CardioPaTh
Cardiovascular
Pathophysiology
& Therapeutics

Characterisation of Pathophysiological Patterns of Coronary Artery Disease

PhD Thesis

Daniel Batista Munhoz, MD, MSc

UNIVERSITÀ DEGLI STUDI DI NAPOLI
FEDERICO II

Cardiovascular Center
OLV Aalst

Characterisation of Pathophysiological Patterns of Coronary Artery Disease

Daniel Batista Munhoz, MD, MSc

06/06/1985, Brasília (Brazil)

Naples, 10/06/2024

Promotor: Prof. Emanuele Barbato

Sapienza Università di Roma Italy

Co-promotor: Dr. Carlos Collet

Cardiovascular Center Aalst, OLV Clinic, Aalst, Belgium

University Federico II of Naples, Faculty of Medicine,
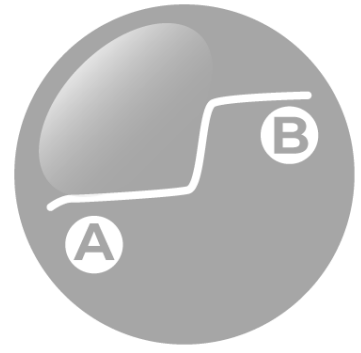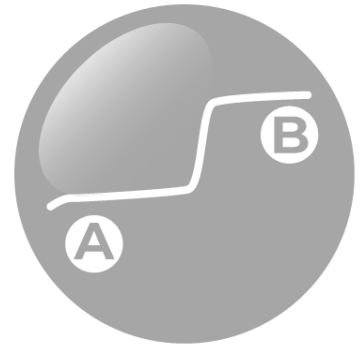
Via Pansini no. 5, 80131 Naples, Italy

TABLE OF CONTENTS

Part A.

General introduction and outline of the thesis

Fractional flow reserve (FFR) measures the reduction of flow caused by an obstructive coronary lesion by comparing distal coronary to aortic pressures during hyperemia. FFR ≤ 0.80 identifies coronary stenoses associated with reversible ischemia.[1] FFR guidance reduces the composite of cardiovascular death, myocardial infarction, and repeat revascularisation compared to angiography alone.[2] Furthermore, in patients with hemodynamically significant stenoses, an FFR-guided PCI strategy reduced cardiovascular outcomes compared to optimal medical therapy alone.[3] Based on the evidence mentioned above, the American and European guidelines recommend using FFR to evaluate patients with intermediate coronary stenoses between 50-90% to define the need for revascularisation.[4,5]

Several studies have shown that PCI restores epicardial conductance, improves myocardial perfusion, relieves angina and potentially reduces spontaneous myocardial infarction (MI).[6-8] These benefits can only be observed if flow-limiting lesions are selected for PCI. Therefore, measuring FFR guides the selection of patients who benefit from PCI. Moreover, deferring patients from PCI based on FFR is safe; patients with flow-limiting lesions based on FFR have a very low rate of adverse events.[9,10]

Despite the enhanced selection of patients for revascularisation provided by coronary physiology, approximately 25% remain symptomatic after a successful PCI.[11] Studies measuring FFR after PCI have shown that in approximately one-third of patients, the intervention results are sub-optimal from the physiologic perspective.[12,13] Low FFR after an angiographic successful PCI has been associated with a higher rate of cardiac death and myocardial infarction.[12] Moreover, the FFR change between the pre and post-intervention has been associated with improved angina and quality of life. Therefore, post-PCI FFR has emerged as a surrogate of the effectiveness of revascularisation with prognostic implications. Recording a pressure pullback curve before PCI allows identifying the presence and location

of focal pressure gradients. Interestingly, performing a pullback has been done since the early days of angioplasty.[14]

However, assessing the pullback curve, a mandatory step for FFR measurements, relied on visual assessment, leading to moderate reproducibility.[15] Recently, the pullback pressure gradient (PPG) has been introduced to quantify the information in the pullback curve. This results in a classification of the pattern of CAD based on a continuous scale from 0 to 1.[16] Vessels with PPG close to 1 indicate focal disease whereas PPG close to 0 indicates diffuse disease. The standardisation of the assessment of the pathophysiological pattern of CAD has facilitated further understanding of CAD and its response to percutaneous treatment.[17] In addition, the widely recognised discrepancy between anatomical and physiological assessments of CAD has been extrapolated to the evaluation of the pattern of the distribution pressure losses.[18] [19]

Extending FFR to the post-PCI stage adds information about the procedure's success. Post-PCI FFR is inversely correlated with the probability of target vessel failure.[12,20] Furthermore, using post-PCI FFR as a trigger to improve the functional outcomes of an intervention using a physiology-guided incremental optimisation strategy (PIOS) is associated with a higher post-PCI FFR.[21] Likewise, PCI optimisation based on intravascular imaging has also been associated with a greater post-PCI FFR when compared to angio-guided PCI.[22] Consequently, FFR after PCI has emerged as a marker of PCI success.

In part B of this thesis, we expand the understanding of pathophysiological patterns of CAD by assessing the PPG's accuracy and reproducibility when derived from different techniques (manual versus motorised). We further evaluate the association between PPG and PCI outcomes and study the influence of PPG on revascularisation decisions. Chapter 1 describes the reproducibility and repeatability of PPG when derived from manual pullbacks, showing an excellent agreement with motorised pullbacks. This finding permitted the

integration of PPG into clinical practice. Chapter 2 addresses the performance of PPG in serial stenoses.

Part C delves into the intricacies of PPG according to specific anatomical characteristics. Chapter 3 deepens the understanding of the mechanistic relationship between vessel volume, myocardial mass and post-PCI FFR. Chapter 4 describes anatomical correlates (vessel types) influencing the relationship between post-PCI FFR and PCI outcomes. This observation of lower post-PCI FFR in the Left Anterior Descending (LAD) artery is validated against clinical outcomes in an individual patient-level (IPD) meta-nalysis presented in Chapter 5. Chapter 6 describes the impact of PPG on PCI optimisation based on coronary physiology.

Part D of this thesis describes novel associations between PPG and atherosclerotic plaque characteristics. Chapter 7 describes the association between focal CAD (high PPG) plaque burden, lipid-rich plaque and thin-cap fibroatheroma (TCFA). Chapter 8 explores the interaction between hemodynamic forces and atherosclerotic plaque phenotypes, particularly concerning plaque rupture. We aimed to establish the association between intracoronary pressure gradients in focal and diffuse CAD and wall shear stress (WSS). Vessels with focal CAD had significantly higher WSS than those with diffuse CAD. Chapter 9 describes the impact of PPG on post-PCI FFR and minimal stent area, and Chapter 10 shows the impact of PPG on patient-reported outcomes, as measured by the 7-item Seattle angina questionnaire(SAQ-7).

In Part E, we present a large-scale prospective validation of the PPG concept starting in Chapter 11 with the rationale and design of the PPG Global study. A single-arm, investigator-initiated, multicenter international study enrolled patients with at least one major epicardial lesion with a distal FFR ≤0.80 and intended to be treated with PCI. The primary endpoint was the predictive capacity of PPG for Post-PCI FFR. The key secondary outcomes included the impact of PPG on treatment decisions, the relationship between baseline PPG and

improvement of angina symptoms one year after PCI (assessed by SAQ-7) and rates of TVF at follow-up. Chapter 12 provides an example of a subject included on PPG Global, aimed at clarifying the role of PPG in cases of discordance between FFR and non-hyperemic pressure indices (NHPR) assessment. The results of the primary endpoint of PPG Global are presented in Chapter 13. PPG demonstrated excellent predictive capacity for optimal revascularisation and PPG influenced treatment decisions. Interestingly, periprocedural MI occurred more frequently in patients with diffuse disease (low PPG) compared to those with focal disease.

The aims of this thesis are 1) To expand the use of coronary physiology to differentiate atherosclerosis phenotypes; 2) To validate the pullback pressure gradient (PPG) as a predictor of PCI outcomes; 3) To determine the usefulness of PPG for clinical decision-making in patients with planned PCI.

REFERENCES

1.   Pijls NH, De Bruyne B, Peels K, et al. Measurement of fractional flow reserve to assess the functional severity of coronary-artery stenoses. *N Engl J Med*. Jun 1996;334(26):1703-8. doi:10.1056/NEJM199606273342604

2.   Tonino PA, De Bruyne B, Pijls NH, et al. Fractional flow reserve versus angiography for guiding percutaneous coronary intervention. *N Engl J Med*. Jan 2009;360(3):213-24. doi:10.1056/NEJMoa0807611

3.   De Bruyne B, Pijls NH, Kalesan B, et al. Fractional flow reserve-guided PCI versus medical therapy in stable coronary disease. *N Engl J Med*. Sep 2012;367(11):991-1001. doi:10.1056/NEJMoa1205361

4.   Knuuti J, Wijns W, Saraste A, et al. 2019 ESC Guidelines for the diagnosis and management of chronic coronary syndromes. *Eur Heart J*. 01 2020;41(3):407-477. doi:10.1093/eurheartj/ehz425

5.   Virani SS, Newby LK, Arnold SV, et al. 2023 AHA/ACC/ACCP/ASPC/NLA/PCNA Guideline for the Management of Patients With Chronic Coronary Disease: A Report of the American Heart Association/American College of Cardiology Joint Committee on Clinical Practice   Guidelines.   *Circulation*.   Aug   29   2023;148(9):e9-e119. doi:10.1161/CIR.0000000000001168

6.   Shaw LJ, Berman DS, Maron DJ, et al. Optimal medical therapy with or without percutaneous coronary intervention to reduce ischemic burden: results from the Clinical Outcomes Utilizing Revascularization and Aggressive Drug Evaluation (COURAGE) trial nuclear   substudy.   *Circulation*.   Mar   2008;117(10):1283-91. doi:10.1161/CIRCULATIONAHA.107.743963

7.   Rajkumar CA, Foley MJ, Ahmed-Jushuf F, et al. A Placebo-Controlled Trial of Percutaneous Coronary Intervention for Stable Angina. *N Engl J Med*. Dec 21 2023;389(25):2319-2330. doi:10.1056/NEJMoa2310610

8.   Chaitman BR, Alexander KP, Cyr DD, et al. Myocardial Infarction in the ISCHEMIA Trial: Impact of Different Definitions on Incidence, Prognosis, and Treatment Comparisons. *Circulation*. Feb 2021;143(8):790-804. doi:10.1161/CIRCULATIONAHA.120.047987

9.   Bech GJ, De Bruyne B, Pijls NH, et al. Fractional flow reserve to determine the appropriateness of angioplasty in moderate coronary stenosis: a randomized trial. *Circulation*. Jun 19 2001;103(24):2928-34. doi:10.1161/01.cir.103.24.2928

10.   Pijls NH, van Schaardenburgh P, Manoharan G, et al. Percutaneous coronary intervention of functionally nonsignificant stenosis: 5-year follow-up of the DEFER Study. *J Am Coll Cardiol*. May 29 2007;49(21):2105-11. doi:10.1016/j.jacc.2007.01.087

11.   Grodzinsky A, Kosiborod M, Tang F, et al. Residual Angina After Elective Percutaneous Coronary Intervention in Patients With Diabetes Mellitus. *Circ Cardiovasc Qual Outcomes*. Sep 2017;10(9)doi:10.1161/CIRCOUTCOMES.117.003553

12.   Hwang D, Koo BK, Zhang J, et al. Prognostic Implications of Fractional Flow Reserve After Coronary Stenting: A Systematic Review and Meta-analysis. *JAMA Netw Open*. Sep 01 2022;5(9):e2232842. doi:10.1001/jamanetworkopen.2022.32842

13.   Jeremias A, Davies JE, Maehara A, et al. Blinded Physiological Assessment of Residual Ischemia After Successful Angiographic Percutaneous Coronary Intervention: The DEFINE PCI   Study.   *JACC   Cardiovasc   Interv*.   10   28   2019;12(20):1991-2001. doi:10.1016/j.jcin.2019.05.054

14.   Meier B. His master's art, Andreas Grüntzig's approach to performing and teaching coronary angioplasty. *EuroIntervention*. May 15 2017;13(1):15-27. doi:10.4244/EIJV13I1A2

15. Toth GG, Johnson NP, Jeremias A, et al. Standardization of Fractional Flow Reserve Measurements. *J Am Coll Cardiol*. Aug 16 2016;68(7):742-53. doi:10.1016/j.jacc.2016.05.067

16. Collet C, Sonck J, Vandeloo B, et al. Measurement of Hyperemic Pullback Pressure Gradients to Characterize Patterns of Coronary Atherosclerosis. *J Am Coll Cardiol*. 10 2019;74(14):1772-1784. doi:10.1016/j.jacc.2019.07.072

17. Sonck J, Collet C, Mizukami T, et al. Motorized fractional flow reserve pullback: Accuracy and reproducibility. *Catheter Cardiovasc Interv*. Sep 01 2020;96(3):E230-E237. doi:10.1002/ccd.28733

18. Tonino PA, Fearon WF, De Bruyne B, et al. Angiographic versus functional severity of coronary artery stenoses in the FAME study fractional flow reserve versus angiography in multivessel evaluation. *J Am Coll Cardiol*. Jun 2010;55(25):2816-21. doi:10.1016/j.jacc.2009.11.096

19. Mintz GS, Painter JA, Pichard AD, et al. Atherosclerosis in angiographically "normal" coronary artery reference segments: an intravascular ultrasound study with clinical correlations. *J Am Coll Cardiol*. Jun 1995;25(7):1479-85. doi:10.1016/0735-1097(95)00088-l

20. Johnson NP, Collet C. Can FFR After Stenting Help Reduce Target Vessel Failure? *JACC Cardiovasc Interv*. Sep 13 2021;14(17):1901-1903. doi:10.1016/j.jcin.2021.08.001

21. Collison D, McClure JD, Berry C, Oldroyd KG. A randomized controlled trial of a physiology-guided percutaneous coronary intervention optimization strategy: Rationale and design of the TARGET FFR study. *Clin Cardiol*. May 2020;43(5):414-422. doi:10.1002/clc.23342

22. Neleman T, van Zandvoort LJC, Tovar Forero MN, et al. FFR-Guided PCI Optimization Directed by High-Definition IVUS Versus Standard of Care: The FFR REACT Trial. *JACC Cardiovasc Interv*. Aug 22 2022;15(16):1595-1607. doi:10.1016/j.jcin.2022.06.018

Part B.

Building a reproducible quantification the FFR pullback curve
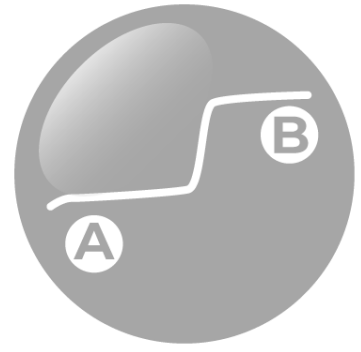
Chapter 1. Development, validation, and reproducibility of the pullback pressure gradient (PPG) derived from manual fractional flow reserve pullbacks

Sonck J, Mizukami T, Johnson NP, Nagumo S, Gallinoro E, Candreva A, Mileva N, Munhoz D, Shinke T, Svanerud J, Barbato E, De Bruyne B, Collet C.

Graphical Abstract

Cohort 1. Comparison between PPG based on motorized and manual pullbacks.	Cohort 2. Reproducibility of the PPG derived from manual pullbacks

Comparison between Manual and Motorized

n = 20
slope = 0.95
Intercept = 0.04
r = 0.89 (95%CI 0.74 to 0.96)
p < 0.001

Motorized Pullback Pressure Gradient (PPG)

PPG Intra reproducibility

n = 25
slope = 0.93
Intercept = 0.04
r = 0.94 (95%CI 0.87 to 0.97)
p < 0.001

Pullback duration and PPG

n = 50
slope = 3.77
Intercept = -0.49
r = 0.02 (95%CI -0.26 to 0.3)
p = 0.869

Manual PPG

PPG Inter reproducibility

n = 25
slope = 0.91
Intercept = 0.06
r = 0.95 (95%CI 0.89 to 0.98)
p < 0.001
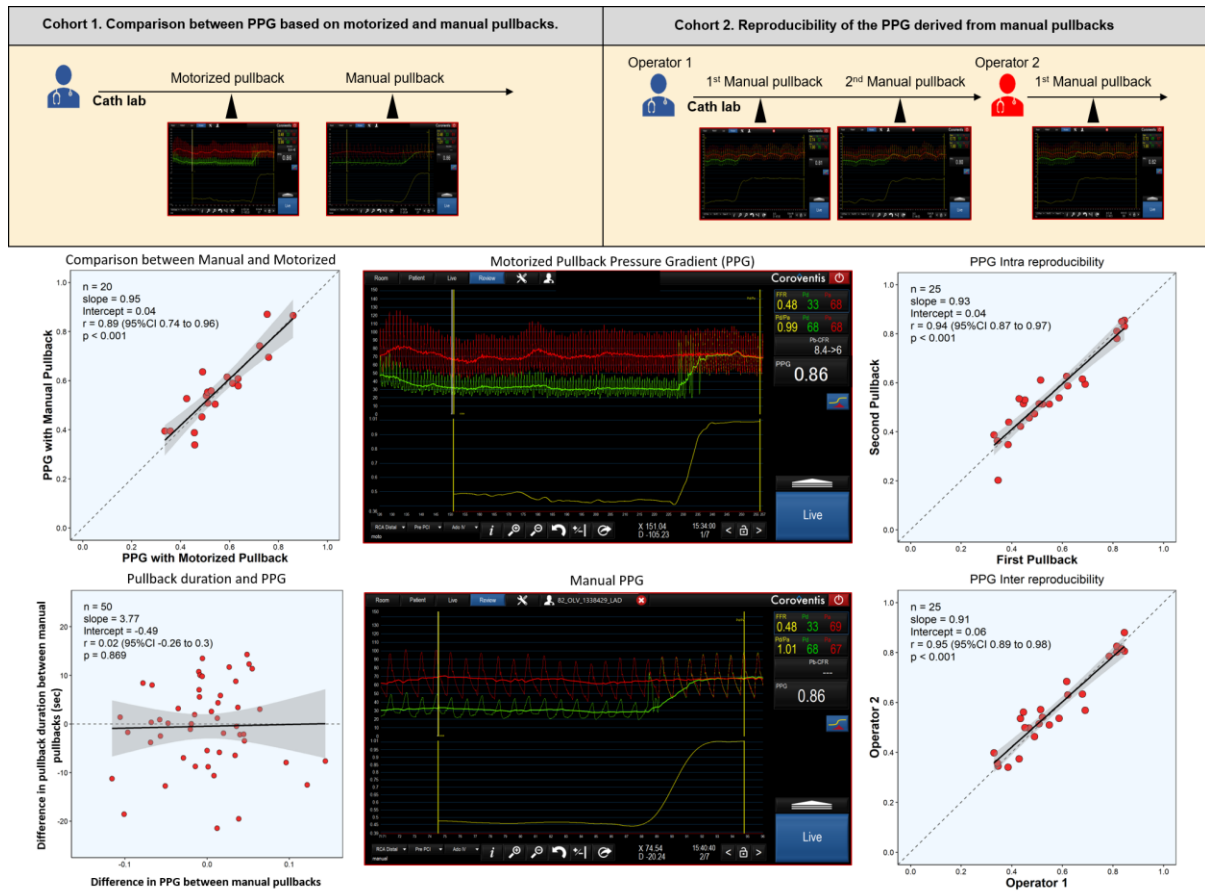
Abstract

Background: FFR pullbacks assess the location and magnitude of pressure drops along the coronary artery. The Pullback Pressure Gradient (PPG) quantifies the FFR pullback curve and provides a numeric expression of focal versus diffuse coronary artery disease. The aim of this study is (1) to validate the PPG using manual FFR pullbacks compared with motorized FFR pullbacks as a reference; and (2) to determine the intra- and inter-operator reproducibility of the PPG derived from manual FFR pullbacks.

Methods: Patients with stable coronary artery disease and an FFR ≤0.80 were included. All patients underwent FFR pullback evaluation either with a motorized device or manually, depending on the study cohort. The agreement of the PPG between repeated pullbacks was assessed using the Bland-Altman method.

Results: Overall 116 FFR pullbacks manoeuvres (96 manual and 20 motorized) were analyzed. There was excellent agreement between the PPG derived from manual and motorized pullbacks (mean difference -0.01 ± 0.07, 95% limits of agreement [LOA] -0.14 to 0.12). The intra- and inter-operator reproducibility of PPG derived from manual pullbacks was excellent (mean difference <0.01, 95% LOA -0.11 to 0.12, and mean difference <0.01, 95% LOA -0.12 to 0.11, respectively). The duration of the pullback maneuver did not impact the reproducibility of the PPG ($r=0.12$, 95% CI -0.29 to 0.49, $p=0.567$).

Conclusion: Manual pullbacks allow for an accurate PPG calculation. The inter- and intra-operator reproducibility of PPG derived from manual pullback was excellent.

Introduction

Intracoronary pressure measurements reflect the physiologic epicardial atherosclerotic burden. [1]A pullback maneuver assesses the distribution and magnitude of pressure loss. [2]A novel metric derived from fractional flow reserve (FFR) pullback curves – the pullback pressure gradient (PPG) – quantifies the pattern of coronary artery disease (CAD) as either focal or diffuse. [3]PPG values close to zero represent diffuse disease; values close to 1 indicate focal CAD. PPG was conceptualized from FFR curves obtained from motorized pullbacks requiring additional hardware in the catheterization laboratory and prolonged adenosine infusions, both leading to longer procedural times and greater patient discomfort that would limit adoption in clinical practice.

An easier approach would be to derive PPG from manual pullbacks. However, manual withdraw of the pressure wire is operator dependent and reproducibility may be hampered. [4]For the practical adoption of the PPG, a mandatory requirement is acceptable test/retest reliability. This general property assumes the utmost importance in the field of coronary physiology where cut-offs are usually applied to guide clinical decision making. [2]

While the usefulness of an intracoronary pullback maneuver is increasingly recognized, there is insufficient data supporting the test/retest reliability of manual FFR pullbacks. [5]The objectives of the current study are: (1) to validate the PPG calculation derived from manual FFR pullbacks compared with motorized FFR pullbacks as a reference, and (2) to assess the intra- and inter-operator reproducibility of the PPG derived from manual FFR pullbacks.

Methods

This prospective, single-center study included patients with stable CAD and clinical indication for FFR interrogation. All patients underwent FFR pullback evaluations either with a motorized device or manually depending on the study cohort. Patients with ostial lesions, severe vessel tortuosity, bifurcation lesions with planned two stent strategy, difficult vessel wiring, STEMI presentation, or severe renal dysfunction with eGFR <30 ml/min/1.73m^2 were excluded. All patients signed informed consent, and the local ethics committee approved the study. The study was funded by the Cardiac Research Institute Aalst. All pressure tracings were analyzed by a core laboratory (CoreAalst BV, Aalst, Belgium).

Calculation of the Pullback Pressure Gradient (PPG)

To expand PPG to manual pullbacks, the original formula was adapted as follows. [3]The original equation combines two equally-weighted parameters:

$$\textbf{PPG} = \frac{\dfrac{\text{Maximal PPG over 20mm}}{\text{Vessel FFR gradient}} + (1 - \dfrac{\text{Length with functional disease}}{\text{Vessel length}})}{2}$$

The *maximal PPG over 20 mm* depicts the magnitude FFR drops over a fixed length; and the *length with functional disease* describes the extent of FFR deterioration (defined as the length, in millimeters, with FFR drop ≥ 0.0015/mm). For manual pullbacks, the original parameters based on absolute distance values (i.e., millimeters) were made relative to the pullback duration. The rationale for this conversion relied on the observed mean pullback length of 98.9 ± 19.3 mm in previous cohorts. [3]Therefore, the adapted equation resulted in:

$$\textbf{PPG} = \frac{\dfrac{\text{Maximal Pressure Gradient over 20\% pullback duration}}{\text{Vessel FFR gradient}} + (1 - \text{proportion of pullback time with FFR deterioration})}{2}$$

where the *maximal pressure gradient over 20% of the pullback duration* calculates the pressure drop over a fixed time window of 20% of the total pullback duration. Likewise, the *percent of pullback time with FFR deterioration* reports the extent of functional deterioration, relative to the total duration of the pullback maneuver, calculated using an equivalent FFR drop cut-off as in the original equation (now 0.0015/% total). The adapted formula has been incoporated in a commercial console and allows for online calculation of the PPG after a manual pullback manoeuvre (Coroventis, Coroventis Research, Uppsala, Sweden) (Figure 1).

Study population

We prospectively recruited two distinct cohorts. The flowchart of patient inclusion is shown in the Supplemental Material Figures S1 and S2. The first cohort of 19 patients (20 vessels) underwent both motorized and manual FFR pullbacks to assess the agreement of PPG values. The second cohort consisted of 22 patients (25 vessels) with repeated manual pullbacks

performed by two operators to assess the inter- and intra-observer reproducibility of PPG values (Figure 2).

Invasive fractional flow reserve analysis

Fractional flow reserve measurements were performed as per standard practice. [6]The pressure wire was positioned at least 20 mm beyond the most distal coronary stenosis in vessels more than 2 mm diameter by visual estimation. The pressure wire position was recorded using a contrast injection annotating the starting point for each pullback manoeuvre to ensure the same initial position among pullbacks. All patients received intra-coronary nitrates administration before FFR measurement. Hyperemia was induced using either adenosine at a dose of 140 μg/kg/min via a peripheral or central vein or intra-coronary papaverine bolus at a dose of 8 mg in the right coronary artery and 12 milligram in the left coronary artery. [7]If significant drift (≥ 0.03) was observed, the FFR measurement was repeated. Pressure wire measurements were performed using CoroFlow version 3.5 (Coroventis Research AB, Uppsala, Sweden). All FFR tracings were assessed by a core laboratory (CoreAalst BV, Aalst, Belgium).

Motorized pullbacks

The detailed procedure has been published elsewhere. [3]Briefly, a pullback device (Volcano R 100, San Diego, California, United States) was adapted to grip the coronary pressure wire (PressureWire X, St Jude Medical, Minneapolis, United States) and set at a speed of 1 mm/s to pull back the pressure-wire to the tip of the guiding catheter during continuous hyperemia.

Manual pullbacks

For manual FFR pullback, the operator withdrew the pressure wire at a steady and constant speed for 20 to 30 seconds during stable hyperemia. When the pressure sensor reached the catheter tip, the recording was stopped. The technique for manual pullbacks is shown in the **Online Video**. For the inter-operator agreement, the second operator remained blinded to the first PPG result.

Statistical analysis

Continuous variables are presented as mean and standard deviation or as median and interquartile range, depending on the distribution. Categorical variables are presented as percentages and counts. Pearson correlation coefficients, intra-class correlation coefficients (ICC), Bland-Altman method, and the coefficient of variation were used to assess the PPG's reproducibility. The study was powered to evaluate the reproducibility of the PPG derived from manual pullbacks. The sample size was calculated assuming a maximal coefficient of variation (COV) of 15% with an 11% two-sided confidence interval for the intra-observer reproducibility and a 20% maximal COV with 15% two-sided confidence interval for the inter-observer reproducibility. The sample size calculation required 20 patients with paired measurements for both the intra- and inter-operator reproducibility analyses. All analyses were perfomed using R (R Foundation for Statistical Computing, Vienna, Austria). COV from duplicate measurements was calculated with MedCalc Statistical Software version 19.3.1 (MedCalc Software, Ostend, Belgium).

Results

Between March 2020 and February 2021, 41 patients were included in two cohorts. Tables 1 and 2 show baseline clinical and procedural characteristics stratified by cohort. A comparison of PPG values between the original and adapted formula using a sample of motorized pullbacks is shown in the Supplemental material Figure S3 and Table T1.

PPG: manual vs motorized pullbacks

Overall, 20 vessels with both manual and motorized FFR pullbacks were included in this analysis. The mean FFR was 0.75 ± 0.13 and 0.75±0.11 before manual and motorized pullbacks, respectively (mean difference <0.01±0.03, lower limit of agreement [LLA] -0.06 and upper limit of agreement [ULA] 0.07). Mean pullback duration was 32.1 ± 7.6 and 103.3 ± 24.8 seconds for manual and motorized pullbacks ($p<0.001$), respectively. Mean PPG derived from manual pullback was 0.57 ± 0.15 whereas mean PPG from motorized pullbacks was 0.56 ± 0.14 (mean difference -0.01±0.07, 95% LLA -0.14 and ULA 0.12;). Figure 3 shows the agreement of the PPG components between manual and motorized pullbacks. A case example is presented in Supplemental Material Figure S4.

Reproducibility of the PPG derived from manual pullbacks

Overall 26 vessels were included in this analysis. In 25 vessels two manual FFR pullbacks were performed by the first operator and in 25 vessels a third pullback was performed by a second operator. The mean FFR of the first, second, and third measurements were 0.68±0.11, 0.69±0.12 and 0.68±0.12, respectively (p=0.920). Mean duration of the first, second, and third pullback maneuver was 35.4±7.3 sec, 35.6±8.9 sec and 36.5±8.8 sec, respectively (p=0.924). Mean PPG derived from the first, second, and third pullbacks was 0.57±0.17, 0.56±0.17 and 0.58±0.16, respectively . There was an excellent intra-observer reproducibility of PPG with a mean difference <0.01±0.06 (95% LOA -0.11, ULA 0.12), COV of 10.7 % (95% CI 7.5 to 14.63) and ICC of 0.94 (0.88 to 0.98). The reproducibility of PPG's components derived from the intra-observer analysis are shown in **Figure 4**. Inter-operator reproducibility was also excellent with a mean difference between PPG of 0.01±0.05 (LLA -0.11, ULA 0.10), COV of 7.6 % (95% CI 5.3 to 9.9) and ICC of 0.95 (95% CI 0.89 to 0.98; Figure 5). The duration of the pullback did not affect the reproducibility of the PPG (r = 0.02, 95% CI -0.26 to 0.30, p= 0.869; Figure 6). A case example is presented in Supplemental Material Figure S5.

All pullback procedures were performed without complications. From all patients, 73% (30/41) underwent PCI without in-hospital adverse events. Eight patients were treated medically and 3 patients were referred to coronary artery bypass grafting.

Discussion

The findings of the present study can be summarized as follows: (1) PPG can be accurately derived from manual pullbacks; (2) both intra- and inter-operator reproducibility of the PPG derived from manual PPG were excellent, and (3) the duration of the pullback manuever did not affect the reproducibility of the PPG.

Fractional flow reserve measured in the distal coronary artery captures the net effect of cumulative pressure losses related to stenoses and diffuse disease. [1,8]An FFR pullback provides a second dimension to the distal measurement by depicting the distribution and magnitude of pressure losses longitudinaly along the coronary vessel. [9]Motorized pullbacks are advantageous because they are operator independent and allow for co-registration of pressure data alongside anatomical images. [10]In contrast, a manual pullback depends on the operator's technique, and pullback speed may vary during the pullback and between operators. This can impact curve morphology, quantification of pressure gradients, and the interpretation of the CAD pattern.[11] Nonetheless, manual pullbacks are practical to perform, reduce procedural

time, and can be done using intra-coronary hyperemic agents such as papaverine. [7]The present study demonstrated that PPG can be derived from manual pullbacks with similar values compared to motorized pullbacks with a mean difference of -0.01±0.07 PPG units. Moreover, the agreement between a manual and motorized pullback for the maximal pressure gradient was excellent at -0.01±0.03 FFR units. The main reason for this agreement is that by using 20% of the duration of the pullback curve as the window for data sampling, the PPG calculation overcomes issues related to different pullback speeds under the assumption of constant pressure wire withdrawal. Lastly, the evaluation of the length of disease, which is based on a threshold relative to total pullback time, was unnafected by the pullback method (mean difference of -0.70±7.57%). Thus, manual pullbacks simplified the assessment of the PPG with excellent accuracy compared to the mechanized approach.

Fractional flow reserve is a highly repeatable metric. [12]Likewise, FFR pullbacks performed with a mechanized device have been shown to have excellent reproducibility. [10]However, the morphology of a pullback curve is sensitive to the pullback technique. Fast pullback maneuvers would likely mask pressure gradients. Similarly, pullback maneuvers with varying speeds may misrepresent the location and magnitude of pressure gradients. In the present study, operators were instructed to performed manual pullback maneuvers aiming at completing the maneuver in 20 to 40 seconds while keeping a constant speed throughout. Following these simple recommendations, PPG derived from repeated manual pullbacks either by the same or a different operator resulted in similar values. Interestingly, the unavoidably different manual pullback times and speeds did not affect the reproducibility of the PPG. These findings provide a practical framework for the standarisation of manual pullback maneuvers.

The current analysis showed a high test/retest reliability of the PPG with excellent intra- and inter-observer reproducibility, together supporting its clinical application. PPG has been incorporated into a commercially-available console (CoroFlow, Coroventis Resreach, Upssala, Sweeden). The online availability of PPG will facilitate the quantification of the pattern of CAD (i.e., focal or diffuse) in clinical practice. [13]Practically, PPG would be indicated once the hemodynamic significance of CAD has been confirmed. PPG refines clinical decision regarding the appropriateness of PCI based on the pattern of CAD, even in cases of serial lesions. [14]Furthermore, PPG anticipates the final FFR value that can be achieved with revascularization. The interpretation of the PPG value should be performed in conjunction with a visual inspection of the pullback curve. This is particualry important for the assessment of

lesion-specific pressure gradients. In patients with low PPG, alternative options to PCI should be considered. On the other hand, vessels with high PPG are optimal candidates for PCI. The ongoing PPG Global registry is evaluating the predictive capacity of PPG to predict post-PCI FFR and the impact of the PPG on clinical decision-making and outcomes (NCT04789317). The results of this study will shed light on the management pathways of patients with focal and diffuse coronary artery disease.

The main limitation of the present study is that it was restricted to a single center; therefore, the extrapolation of these results to operators with different levels of expertise in coronary physiology requires further investigation.

Conclusion

PPG can be derived from manual FFR pullbacks, resulting in similar values compared to motorized pullbacks. The inter- and intra-operator reproducibility of the PPG derived from a manual pullback was excellent. Further studies are require to determined the clinical benefit of a PPG-guided PCI strategy.

Figure 1. Pullback Pressure Gradient (PPG) interface

Coroventis screen showing a FFR pullback with Pd in green, Pa in red and a corresponding distal FFR value of 0.48 in yellow. The vertical yellow lines indicate the start and end of the pullback (yellow horizontal line). The PPG equals 0.86, indicating focal coronary artery disease.

Figure 2. Study design and procedures.
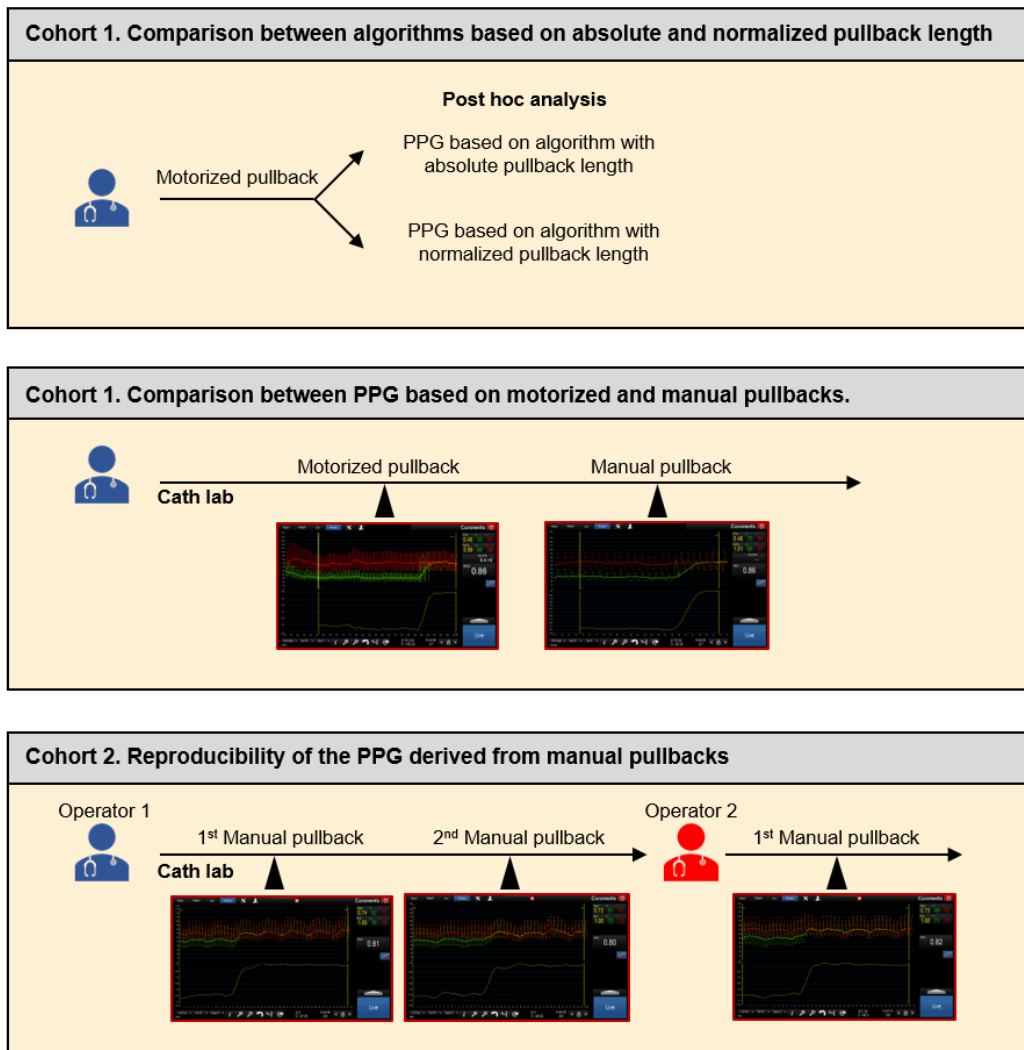
Figure 3. Agreement on the Pullback Pressure Gradient (PPG) and its components between manual and motorized pullbacks.
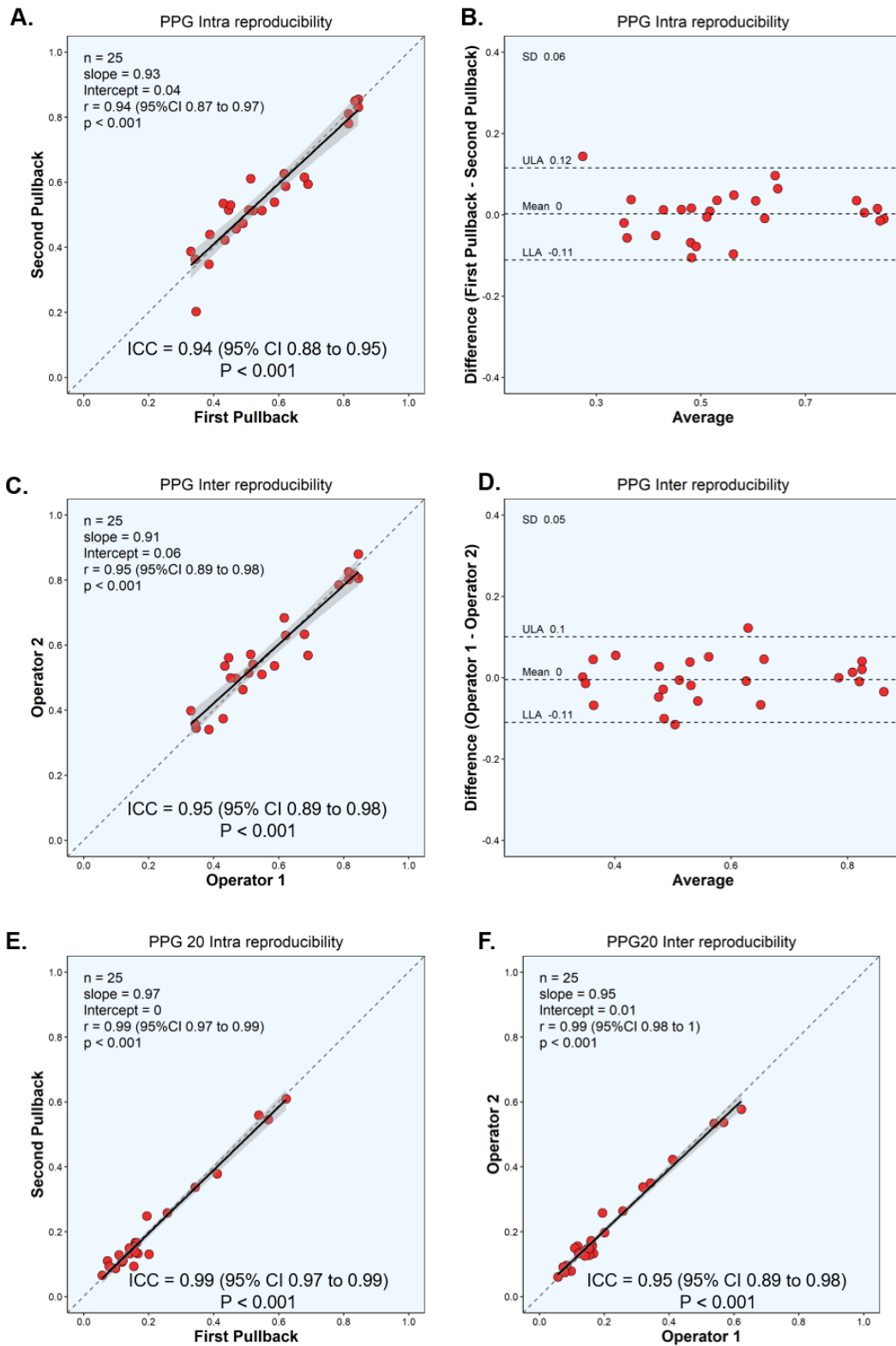
Figure 4. Intra-operator agreement on the Pullback Pressure Gradient (PPG) (Panel A and B) and its components (percentage of disease in panels C and D and PPG 20 millimeter in panels E and F) between repeated manual pullbacks.
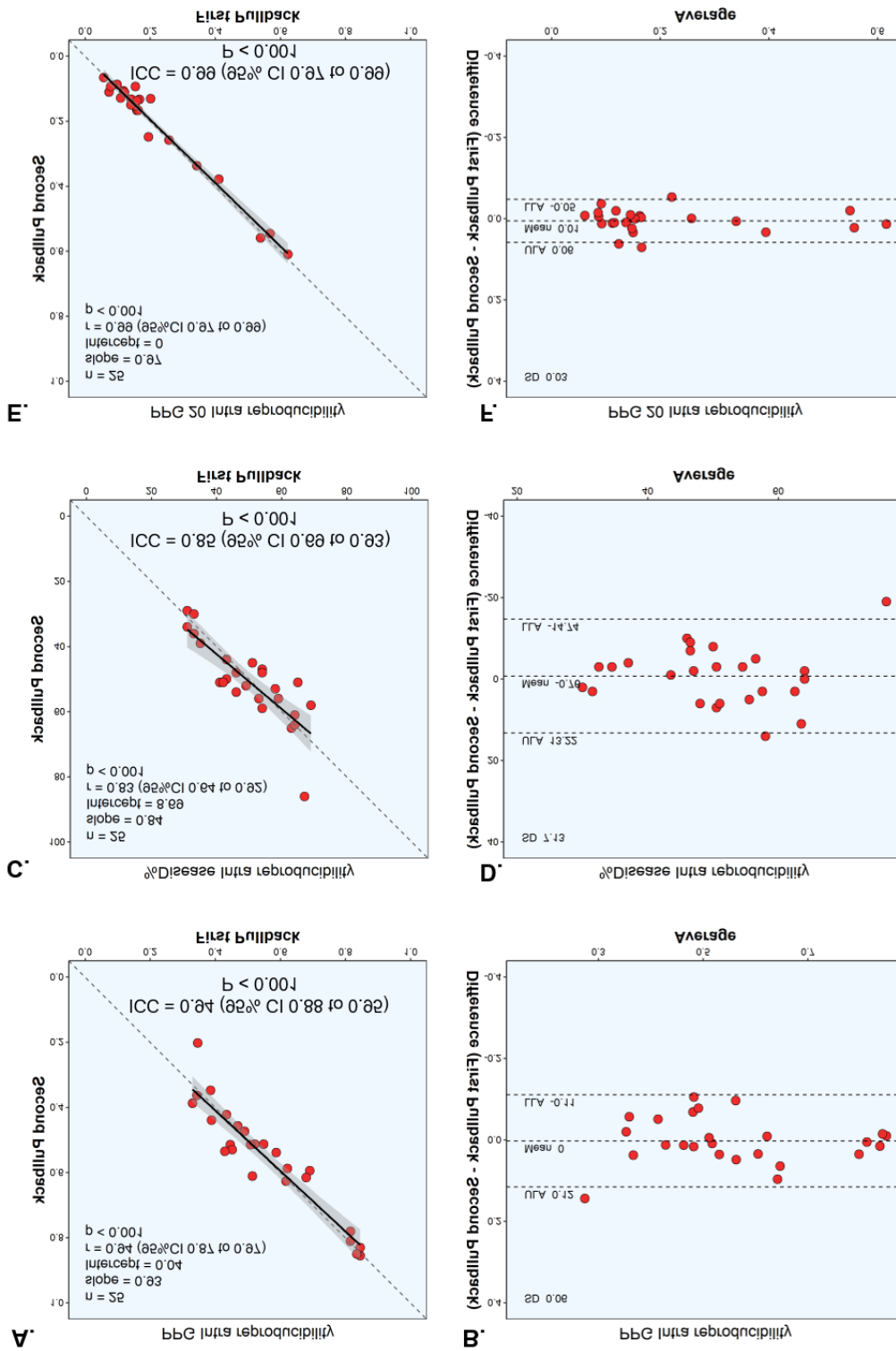
Figure 5. Inter-operator agreement on the Pullback Pressure Gradient (PPG) (Panel A and B) and its components (percentage of disease in panels C and D and PPG 20 millimeter in panels E and F) between repeated manual pullbacks.
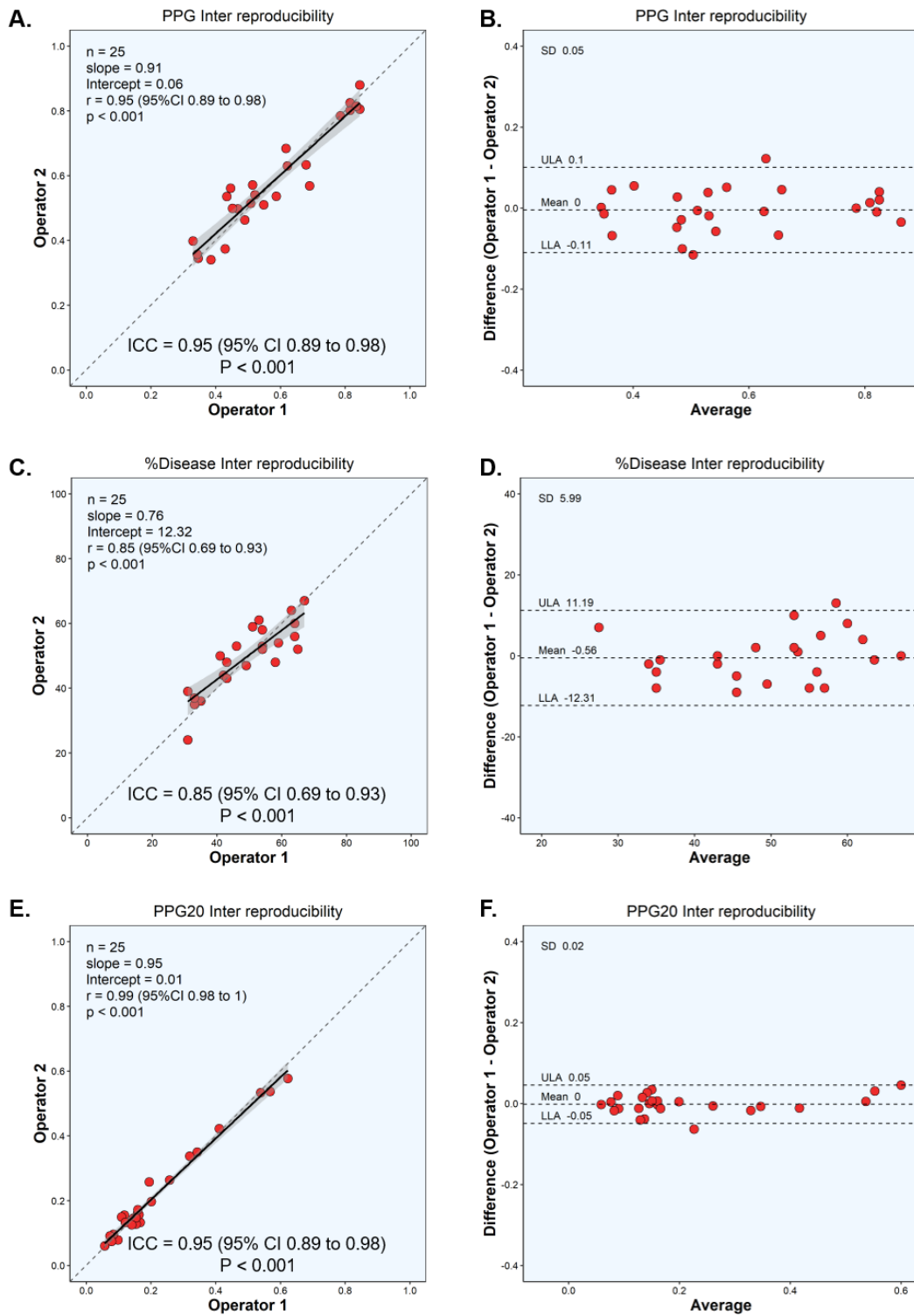
Figure 6: Relationship between the difference in duration of the manual pullbacks and

reproducibility of the PPG
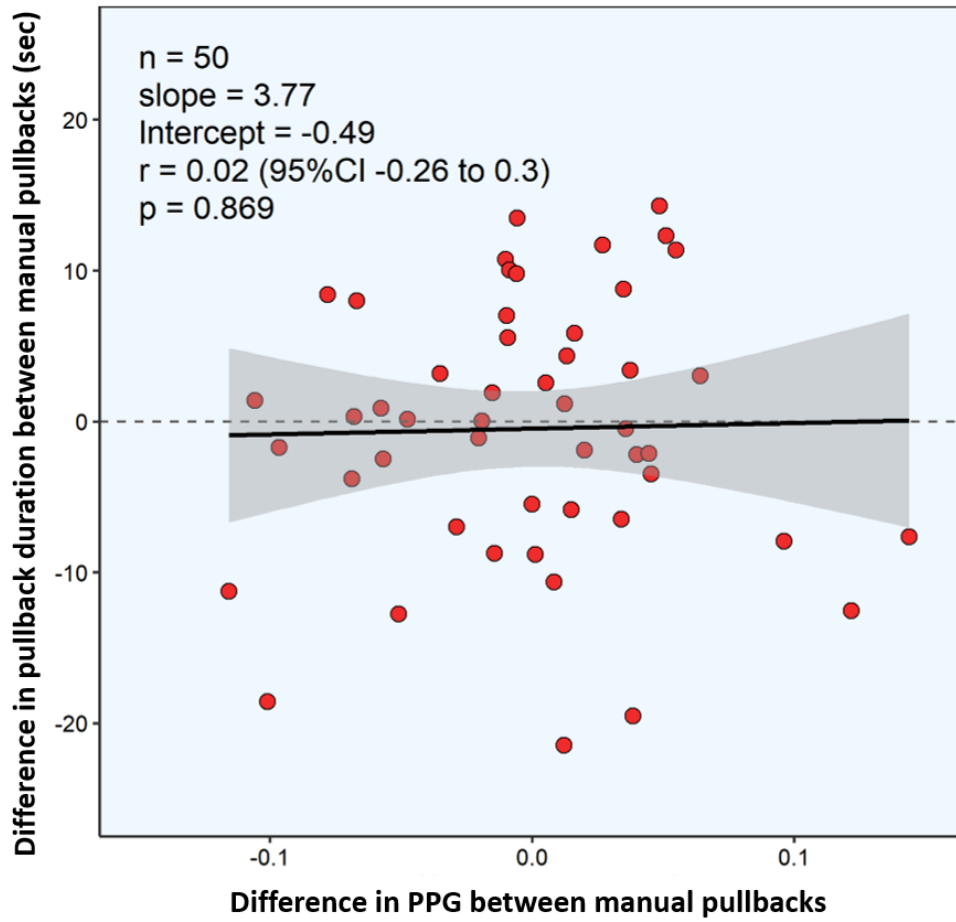
Supplemental figure S1. Agreement on PPG values and its components derived from motorized pullbacks between the original and adapted formula.

23 patients, 24 vessels

Exclusions: 4 patients and vessels
Procedural artefact n = 1
Unstable hyperemia n = 3

19 patients and 20 vessels with motorized and manual pullback
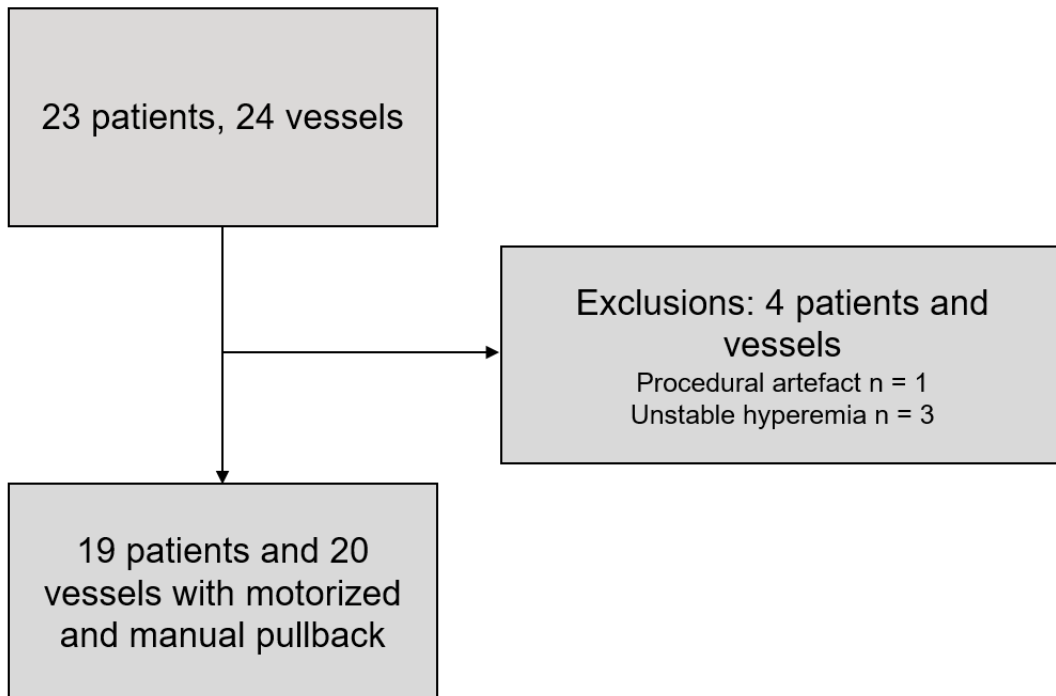
Supplemental figure S2. Flowchart of cohort 1 (motorized and manual pullback).

Patients with repeated manual
pullbacks
from 9/Mar/2020 to 29/July/2020
n = 22 pts

Exclusions: 0 patients, 2
vessels
1 vessel without repeated pullback by
first operator
1 vessel without second operator
pullback

Analyzable cases (22 patients)
Intra rater analysis: 25 vessels
Inter rater analysis: 25 vessels
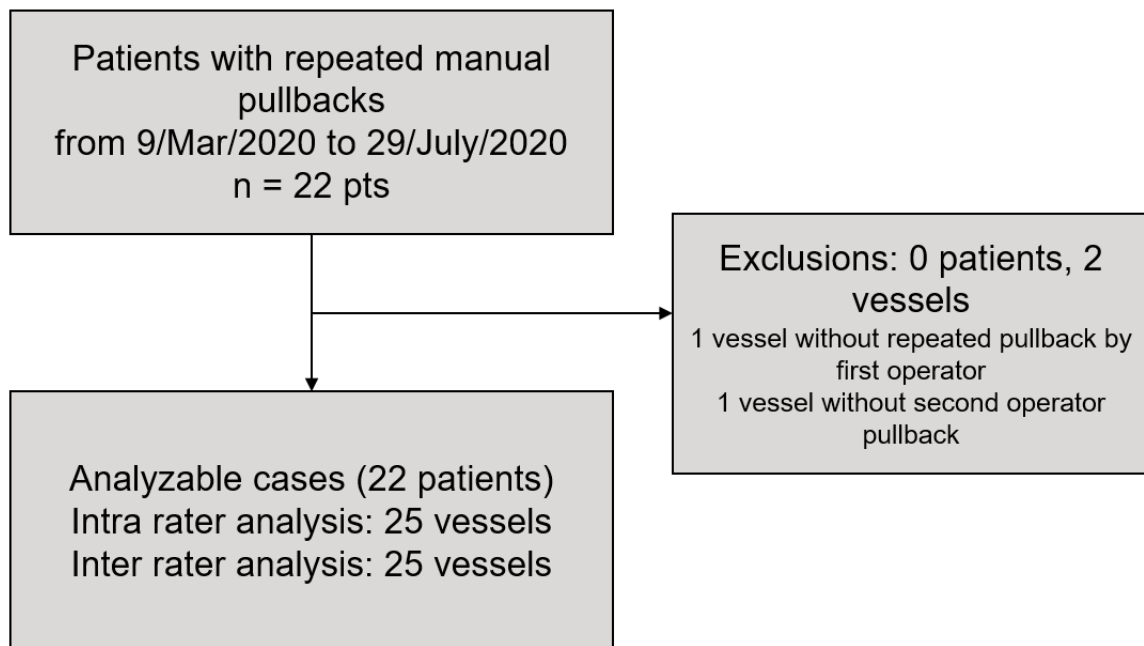
Supplemental figure S3. Flowchart of cohort 2 (repeated manual pullbacks).
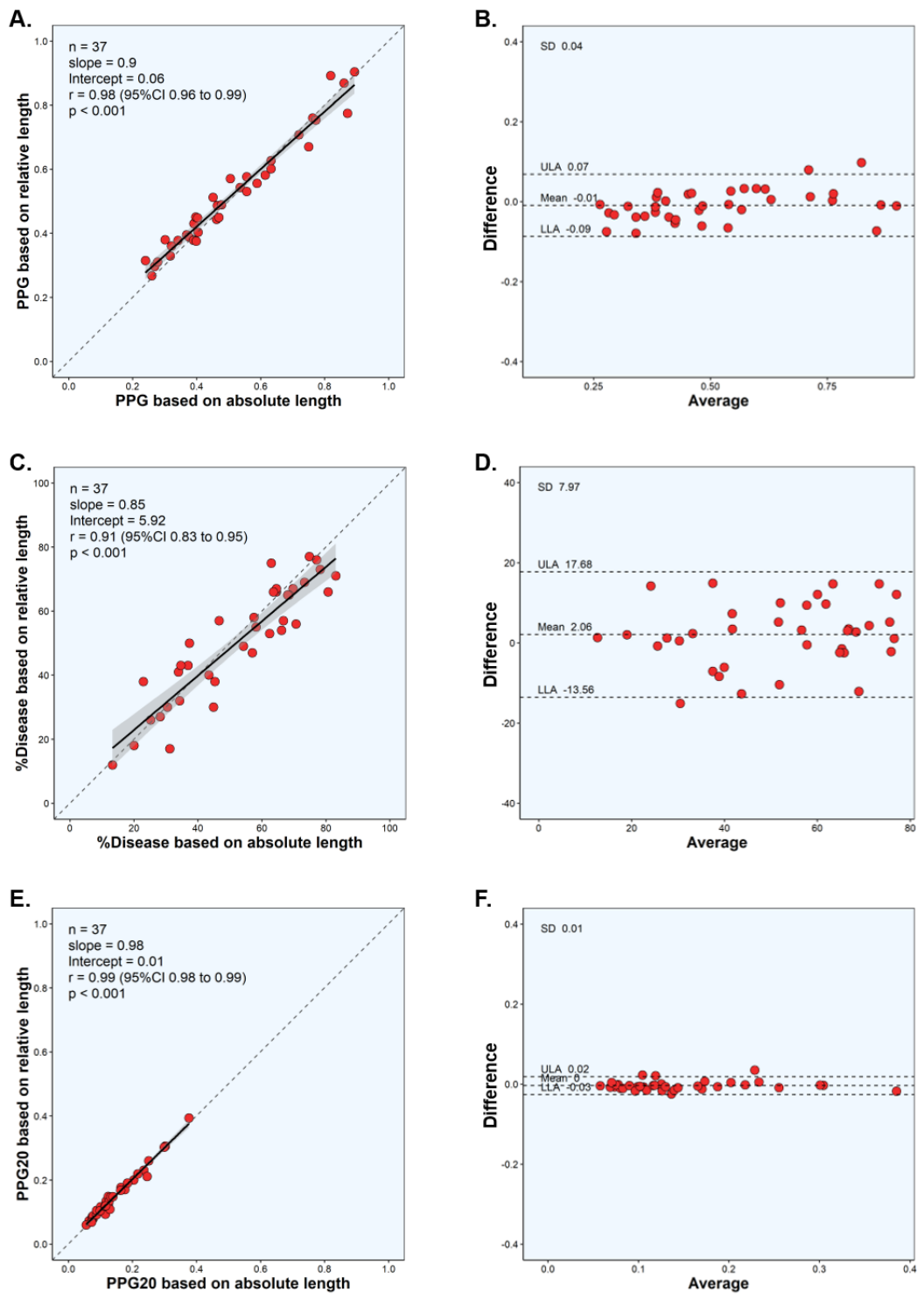
Supplemental Figure S4. Case example of a patient from cohort 1.

Motorized Pullback

Manual Pullback

Supplemental Figure S5. Case example of a patient from cohort 2.

Operator 1. 1st Pullback

Operator 1. 2nd Pullback

Operator 2

REFERENCES

1.   De Bruyne B, Hersbach F, Pijls NH, et al. Abnormal epicardial coronary resistance in patients with diffuse atherosclerosis but "Normal" coronary angiography. *Circulation*. Nov 13 2001;104(20):2401-6.

2.   Knuuti J, Wijns W, Saraste A, et al. 2019 ESC Guidelines for the diagnosis and management of chronic coronary syndromes: The Task Force for the diagnosis and management of chronic coronary syndromes of the European Society of Cardiology (ESC). *European heart journal*. 2019;doi:10.1093/eurheartj/ehz425

3.   Collet C, Sonck J, Vandeloo B, et al. Measurement of Hyperemic Pullback Pressure Gradients to Characterize Patterns of Coronary Atherosclerosis. *Journal of the American College of Cardiology*. 2019;74(14):1772-1784. doi:10.1016/j.jacc.2019.07.072

4.   Higashioka D, Shiono Y, Kubo T, et al. The inter-study reproducibility of instantaneous wave-free ratio and angiography coregistration. *J Cardiol*. May 2020;75(5):507-512. doi:10.1016/j.jjcc.2019.09.016

5.   Collison D, Didagelos M, Aetesam-Ur-Rahman M, et al. Post-stenting fractional flow reserve vs coronary angiography for optimisation of percutaneous coronary intervention: TARGET-FFR trial. *European heart journal*. Jul 19 2021;doi:10.1093/eurheartj/ehab449

6.   Toth GG, Johnson NP, Jeremias A, et al. Standardization of Fractional Flow Reserve Measurements. *Journal of the American College of Cardiology*. Aug 16 2016;68(7):742-53. doi:10.1016/j.jacc.2016.05.067

7.   Mizukami T, Sonck J, Gallinoro E, et al. Duration of Hyperemia With Intracoronary Administration of Papaverine. *Journal of the American Heart Association*. Feb 2 2021;10(3):e018562. doi:10.1161/jaha.120.018562

8.   Pijls NH, De Bruyne B, Bech GJ, et al. Coronary pressure measurement to assess the hemodynamic significance of serial stenoses within one coronary artery: validation in humans. *Circulation*. Nov 7 2000;102(19):2371-7.

9.   Matsuo A, Shimoo S, Takamatsu K, et al. Visualization of the improvement of myocardial perfusion after coronary intervention using motorized fractional flow reserve pullback curve. *Cardiovascular intervention and therapeutics*. Apr 2018;33(2):99-108. doi:10.1007/s12928-016-0448-3

10.   Sonck J, Collet C, Mizukami T, et al. Motorized fractional flow reserve pullback: Accuracy and reproducibility. *Catheter Cardiovasc Interv*. Sep 1 2020;96(3):E230-e237. doi:10.1002/ccd.28733

11.   Rajkumar CA, Shun-Shin M, Seligman H, et al. Placebo-Controlled Efficacy of Percutaneous Coronary Intervention for Focal and Diffuse Patterns of Stable Coronary Artery Disease. *Circulation Cardiovascular interventions*. Aug 3 2021:Circinterventions120009891. doi:10.1161/circinterventions.120.009891

12.   Johnson NP, Johnson DT, Kirkeeide RL, et al. Repeatability of Fractional Flow Reserve Despite Variations in Systemic and Coronary Hemodynamics. *JACC Cardiovascular interventions*. Jul 2015;8(8):1018-1027. doi:10.1016/j.jcin.2015.01.039

13.   Biscaglia S, Uretsky B, Barbato E, et al. Invasive Coronary Physiology After Stent Implantation: Another Step Toward Precision Medicine. *JACC Cardiovascular interventions*. Feb 8 2021;14(3):237-246. doi:10.1016/j.jcin.2020.10.055

14.   Candreva A, Mizukami T, Sonck J, et al. Hyperemic hemodynamic characteristics of serial coronary lesions assessed by pullback pressure gradients. *Catheter Cardiovasc Interv*. Jul 15 2021;doi:10.1002/ccd.29868
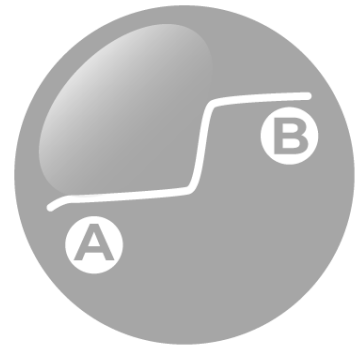
Chapter 2. Hyperemic hemodynamic characteristics of serial coronary lesions assessed by pullback pressure gradients.

Candreva A, Mizukami T, Sonck J, Munhoz D, Nagumo S, Di Gioia G, Gallinoro E, Mileva N, Bartunek J, Wyffels E, Barbato E, De Bruyne B, Perera D, Collet C.

Abstract

Objectives

To characterize hemodynamics of serial coronary stenoses using fractional flow reserve (FFR) pullbacks and the pullback pressure gradients (PPG) index.

Background

The cross-talk between stenoses within the same coronary artery makes the prediction of the functional contribution of each lesion challenging.

Methods and results

One-hundred seventeen patients undergoing coronary angiography for stable angina were prospectively recruited. Serial lesions were defined as two or more narrowings with visual diameter stenosis >50% on conventional angiography. Motorized FFR pullback tracings were obtained at 1 mm/s. Pullbacks were visually adjudicated as presenting two, one, and no focal pressure drops. The pattern of disease (i.e., focal or diffuse) was quantified using the PPG index. Twenty-five vessels presented serial lesions (mean PPG 0.48 ± 0.17). Two, one or no focal pressure drops were observed in 40% ($n = 10$; PPG 0.59 ± 0.17), 52% ($n = 13$; PPG 0.44 ± 0.12) and 8% of cases ($n = 2$; PPG 0.27 ± 0.01; p-value = 0.01). Distal FFR was similar between vessels with two, one and no focal pressure drops in the pullback curve (p-value = 0.27). The PPG index independently predicted the presence of two focal pressure drops in the pullback curve ($p = 0.04$).

Conclusions

FFR pullbacks in serial coronary lesions exhibit three distinct functional patterns. High PPG was associated with pullback curves presenting two pressure drops. The PPG provides a quantitative assessment of the pattern of coronary artery disease in cases with serial lesions and might be useful to assess the appropriateness of percutaneous revascularization.

Introduction

The presence of more than one stenosis within the same coronary artery is common.[1] These serial stenoses often represent a physiological conundrum because of the interaction (cross talk) between the different stenoses. This prevents merely summing up the transstenotic pressure gradients taken in isolation.[2] As a consequence, isolating the functional contribution of each lesion in a serial circuit either in resting or hyperemic conditions remains challenging.[3]

Traditionally, serial lesions have been defined based on coronary angiography.[4] Nonetheless, this approach neglects the known discordance between angiographic stenosis and its physiological effect, which is further affected by the distance between the stenoses and the microcirculatory function.[5] Intracoronary pressure pullbacks are essential to understand the physiological effect of serial lesions.[3, 6] The idealized model is represented by a pressure curve with two focal pressure drops in a pullback curve. Nonetheless, vessels with angiographic serial lesions might also present diffuse pressure losses without evident drops.[6]

The pullback pressure gradient (PPG) index quantifies the functional pattern of coronary artery disease (CAD) as either focal or diffuse. Values close to one represent focal CAD whereas values close to zero characterize diffuse CAD.[6] The PPG index lumps a metric of focality (i.e., maximal pressure gradient over 20 mm) with a metric of diffuseness (i.e., length of functional disease) and may aid in defining the pattern of disease in vessels with serial lesions. The present study aims at characterizing the functional pattern of CAD in vessels with serial lesions using mechanized FFR pullbacks and the PPG.

Materials and Method

Study design

This was a prospective, multicenter registry (NCT03824600) enrolling patients undergoing clinically indicated coronary angiography. A complete study description was presented elsewhere.[6] The study was approved by the investigational review board or ethics committee at each participating center, and all patients gave written informed consent.

Briefly, FFR measurements during continuous intravenous adenosine infusion at a dose of 140 mg/kg/min were obtained for coronary lesions with 30%–70% diameter stenosis.[7] Vessels with distal FFR ≥0.95 were considered without functional disease and excluded from the study. Motorized FFR pullback curves were collected in all studied patients by withdrawing at the controlled speed of 1 mm/s the pressure wire sensor (PressureWire X, St. Jude Medical, Minneapolis, MN) up to the tip of the guiding catheter. Quantitative coronary angiography (QCA) and FFR pullback tracings were co-registered.

An independent core laboratory (CoreAalst BV, Aalst, Belgium) analyzed coronary angiogram using a validated software package (CAAS Workstation 8.1, Pie Medical Imaging, Maastricht, The Netherlands). Serial lesions were angiographically defined as the presence of two or more narrowings with visual diameter stenosis >50%, separated at least by three times the reference vessel diameter in the same coronary vessel.[4] The distance between proximal and distal lesion was assessed in mm from the distal edge of the proximal lesion up to the proximal edge of the distal lesion.

FFR pullback curves were visually adjudicated by two independent observers (C.C. and J.S.) as presenting no pressure drop ("no drop"), one pressure drop ("one drop") and two pressure drops ("two drops"), see Figure 1. The presence of pressure drops was defined visually as step ups in the FFR curve of at least five FFR units in <20 mm. In addition, pressure drops were quantified as the maximal FFR gradient over 20 mm of length. The length of functional disease was defined as the length, in millimeters, with FFR drop ≥ 0.0015/mm. Trans-stenotic difference in FFR (delta lesion FFR) was determined. The PPG index was calculated as previously described.[6] The study was approved by the investigational review board or ethics committee at each participating center. Signed informed consent was obtained by all enrolled patients.

Serial lesions were independently adjudicated by visual inspection of patients coronary angiograms (upper panels) as presenting two or more narrowings (arrows) with visual diameter stenosis >50%, separated at least by three times the reference vessel diameter in the same coronary vessel. In turn, the visual analysis of the pullback pressure gradients (PPG) tracings was used to categorized the pressure drop patterns along the vessel presenting a serial lesion, thus resulting in three patterns (lower panels): absence of focal drops (left), presence of only one focal drop, either proximally or distally, (central panel), and presence of two focal pressure drops (right). FFR, fractional flow reserve; PPG, pullback pressure gradient

Statistical analysis

For the present study, vessels were considered independent observations. Continuous variables with normal distribution are presented as mean $\pm$ SD and non-normally distributed variables as median (interquartile range [IQR]). Categorical variables are presented as percentages. Chi-squared tests were used for comparing categorical variables, while Student's *t* (or Mann–Whitney tests as appropriate) for continuous ones. The one-way analysis of variance (or Kruskal–Wallis tests) was used for comparing more than two continuous variables. Interobserver agreement for the visual functional pattern adjudication was assessed with the Cohen's kappa method. Finally, anatomical and functional variables of interest were

entered into a multivariate model. A p-value <0.05 was considered significant. All statistical analyses were performed using R statistical software (R Foundation for Statistical Computing, Vienna, Austria).

Results

Between November 2017 and January 2019, 85 vessels from 72 patients presented at least one functionally significant lesion. Among these, 25 vessels from 23 patients presented serial lesions and were included in the present study (Figure 2). Motorized FFR pullbacks and PPG index were obtained in all cases. In all but one case, two stenoses were angiographically identifiable, and in one case, three. We included 51 stenoses in the final analysis.

Baseline characteristics

Clinical, angiographic and functional characteristics at baseline are listed in Table 1. Mean age was 68.7 ± 8.2 years, males in 90.9%, and multivessel disease was present in 73.9%. Mean diameter stenosis was 46.4 ± 15.6%, minimal lumen area 1.36 ± 0.45 mm^2 and mean lesion length was 22.8 ± 10.5 mm. Mean distal FFR was 0.77 ± 0.07 and 72% of the vessels had an FFR ≤0.80. Functional disease was observed in 53.5 ± 20.6% of the vessel length and the mean maximal pressure gradient over 20 mm was 0.10 (IQR 0.07–0.14) FFR units.

The distance between proximal and distal lesion was 55.5 ± 26.0 mm. The angiographic severity of the proximal and distal lesions was comparable (diameter stenosis 44.8 ± 15.5% proximal vs. 48.0 ± 16.2% distal, $p = 0.49$), Table 2. Lesion length was longer for the distal lesions (20.0 ± 8.8 mm proximal vs. 26.2 ± 10.9 mm distal, $p = 0.03$). Translesional FFR gradient was comparable between proximal and distal lesions (0.08 ± 0.06 proximal vs. 0.08 ± 0.04 distal, $p = 0.88$).

In comparison with vessels presenting a single lesion, vessels with serial lesion by angiography had a lower distal FFR (0.83 ± 0.07 vs. 0.77 ± 0.08, $p = 0.001$), longer functional disease (33.3 ± 19.1 mm vs. 53.5 ± 19.9 mm, $p < 0.001$), and lower PPG index (0.61 ± 0.17 vs. 0.48 ± 0.17, $p = 0.002$), Table 3.

Functional patterns of CAD

Visual assessment of the FFR pullback curves resulted in two vessels (8%) presenting no pressure drop, 13 (52%) vessels presenting one drop and 10 (40%) vessels two pressure drops, Figure 3. These three functional disease phenotypes had similar baseline clinical characteristics, Table S1. Mean distal FFR values were similar between vessels with no visible pressure curve drops, one or two drops (0.77 ± 0.02 vs. 0.74 ± 0.10 vs. 0.80 ± 0.06, $p = 0.27$, respectively), Table 4. PPG was significantly higher in vessels with two pressure drops versus one pressure drop and no pressure drop ($p = 0.01$, Figure 4). Multivariate analysis showed that

the PPG index was the only independent predictor ($p = 0.04$) of an FFR pullback curve presenting two pressure drops (Table 5). An increment of 0.1 PPG unit was associated with doubled the odds for the two-drop functional phenotype (OR = 2.3 95% CI 1.2–5.6, $p = 0.02$).

3.3 Procedural characteristics

All coronary arteries with serial lesions and distal FFR ≤0.80 were revascularized (Table S2). PCI was performed in 52.0% and coronary artery bypass graft in 24.0%. In patients undergoing PCI, two stents were placed in 61.5% of PCI cases.

Discussion

The present study describes the physiological patterns observed in vessels with serial coronary stenoses utilizing motorized pullback pressure tracings during pharmacological induced hyperemia. The main findings can be summarized as follows: (i) significant functional disease is frequent in cases of angiographic serial coronary lesions; (ii) at the lesion level, diameter stenosis and trans-stenotic FFR gradients were comparable between proximal and distal lesions; (iii) three distinct functional phenotypes were observed, that is, diffuse functional disease without FFR step-ups, FFR pullback curves with one step-up and FFR pullback curves with two step-ups; (iv) the functional pattern with two pressure drops was identified by the PPG index, the higher the PPG index the higher the likelihood of FFR pullback curves with two step-ups.

In this way, the present study expands on the application of the recently introduced PPG index[6] providing a further validation of the index in patients with serial coronary lesions.

Serial lesions: A complex CAD phenotype

Patients presenting serial coronary lesions represent a population with advanced CAD[1] in which treatment strategies can be challenging. Firstly, while the decision to treat the vessel can be based on the distal FFR measurement,[8, 9] the decision of which lesion to treat is less evident. Secondly, when decided to treat one of the two lesions either based on anatomically severity or the lesion with the greatest pressure drop at the pullback curve, the resulting post-PCI FFR can be difficult to be estimated. In fact, increased flow conditions interact with the residual disease, potentially leading to higher pressure gradients,[10] as demonstrated with both hyperemic and resting pressure-based indices.[3]

In the present analysis, proximal and distal lesions appeared comparable in terms of angiographic severity, and the magnitudes of apparent pressure drops. Similarly, at the vessel level, the distal FFR was not able to differentiate functional patterns. In contrast, FFR pullback tracings discriminate three functional CAD patterns based on the presence of one, two or absence of focal pressure drops.[10]

Application of pressure pullbacks and PPG index in serial lesions

Clinically, identification of a step-up in a pullback pressure curve is an essential element in the decision-making process concerning the appropriateness of PCI. Despite whatsoever angiographic appearance, PCI in segments without pressure losses or step-ups results in negligible increase in epicardial conductance. In contrast, the presence of a step-up may translate in clinical benefit of PCI in terms of gain in conductance.[11] In serial lesions, an FFR pullback-guided revascularization strategy was found safe and effective, while minimizing unnecessary coronary interventions.[8]

The results of the present study highlight the usefulness of the FFR pullbacks in cases of serial lesions (i) to define the pattern of functional CAD, (ii) to assess the appropriateness of percutaneous revascularization, and (iii) to guide the PCI strategy. The PPG index was higher in vessels exhibiting a functional pattern of disease with two pressure drops and emerged as the only independent predictor of FFR pullbacks curves with two pressure drops. This could be analytically explained by the length of functional disease, component of the PPG formula, that was significantly lower in the serial lesion phenotype with two pressure drops, Figure 5. The PPG index was able to inform about functional pattern with two focal pressure drops. Therefore, it can be hypothesized that in vessels with serial lesions and high PPG value, PCI may translate in higher post-PCI FFR. This hypothesis warrants further investigation.

Study limitations

Small sample size and lack of a clinical outcome analysis represent the major limitations to the current study. Moreover, in the cases undergoing PCI, FFR after PCI was not collected. In addition, clinical applicability of motorized FFR pullback with long hyperemic times is questionable. Further limitations of the present study – including feasibility of the PPG derivation by motorized hyperemic pullback – were discussed previously.[6]

Conclusion

Serial coronary lesions represent a population of interest with advanced CAD. Physicians are challenged to whether or not, and which lesion to treat with PCI. Increasing evidence supports the usefulness of pullback pressure tracings to better understand the functional pattern of CAD.

The present study further informs about the clinical value of FFR pullback maneuvers in the clinical routine, offering a pathophysiological classification of serial coronary lesions based on pullback tracings (no drop, one drop, two drops). Each of these patterns may justify a diverse therapeutic management.

In addition, the PPG index, a novel physiology metrics able to characterize CAD patterns, identified serial coronary lesions with two focal drops. This serial-lesion functional

phenotype might be the best suited for PCI. Future studies should address the impact on a PPG guided PCI strategy on outcomes in serial coronary lesions.

TABLE 1. Baseline clinical, angiographic, and physiological characteristics (patient $N = 23$)

Clinical characteristics	
Male, n(%)	20 (90.9)
Age, years	68.74 ± 8.18
BMI, kg/m²	28.26 ± 4.38
CCS ≥ 2, n(%)	15 (65.22)
MVD, n(%)	17 (73.91)
LVEF, %	57.61 ± 6.19
CrCl, ml/min	77.32 ± 22.71
Hypertension, n(%)	17 (73.91)
Diabetes mellitus, n(%)	9 (39.13)
- Under insulin, n(%)	1 (4.35)
Hyperlipidaemia, n(%)	22 (95.65)
Family history for CAD, n(%)	3 (13.04)
Active smoking status, n(%)	0 (0.0)
Previous PAD, n(%)	1 (4.35)
Previous CVI, n(%)	2 (8.70)

Previous PCI, *n*(%)	7 (30.43)
Previous MI, *n*(%)	3 (13.05)
Angiographic characteristics	
Vessels presenting serial lesions	25
LAD, *n*(%)	18 (72.0)
LCX/Ramus, *n*(%)	4 (16.0)
RCA, *n*(%)	3 (12.0)
Quantitative coronary angiography	
Lesions	51[a]
Diameter stenosis, %	46.43 ± 15.62
Minimal lumen area, mm^2	1.36 ± 0.45
Reference vessel diameter, mm	2.58 ± 0.65
Lesion length, mm	22.83 ± 10.46
Distance from ostium to proximal stenosis, mm	33.22 ± 23.51
Distance between proximal and distal stenoses, mm	55.51 ± 25.96
QCA tracing contour correction	10.18 ± 7.92
Functional characteristics	

Vessels presenting serial lesions	25
Distal FFR	0.77 ± 0.07
Distal FFR ≤0.80	18 (72.0)
Delta lesion FFR	0.16 ± 0.08
Proximal FFR (drift)	0.99 ± 0.01
Pullback length, mm	98.6 ± 20.81
PPG index	0.48 ± 0.17
Maximal PPG over 20 mm	0.099 (0.072–0.141)
Vessel length with functional disease, mm	53.52 ± 20.57
Percent vessel length with functional disease, %	54 ± 18

[a] One vessel presented three serial lesions. The third lesion in this vessel was not included in the analysis.

Note: Values are *n* (%), mean ± SD, *n*, or median (interquartile range).

Abbreviations: BMI, body mass index; CAD, coronary artery disease; CCS, Canadian Cardiovascular Society classification of angina; CrCl, creatinine clearance; CVI, cerebrovascular injury; FFR, fractional flow reserve; MVD, multivessel disease; LAD, left anterior descending artery; LCX, left circumflex artery; LVEF, left ventricle ejection fraction; MI, myocardial infarction; PAD, peripheral artery disease; PCI, percutaneous coronary intervention; PPG, pullback pressure gradients; QCA, quantitative coronary angiography; RCA, right coronary artery.

TABLE 2. Anatomical and functional characteristics at lesion level (lesion $N = 50$[a])

	Proximal lesion	Distal lesion	p-value (two-tailed)
Lesions	25	25	-
Diameter stenosis, %	44.84 ± 15.47	47.96 ± 16.24	0.490
- Minimal lumen area, mm^2	1.36 ± 0.45	1.12 ± 0.33	< 0.001
- Reference vessel diameter, mm	2.98 ± 0.62	2.21 ± 0.38	< 0.001
Lesion length, mm	20.05 ± 8.82	26.24 ± 10.94	0.032
Distance from ostium to proximal edge of the lesion, mm	17.90 ± 14.26	47.03 ± 21.14	< 0.001
Delta lesion FFR	0.08 ± 0.06	0.08 ± 0.04	0.885
QCA tracing contour correction	9.72 ± 8.58	10.72 ± 7.51	0.063

[a] One vessel presented three serial lesions. In this case, the lesion more distally located was excluded from the analysis.

TABLE 3. Comparison of angiographical and functional characteristics for vessels presenting a visually defined single lesion versus serial lesions

	Single lesion (vessel $N = 60$)	Serial lesion (vessel $N = 25$)	p-value (two-tailed)
Diameter stenosis, %	45.5 ± 13.07	46.5 ± 10.9	0.73
Vessel length with functional disease, mm	33.3 ± 19.1	53.5 ± 19.9	< 0.001
Distal FFR	0.83 ± 0.07	0.77 ± 0.08	0.001
FFR≤0.80	19.0 (31.7%)	18.0 (72.0%)	< 0.001
Pullback length, mm	99.0 ± 19.1	98.6 ± 20.0	0.93
Maximal PPG over 20 mm	0.10 (0.05–0.12)	0.12 (0.07–0.13)	0.22
PPG Index	0.61 ± 0.17	0.48 ± 0.17	0.002

TABLE 4. Angiographic and functional characteristics of interest stratified by functional class (vessel $N = 25$)

Functional pressure pullback pattern			
	No drop ($N = 2$)	**One drop ($N = 13$)**	**Two drops ($N = 10$)** **p-value (two-tailed)**
Diameter stenosis, %	37.2 ± 6.72	44.3 ± 11.4	51.2 ± 9.3	0.15
Distal FFR	0.77 ± 0.02	0.74 ± 0.1	0.80 ± 0.06	0.27
PPG Index	0.27 ± 0.01	0.44 ± 0.12	0.59 ± 0.17	0.01
Max. pressure drop over 20 mm	0.07 (IQR 0.06–0.07)	0.12 (IQR 0.07–0.13)	0.12 (IQR 0.07–0.15)	0.37
Length of functional disease, mm	77.5 ± 4.95	60.8 ± 18.3	39.3 ± 13.2	0.003

TABLE 5. Uni- and multivariate analyses for the detection of pullback curves with two pressure drops

Variable	p-value
Univariate model	
Diameter stenosis (%)	0.08
Lesion length (mm)	0.79
PPG index	0.02
Multivariate model	
Diameter stenosis (%)	0.22
Lesion length (mm)	0.47
PPG index	0.04

- Abbreviation: AIC, akaike information criterion.

Figure 1

Serial lesions were independently adjudicated by visual inspection of patients coronary angiograms (upper panels) as presenting two or more narrowings (arrows) with visual diameter stenosis >50%, separated at least by three times the reference vessel diameter in the same coronary vessel. In turn, the visual analysis of the pullback pressure gradients (PPG) tracings was used to categorized the pressure drop patterns along the vessel presenting a serial lesion, thus resulting in three patterns (lower panels): absence of focal drops (left), presence of only one focal drop, either proximally or distally, (central panel), and presence of two focal pressure drops (right). FFR, fractional flow reserve; PPG, pullback pressure gradient

Figure 2

Flowchart of the patients included in the study. Twenty-five vessels of 23 patients were adjudicated to present a serial lesion consisting of at least two stenosis (three in one case). In all cases, valid pullback pressure gradient tracings for the digital postprocessing and analysis were successfully performed. FFR, fractional flow reserve
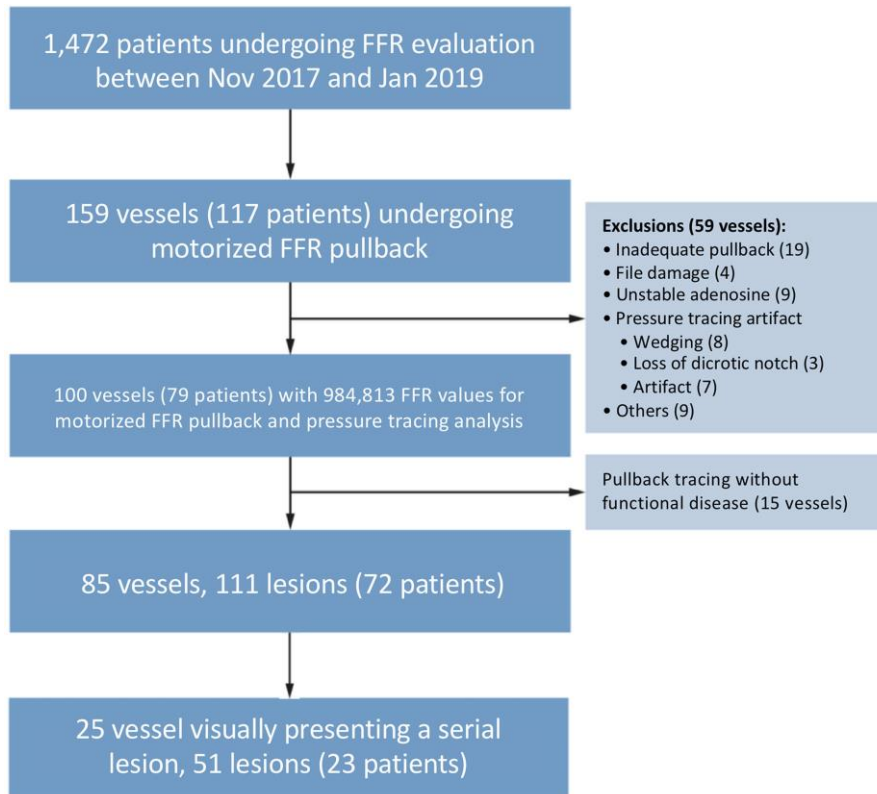
Figure 3

Flowchart of the patients included in the study. Twenty-five vessels of 23 patients were adjudicated to present a serial lesion consisting of at least two stenosis (three in one case). In all cases, valid pullback pressure gradient tracings for the digital postprocessing and analysis were successfully performed. FFR, fractional flow reserve
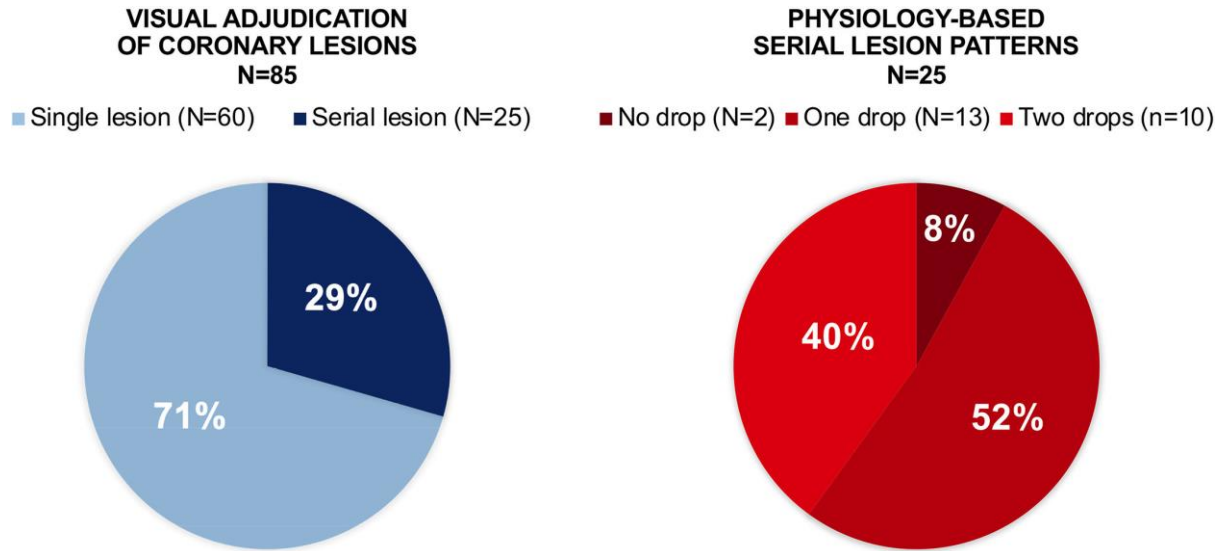
Figure 4

Distributions of the fractional flow reserve (left panel) and pullback pressure gradient index (right panel) according to the adjudicated functional pattern, underlining the inability for the distal FFR to capture difference among the three functional patterns. On the other hand, higher PPG index values were significantly associated with the two focal serial lesion pattern. FFR, functional flow reserve; PPG, pullback pressure gradient
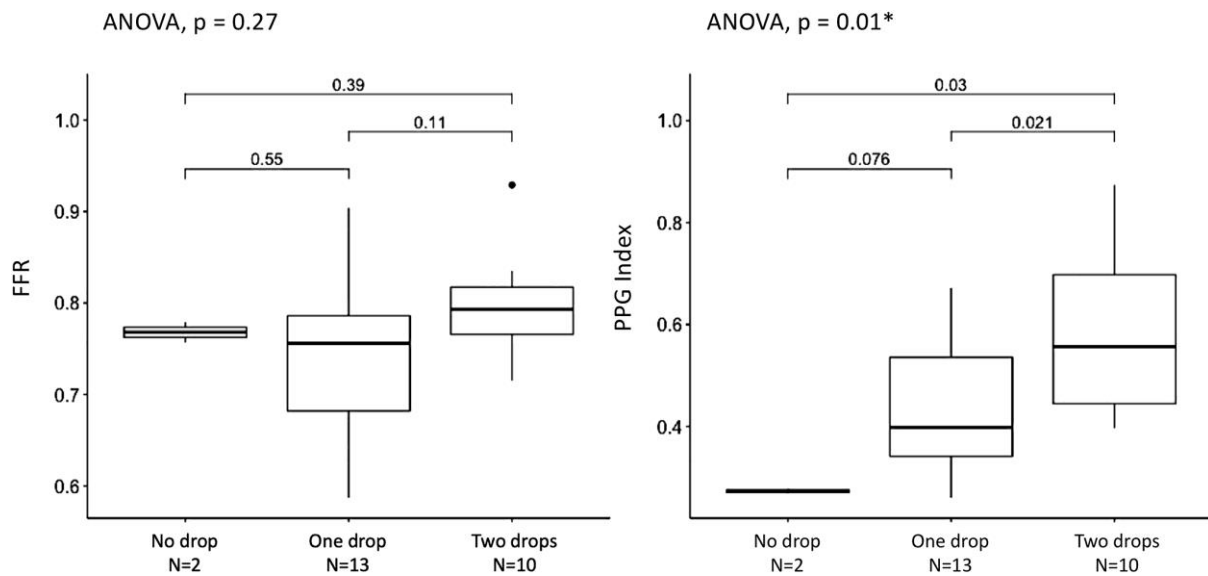
Figure 5

Distribution of two components of the pullback pressure gradient index equation, namely the maximal pressure gradients over 20 mm (left panel) and the length of functional disease (right panel), according to the three functional disease patterns. While the max PPG over 20 mm mean did not differ significantly between the groups, serial lesion presenting two pressure stenoses were significantly associated with shorter diseased vessel segments. KW, Kruskal–Wallis; ANOVA, (one way) analysis of variance
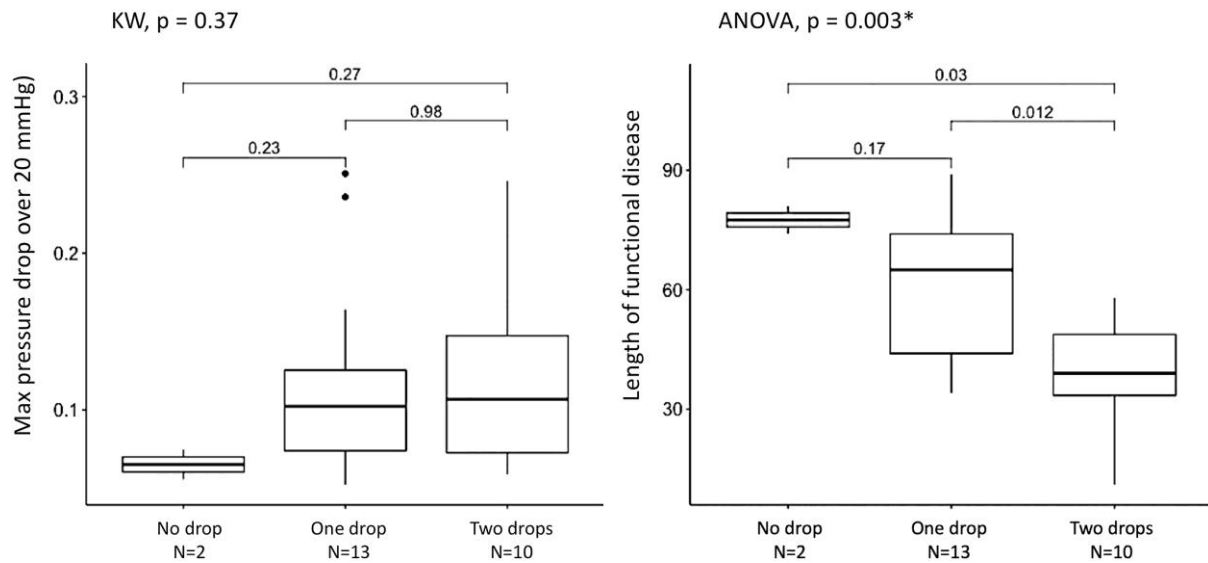
REFERENCES

1. Humphries JO, Kuller L, Ross RS, Friesinger GC, Page EE. Natural his-tory of ischemic heart disease in relation to arteriographic findings: atwelve year study of 224 patients. Circulation. 1974;49(3):489-497.

2. Siyeong J, Gu L. Hemodynamic interference of serial Stenoses and itsimpact on FFR and iFR measurements. Appl Sci. 2019;9:279.

3. Modi BN, Rahman H, Ryan M, et al. Comparison of fractional flowreserve, instantaneous wave-free ratio and a novel technique for assessing coronary arteries with serial lesions. EuroIntervention.2020;16(7):577-583.

4. Sianos G, Morel MA, Kappetein AP, et al. The SYNTAX score: anangiographic tool grading the complexity of coronary artery disease.EuroIntervention. 2005;1(2):219-227.

5. De Bruyne B, Pijls NH, Heyndrickx GR, Hodeige D, Kirkeeide R,Gould KL. Pressure-derived fractional flow reserve to assess serialepicardial stenoses: theoretical basis and animal validation. Circula-tion. 2000;101(15):1840-1847.

6. Collet C, Sonck J, Vandeloo B, et al. Measurement of hyperemicpullback pressure gradients to characterize patterns of coronary ath-erosclerosis. J Am Coll Cardiol. 2019;74(14):1772-1784.

7. Toth GG, Johnson NP, Jeremias A, et al. Standardization of fractionalflow reserve measurements. J Am Coll Cardiol. 2016;68(7):742-753.

8. Kim HL, Koo BK, Nam CW, et al. Clinical and physiological outcomesof fractional flow reserve-guided percutaneous coronary interventionin patients with serial stenoses within one coronary artery. JACCCardiovasc Interv. 2012;5(10):1013-1018.

9. Pijls NH, De Bruyne B, Bech GJ, et al. Coronary pressure measure-ment to assess the hemodynamic significance of serial stenoseswithin one coronary artery: validation in humans. Circulation. 2000;102(19):2371-2377.

10. Modi BN, De Silva K, Rajani R, Curzen N, Perera D. Physiology-guidedManagement of Serial Coronary Artery Disease: a review. JAMA Cardiol. 2018;3(5):432-438.

11. Lee SH, Shin D, Lee JM, et al. Automated algorithm using pre-intervention fractional flow reserve pullback curve to predict post-intervention physiological results. JACC Cardiovasc Interv. 2020;13(22):2670-2684.
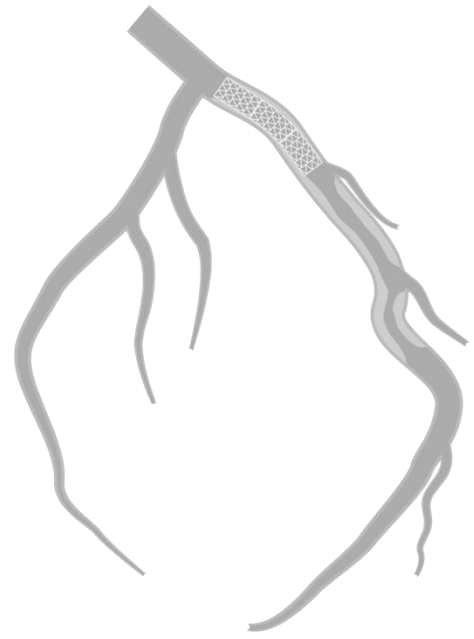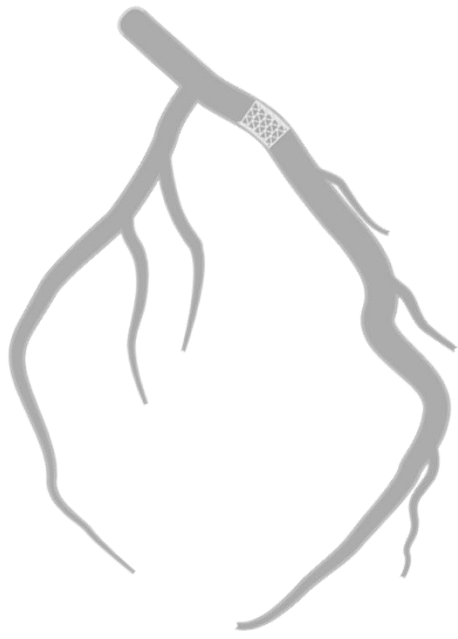
Part C.

Post-PCI FFR as a predictor of PCI success
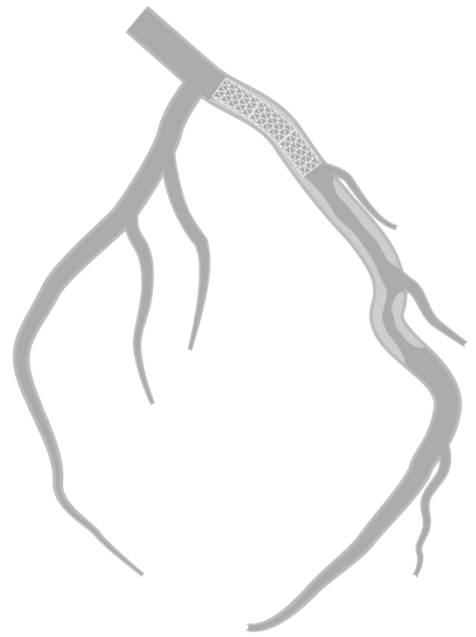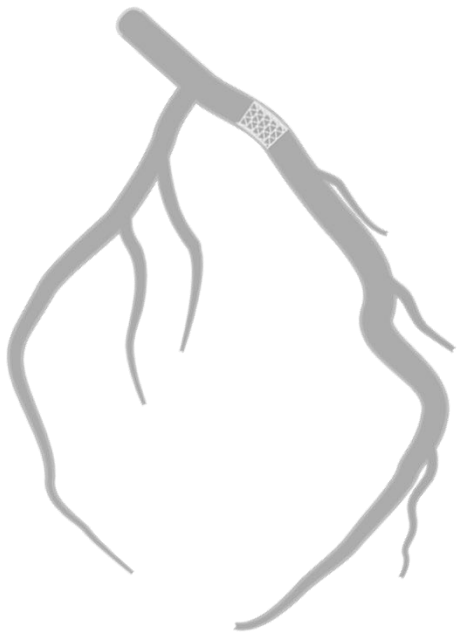
Chapter 3. Relationship between coronary volume, myocardial mass, and post-PCI fractional flow reserve

Mileva N, Ohashi H, Paolisso P, Leipsic J, Mizukami T, Sonck J, Norgaard BL, Otake H, Ko B, Maeng M, Munhoz D, Nagumo S, Belmonte M, Vassilev D, Andreini D, Barbato E, Koo BK, De Bruyne B, Collet C.

Abstract

Background: FFR measured after PCI carries prognostic information. Yet, myocardial mass subtended by a stenosis influences FFR. We hypothesized that a smaller coronary lumen volume and a large myocardial mass might be associated with lower post-PCI FFR.

Aim: We sought to assess the relationship between myocardial mass and post percutaneous coronary intervention (PCI) fractional flow reserve (FFR).

Methods: This was a sub-analysis with an international prospective study of patients with significant lesions (FFR≤0.80) undergoing PCI. Territory-specific myocardial mass was calculated from coronary computed tomography angiography (CCTA) using a novel algorithm. Vessel volume was extracted from quantitative CCTA analysis. Resting full-cycle ratio (RFR) and FFR were measured before and after PCI. Coronary lumen volume (V) and its related myocardial mass (M), and the percent of total myocardial mass (%M) were correlated with post-PCI FFR.

Results: We studied 120 patients (123 vessels: 94 LAD, 13 LCX, 16 RCA). Mean vessel-specific mass was 61 ± 23.1 g (%M 39.6 ± 11.7%). The mean post-PCI FFR was 0.88 ± 0.06 FFR units. Post-PCI FFR values were lower in vessels subtending higher mass (0.87 ± 0.05 vs 0.89 ± 0.07, p=0.047), and in vessels with lower V/M ratio (0.87 ± 0.06 vs 0.89 ± 0.07, p=0.02). V/M ratio correlated significantly with post-PCI RFR and FFR (RFR r=0.37, 95% CI 0.21-0.52 p<0.001 and FFR r=0.41, 95% CI 0.26-0.55, p<0.001).

Conclusion: Post-PCI RFR and FFR are associated with the subtended myocardial mass and the coronary volume to mass ratio. Vessels with higher mass and lower V/M ratio have lower post-PCI RFR and FFR.

Introduction

In coronary arteries, discordance between the angiographic degree of stenosis and its functional severity is common. [1]Aside from stenosis severity, several other co-variables influence FFR such collateral flow, microvascular function and the myocardial mass subtended by the vessel. For a given coronary morphology, a higher mass translates into higher coronary blood flow which, in turn, generate larger pressure gradients. Therefore, myocardial mass is one of the determinants of fractional flow reserve (FFR).[2] Myocardial mass and its relationship with vessel volume, the so-called volume mass (V/M) ratio, have been associated with lower FFR values. [3-5]Furthermore, V/M mismatch has been proposed as a possible cause of ischemia in patients with non-obstructive coronary arteries (INOCA). [6]

Post-PCI FFR is considered a physiological prognostic marker. Patients with low post-PCI FFR have been shown to have a worse prognosis compared to higher post-PCI FFR values. [7,8]Post-PCI FFR might be also affected by the subtended myocardial mass. Yet, after PCI there are additional procedural related factors that might not present at baseline (e.g. distal embolization, iatrogenic coronary microvascular dysfunction, etc.). There is no data assessing the relationship between myocardial mass and post-PCI FFR.

Assessing myocardial mass in clinical practice has been facilitated by the advancement in the field of cardiac CT. Recently, dedicated algorithms have been developed to quantify the vessel-specific mass based on coronary computed tomography angiography (CCTA). [4,9,10]Moreover, CCTA provides lumen volume calculations. Thus, V/M ratio is a metric that is readily available from CCTA scans. We hypothesized that the vessel-specific myocardial mass, as well as the ratio of the coronary lumen volume to the vessel-specific myocardial mass (V/M), may influence FFR after PCI.

Material and methods

Study population

This is a sub-analysis of the Prospective Evaluation of a Virtual Non-invasive Percutaneous Intervention Planner in Patients with Coronary Artery Disease: Precise PCI Plan (P3) study. The design and results of this study have been described in detail previously. [11]Briefly, the P3 study was an investigator-initiated, controlled, multicentre, prospective study of patients with chronic coronary syndromes referred for PCI. Patients with CCTA performed within the standard of care showing a significant epicardial lesion and an invasive FFR measurement ≤0.80 were included. Patients underwent a PCI protocol guided by optical coherence tomography (OCT) with pre-and post-stent FFR evaluations. Patients with severely

calcified vessels, bifurcation or ostial lesions, left main disease, severe vessel tortuosity, previous revascularization, and atrial fibrillation were excluded. The study protocol was approved by the investigational review board or ethics committee at each participating centre. All patients signed informed consent before the study procedures. The protocol was registered as NCT03782688.

Invasive procedure and FFR measurements

Coronary angiograms were acquired in two projections separated at least by 30 degrees after administering intracoronary nitro-glycerine. Three-dimensional quantitative coronary angiography (3D-QCA) was performed before and after PCI using a validated software (CAAS 8.2, Pie Medical Imaging, Maastricht, the Netherlands). FFR measurements were performed following current recommendations. [12]A continuous intravenous adenosine infusion was given at a dose of 140 mg/kg/min via a peripheral or central vein to obtain steady-state hyperaemia for at least 2 min. If FFR drift (>0.03) was observed, the FFR was repeated. FFR was defined as the lowest ratio between distal and proximal coronary pressures during hyperaemia. Resting full-cycle ratio (RFR) was defined as the lowest distal coronary-to-aortic pressure value for each heartbeat averaged over five heart cycles and it was automatically calculated offline using CoroFlow version 3.6 (Coroventis Research, Uppsala, Sweden). OCT was performed after PCI using 75 mm pullbacks acquired using Dragonfly OPTIS Imaging Catheter (Abbott Vascular, St. Paul, MN, USA). An automated algorithm defined minimal stent area (MSA).

Coronary computed tomography angiography image acquisition and analyses

Coronary CTAs were performed using the latest generation CT scanners. Local imaging acquisition guidelines were followed with the recommendation for the use of nitrates prior to CT acquisition and beta-blockers in cases of heart rate higher than 65 b.p.m. [11,13]Target major epicardial coronary artery and its branches > 1.8 mm diameter were segmented, and vessel, lumen was quantified using a validated software (QAngio CT, Medis Medical Imaging, the Netherlands).[14] Coronary volume was normalized by vessel length (vessel volume/vessel length x 100). In order to reflect the lumen volume after PCI, the proximal and distal lumen diameter references were extrapolated mimicking the effects of PCI (Supplementary Figure S1).

Myocardial mass quantification

Vessel-specific myocardial mass was quantified from the CCTA images using Voronoi's algorithm with dedicated software (3D Synapse 3D, Fujifilm Healthcare Solutions, Holdings America Corporation).[9] Briefly, in Voronoi's algorithm voxel in the left ventricle (LV) myocardium is partitioned into perfusion volumes according to their distance to the

closest supplying coronary artery and then linked to the nearest voxel on the adjacent coronary artery. [10,15,16]Subsequently, the algorithm automatically calculates the territory by aggregating all myocardial voxels associated with the voxels of the coronary artery that are distal to the seed point. The software automatically provides the territory-specific myocardial mass volume and in percent of the LV mass. Myocardial mass gram is further obtained by multiplying the myocardial mass volume by the specific gravity of the myocardium (1.05 g/ml). [17,18]The values of vessel-specific myocardial mass, in grams (M), and the ratio of the M over the whole LV myocardial mass (%M) were used to assess the association with invasive physiology measurements. Furthermore, V/M ratio was defined as the ratio of normalized lumen volume, and the %M was calculated.

Study objectives

The primary objective was to evaluate the association between the vessel-specific myocardial mass and V/M ratio with post-PCI FFR.

Statistical analysis

Continuous variables with normal distribution are presented as mean ± SD and non-normally distributed variables as median (interquartile range). Categorical variables are presented as counts and percentages. Patients were stratified according to the median V/M value. The T-tests were used to compare the difference between these groups. Pearson's test was performed to assess for correlation between myocardial mass, V/M ratio and post-PCI FFR. Regression analysis was performed to adjust the relationship between V/M ratio and post-PCI FFR for minimal stent area, and residual diameter stenosis by 3D-QCA. A p-value <0.05 was considered statistically significant. All statistical analyses were performed with the use of R statistical software (R Foundation for Statistical Computing, Vienna, Austria).

Results

Patient and lesion characteristics

Overall, 132 patients and 135 vessels were included. After exclusion of cases with suboptimal CCTA quality for analysis, the final population consisted of 120 patients (123 vessels, 94 LAD, 13 LCX, 16 RCA; Supplemental Material Figure S2). The mean age was 64.3±9.9 years, 79% were male and 24% had diabetes. Patients' demographic and baseline data stratified by V/M are shown in **Table 1**. Baseline lesion and physiological characteristics are shown in **Table 2**. The majority of lesions (**75.7%**) were located in the left anterior descending (LAD) coronary artery. The mean baseline FFR was 0.66±0.13. The mean value of vessel-specific M was 61.0±23.1 g (median 59.1 g [IQR 44.3 to 72.4]). The mean value of V/M ratio was 8.2±4.6 (median 7.5 [IQR 5.3 to 9.4]).

The relationship between myocardial mass and baseline RFR and FFR is shown in Supplemental Material Figure S3. There were no differences in pre-PCI FFR or RFR in patients with high or low V/M (**Table 2**). Among patients with a low V/M ratio, there were significantly more LAD as compared to cases with high V/M ratio. Moreover, V/M ratio was significantly lower in the LAD compared to non-LAD (4.97±1.3 vs 7.70±2.1, p-value<0.001) whereas %M was significantly higher in LAD as compared to non-LAD (42.8±10.3% vs 29.4±10.2%, p<0.001). The mean V/M ratio was significantly lower for the LAD compared to RCA and LCx (7.1±3.3 LAD vs. 13.0±7.3 RCA vs. 10.6±3.7 LCx, p<0.001). Two representative cases with high and low V/M ratio are shown in **Figure 1**.

Myocardial mass, V/M ratio and post-PCI FFR

The mean post-PCI RFR and FFR were 0.92±0.05 and 0.88±0.06 units, respectively. The distribution of post-PCI pressure ratios shown in **Figure 2**. The vessels subtending higher %M had similar RFR (0.91±0.04 high %M vs. 0.92±0.06 low %M, p=0.178) and lower post-PCI FFR compared to vessels with lower %M FFR 0.87±0.05 high %M vs. 0.89±0.07 low %M, p=0.047; **Figure 3**). %M, as continuous variable, was negatively and significantly correlated with post-PCI RFR and FFR (r=-0.25, CI 95% -0.41 to -0.07, p=0.006 and r=-0.35, CI 95% -0.18 to -0.19, p<0.001). Vessels with low V/M had lower post-PCI RFR and FFR (RFR 0.91±0.05 low V/M vs. 0.93±0.05 high V/M, p-value=0.04 and FFR 0.87±0.06 low V/M vs 0.89±0.07 high V/M, p=0.02) and V/M, as a continuous variable, was significantly correlated with both post-PCI RFR and FFR (RFR r=0.37, 95% CI 0.21-0.52 p<0.001 and FFR r=0.41, 95% CI 0.26-0.55, p<0.001; **Figure 4**). The association of V/M with post-PCI FFR was independent of residual diameter stenosis (by QCA) and OCT-minimum stent area (point estimate 0.006; 95% CI: 0.003 to 0.008; p< 0.001 and point estimate 0.006; 95% CI: 0.003 to 0.008; p< 0.001, respectively).

Discussion

The findings of the present study can be summarized as follows: After PCI, lower RFR and FFR values were found in vessels supplying a larger myocardial mass. The resultant low V/M suggests that pressure losses after successful PCI may arise, at least in part, due to a mismatch between coronary artery lumen volume and myocardial demand, a situation that was found particularly frequent in the LAD. The moderate association between mass and post-PCI resting and hyperaemic indexes was independent of residual stenosis.

Allometric scaling laws have been proposed to relate anatomic and physiologic variables to organism size. [19]These laws have also been applied to relate these variables to organ size. [20]The general form of the scaling law between organ perfusion and organ mass is

$Q \approx M^{3/4}$. In a porcine model, Choy et al. found a very tight relationship between myocardial flow and mass as well as between coronary artery volume and myocardial mass. [21]Accordingly, Taylor et al. have shown that patients with coronary artery disease have large variations in coronary artery volume and that FFR was significantly lower in arteries with a small vascular volume and perfusing a large myocardial mass, i.e. arteries with a small V/M ratio. [4]The V/M ratio, therefore, appears as a measure of the capability of the epicardial coronary arteries to supply blood according to the myocardial demand. It is important to note that the discrepancy in the V/M ratio may be one of the reasons for the observed different FFR values in the LAD versus non-LAD vessels. It has been confirmed that in regions with larger amount of myocardial mass (as the zones supplied by LAD) the absolute myocardial blood flow is greater than in regions supplied by RCA or LCX. [22-24]Thus, meaning, that in a condition of higher flow, coronary lesions with equal anatomical stenosis will produce a greater gradient and a lower FFR compared to those with lower flow. Furthermore, the RCA have higher lumen volume compared to the LAD due to the progressive physiologic tapering of the latter. [25]Consequently, our results are in accordance with evidence of smaller V/M ratio in the LAD compared to that in the non-LAD arteries. [26]It is noteworthy that previous studies assessed the association of V/M and FFR on a patient level. [4,27]To the best of our knowledge, our study is the first to assess the relationship between vessel-specific mass and resultant V/M ratio and post-PCI RFR and FFR. This was feasible thanks to the advent of dedicated mass extraction algorithms that can be applied to conventional CCTA. Vessel-specific V/M implies the association between blood supply and myocardial demand for each coronary vessel. The specific territory Voronoi's algorithm has been validated in the swine model and showed excellent accuracy in measuring myocardial mass at risk. Furthermore, Voronoi's CT-derived myocardial mass is highly reproducible and to correlate with the ischemic burden.

In the present study, resting and hyperemic pressure ratios after PCI were equally affected by the myocardial mass subtended by the vessel. The results of the present study suggest that post-PCI FFR should be interpreted by accounting for the subtended mass. In vessels with higher myocardial mass, post-PCI RFR and FFR were lower compared to vessels with lower subtended mass. Therefore, in vessels with large mass, predominantly represented by the LAD, lower RFR and FFR values should be expected. This was independent of residual disease assessed by diameter stenosis by 3D-QCA and MSA by OCT. Conversely, vessels with lower mass showed higher post-PCI RFR and FFR values.

Limitations

The present study has several limitations. First, most of the vessels included in our analysis are LAD, thus, the study was not powered to assess the variation in V/M ratio and its impact on post-PCI FFR across the different coronary arteries; we partly circumvent this issue by grouping the RCA and LCx and compared them to LAD. Second, by study design, all patients had a pre-PCI FFR ≤0.80; this selection criterion introduced bias for assessing the relationship between pre-PCI FFR and myocardial mass. Third, the coronary microvascular or collateral flow, were not available in the current analysis. Fourth, the correlation between myocardial mass and FFR described in the present study did not account for the potential effect of hydrostatic forces that inevitably affect LAD and non-LAD differently when sensored tip wires are used for the measurements. [28]Fifth, the presented observations are also not generalizable to patients with severely calcified vessels, bifurcation or ostial lesions, left main disease, patients with severe vessel tortuosity, history of previous revascularization or atrial fibrillation since these patients were excluded according to the study protocol.

Conclusion

Fractional flow reserve and non-hyperaemic pressure ratios after PCI are associated with the subtended myocardial mass and the ratio of coronary volume to subtended mass. Vessel with higher myocardial mass have lower post-PCI RFR, and FFR values, and vessels with higher V/M ratio have higher post-PCI RFR and FFR.

Table 1. Baseline patient characteristics.

Variables	Overall	Low V/M <7.5	High V/M ≥7.5	P-value
N	120	60	60	
Age, years (mean ± SD)	64.3±9.00	65.0±8.8	63.6±9.2	0.40
Sex, Male, n (%)	95 (79.2)	46 (76.7)	49 (81.7)	0.65
BMI, kg/m2 (mean ± SD)	26.9±3.3	27.0±3.3	26.7±3.3	0.57
Dyslipidaemia, n (%)	95 (79.2)	44 (73.3)	51 (85.0)	0.18
Hypertension, n (%)	70 (58.3)	27 (45.0)	43 (71.7)	0.005
Diabetes mellitus, n (%)	29 (24.2)	9 (15.0)	20 (33.3)	0.03
Current smoker, n (%)	28 (23.3)	12 (20.0)	16 (26.7)	0.52
Creatinine, mg/dL	0.94±0.20	0.94±0.20	0.94±0.20	0.880
Clinical presentation				0.354
Silent ischemia, n (%)	28 (23.3)	15 (25.0)	13 (21.7)	
Stable angina CCS I, n (%)	37 (30.8)	18 (30.0)	19 (31.7)	
Stable angina CCS II, n (%)	44 (36.7)	24 (40.0)	20 (33.3)	
Stable angina CCS III, n (%)	8 (6.7)	2 (3.3)	6 (10.0)	
Stable angina CCS IV, n (%)	1 (0.8)	1 (1.7)	0 (0.0)	
Unstable angina, n (%)	2 (1.7)	0 (0.0)	2 (3.3)	

V/M volume to mass ratio; BMI Body mass index

* In patients with two vessels treated (n=3), the one with the lowest V/M was used for the patient level analysis.

Table 2. Pre-PCI lesion characteristics stratified by V/M.

Variables	Overall	Low V/M <7.5	High V/M ≥7.5	P-value
N	123	61	62	
Number of vessels, n (%)				0.01
LAD	94 (76.4)	54 (88.5)	40 (64.5)	
LCX	13 (10.6)	3 (4.9)	10 (16.1)	
RCA	16 (13.0)	4 (6.6)	12 (19.4)	
Coronary lumen volume (mm^3), mean ± SD	390.2 ± 172.0	314.3 ± 104.8	464.9 ± 192.3	< 0.001
Coronary lumen volume (normalized, mm^3), mean ± SD	299.4 ± 127.7	226.3 ± 72.5	371.2 ± 129.8	< 0.001
Vessel-specific myocardial mass (g), mean± SD	61.0 ± 23.1	68.23± 24.3	53.9± 19.5	<0.001
Present myocardial mass (%), mean ± SD	39.6 ± 11.7	44.43± 10.8	34.9± 10.7	< 0.001
V/M, mean ± SD	8.23 ± 4.6	5.16± 1.3	11.3± 4.6	<0.001
Lesion length, QCA, mm (mean ± SD)	25.4 ± 14.4	24.2 ± 11.5	26.5 ± 16.7	0.389
Vessel length, QCA, mm (mean ± SD)	133.3 ± 30.74	141.8 ± 28.89	124.9 ± 30.42	0.002
Mean reference diameter, QCA, mm (mean ± SD)	2.70 ± 0.50	2.78 ± 0.46	2.63 ± 0.53	0.09
Minimal lumen diameter, QCA, mm (mean ± SD)	1.29 ± 0.41	1.29 ± 0.42	1.30 ± 0.41	0.86
Diameter stenosis, QCA, % (mean ± SD)	51.4 ± 14.3	53.6 ± 13.9	49.21 ± 14.4	0.089

Baseline physiology				
RFR pre-PCI (mean ± SD) *	0.77±0.18	0.76± 0.19	0.77±0.18	0.922
FFR pre-PCI (mean ± SD) **	0.66±0.13	0.67±0.14	0.66±0.13	0.64
Procedural				
Number of stents per vessel, (mean ± SD)	1.27 ± 0.54	1.20 ± 0.48	1.34 ± 0.60	0.15
Stent diameter, mm (mean ± SD)	3.23 ± 0.95	3.15 ± 0.78	3.31 ± 1.08	0.36
Stent length, mm (mean ± SD)	35.0 ± 16.3	32.2 ± 14.2	37.7 ± 17.9	0.06
Pre-dilatation, n (%)	113 (91.9)	56 (91.8)	57 (91.9)	0.48
Post-dilatation, n (%)	111 (90.2)	55 (90.1)	56 (90.3)	0.50

QCA quantitative coronary angiography; SD standard deviation; OCT optical coherence tomography; PCI percutaneous coronary intervention; V/M volume to mass ratio; FFR fractional flow reserve

* Available for 107 lesions. (Low V/M 53 lesions, High V/M 54 lesions)

** Available for 116 lesions. (Low V/M 56 lesions, High V/M 60 lesions)

Table 3. Post-PCI lesion characteristics stratified by V/M.

Variables	Overall (n=123)	Low V/M <7.5	High V/M ≥7.5	P-value
N	123	61	62	
FFR post-PCI (mean ± SD)	0.88±0.06	0.87±0.06	0.89±0.07	0.02
RFR post-PCI (mean ± SD)	0.92±0.05	0.91±0.05	0.93±0.05	0.04
Mean reference diameter, QCA, mm (mean ± SD)	2.86±0.48	2.86 ± 0.47	2.87 ± 0.49	0.91
Minimal lumen diameter, QCA, mm (mean ± SD)	2.76±0.46	2.73 ± 0.43	2.78 ± 0.49	0.57
Residual Diameter stenosis, QCA, % (mean ± SD)	2.61±11.2	3.57 ±10.95	1.66±11.4	0.35
Minimal stent area, OCT, mm^2 (mean ± SD)*	5.53±2.06	5.49±1.65	5.56±2.33	0.88

* Available for 102 lesions. (Low V/M 46 lesions, High V/M 56 lesions)

FFR fractional flow reserve; RFR resting-full-cycle ratio; QCA quantitative coronary angiography; SD standard deviation; OCT optical coherence tomography; PCI percutaneous coronary intervention; V/M volume to mass ratio

Figure 1. Case examples of myocardial mass and post-PCI FFR.

Panel A shows a coronary CT angiography of a Right Coronary artery (RCA) with a post-PCI FFR of 0.99 with a V/M ratio of 30.0 (Coronary volume 497.3mm^3; %M 16.6%). Panel B shows a Left Anterior Descending artery with a post-PCI FFR of 0.79 and a V/M ratio of 5.0 (Coronary volume 150.3mm^3; %M 29.9%). The case examples depict the effect of V/M on post-PCI FFR.

PCI percutaneous coronary intervention; FFR fractional flow reserve; %M percent myocardial mass; V/M volume to mass ratio.

A

FFR 0.99

B

FFR 0.79
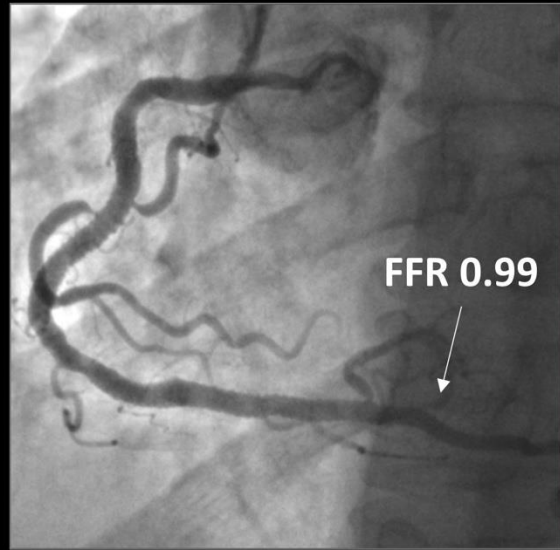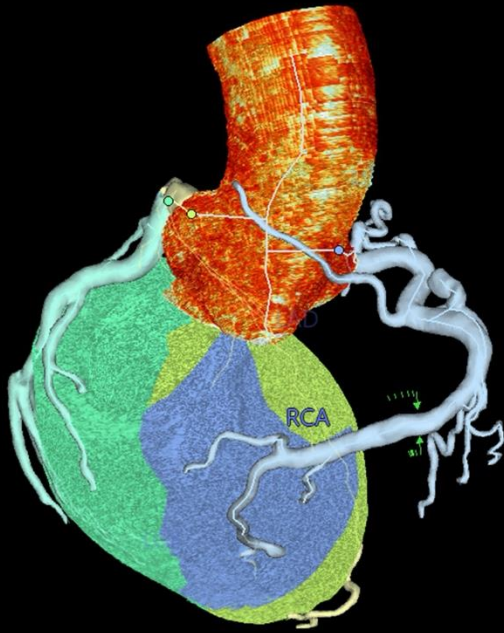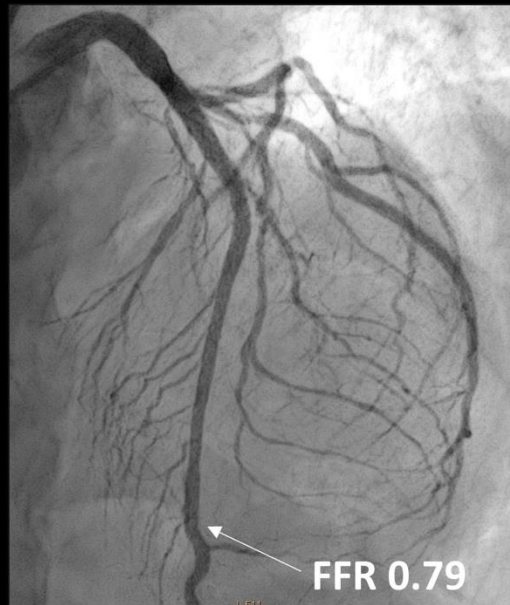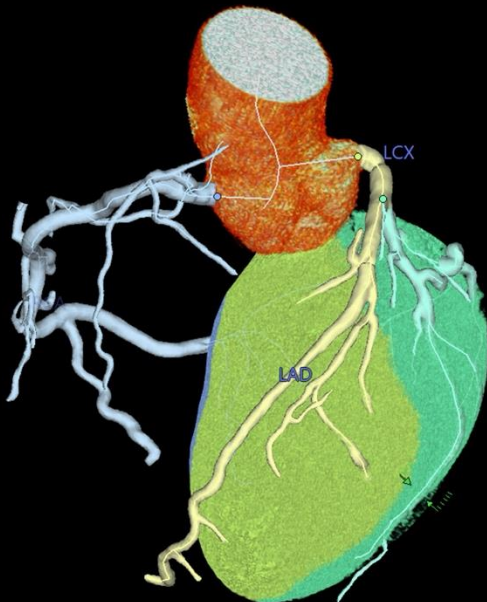
Figure 2. Distribution of post-PCI resting full-cycle ratio and fractional flow reserve.
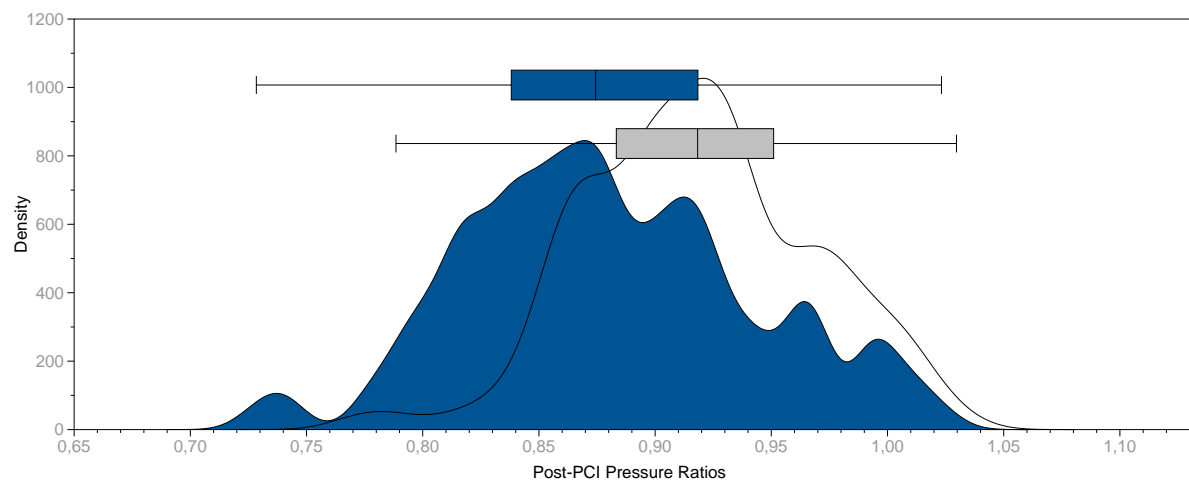
Figure 3. Percent myocardial mass and post-PCI resting and hyperaemic pressure ratios.

Panels A and B show box plots comparing post-PCI RFR and FFR values in vessels with low and high percent mass (%M), respectively. Panels B and C show the relationship between %M and post-PCI RFR and FFR, respectively. Panel E shows the distribution of vessel-specific %M stratified by coronary vessel.

PCI percutaneous coronary intervention; RFR resting full-cycle ratio; FFR fractional flow reserve; %M percent myocardial mass.
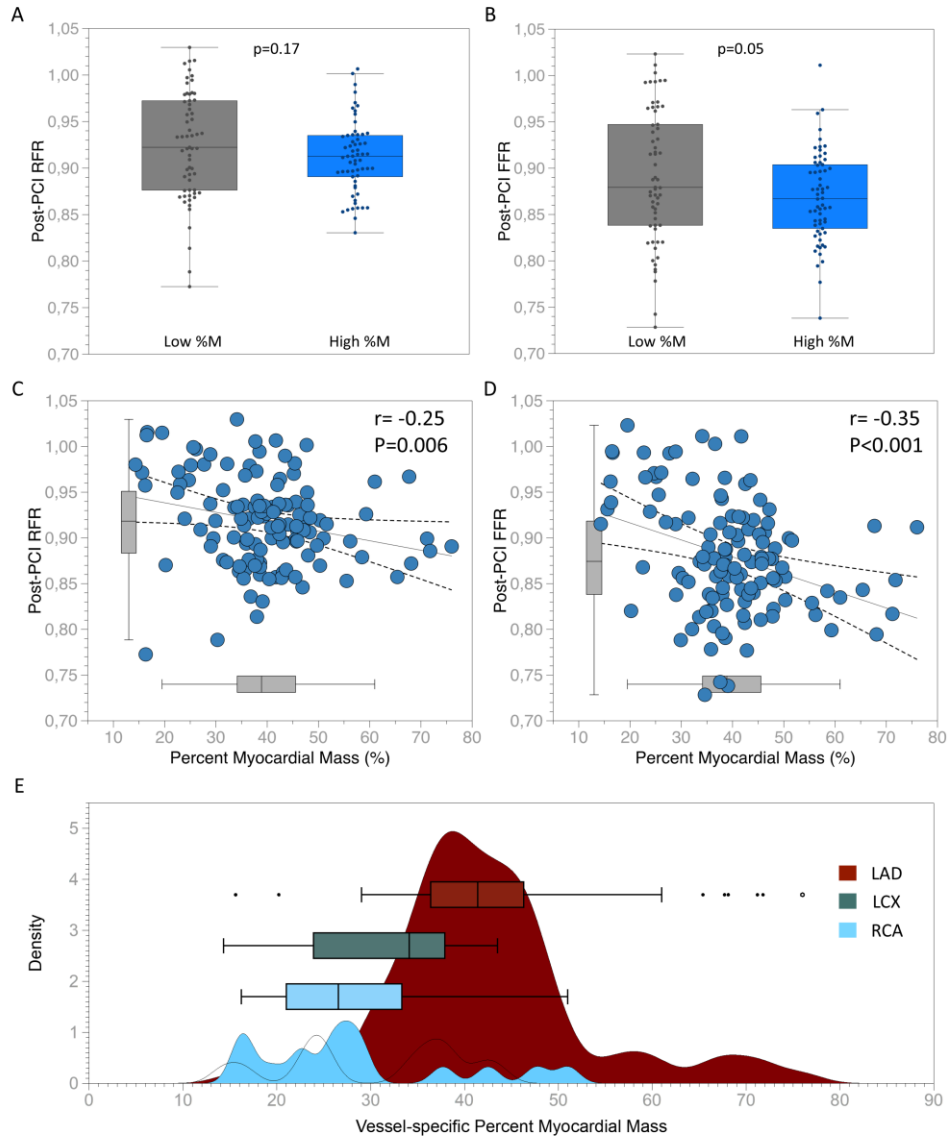
Figure 4. Volume to mass ratio and post-PCI resting and hyperaemic pressure ratios.

Panels A and B show box plots comparing post-PCI RFR and FFR values in vessels with low and high volume to mass ratio (V/M), respectively. Panels B and C show significant relationships between V/M and post-PCI RFR and FFR, respectively. Panel E shows the distribution of vessel-specific V/M stratified by coronary vessel.

PCI percutaneous coronary intervention; RFR resting full-cycle ratio; FFR fractional flow reserve; V/M volume to mass ratio

85
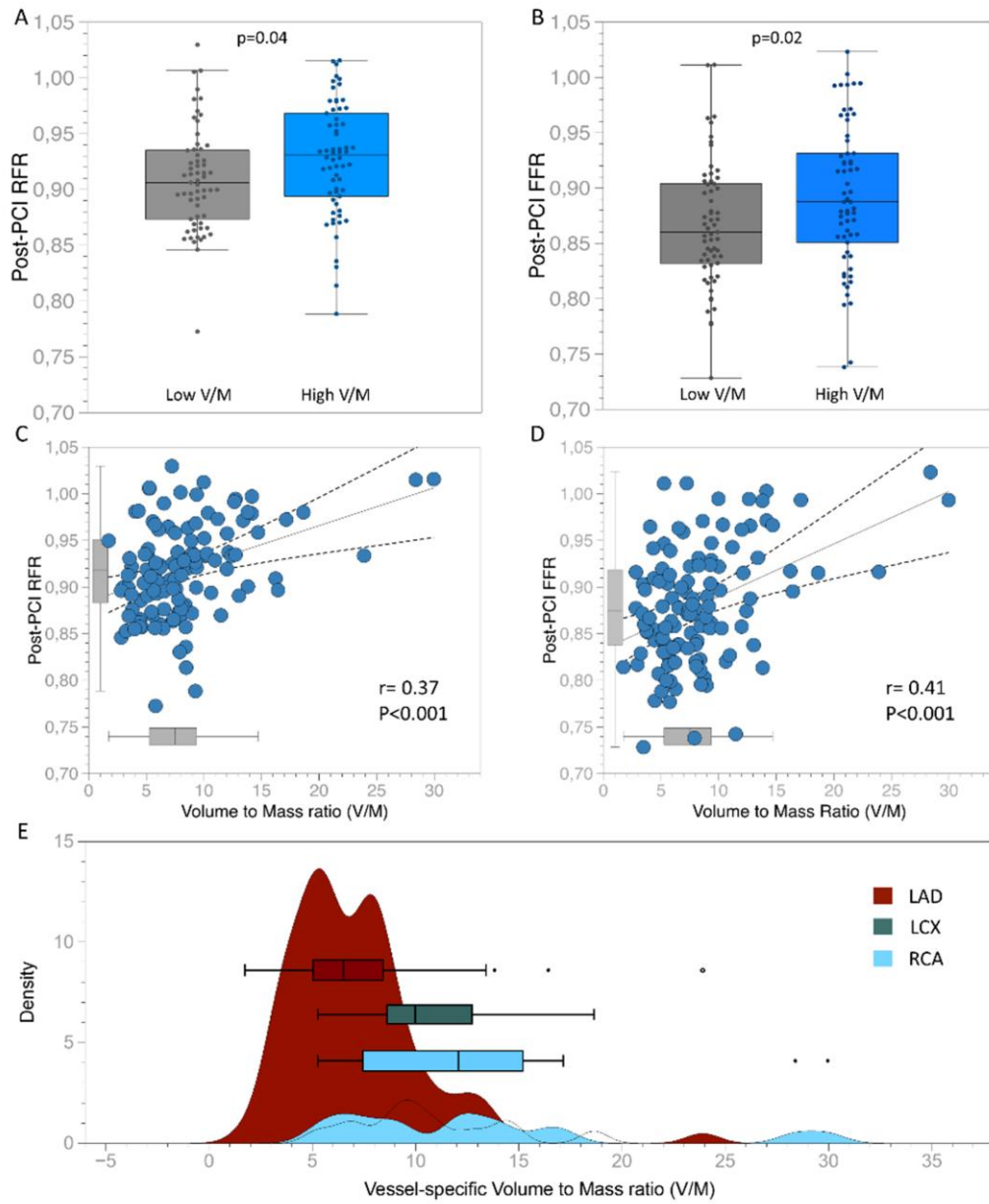
REFERENCES

1.   Toth G, Hamilos M, Pyxaras S, et al. Evolving concepts of angiogram: fractional flow reserve discordances in 4000 coronary stenoses. *Eur Heart J*. Oct 21 2014;35(40):2831-8. doi:10.1093/eurheartj/ehu094

2.   De Bruyne B, Sarma J. Fractional flow reserve: a review: invasive imaging. *Heart*. Jul 2008;94(7):949-59. doi:10.1136/hrt.2007.122838

3.   Kim HY, Lim HS, Doh JH, et al. Physiological Severity of Coronary Artery Stenosis Depends on the Amount of Myocardial Mass Subtended by the Coronary Artery. *JACC Cardiovasc Interv*. Aug 8 2016;9(15):1548-60. doi:10.1016/j.jcin.2016.04.008

4.   Taylor CA, Gaur S, Leipsic J, et al. Effect of the ratio of coronary arterial lumen volume to left ventricle myocardial mass derived from coronary CT angiography on fractional flow reserve. *J Cardiovasc Comput Tomogr*. Nov 2017;11(6):429-436. doi:10.1016/j.jcct.2017.08.001

5.   Yang DH, Kang SJ, Koo HJ, et al. Incremental Value of Subtended Myocardial Mass for Identifying FFR-Verified Ischemia Using Quantitative CT Angiography: Comparison With Quantitative Coronary Angiography and CT-FFR. *JACC Cardiovasc Imaging*. Apr 2019;12(4):707-717. doi:10.1016/j.jcmg.2017.10.027

6.   Grover R, Leipsic JA, Mooney J, et al. Coronary lumen volume to myocardial mass ratio in primary microvascular angina. *J Cardiovasc Comput Tomogr*. Nov 2017;11(6):423-428. doi:10.1016/j.jcct.2017.09.015

7.   Johnson NP, Toth GG, Lai D, et al. Prognostic value of fractional flow reserve: linking physiologic severity to clinical outcomes. *J Am Coll Cardiol*. Oct 21 2014;64(16):1641-54. doi:10.1016/j.jacc.2014.07.973

8.   Piroth Z, Toth GG, Tonino PAL, et al. Prognostic Value of Fractional Flow Reserve Measured Immediately After Drug-Eluting Stent Implantation. *Circ Cardiovasc Interv*. Aug 2017;10(8)doi:10.1161/CIRCINTERVENTIONS.116.005233

9.   Guibas L, Stolfi J. Primitives for the manipulation of general subdivisions and the computation of Voronoi. *ACM Transactions on Graphics*. 1985;4(2):74-123. doi:10.1145/282918.282923

10.   Ide S, Sumitsuji S, Yamaguchi O, Sakata Y. Cardiac computed tomography-derived myocardial mass at risk using the Voronoi-based segmentation algorithm: A histological validation study. *J Cardiovasc Comput Tomogr*. May - Jun 2017;11(3):179-182. doi:10.1016/j.jcct.2017.04.007

11.   Nagumo S, Collet C, Norgaard BL, et al. Rationale and design of the precise percutaneous coronary intervention plan (P3) study: Prospective evaluation of a virtual computed tomography-based percutaneous intervention planner. *Clin Cardiol*. Apr 2021;44(4):446-454. doi:10.1002/clc.23551

12.   Toth GG, Johnson NP, Jeremias A, et al. Standardization of Fractional Flow Reserve Measurements. *J Am Coll Cardiol*. Aug 16 2016;68(7):742-53. doi:10.1016/j.jacc.2016.05.067

13.   Abbara S, Blanke P, Maroules CD, et al. SCCT guidelines for the performance and acquisition of coronary computed tomographic angiography: A report of the society of Cardiovascular Computed Tomography Guidelines Committee: Endorsed by the North American Society for Cardiovascular Imaging (NASCI). *J Cardiovasc Comput Tomogr*. Nov-Dec 2016;10(6):435-449. doi:10.1016/j.jcct.2016.10.002

14.   Boogers MJ, Broersen A, van Velzen JE, et al. Automated quantification of coronary plaque with computed tomography: comparison with intravascular ultrasound using a dedicated registration algorithm for fusion-based quantification. *Eur Heart J*. Apr 2012;33(8):1007-16. doi:10.1093/eurheartj/ehr465

15. Sumitsuji S, Ide S, Siegrist PT, et al. Reproducibility and clinical potential of myocardial mass at risk calculated by a novel software utilizing cardiac computed tomography information. *Cardiovasc Interv Ther*. Jul 2016;31(3):218-25. doi:10.1007/s12928-015-0370-0

16. van Driest FY, Bijns CM, van der Geest RJ, et al. Correlation between quantification of myocardial area at risk and ischemic burden at cardiac computed tomography. *Eur J Radiol Open*. 2022;9:100417. doi:10.1016/j.ejro.2022.100417

17. Gheorghe AG, Fuchs A, Jacobsen C, et al. Cardiac left ventricular myocardial tissue density, evaluated by computed tomography and autopsy. *BMC Med Imaging*. Apr 12 2019;19(1):29. doi:10.1186/s12880-019-0326-4

18. Jackowski C, Schweitzer W, Thali M, et al. Virtopsy: postmortem imaging of the human heart in situ using MSCT and MRI. *Forensic Sci Int*. Apr 20 2005;149(1):11-23. doi:10.1016/j.forsciint.2004.05.019

19. West GB, Brown JH, Enquist BJ. A general model for the origin of allometric scaling laws in biology. *Science*. Apr 4 1997;276(5309):122-6. doi:10.1126/science.276.5309.122

20. Upton RN. Organ weights and blood flows of sheep and pig for physiological pharmacokinetic modelling. *J Pharmacol Toxicol Methods*. Nov-Dec 2008;58(3):198-205. doi:10.1016/j.vascn.2008.08.001

21. Choy JS, Kassab GS. Scaling of myocardial mass to flow and morphometry of coronary arteries. *J Appl Physiol (1985)*. May 2008;104(5):1281-6. doi:10.1152/japplphysiol.01261.2007

22. Sdringola S, Johnson NP, Kirkeeide RL, Cid E, Gould KL. Impact of unexpected factors on quantitative myocardial perfusion and coronary flow reserve in young, asymptomatic volunteers. *JACC Cardiovasc Imaging*. Apr 2011;4(4):402-12. doi:10.1016/j.jcmg.2011.02.008

23. Keulards DCJ, Fournier S, van 't Veer M, et al. Computed tomographic myocardial mass compared with invasive myocardial perfusion measurement. *Heart*. Oct 2020;106(19):1489-1494. doi:10.1136/heartjnl-2020-316689

24. Fournier S, Keulards DCJ, van 't Veer M, et al. Normal values of thermodilution-derived absolute coronary blood flow and microvascular resistance in humans. *EuroIntervention*. Jul 20 2021;17(4):e309-e316. doi:10.4244/EIJ-D-20-00684

25. Ihdayhid AR, Thakur U, Yap G, et al. Ethnic differences in coronary anatomy, left ventricular mass and CT-derived fractional flow reserve. *J Cardiovasc Comput Tomogr*. May-Jun 2021;15(3):249-257. doi:10.1016/j.jcct.2020.09.004

26. Seiler C, Kirkeeide RL, Gould KL. Basic structure-function relations of the epicardial coronary vascular tree. Basis of quantitative coronary arteriography for diffuse coronary artery disease. *Circulation*. Jun 1992;85(6):1987-2003. doi:10.1161/01.cir.85.6.1987

27. van Diemen PA, Schumacher SP, Bom MJ, et al. The association of coronary lumen volume to left ventricle mass ratio with myocardial blood flow and fractional flow reserve. *J Cardiovasc Comput Tomogr*. Jul - Aug 2019;13(4):179-187. doi:10.1016/j.jcct.2019.06.016

28. Bland JM, Altman DG. Correlation in restricted ranges of data. *BMJ*. Mar 11 2011;342:d556. doi:10.1136/bmj.d556
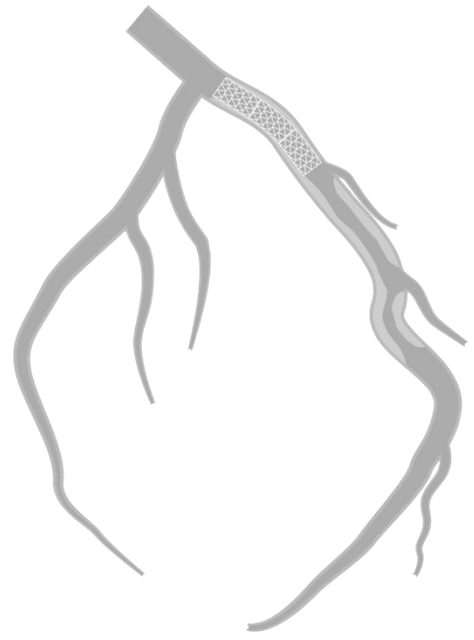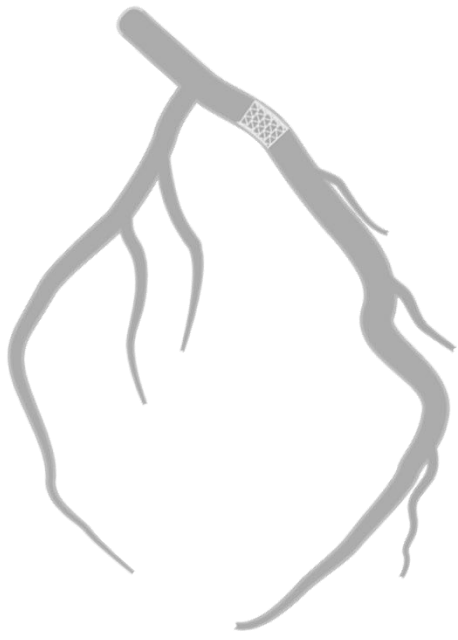
Chapter 4. Triggering Stent Optimization by Coronary Physiology

Munhoz D, Sakai K, Collet C, Mizukami T.

In reporting the results of FFR-REACT, the vessel distribution shows a predominance of Left Anterior Descending arteries (LAD) compared to non-LAD vessels (74 % vs. 25%).[1] Intracoronary pressure measurements in the LAD are affected by the hydrostatic pressure leading to lower fractional flow reserve (FFR) values. The LAD runs approximately 5 cm above the ostium of the left main stem resulting in a progressive reduction of the coronary pressure when measured with sensor tip pressure wires. Theoretically, the highest possible FFR in a normal LAD would be 0.96, and trans-stent pressure gradients are invariably present in LAD while the opposite situation occurs in the right coronary artery (RCA).[2] For this reason, inclusion criteria of post-PCI FFR <0.90 generated a selection bias towards more LAD. [3,4]It would be of interest to compare vessel type between patients included in the trial and those with post-PCI ≥ 0.90 allocated to the registry. In addition, understanding how post-PCI physiology (post-PCI FFR, trans-stent pressure gradients, and the rate of patients with FFR ≤0.80) differed between LAD and non-LAD vessels could inform practitioners on the inter-vessel differences in coronary physiology that appear to be more apparent in the post-PCI phase.

REFERENCES

1.   Neleman T, van Zandvoort LJC, Tovar Forero MN, et al. FFR-Guided PCI Optimization Directed by High-Definition IVUS Versus Standard of Care: The FFR REACT Trial. *JACC Cardiovasc Interv*. Aug 22 2022;15(16):1595-1607. doi:10.1016/j.jcin.2022.06.018

2.   Kawaguchi Y, Ito K, Kin H, et al. Impact of Hydrostatic Pressure Variations Caused by Height Differences in Supine and Prone Positions on Fractional Flow Reserve Values in the Coronary Circulation. *J Interv Cardiol*. 2019;2019:4532862. doi:10.1155/2019/4532862

3.   Diletti R, Masdjedi K, Daemen J, et al. Impact of Poststenting Fractional Flow Reserve on Long-Term Clinical Outcomes: The FFR-SEARCH Study. *Circulation Cardiovascular interventions*. Mar 2021;14(3):e009681. doi:10.1161/circinterventions.120.009681

4.   Hwang D, Lee JM, Lee HJ, et al. Influence of target vessel on prognostic relevance of fractional flow reserve after coronary stenting. *EuroIntervention*. Aug 29 2019;15(5):457-464. doi:10.4244/EIJ-D-18-00913
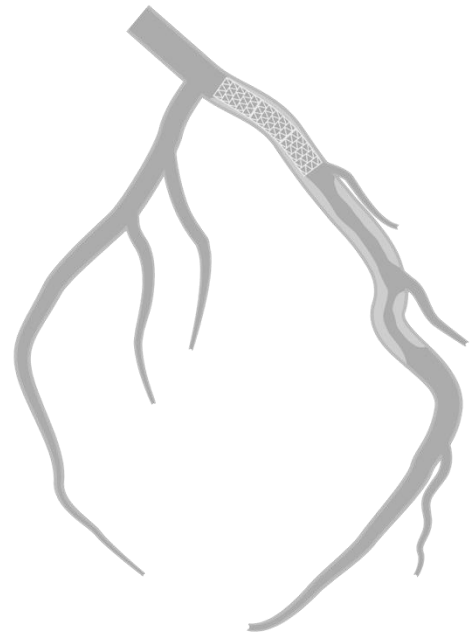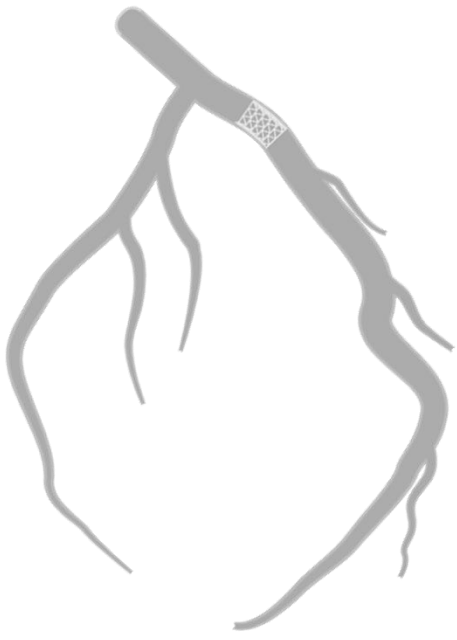
Chapter 5. Impact of Post-PCI FFR Stratified by Coronary Artery

Collet C, Johnson NP, Mizukami T, Fearon WF, Berry C, Sonck J, Collison D, Koo BK, Meneveau N, Agarwal SK, Uretsky B, Hakeem A, Doh JH, Da Costa BR, Oldroyd KG, Leipsic JA, Morbiducci U, Taylor C, Ko B, Tonino PAL, Perera D, Shinke T, Chiastra C, Sposito AC, Leone AM, Muller O, Fournier S, Matsuo H, Adjedj J, Amabile N, Piróth Z, Alfonso F, Rivero F, Ahn JM, Toth GG, Ihdayhid A, West NEJ, Amano T, Wyffels E, Munhoz D, Belmonte M, Ohashi H, Sakai K, Gallinoro E, Barbato E, Engstrøm T, Escaned J, Ali ZA, Kern MJ, Pijls NHJ, Jüni P, De Bruyne B.

Meta-analysis of individual patient-level data

2.760 patients
3.336 vessels

9 studies
4 randomized trials
5 observational studies
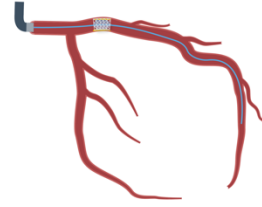
Post-PCI FFR

Mean post-PCI FFR & predicted capacity of TVF stratified by vessel

0.93 LCX

0.91 RCA

0.86 LAD

Non-LAD
AUC 0.66 (95% CI 0.59 to 0.73)

LAD
AUC 0.52 (95% CI 0.47 to 0.58)

Sensitivity

1-Specificity
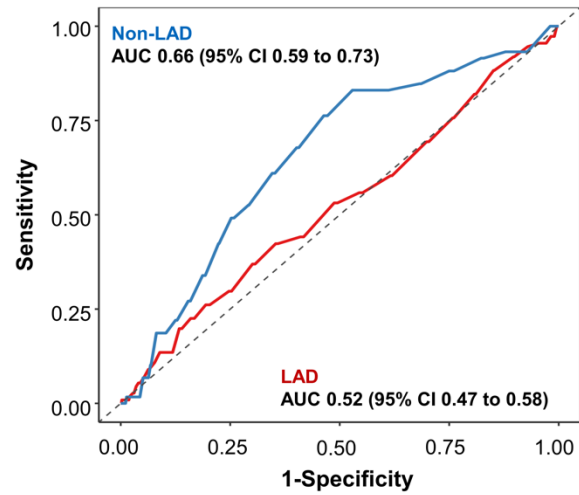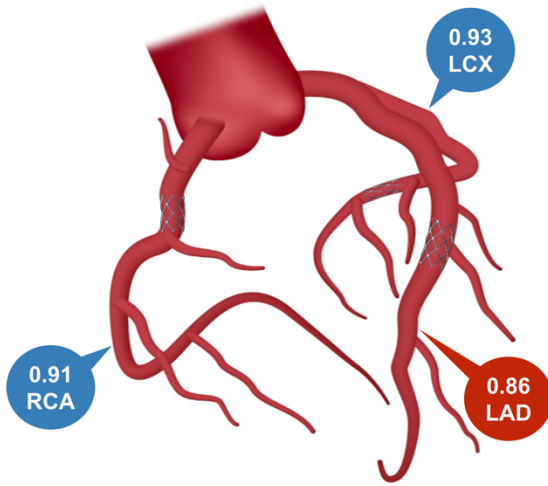
Risk of TVF stratified by post-PCI FFR in LAD and non-LAD

LAD

Adjusted HR 0.47
(95% CI 0.31 – 0.70), P < 0.001

Low Post-PCI FFR

High Post-PCI FFR

Event Probability

Years Since Index Procedure

Non LAD

Adjusted HR 0.24
(95% CI 0.12 – 0.48), P < 0.001

Low Post-PCI FFR

High Post-PCI FFR

Event Probability

Years Since Index Procedure
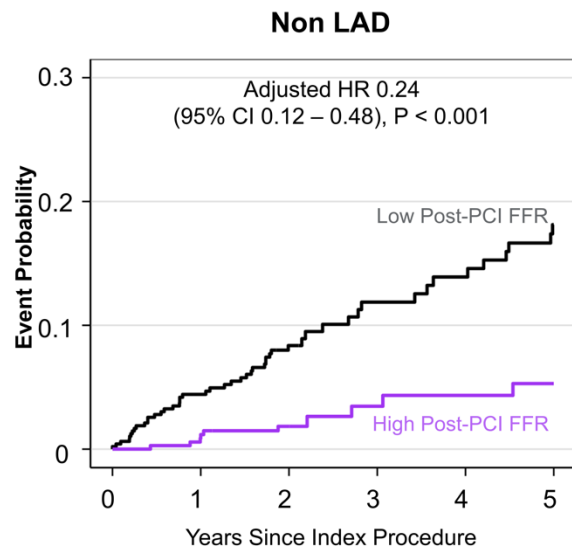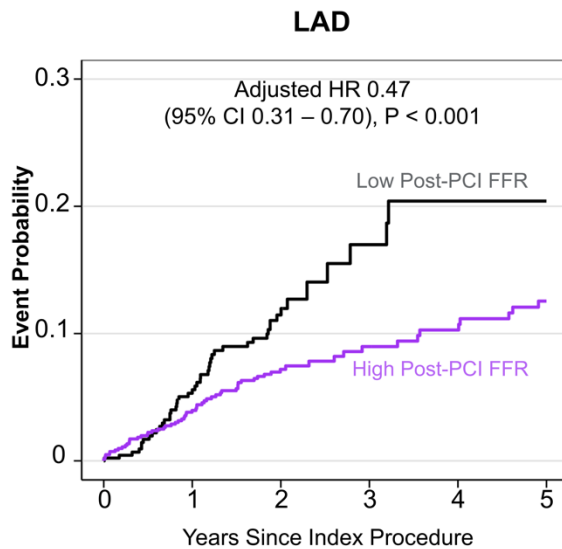
Abstract

Background: Low fractional flow reserve (FFR) after PCI has been associated with adverse clinical outcomes. Hitherto, this assessment has been independent of the epicardial vessel interrogated.

Objectives: To assess the predictive capacity of post-PCI FFR for target vessel failure (TVF) stratified by coronary artery.

Methods: A systematic review and individual patient-level data meta-analysis of randomized clinical trials and observational studies with protocol-recommended post-PCI FFR assessment. The difference in post-PCI FFR between LAD and non-LAD was assessed using a random-effect models meta-analysis of mean differences. TVF was defined as a composite of cardiac death, target vessel myocardial infarction, and clinically-driven target vessel revascularization.

Results: Overall, 3,336 vessels (2,760 patients) with post-PCI FFR measurements were included in 9 studies. The weighted mean post-PCI FFR was 0.89 (95% CI 0.87 to 0.90) and differed significantly between coronary vessels (LAD 0.86, 95% CI 0.85 to 0.88 vs. non-LAD 0.93, 95% CI 0.91 to 0.94, p-value <0.001). Post-PCI FFR was an independent predictor of TVF, with its risk increasing by 52% for every reduction of 0.10 FFR units and this was mainly driven by TVR. In the LAD, post-PCI FFR was 0.064 units (95% CI 0.082 to 0.045) lower than non-LAD, and the predicted capacity for TVF was poor for the LAD (AUC 0.52, 95% CI 0.47 to 0.58) and moderate for non-LAD (0.66, 95% CI 0.59 to 0.73; p-value LAD vs non-LAD = 0.005).

Conclusion: The LAD is associated with a lower post-PCI FFR than non-LAD arteries, emphasizing the importance of interpreting post-PCI FFR on a vessel-specific basis. While higher post-PCI FFR was associated with improved prognosis, its predictive capacity for events differs between the LAD and non-LAD arteries, being poor in the LAD and moderate in non-LAD vessels.

Introduction

Fractional flow reserve (FFR) was developed and validated to quantify the relative reduction in normal maximum flow due to an epicardial stenosis.[1,2] Based on a substantial body of evidence, an FFR between 0.75-0.80 has entered the guidelines as a metric to determine the appropriateness of revascularization, and an FFR of ≤0.75 can be used to define more severe flow impairment that is of prognostic relevance.[3] The utility of FFR to guide revascularization decisions has been demonstrated in numerous clinical trials among patients across the spectrum of coronary artery disease. [4,5]

Successful PCI re-establishes epicardial conductance and improves myocardial perfusion. Consequently, FFR measured after PCI can quantify the degree of functional revascularization. Several studies have observed that in a sizable proportion of patients, epicardial hemodynamics remain abnormal despite angiographically successful PCI. [6,7] [8] Moreover, post-PCI FFR has been proposed as a clinical target to optimize PCI and as a surrogate endpoint for clinical outcomes. [9,10] [11] [12]

FFR measurements after PCI are increasingly performed both in the context of clinical studies and in routine practice. Hitherto, post-PCI FFR had been proposed as a metric reflecting the degree of residual flow limitation in coronary vessels. Historically and in contemporary practice, this assessment has been independent of the specific epicardial vessel interrogated. Nevertheless, post-PCI FFR measured in the left anterior descending (LAD) artery has been reported to be lower than in non-LAD vessels. [13]The clinical implications and mechanisms of this finding remain to be elucidated.

There are four main goals of this paper:

(1) to present individual patient-level data (IPD) summarizing post-PCI FFR stratified by coronary artery;

(2) to investigate the predictive power of vessel-specific post-PCI FFR for target vessel failure;

(3) to describe the mechanisms that account for inter-vessel differences in post-PCI FFR values;

(4) to provide recommendations for clinicians and trialists about the use and interpretation of post-PCI FFR measurements.

Methods

Two independent reviewers (C.C. and T.M.) systematically searched MEDLINE/Embase/CENTRAL applying the search terms 'fractional flow reserve" and "post-PCI". The search was conducted in December 2021. No restrictions were applied concerning

language. Data were obtained from fully published articles. The principal investigator for each of the studies included was contacted for individual patient-level data. We included randomized clinical trials or observational studies with patients who (i) underwent PCI for obstructive coronary artery disease; (ii) post-PCI FFR was measured and (iii) patient-level data was obtained. The same two investigators extracted data in agreement with PRISMA (Preferred Reporting Items for Systematic Reviews and Meta-Analyses) guidelines. Bias assessment was performed using the Cochrane Collaboration's tool. There was no funding available for this systematic review and IPD. This systematic review and meta-analysis were registered in PROSPERO (CRD42021274567).

The primary outcome of interest was the predictive capacity of post-PCI FFR for target vessel failure (TVF), defined as a composite of cardiac death, target vessel myocardial infarction (MI), and clinically-driven target vessel revascularization (TVR) stratified by coronary artery. Peri-procedural myocardial infarction was not included as a TVF component. The secondary outcome of interest was determining the difference between post-PCI FFR units between LAD and non-LAD vessels.

Statistical analysis

Continuous variables are presented as means and standard deviation, and categorical variables as percentages and counts. The difference in post-PCI FFR between LAD and non-LAD was assessed using a random-effects models meta-analysis of mean differences. Differences between LAD and non-LAD arteries stratified by randomized and observational studies were compared using random-effects models and interaction testing. Random-effects models were stratified by trial to assess independent predictors of low post-PCI FFR. For assessing independent predictors of post-PCI-FFR, the model was adjusted for age, hypertension, dyslipidemia, diabetes mellitus, vessel type, pre-PCI FFR, number of stents, and stent length. All patients included in the analysis of the clinical outcomes were treated with second-generation drug-eluting stents. Receiver-operating characteristic curves (ROC) were used to define the best cutoff to predict TVF stratified by vessel (i.e., LAD versus non-LAD). Youden's index defined the best cutoff to predict TVF in LAD and non-LAD. ROC curves between LAD and non-LAD were compared using the DeLong test. Subsequently, survival curves were created using the vessel-specific cutoff. In addition, vessel-specific cutoffs were verified by maximally selected rank statistics and Cox regression using FFR bins every 0.05 units to detect the maximal hazard ratio.

Random-effect models with random intercepts and slopes were created to assess the relationship between post-PCI FFR and TVF. To account for multiple observations per patient

mixed effect models were stratified by trial and by patient. For assessing predictors of TVF, the model was adjusted by known clinical and procedural characteristics associated with adverse prognoses. Variables showing a significant association with TVF were included in the multivariable model. Finally, the analysis was complemented by a bivariate meta-analysis to assess the prognostic performance of post-PCI FFR for TVF. These results are presented as accuracy, sensitivity, specificity, positive predictive value (PPV), negative predictive value (NPV), positive likelihood ratio (PLR), and negative likelihood ratio (NLR) for post-PCI FFR to detect TVF using the vessel-specific cutoffs derived from the ROC analyses (i.e., 0.83 for LAD and 0.93 for non-LAD). All analyses were performed with R (R Foundation for Statistical Computing, Vienna, Austria).

Results

We identified 54 studies with protocol-recommended post-PCI FFR assessments. The systematic review flowchart and preferred reporting items for systematic reviews and meta-analyses (PRISMA) checklist are shown in Supplemental Material Tables S1 and S2. After contacting principal investigators, individual patient-level data from four randomized clinical trials and five observational studies encompassing 2,760 patients with 3,336 vessels with post-PCI FFR measurements were obtained. Bias assessment is reported in Supplementary Material Table S3.

1. Post-PCI FFR stratified by coronary artery

Overall, 3,336 vessels with post-PCI FFR measurements were included in 9 studies. The design, baseline, and procedural characteristics stratified by study are shown in Supplemental Material Tables S4 and S5. [7 9 11 14 15 16 17,18] The weighted mean age of patients was 63.1 (95% CI 61.4 to 64.8), 83.1% were males, and diabetes was present in 32.1%. The weighted mean pre-PCI FFR was 0.65 (95% CI 0.62 to 0.69) and was similar between vessel (LAD 0.66, 95% CI 0.63 to 0.69 vs. non-LAD 0.65, 95% CI 0.61 to 0.69; mean difference 0.007, 95% CI -0.023 to -0.037). The mean number of stents implanted per vessel was 1.26±0.56, and the mean stent length was 28.1±14.8 mm.

Post-PCI FFR was measured in LAD: 1,872 (56.1%), LCX: 630 (18.9%) and RCA: 834 (25.0%). The weighted mean post-PCI FFR was 0.89 (95% CI 0.87 to 0.90) and differed significantly between coronary vessels (LAD 0.86, 95% CI 0.85 to 0.88 vs. non-LAD 0.93, 95% CI 0.91 to 0.94, p-value <0.001), p-value <0.001; Figure 1 and Table 1). The distributions of pre-and post-PCI FFR are shown in Supplemental Material Figures S1 and S2. In the LAD, post-PCI FFR was 0.064 (95% CI 0.082 to 0.045) FFR units lower than non-LAD. This difference was consistent between randomized and observational trials (-0.057, 95% CI -0.104

to -0.011 FFR units in randomized trials vs. -0.070, 95% CI: -0.095 to -0.045 FFR units in observational studies, p-value = 0.473; Supplemental Material Figure S3). The LAD vessel, pre-PCI FFR, diabetes mellitus, and stent number and length were independent predictors of low post-PCI FFR (Supplemental Material Table S6).

2. Prognostic capacity of post-PCI FFR for target vessel failure

Two randomized clinical trials and three observational studies encompassing 1,864 patients treated with second-generation DES reported mid-term clinical outcomes (Table 2). Overall, 2,184 post-PCI FFR measurements were included: LAD 1,301 (59.6%), LCX 386 (17.7%) and RCA 496 (22.7%). The median follow-up was 2.00 [IQR 1.46-4.61] years. Baseline patient and procedural characteristics are shown in Supplemental Material Tables S4 and S5.

Overall, TVF occurred in 161 patients (24 cardiac death, 43 TV-MI, and 132 TVR). Overall, post-PCI FFR had a poor predictive capacity for TVF with an AUC of 0.58 (95% CI: 0.54 to 0.62). When stratified by vessel, the predictive capacity of post-PCI FFR for TVF showed an AUC of 0.52 (95% CI: 0.47 to 0.58) for the LAD and an AUC of 0.66 (95% CI: 0.59 to 0.73) for non-LAD (p-value LAD vs. non-LAD = 0.005) (Figure 2). The predicted capacity of post-PCI FFR for TVF was mainly driven by TVR. Overall, the risk of TVF increased by 52% per every reduction of 0.10 FFR units (Supplemental Material Figure S4). Post-PCI FFR was significantly associated with adverse events both in LAD and non-LAD groups; patients with low post-PCI FFR in LAD and non-LAD had higher rates of TVF (Figure 3). Survival curves of TVF components stratified by low and high post-PCI FFR are shown in Figure 4. Clinical and procedural characteristics of patients with and without TVF are shown in Table 3. In a multivariable analysis adjusting for clinical and procedural variables, age and post-PCI FFR emerged as the only independent predictor of adverse events (Supplemental Material Tables S7 and S8). The thresholds derived from Youden indexes corresponded to maximal hazard ratios for TVF for LAD and non-LAD, respectively (Supplemental Material Table S9 and Figure S5). High post-PCI FFR, according to vessel-specific cut-offs, conferred high negative predictive values for TVF (LAD: 92%, 95% CI: 90 – 94 and non-LAD: 96% 95% CI: 94 – 98; Supplemental Material Table S10). The change in FFR (functional gain) was not associated with TVF (Supplemental Material Figure S6).

When the composite of cardiac death and TV-MI was analysed, patients with low post-PCI FFR had an increased risk of cardiac death or TV-MI (adjusted HR 0.58, 95% Cl 0.36 to 0.93, p-value =0.025); this increased risk was observed in LAD and non-LAD vessels. As for

TVF, the predicted capacity of post-PCI FFR for TV-MI and cardiac death was poor in LAD and moderate in non-LAD (Figure 5).

Discussion

The present individual patient data (IPD) analysis provides evidence linking post-PCI FFR to adverse clinical outcomes. The risk of TVF increased by 52% with every 0.10 units decrease in post-PCI FFR. Patients with low post-PCI had an increased risk of cardiac death and MI than those with high post-PCI FFR. Moreover, post-PCI FFR was the only independent predictor of TVF. The novelty of the present analysis lies in the differentiation of post-PCI FFR values among coronary vessels. Specifically, post-PCI FFR was significantly lower in LAD vs non-LAD by 0.06 (95% CI: 0.05 to 0.08) FFR units. Additionally, the predictive capacity of post-PCI FFR for TVF varies between vessels, with poorer performance observed in the LAD and moderate performance observed in non-LAD vessels. The predictive capacity of post-PCI for the outcomes was mainly driven by TVR.

Post-PCI FFR has been identified in several independent cohorts as a prognostic marker. Several factors, including patient characteristics, diffuse disease, atherosclerotic plaque composition, and PCI technique, have been shown to influence FFR after PCI. [199] [20] Moreover, adrenergic stimulation due to stress and anxiety, pre-hydration, contrast volume, ischemic time due to prolonged coronary manipulation, microvascular dysfunction due to microparticles embolization, temporary or persistent slow flow/no-reflow phenomena can affect post-PCI FFR. Clinically, low post-PCI FFR can result from two mechanisms identifiable using longitudinal vessel assessment. Pressure deterioration can occur gradually along the coronary vessel with homogeneously distributed pressure gradients (i.e., residual diffuse disease), or focal pressure gradients may arise from stent under-expansion and residual (or unmasked) focal stenoses. Thus, beyond low post-PCI FFR, understanding residual functional disease necessitates longitudinal vessel interrogation with pressure pullbacks. The FFR REACT trial addressed this question by assessing the impact of PCI optimization directed by IVUS in patients with post-PCI FFR <0.90. The use of IVUS translated into higher post-PCI FFR; however, this strategy failed to improve clinical outcomes at one year. [21]A recent meta-analysis, confirmed the prognostic value of post-PCI FFR by demonstrating that reduced FFR after DES implantation was associated with TVF and cardiac death or TV-MI. [22]The present analysis expands those findings by exposing the need for a different interpretation of post-PCI FFR according to the coronary artery. Low post-PCI FFR values in the LAD are common, and despite their association with outcomes, its predictive capacity for events was

poor. In contrast, post-PCI FFR in non-LAD appears to bear superior predictive capacity for TVF than in the LAD.

Two fundamental mechanisms contribute to differential FFR values in LAD versus non-LAD: the difference in subtended myocardial mass and the hydrostatic effect. [23][24] [25] The LAD subtends larger mass, leading to higher blood flow and pressure losses. Hydrostatic effects arise in a supine patient because the mid to distal segment of the LAD runs approximately 5 cm above the ostium of the left main stem, and when the digital sensor of wire is placed in this location, a slight hydrostatic gradient is invariably generated. [26][27] [28] Conversely, the distal LCX and right posterolateral branches course about 3-4 cm below the ostium and the opposite phenomenon is observed. [29]These differences may explain circa 0.04 FFR units in a single vessel. These findings have been observed with resting and hyperemic pressure ratios[26]. Because of the range of the metrics, hydrostatic effect impact non-hyperaemic pressure ratios almost twice as much as FFR, given the lower range of P_d/P_a values during resting conditions.[28] Notably, the average difference in our cohort between LAD and non-LAD vessels was 0.064, consistent with the expectation regarding hydrostatic effects (LAD 0.04 lower from a 5-cm elevation, LCX or RCA 0.02 higher, due to a 3-4 cm depression; net difference 0.06). The abovementioned mechanisms may influenced the predictive capacity of post-PCI FFR in LAD vs. non-LAD for TVF.

The primary goals of assessing intracoronary physiology are identifying large epicardial gradients to explain clinical signs and symptoms and distinguishing focal gradients (amenable to revascularization) from diffuse gradients (less suitable for revascularization). A comprehensive and carefully studied FFR pullback before initiating PCI and after stent implantation will likely result in more personalized procedural planning, leading to better patient selection and a higher degree of functional revascularization.

Limitations

The present IPD analysis has several limitations. First, information about the use of intravascular imaging guidance was not available. Therefore, we can only hypothesize about the impact of intravascular imaging on post-PCI FFR and clinical outcomes. Second, FFR pullback curves pre- or post-PCI were not accessible in all studies. Third, randomized and observational data were combined for the analysis, and outcomes data were available only for five studies (2 RCTs and three observational studies). Fourth, not all operators and event adjudication processes were blinded to the post-PCI FFR results. This may have introduced bias in the management of patients after PCI. Fifth, FFR tracings were not analysed by an independent Core Laboratory.

Conclusion and Recommendations

We believe that the current data on post-PCI FFR support the following recommendations:

1. Post-PCI FFR should be interpreted in a vessel-specific manner. Due mainly to hydrostatic effects and myocardial mass, the LAD coronary artery is associated with a lower post-PCI FFR than non-LAD arteries.

2. Post-PCI FFR can be considered a metric of functional revascularization. While influenced by procedural technique, post-PCI FFR is largely determined by the coronary artery (LAD vs. non-LAD) and, as shown by other studies, by the baseline phenotype of CAD (focal vs. diffuse).

3. Although a higher post-PCI FFR reduces the probability of adverse events, its predictive value was poor for the LAD and moderate for non-LAD. There is insufficient evidence to support post-PCI FFR as a surrogate marker of outcomes in clinical practice. Further investigation is necessary to understand if additional PCI in response to post-PCI FFR data can improve clinical outcomes.

Table 1. Anatomical and functional characteristics stratified by vessel.

Variables	LAD	LCX	RCA	*P*-value
Number of vessels	1872	630	834	
Diameter stenosis (%), mean ± SD[¶]	64.4 ± 13.9	70.1 ± 14.0	69.8 ± 13.7	<0.001
Lesion length (mm), mean ± SD[¶¶]	20.6 ± 11.5	16.8 ± 9.1	18.8 ± 11.5	<0.001
FFR pre-PCI, mean ± SD[¶¶¶]	0.66 ± 0.13	0.65 ± 0.14	0.64 ± 0.15	0.003
FFR post-PCI, mean ± SD	0.86 ± 0.06	0.93 ± 0.06	0.91 ± 0.06	<0.001
Functional gain*, mean ± SD[¶¶¶]	0.20 ± 0.13	0.28 ± 0.15	0.27 ± 0.16	<0.001
Relative functional gain**, mean ± SD [§]	54.01 ± 21.39	75.82 ± 22.37	71.73 ± 21.12	<0.001
Number of stents, mean ± SD [§ §]	1.28 ± 0.54	1.15 ± 0.42	1.32 ± 0.67	<0.001
Total stent length (mm) [§§§], mean ± SD	28.82 ± 14.24	23.32 ± 10.91	30.14 ± 17.62	<0.001

LAD Left anterior descending artery. LCX Left circumflex. RCA Right coronary artery. FFR Fractional flow reserve. PCI Percutaneous coronary interventions. SD Standard deviation.

* Post PCI FFR minus pre-PCI FFR.

** Post PCI FFR minus pre-PCI FFR / (1 minus pre-PCI FFR).

[¶] Data available for 1,848 vessels.

[¶¶] Data available for 1,815 vessels.

[¶¶¶] Data available for 2,734 vessels.

[§] Data available for 2,731 vessels.

[§§] Data available for 3,282 vessels.

[§§§] Data available for 3,272 vessels.

Table 2. Clinical events stratified by study.

Variables	Overall	3V FFR FRIENDS	ARKANSAS Registry	COE-PERSPECTIVE	FAME 2	TARGET-FFR
Number of patients	1,864	266	330	742	287	239
Number of vessels	2,184	337	347	937	324	239
Target vessel failure, n (%)	161 (8.6)	19 (7.1)	57 (17.3)	33 (4.4)	51 (17.8)	1 (0.4)
Cardiac death or myocardial infarction, n (%)	66 (3.5)	2 (0.8)	31 (9.4)	7 (0.9)	25 (8.7)	1 (0.4)
Cardiac death, n (%)	24 (1.3)	0 (0.0)	12 (3.6)	6 (0.8)	5 (1.7)	1 (0.4)
Myocardial infarction, n (%)	43 (2.3)	2 (0.8)	20 (6.1)	1 (0.1)	20 (7.0)	0 (0.0)
Target vessel revascularization, n (%)	132 (7.2)	19 (7.1)	46 (13.9)	27 (3.6)	40 (13.9)	0 (0.0)

Table 3.

Variables	No TVF	TVF	P- value
Number of patients	1703	161	
Age (yrs), mean ± SD	63.17 ± 9.44	65.50 ± 8.45	0.003
Gender (male), n (%)	1420 (83.4)	136 (84.5)	0.807
BMI, mean ± SD¶	29.06 ± 4.93	28.84 ± 4.45	0.755
Hypertension, n (%)	1156 (67.9)	130 (80.7)	0.001
Dyslipidemia, n (%)	1074 (63.1)	125 (77.6)	<0.001
Diabetes mellitus, n (%)	579 (34.0)	73 (45.3)	0.005
Smoking, n (%)	587 (34.5)	52 (32.3)	0.636
Family history of CAD, n (%)¶	273 (57.6)	18 (34.6)	0.003
Prior PCI, n (%)¶	133 (28.1)	14 (26.9)	0.992
Prior MI, n (%)	249 (17.4)	28 (26.9)	0.022
Number of vessels	2014	170	
Vessel (%)			0.280
LAD	1190 (59.1)	111 (65.3)	
LCX	361 (17.9)	25 (14.7)	
RCA	463 (23.0)	34 (20.0)	
FFR pre-PCI, mean ± SD§	0.66 ± 0.13	0.67 ± 0.13	0.975
FFR post-PCI, mean ± SD	0.88 ± 0.07	0.86 ± 0.07	0.001
High post-PCI FFR, n (%)	1157 (57.4)	74 (43.5)	0.001
Functional gain*, mean ± SD§	0.21 ± 0.14	0.20 ± 0.14	0.237
Relative functional gain**, mean ± SD§	60.29 ± 23.41	54.97 ± 25.37	0.008
Number of stents, mean ± SD§§	1.24 ± 0.52	1.28 ± 0.57	0.263
Total stent length (mm), mean ± SD	29.92 ± 14.87	27.19 ± 13.19	0.021
Diameter stenosis (%), mean ± SD§§§	67.26 ± 14.08	64.41 ± 10.76	0.139
Lesion length (mm), mean ± SD§§§§	20.13 ± 11.35	20.87 ± 9.66	0.630

TVF Target vessel failure. BMI Body mass index. CAD Coronary artery disease. MI Myocardial infarction. LAD Left anterior descending artery. LCX Left circumflex. RCA Right coronary artery. FFR Fractional flow reserve. PCI Percutaneous coronary interventions. SD Standard deviation.

High post-PCI FFR was defined using FFR more than 0.83 and 0.93 cutoff for LAD and non-LAD, respectively.

* Post PCI FFR minus pre-PCI FFR.

** Post PCI FFR minus pre-PCI FFR / (1 minus pre-PCI FFR).

¶ Data available for 526 patients.

¶¶ Data available for 1,533 patients.

§ Data available for 1,822 vessels.

§§ Data available for 2,181 vessels.

§§§ Data available for 1,503 vessels.

§§§§ Data available for 1,481 vessels.

Figure 1. Overview of included studies with post-PCI FFR and functional gain stratified by vessel.

In the top panel, the type of study (randomized vs. observational), study name and number of patients and vessels included in the present analysis.

In the lowest panels, A) shows the distribution of post-PCI FFR stratified by coronary artery, B) box plot of post-PCI FFR stratified by coronary artery. The thick black line in the box plot represents the median value, the box limits the 25th and 75th percentile, and the vertical line the range of the values and C) functional gain (post-PCI FFR minus pre-PCI FFR) stratified per coronary artery.

Randomized Clinical Trials

Observational studies

| FAME 1 | FAME 2 | TARGET-FFR | DOCTORS | PRECISE PCI PLAN | DEFINE FLOW | ARKANSAS Registry | COE-PERSPECTVE | 3V FFR FRIENDS |

352 patients
496 vessels

287 patients
324 vessels

239 patients
239 vessels

151 patients
240 vessels

108 patients
111 vessels

49 patients
50 vessels

566 patients
602 vessels

742 Patients
937 Vessels
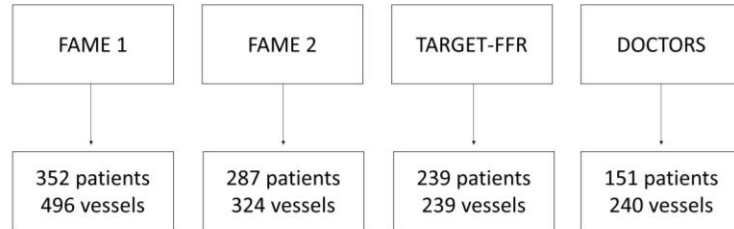
266 Patients
337 Vessels
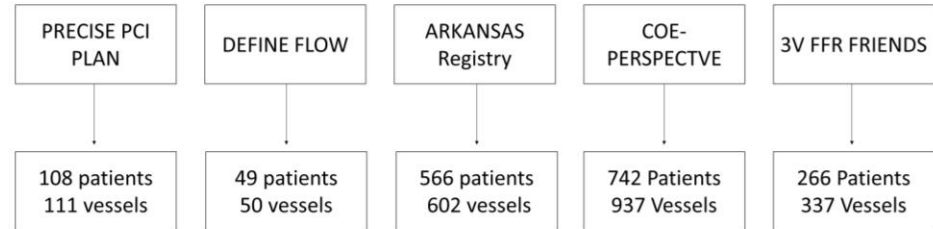
Total 9 studies comprising 3.336 post-PCI FFR measurements in 2.760 patients

A

LAD
0.86 ± 0.06
0.86 [0.82 – 0.90]

LCX
0.93 ± 0.06
0.94 [0.89 – 0.97]

RCA
0.91 ± 0.06
0.92 [0.88 – 0.96]

FFR post PCI

B

Vessel

C

LAD
0.20 ± 0.13
0.16 [0.10 – 0.26]

LCX
0.28 ± 0.15
0.25 [0.17 – 0.38]

RCA
0.27 ± 0.16
0.23 [0.14 – 0.38]

Delta FFR

LAD   LCX   RCA
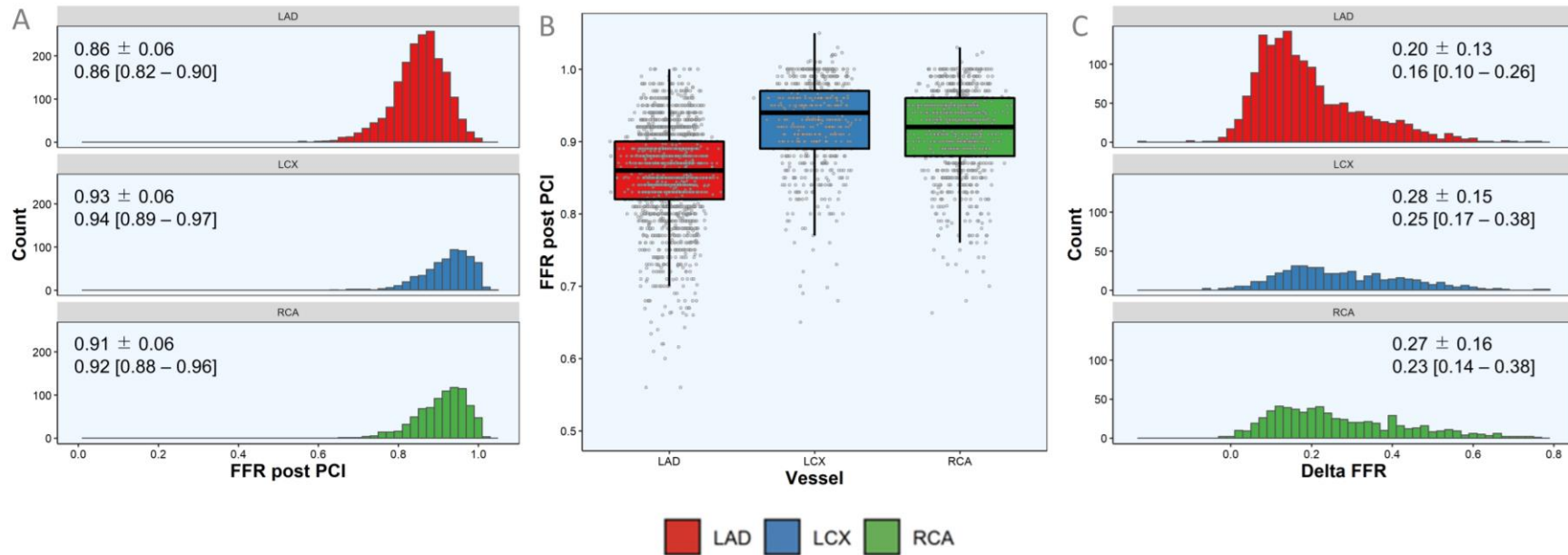
Figure 2. Receiver-operating characteristic (ROC) curves of post-PCI FFR to predict target vessel failure in all vessels and stratified by LAD versus non-LAD.
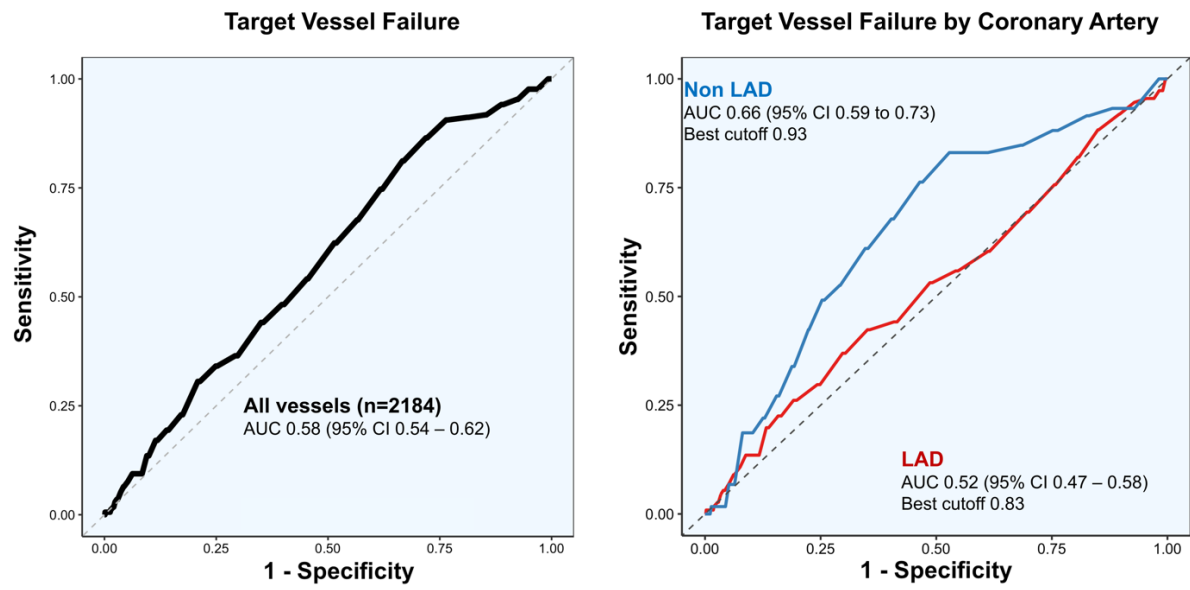
Figure 3. Risk of target vessel failure according to post-PCI FFR value stratified by vessel. In the top panel, Kaplan-Meier curves for target vessel failure (TVF) in vessels with low FFR (black) and high (purple) post-PCI FFR. From left to right, comparisons of TVF in vessels with low vs. high post-PCI FFR, including all vessels, LAD, and non-LAD, are displayed. Post-PCI FFR cut-off were 0.83 and 0.93 for LAD and non-LAD, respectively. The lowest panel shows the distribution of post-PCI values and risk of TVF. The colors (red, blue and green) identify the tertiles of post-PCI FFR in all vessels, LAD, and non-LAD, respectively. The grey bars depict the distribution of events. The best fit line of the logistic regression analysis is shown with its confidence interval (yellow shade).
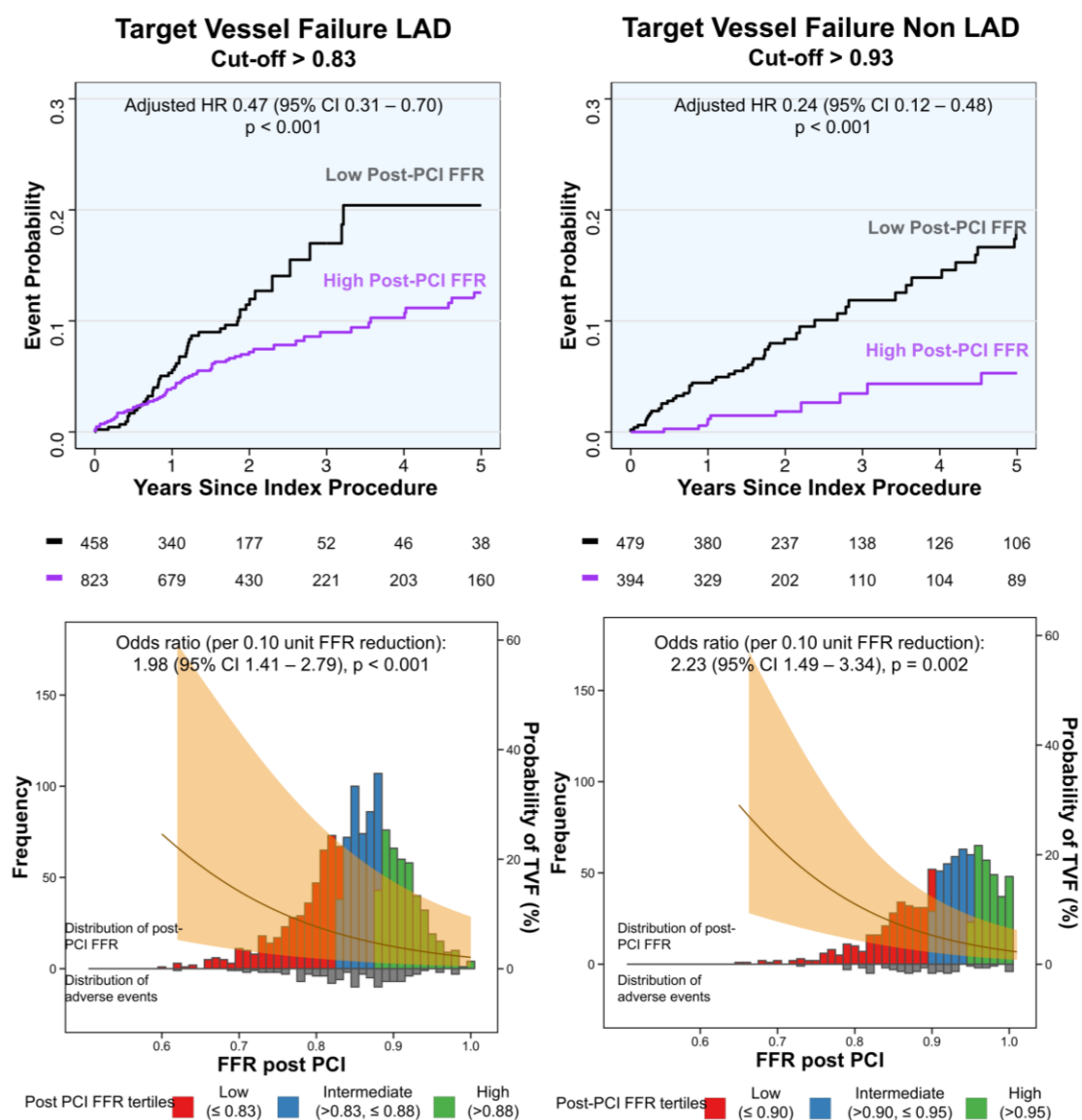
Figure 4. Target vessel revascularization, clinically-indicated target-vessel myocardial infarction and cardiac death in patients with high and low post-PCI FFR.

Each row shows a component of target vessel failure (TVF); from top to bottom target vessel revascularisation, target vessel myocardial infarction and cardiac death. From left to right, all coronary vessels, only LAD and, in the right non-LAD. Patients with high post-PCI FFR are depicted by the purple line, whereas low post-PCI in represented by a black line in the survival curves. Low and high post-PCI FFR was defined using 0.830 and 0.93 cutoff for LAD and non-LAD, respectively.
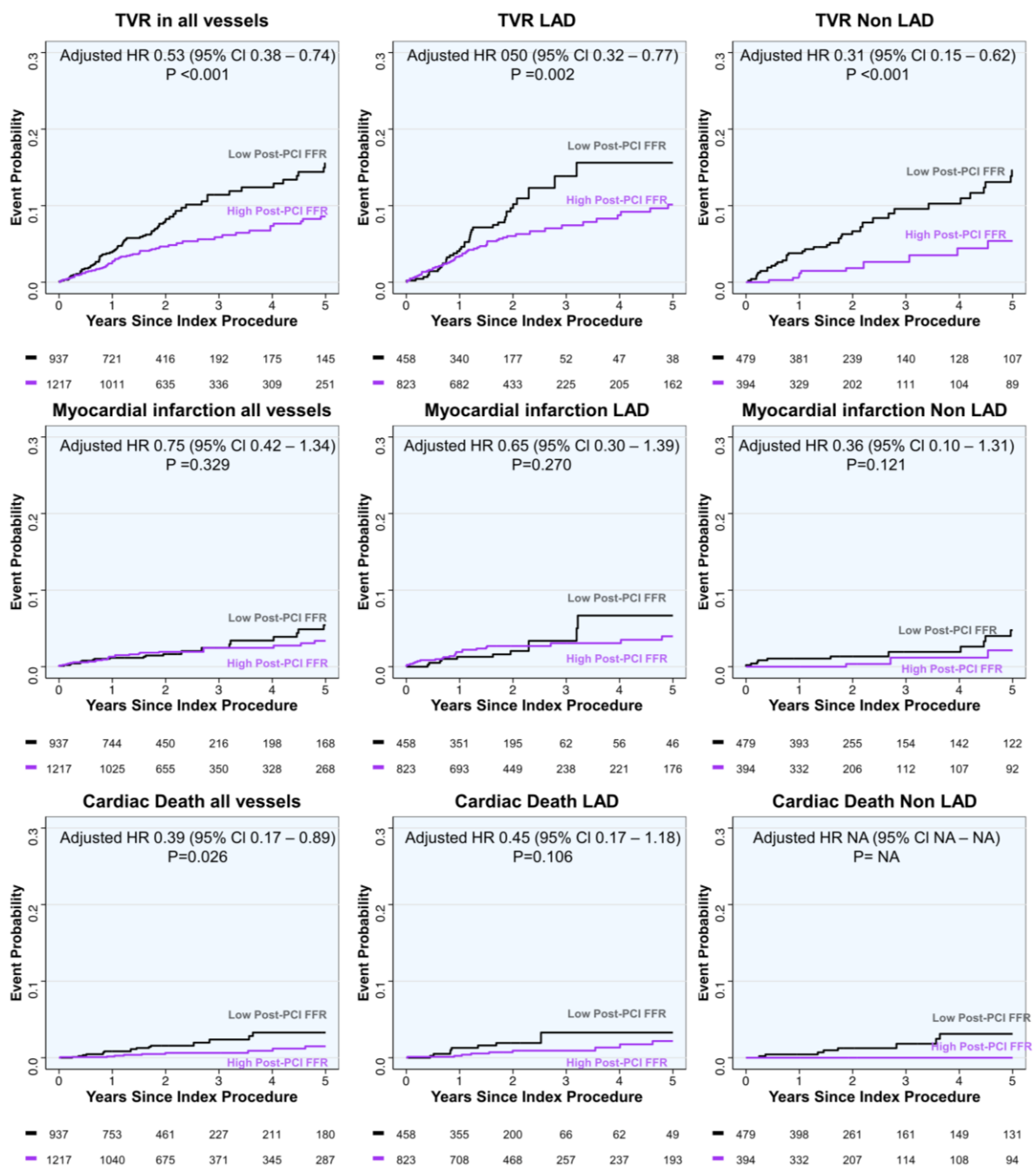
Figure 5. Predictive capacity of post-PCI FFR for cardiac death and myocardial infarction and survival stratified by high and low post-PCI FFR. The top panel shows the ROC curves for the ability of post-PCI FFR to predict cardiac death and myocardial infarction. The bottom panel shows the Kaplan-Meier curves stratified by high or low post-PCI FFR in all vessel, LAD and non-LAD.

Cardiac Death or Myocardial Infarction

All vessels (n=2184)
AUC 0.56 (95% CI 0.49 – 0.62)
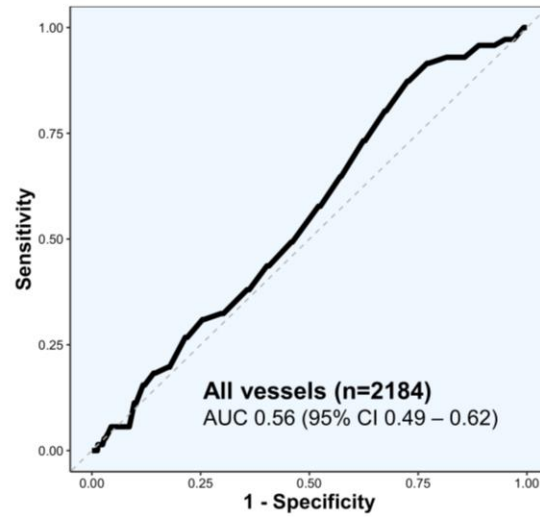
Cardiac Death or Myocardial Infarction by Coronary Artery

LAD: AUC 0.52 (95%CI 0.43 - 0.60)
Non-LAD: AUC 0.64 (95%CI 0.53-0.75)
P-value LAD vs non-LAD= 0.074

cat — LAD — non_LAD
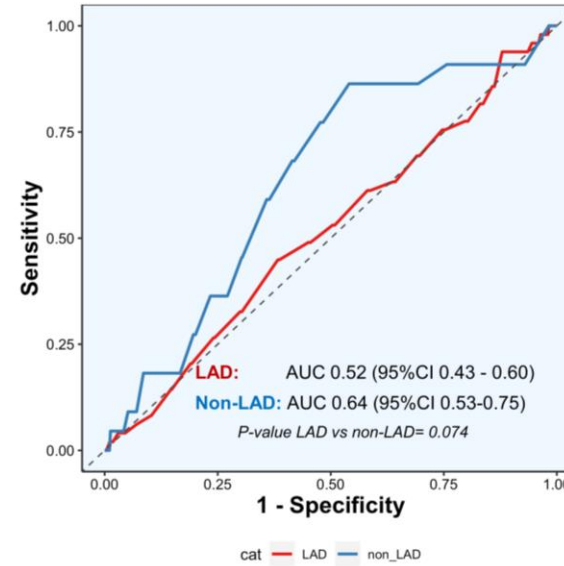
Cardiac Death or Myocardial Infarction in all vessels

Adjusted HR 0.58 (95% CI 0.36– 0.93)
P =0.025

Low Post-PCI FFR
High Post-PCI FFR
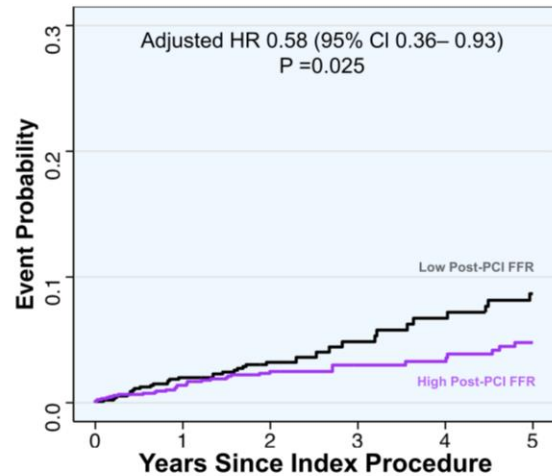
| 937 | 743 | 449 | 215 | 197 | 167 |
| 1217 | 1026 | 656 | 351 | 329 | 269 |

Cardiac Death or Myocardial Infarction in LAD

Adjusted HR 0.53 (95% CI 0.29 – 0.97)
P =0.039

Low Post-PCI FFR
High Post-PCI FFR
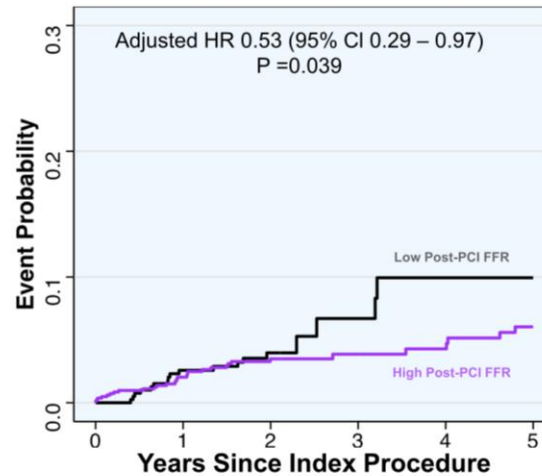
| 458 | 350 | 194 | 61 | 55 | 45 |
| 823 | 694 | 450 | 239 | 222 | 177 |

Cardiac Death or Myocardial Infarction in Non LAD

Adjusted HR 0.20 (95% CI 0.06 – 0.67)
P =0.009

Low Post-PCI FFR
High Post-PCI FFR
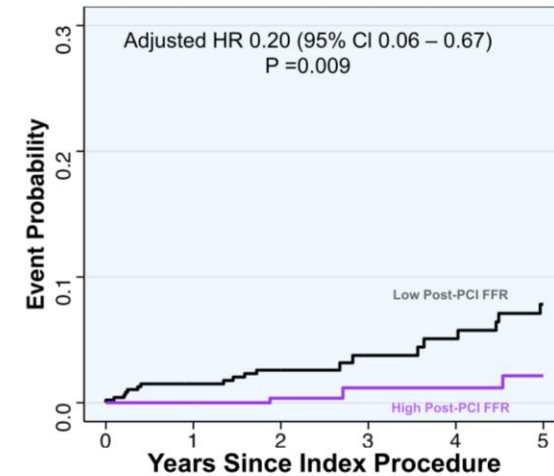
| 479 | 393 | 255 | 154 | 142 | 122 |
| 394 | 332 | 206 | 112 | 107 | 92 |

113

References

1.   Pijls NH, van Son JA, Kirkeeide RL, De Bruyne B, Gould KL. Experimental basis of determining maximum coronary, myocardial, and collateral blood flow by pressure measurements for assessing functional stenosis severity before and after percutaneous transluminal coronary angioplasty. *Circulation*. Apr 1993;87(4):1354-67.

2.   De Bruyne B, Baudhuin T, Melin JA, et al. Coronary flow reserve calculated from pressure measurements in humans. Validation with positron emission tomography. *Circulation*. Mar 1994;89(3):1013-22. doi:10.1161/01.cir.89.3.1013

3.   Knuuti J, Wijns W, Saraste A, et al. 2019 ESC Guidelines for the diagnosis and management of chronic coronary syndromes: The Task Force for the diagnosis and management of chronic coronary syndromes of the European Society of Cardiology (ESC). *European heart journal*. 2019;doi:10.1093/eurheartj/ehz425

4.   van Nunen LX, Zimmermann FM, Tonino PA, et al. Fractional flow reserve versus angiography for guidance of PCI in patients with multivessel coronary artery disease (FAME): 5-year follow-up of a randomised controlled trial. *Lancet (London, England)*. Nov 7 2015;386(10006):1853-60. doi:10.1016/s0140-6736(15)00057-4

5.   Zimmermann FM, Omerovic E, Fournier S, et al. Fractional flow reserve-guided percutaneous coronary intervention vs. medical therapy for patients with stable coronary lesions: meta-analysis of individual patient data. *European Heart Journal*. 2018;40(2):180-186. doi:10.1093/eurheartj/ehy812

6.   Piroth Z, Toth GG, Tonino PAL, et al. Prognostic Value of Fractional Flow Reserve Measured Immediately After Drug-Eluting Stent Implantation. *Circulation Cardiovascular interventions*. Aug 2017;10(8)doi:10.1161/circinterventions.116.005233

7.   Agarwal SK, Kasula S, Hacioglu Y, Ahmed Z, Uretsky BF, Hakeem A. Utilizing Post-Intervention Fractional Flow Reserve to Optimize Acute Results and the Relationship to Long-Term Outcomes. *JACC Cardiovasc Interv*. May 23 2016;9(10):1022-31. doi:10.1016/j.jcin.2016.01.046

8.   Jeremias A, Davies JE, Maehara A, et al. Blinded Physiological Assessment of Residual Ischemia After Successful Angiographic Percutaneous Coronary Intervention: The DEFINE PCI Study. *JACC Cardiovasc Interv*. Oct 28 2019;12(20):1991-2001. doi:10.1016/j.jcin.2019.05.054

9.   Meneveau N, Souteyrand G, Motreff P, et al. Optical Coherence Tomography to Optimize Results of Percutaneous Coronary Intervention in Patients with Non-ST-Elevation Acute Coronary Syndrome: Results of the Multicenter, Randomized DOCTORS Study (Does Optical Coherence Tomography Optimize Results of Stenting). *Circulation*. Sep 27 2016;134(13):906-17. doi:10.1161/circulationaha.116.024393

10.   Burzotta F, Leone AM, Aurigemma C, et al. Fractional Flow Reserve or Optical Coherence Tomography to Guide Management of Angiographically Intermediate Coronary Stenosis: A Single-Center Trial. *JACC Cardiovascular interventions*. Jan 13 2020;13(1):49-58. doi:10.1016/j.jcin.2019.09.034

11.   Collison D, Didagelos M, Aetesam-Ur-Rahman M, et al. Post-stenting fractional flow reserve vs coronary angiography for optimisation of percutaneous coronary intervention: TARGET-FFR trial. *European heart journal*. Jul 19 2021;doi:10.1093/eurheartj/ehab449

12.   Diletti R, Masdjedi K, Daemen J, et al. Impact of Poststenting Fractional Flow Reserve on Long-Term Clinical Outcomes: The FFR-SEARCH Study. *Circ Cardiovasc Interv*. Mar 2021;14(3):e009681. doi:10.1161/circinterventions.120.009681

13.   Hwang D, Lee JM, Lee HJ, et al. Influence of target vessel on prognostic relevance of fractional flow reserve after coronary stenting. *EuroIntervention*. Aug 29 2019;15(5):457-464. doi:10.4244/eij-d-18-00913

14.   Tonino PA, De Bruyne B, Pijls NH, et al. Fractional flow reserve versus angiography for guiding percutaneous coronary intervention. *The New England journal of medicine*. Jan 15 2009;360(3):213-24. doi:10.1056/NEJMoa0807611

15.   De Bruyne B, Pijls NH, Kalesan B, et al. Fractional flow reserve-guided PCI versus medical therapy in stable coronary disease. *N Engl J Med*. Sep 13 2012;367(11):991-1001. doi:10.1056/NEJMoa1205361

16.   Nagumo S, Collet C, Norgaard BL, et al. Rationale and design of the precise percutaneous coronary intervention plan (P3) study: Prospective evaluation of a virtual computed tomography-based percutaneous intervention planner. *Clin Cardiol*. Mar 3 2021;doi:10.1002/clc.23551

17.   Lee JM, Koo BK, Shin ES, et al. Clinical implications of three-vessel fractional flow reserve measurement in patients with coronary artery disease. *Eur Heart J*. Mar 14 2018;39(11):945-951. doi:10.1093/eurheartj/ehx458

18.   Johnson NP, Matsuo H, Nakayama M, et al. Combined Pressure and Flow Measurements to Guide Treatment of Coronary Stenoses. *JACC: Cardiovascular Interventions*. 2021;14(17):1904-1913. doi:doi:10.1016/j.jcin.2021.07.041

19.   Ando H, Takashima H, Suzuki A, et al. Impact of lesion characteristics on the prediction of optimal poststent fractional flow reserve. *Am Heart J*. Dec 2016;182:119-124. doi:10.1016/j.ahj.2016.09.015

20.   Sonck J, Nagumo S, Norgaard BL, et al. Clinical Validation of a Virtual Planner for Coronary Interventions Based on Coronary CT Angiography. *JACC: Cardiovascular Imaging*. 0(0)doi:doi:10.1016/j.jcmg.2022.02.003

21.   Neleman T, van Zandvoort LJC, Tovar Forero MN, et al. FFR-Guided PCI Optimization Directed by High-Definition IVUS Versus Standard of Care: The FFR REACT Trial. *JACC Cardiovasc Interv*. Aug 22 2022;15(16):1595-1607. doi:10.1016/j.jcin.2022.06.018

22.   Hwang D, Koo BK, Zhang J, et al. Prognostic Implications of Fractional Flow Reserve After Coronary Stenting: A Systematic Review and Meta-analysis. *JAMA Netw Open*. Sep 1 2022;5(9):e2232842. doi:10.1001/jamanetworkopen.2022.32842

23.   Leone AM, De Caterina AR, Basile E, et al. Influence of the amount of myocardium subtended by a stenosis on fractional flow reserve. *Circ Cardiovasc Interv*. Feb 2013;6(1):29-36. doi:10.1161/circinterventions.112.971101

24.   Leone AM, De Caterina AR, De Maria GL, et al. Three-dimensional quantitative coronary angiography and quantification of jeopardised myocardium to predict functional significance of intermediate coronary artery stenosis. *EuroIntervention*. Jul 2015;11(3):308-18. doi:10.4244/eijv11i3a58

25.   Mileva N, Ohashi H, Paolisso P, et al. Relationship between coronary volume, myocardial mass, and post-PCI fractional flow reserve. *Catheter Cardiovasc Interv*. Apr 27 2023;doi:10.1002/ccd.30664

26.   Kawaguchi Y, Ito K, Kin H, et al. Impact of Hydrostatic Pressure Variations Caused by Height Differences in Supine and Prone Positions on Fractional Flow Reserve Values in the Coronary Circulation. *J Interv Cardiol*. 2019;2019:4532862. doi:10.1155/2019/4532862

27.   Härle T, Luz M, Meyer S, et al. Influence of hydrostatic pressure on intracoronary indices of stenosis severity in vivo. *Clin Res Cardiol*. Mar 2018;107(3):222-232. doi:10.1007/s00392-017-1174-2

28.   Üveges Á, Tar B, Jenei C, et al. The impact of hydrostatic pressure on the result of physiological measurements in various coronary segments. *Int J Cardiovasc Imaging*. Jan 2021;37(1):5-14. doi:10.1007/s10554-020-01971-w

29.   Courtois M, Fattal PG, Kovács SJ, Jr., Tiefenbrunn AJ, Ludbrook PA. Anatomically and physiologically based reference level for measurement of intracardiac pressures. *Circulation*. Oct 1 1995;92(7):1994-2000. doi:10.1161/01.cir.92.7.1994

Chapter 6. Fractional Flow Reserve-Guided Stent Optimisation in Focal and Diffuse Coronary Artery Disease.

Ohashi H, Collison D, Mizukami T, Didagelos M, Sakai K, Aetesam-Ur-Rahman M, Munhoz D, McCartney P, Ford TJ, Lindsay M, Shaukat A, Rocchiccioli P, Brogan R, Watkins S, McEntegart M, Good R, Robertson K, O'Boyle P, Davie A, Khan A, Hood S, Eteiba H, Amano T, Sonck J, Berry C, De Bruyne B, Oldroyd KG, Collet C.

Abstract: Assessing coronary physiology after stent implantation facilitates optimisation of percutaneous coronary intervention (PCI). Coronary artery disease (CAD) patterns can be characterised by the pullback pressure gradient (PPG) index. The impact of focal vs diffuse disease on the effectiveness of a physiology-guided incremental optimisation strategy (PIOS) is unknown. This is sub-study of the TARGET-FFR randomised clinical trial (NCT03259815). The study protocol directed that optimisation be attempted for patients in the PIOS arm when post-PCI FFR was < 0.90. 114 patients (n=61 PIOS and 53 controls) with both pre-PCI fractional flow reserve (FFR) pullbacks and post-PCI FFR were included. A PPG ≥ 0.74 defined focal CAD. PPG was correlated significantly with post-PCI FFR (r = 0.43, 95% CI 0.26 to 0.57, p-value < 0.001) and normalised delta FFR (r = 0.49, 95% CI 0.34 to 0.62, p-value < 0.001). PIOS was more frequently applied to vessels with diffuse CAD (6% focal vs. 42% diffuse, p-value = 0.006). In patients randomised to PIOS, those with focal disease achieved higher post-PCI FFR than patients with diffuse CAD (0.93 ± 0.05 vs 0.83 ± 0.07, p<0.001). There was a significant interaction between CAD patterns and the randomisation arm for post-PCI FFR (p-value for interaction = 0.004). Physiology-guided stent optimisation was applied more frequently to vessels with diffuse disease; however, patients with focal CAD at baseline achieved higher post-PCI FFR.

1. Introduction

Optimisation of percutaneous coronary intervention (PCI) is advocated to reduce stent failure and improve patient outcomes[1]. After stent implantation, intravascular imaging can be used to optimise stent expansion, correct malapposition, and detect residual disease[2,3]. Fractional flow reserve (FFR) can also be used to optimise PCI by identifying physiologically sub-optimal results and guide additional intervention[4,5]. Performing additional interventions in segments of residual pressure losses translates into higher post-PCI FFR values, which may positively influence prognosis[4,6,7]. Recently, the TARGET-FFR (Trial of Angiography vs. Pressure-Ratio-Guided Enhancement Techniques-Fractional Flow Reserve) trial assessed the efficacy of a routine post-PCI physiology-guided incremental optimisation strategy (PIOS) in achieving optimal post-PCI FFR results (FFR $\geq$ 0.90). Patients randomised to the PIOS arm with post-PCI FFR < 0.90 were treated according to a pre-specified protocol based on the findings of the post-PCI FFR pullback (Figure S1). Whilst PIOS improved post-PCI FFR and reduced the proportion of patients with a post-PCI FFR $\leq$ 0.80, there was no significant difference between groups in the proportion of patients achieving an optimal post FFR value of $\geq$ 0.90[5]. The pullback pressure gradient (PPG) is a new metric derived from FFR pullbacks that can differentiate focal from diffuse coronary artery disease (CAD)[8]. Although CAD patterns impact post-PCI physiology, their influence on the efficacy of PCI optimisation is unknown. Thus, we sought to investigate the impact of baseline CAD patterns, defined by the PPG, on the effectiveness of physiology-guided PCI optimisation in the TARGET-FFR trial.

2. Materials and Methods

2.1. Study population

This study is a post hoc analysis of the TARGET-FFR study. Briefly, TARGET-FFR was a prospective, single-centre, randomized, controlled, parallel-group, blinded clinical trial conducted at the Golden Jubilee National Hospital in Glasgow, UK[5]. The study is registered at ClinicalTrials.gov identifier NCT03259815. Patients undergoing PCI for either stable angina, medically-stabilised non-ST-segment elevation myocardial infarction (NSTEMI), or staged completion of non-culprit vessel revascularization following either NSTEMI or ST-segment elevation myocardial infarction (STEMI) were eligible for inclusion. A list of the inclusion and exclusion criteria is provided in Table S1. All patients signed informed consent before any study procedure. Patients were randomised to either PIOS or control group[5]. For the present analysis, patients with both pre-PCI FFR pullbacks and post-PCI FFR were considered for

inclusion. Coronary physiology data were analysed by a core laboratory (CoreAalst BV, Aalst, Belgium).

2.2. Procedures

The details of the coronary physiology measurements and PCI have been described previously.[5] FFR measurements were performed using the PressureWire X Guidewire (Abbott Laboratories, IL, USA). Following administration of a 200 ug bolus of intracoronary nitrate, the pressure wire sensor was positioned at the tip of the guide catheter and equalised with the aortic pressure. The pressure wire was then advanced to position the sensor in the distal third of the vessel. Hyperaemia was induced by infusion of adenosine into an antecubital vein at a rate of 140 ug/kg/min[9]. Pre-PCI FFR pullbacks were performed manually, their use and interpretation were left to the operator's discretion. After angiographically successful PCI, patients were randomised 1:1 to either the PIOS or control groups. In patients randomised to the PIOS group with post-PCI FFR <0.90, operators planned additional interventions based on the findings of the post-PCI FFR pullback according to the incremental optimisation protocol (Figure S1). Following these additional optimisation measures, FFR was re-assessed, and the procedure was completed. In the control group, post-PCI FFR and pullback information were acquired but concealed from the operator. The use of adjunctive intravascular imaging was left to the operator's discretion.

2.3. Characterisation of CAD Patterns

The PPG index was calculated off line from the manual pre-PCI FFR pullbacks. Details of the PPG calculation have been described in detail elsewhere[8]. In brief, the PPG combines two parameters extracted from FFR pullback curves 1) the maximal pressure gradient over 20% of the pullback duration, and 2) the length of functional disease computed using a FFR threshold per unit of time. PPG values close to 1 represent focal disease and values close to 0 characterise diffuse CAD. The PPG was calculated using a commercially available console (Coroflow v3.5, Coroventis Research AP, Uppsala, Sweden). Pressure tracings with ventricularisation, absence of a dicrotic notch, drift of more than 0.05 FFR units, unstable hyperaemic conditions during the pullback manoeuvre, pullback duration less than 15 seconds, and pullback curves with major artifacts were excluded. Delta FFR was normalised by pre-PCI FFR ([final post-PCI FFR minus pre-PCI FFR divided by one minus pre-PCI FFR] by a factor of one hundred). Post-PCI FFR pullbacks were also quantitatively analysed to determine the magnitude of residual focal pressure gradients. The residual PPG was defined as the maximal pressure gradient, in absolute FFR units, over 20% of the duration of the pullback curve (i.e.,

the first component of the PPG equation). To assesses the outcomes of PIOS stratified by CAD patterns, the population was divided into tertiles according to the baseline PPG distribution, and the highest tertile considered as focal disease, whereas the intermediate and low tertiles, comprising patients with both mixed (focal and diffuse) and diffuse CAD, were considered as diffuse disease[10]. The objective of the present analysis was to investigate the effect of PPG-defined focal vs diffuse disease on the efficacy of PIOS in improving post-PCI FFR.

2.4. Statistical Analysis

Data are expressed as mean ± SD and median [interquartile range] for normally and non-normally distributed data, respectively. Categorical variables are expressed as frequencies and percentages (%). Continuous variables were compared using the Student's t-test (or Mann–Whitney tests as appropriate), and categorical variables were compared using the Chi-square (or Fisher's exact test as appropriate). Differences across the groups were compared with the Kruskal-Wallis H test. Predictors of the post-PCI FFR value were assessed using univariate and multivariate regression analyses. The variables included in the multivariate analysis were selected based on their known association with final post-PCI FFR[11,12]. A formal interaction testing was performed between the randomization arm (PIOS or controls) and PPG for the outcome of post-PCI FFR. Receiver operating characteristic (ROC) curve analyses were used to assess the capacity of residual PPG for predicting final post-PCI FFR ≥ 0.90. All analyses were performed in the intention-to-treat population in patients with pre-PCI FFR pullbacks suitable for PPG calculation. A 2-sided p-value of 0.05 or less was considered statistically significant. All statistical analyses were performed with R statistical software (R Foundation for Statistical Computing, Vienna, Austria).

3. Results

3.1. Study Population

Between February 2018 and November 2019, 260 patients were randomized. Of these, 192 patients had pre-PCI FFR pullbacks (PIOS n=98 and control n=94). Finally, 114 patients (61 patients in the PIOS group and 53 patients in the control group) with pullbacks of sufficient quality for PPG calculation were included in the analysis. The study flowchart is shown in **Figure S2.**

3.2. Baseline Characteristics

Baseline clinical, procedural, and functional characteristics stratified by the randomization arms are shown in **Table 1**. The mean age was 59.8 ± 8.1 years, 85.1% were male, and the LAD was the most frequently treated vessel in 63.2%. There were no significant

differences in clinical, procedural, or functional baseline characteristics between PIOS and controls. Overall, the mean FFR increased after PCI from 0.62 ± 0.14 to 0.85 ± 0.07 ($p < 0.001$). There was no difference in the final post-PCI FFR between PIOS and controls (0.86 ± 0.08 vs. 0.85 ± 0.07, p-value = 0.27).

3.3. Baseline CAD patterns and final post-PCI FFR

The mean PPG value was 0.65 ± 0.14, and focal disease was defined as PPG ≥ 0.74 (highest tertile). The PPG was moderately correlated with normalised delta FFR and final post-PCI FFR (**Figure 1**). Patients with focal disease achieved significantly larger changes in FFR after PCI leading to higher final post-PCI FFR than patients with diffuse CAD (normalised delta FFR $72.0 \pm 20.3\%$ in focal vs $52.5 \pm 19.2\%$ in diffuse, $p<0.001$). In addition, patients with focal CAD achieved higher post-PCI CFR (**Table S2**). The proportion of patients achieving optimal final post PCI FFR ≥ 0.90 was significantly higher in focal disease (52.6% vs. 15.8%, p-value < 0.001). In the multivariate analysis, pre-PCI FFR and PPG were independently associated with final post-PCI FFR (**Table S3**).

3.4. Stent optimisation in focal and diffuse disease

Post-PCI physiological results stratified by CAD patterns and randomisation arm are shown in **Table 2**. Immediately after stenting, patients with focal CAD had higher post-PCI FFR compared to diffuse disease (0.93 ± 0.05 focal PIOS vs. 0.83 ± 0.07 diffuse PIOS vs. 0.87 ± 0.07 focal controls vs. 0.83 ± 0.07 diffuse controls). In the PIOS arm, optimisation was applied more frequently to vessels with diffuse CAD (6% (1/18) vs. 42% (18/43), p-value = 0.006). In the 18 patients with diffuse CAD in the PIOS group who received additional optimisation, PIOS, FFR improved from 0.76 ± 0.09 to 0.83 ± 0.05, p-value < 0.01 (**Figures 2 and Table S4**). However, when comparing post-PCI FFR values between patients with diffuse disease, PIOS did not result in higher post-PCI FFR compared to controls (0.83 ± 0.07 PIOS vs. 0.83 ± 0.07 control, p-value = 0.90, **Figure S3**). In contrast, patients with focal CAD achieved higher post-PCI FFR, and those with focal CAD randomized to PIOS achieved significantly higher final post-PCI FFR (0.93 ± 0.05 focal PIOS vs 0.83 ± 0.07 diffuse PIOS vs 0.87 ± 0.07 focal controls vs 0.83 ± 0.07 diffuse controls; p-value<0.001, **Figure S3**). Moreover, there was a significant interaction between PPG and the randomization arm for post-PCI FFR (p-value for interaction = 0.004; **Figure 3**). The proportion of patients achieving post-PCI FFR ≥ 0.90 stratified by CAD patterns and randomization arm is shown in **Figure S4.**

3.5. Residual PPG and final post-PCI FFR

The mean residual diameter stenosis was $15.0 \pm 8.8\%$ and there was no difference between focal and diffuse CAD ($16.0 \pm 9.9\%$ focal vs. $14.5 \pm 8.2\%$ diffuse, p-value = 0.41) or between PIOS and controls ($14.5 \pm 9.2\%$ PIOS vs. $15.6 \pm 8.4\%$ control, p-value = 0.50). The mean residual PPG derived from post-PCI FFR pullbacks was 0.07 ± 0.04. Residual PPG strongly conditioned final post-PCI FFR ($R^2 = 0.64$, 95% CI 0.50 to 0.74, P <0.001; Figure 4A). Residual PPG was not significantly different between patients randomised to PIOS versus controls (0.06 ± 0.04 PIOS vs. 0.07 ± 0.04 controls, p-value = 0.06). However, patients with focal CAD randomised to PIOS had the lowest residual PPG (0.04 ± 0.02 focal PIOS vs. 0.07 ± 0.04 focal control, 0.07 ± 0.04 diffuse PIOS vs. 0.08 ± 0.04 diffuse control, ANOVA p-value = 0.008, Figure 4B). Residual PPG predicted final post-PCI FFR ≥ 0.90 with an AUC of 0.93 (95% CI: 0.87–0.99, p < 0.001, Figure 4C).

3.6. Clinical outcomes

At a median follow-up of 2 years, only one target vessel failure (TVF) occurred. This patient, randomised to PIOS with focal disease, suffered a presumed cardiac death 17 months after the procedure. There were no differences in TVF between PIOS and controls or between patients with focal or diffuse CAD.

4. Discussion

The main findings of the present study can be summarized as follows: 1) CAD patterns, defined by the PPG index, correlated with post-PCI FFR and delta FFR. Patients with focal disease achieved higher post-PCI FFR compared to those with diffuse CAD; 2) Physiology-guided PCI optimisation was more frequently applied to patients with diffuse CAD (as the incidence of post-PCI FFR < 0.90 was higher). However, despite higher use of optimisation, final FFR values in patients with diffuse disease did not differ between PIOS and controls; 3) There was a significant interaction between the PPG and the randomization arm for post-PCI FFR; patients with focal disease randomized to PIOS achieved the highest post-PCI FFR and 4) post-PCI FFR was largely determined by focal residual pressure gradients, the residual PPG index, which was significantly lower in patients with focal disease randomised to stent optimisation.

The PPG is the first quantitative metric to differentiate focal from diffuse disease. In line with previous publications, the PPG correlated with post-PCI and delta FFR[13]. Patients with high PPG (focal disease) achieved significantly higher post-PCI FFR and delta FFR. We demonstrated that improvement in coronary blood flow with PCI partially depends on the baseline pattern of disease. The higher post-PCI FFR in focal disease was observed

independent of the application of physiology-guided stent optimisation. In contrast, in diffuse disease, additional optimisation had limited value in terms of post-PCI FFR and in this group the final FFR was similar between patients randomized to PIOS and controls. The advent of PPG, a reproducible metric for quantifying the physiological pattern of CAD, will facilitate the study of treatment options stratified by disease patterns.

TARGET-FFR was the first randomized trial assessing the feasibility of routine post-PCI FFR-guided optimisation strategy[14]. As shown in this study, physiologic outcomes after PCI are influenced by the baseline CAD pattern. By design, TARGET-FFR applied of physiology guided stent optimisation to patients with predominantly diffuse disease because these additional manoeuvres were triggered by low post-PCI FFR, a proxy of diffuse disease. In addition, the high proportion of vessels with diffuse CAD in the study limited the efficacy of PIOS in improving the post-PCI FFR. Likewise, the mechanism leading to higher post-PCI FFR in patients with focal CAD randomized to PIOS is likely unrelated to the application of optimisation manoeuvres since only one patient with focal CAD in the PIOS group received an additional intervention. Nonetheless, it can be hypothesised that patients with focal disease pre-PCI and a suboptimal functional result after stenting might have additional targets for optimisation (e.g., unmasked focal pressure gradients either arising from the untreated segments) may lead to improved post-PCI physiology. The hypothesis that functionally-guided PCI optimisation is more effective in focal vs diffuse disease requires further investigation.

There are mainly three mechanisms leading to unsatisfactory PCI results. First, the presence of residual pressure gradients within the stented segment, mainly associated with stent under-expansion or issues at the stent edges[15,16]. Second, focal pressure gradients distal or proximal to the treated segment; and third, diffuse residual disease. The first two can potentially be addressed by additional post-dilation or PCI with a resultant improvement in intracoronary haemodynamics. In this study, half of the cases were optimised with additional in stent post-dilation and half underwent an additional PCI. Nonetheless, in the setting of diffuse disease optimisation manoeuvres will result in minor coronary physiology improvement as shown in this cohort by the little increase in FFR from 0.80 ± 0.09 immediately after stenting to 0.83 ± 0.07 after optimisation. In this work, we also introduced residual PPG as a metric to quantify residual pressure gradients. Distinctive from the original study protocol, where residual focal pressure gradients were assessed visually, the residual PPG provides an automatic quantification of residual focal gradients after stenting. This new approach leverages on the

original PPG formula adapted to the post-PCI setting to quantify focal pressure drops in absolute FFR units. As anticipated, residual PPG was strongly associated with post-PCI FFR with an AUC of 0.93 (95% CI: 0.87–0.99). Interestingly, residual PPG was significantly lower in patients with focal CAD assigned to PIOS highlighting the influence of the baseline pattern of disease and potentially the value of optimisation in the magnitude of residual focal gradients after PCI. The clinical relevance of focal residual trans-lesional gradients using angiography-derived FFR software in the post-PCI phase has previously been suggested by one study[17]. Nonetheless, further studies are required to better understand the clinical implications of residual PPG better. The importance of this study is identifying which patients benefit from additional physiology-guided optimization. Patients randomized to PIOS with focal CAD patterns achieved greater improvement in post-PCI FFR when compared to patients with diffuse CAD. Therefore, CAD pattern by PPG before stenting identifies patients likely to achieve high post-PCI FFR.

This study has several limitations. First, pre-PCI FFR pullbacks were only performed in 74% (192/260) of cases, of which 59.3% (114/192) were deemed suitable for PPG calculation. However, this attrition of the sample size was equally distributed between the two arms, and the benefit of randomisation in terms of baseline risk distribution was preserved. Second, the study was not powered to assess clinical outcomes; the primary objective was post-PCI FFR, a surrogate endpoint of adverse events after PCI. Third, the PPG and residual PPG were calculated off-line, limiting the evaluation of the clinical utility of these metrics. Nonetheless, quantification of pullback data has the potential to standardise diagnosis and treatment pathways accounting for CAD patterns and residual disease. Further studies are required to better understand the pattern of CAD assessed by non-invasively assessment through coronary blood flow models[18-20]. Finally, this is a post hoc analysis of randomized clinical trials and all the findings presented in this study should be interpreted as hypothesis generating.

5. Conclusions

Baseline coronary artery disease patterns influence FFR after PCI. Patients with diffuse disease (low PPG) achieve lower post-PCI FFR compared to those with focal CAD. Physiology-guided stent optimisation was applied more frequently to vessels with diffuse disease; however, patients with focal CAD at baseline achieved higher post-PCI FFR. Characterising coronary artery disease patterns with the PPG before stenting identifies patients likely to achieve high post-PCI FFR.

Table 1. Baseline characteristics

Variables	All	PIOS	Control	p-value
N	114	61	53	
Clinical characteristics				
Gender (male), n (%)	97 (85.1)	53 (86.9)	44 (83.0)	0.75
Age (years), mean ± SD	59.8±8.1	59.3±8.0	60.4±8.2	0.45
BMI, mean ± SD	29.7±4.7	29.4±4.3	30.1±5.2	0.46
Family history, n (%)	75 (65.8)	40 (65.6)	35 (66.0)	1.00
Smoking, n (%)	80 (70.2)	44 (72.1)	36 (67.9)	0.78
Hypertension, n (%)	50 (43.9)	29 (47.5)	21 (39.6)	0.51
Dyslipidaemia, n (%)	65 (57.0)	33 (54.1)	32 (60.4)	0.63
Diabetes mellitus, n (%)	23 (20.2)	10 (16.4)	13 (24.5)	0.40
History of stroke, n (%)	7 (6.1)	5 (8.2)	2 (3.8)	0.56
Chronic kidney disease, n (%)	3 (2.6)	2 (3.3)	1 (1.9)	1.00
Prior PCI, n (%)	51 (44.7)	31 (50.8)	20 (37.7)	0.23
Prior MI, n (%)	50 (43.9)	29 (47.5)	21 (39.6)	0.51
Prior CABG, n (%)	0	0	0	NA
Symptomatic angina, n (%)	95 (69.2)	53 (86.9)	42 (79.2)	0.95
CCS I	21 (22.1)	12 (22.6)	9 (21.4)	
CCS II	48 (50.5)	26 (49.1)	22 (52.4)	
CCS III	26 (27.4)	15 (28.3)	11 (26.2)	
CCS IV	0 (0)	0 (0)	0 (0)	
Clinical presentation, n (%)				0.22
Stable angina	29 (25.4)	13 (21.3)	16 (30.2)	
ACS - NSTEMI	44 (38.6)	21 (34.4)	23 (43.4)	
ACS - Unstable Angina	1 (0.9)	1 (1.6)	0 (0.0)	
Staged PCI	40 (35.1)	26 (42.6)	14 (26.4)	
Procedural characteristics				
Vessel, n (%)				0.99
LAD	72 (63.2)	38 (62.3)	34 (64.2)	
Non-LAD	42 (36.8)	23 (37.7)	19 (35.8)	
QCA diameter stenosis (%), mean	61.0	60.9	61.2	0.92
QCA lesion length (mm), median [IQR]	10.8 [7.96, 13.2]	10.7 [8.34, 13.6]	10.9 [6.93, 13.0]	0.73
Intravascular imaging, n (%)	22 (19.3)	10 (16.4)	12 (22.6)	0.55
IVUS, n (%)	19 (86.4)	10 (100)	9 (77.4)	
OCT, n (%)	3 (13.6)	0 (0.0)	3 (23.1)	

Stent diameter (mm), median [IQR]	3.00 [3.0, 3.5]	3.00 [3.0, 3.5]	3.00 [3.0, 3.5]	0.45
Stent length (mm), median [IQR]	32.0 [23.0, 38.0]	32.0 [23.0, 38.0]	28.0 [23.0, 38.0]	0.76
Number of stents per patients, median [IQR]	1.00 [1.00, 2.00]	1.00 [1.00, 2.00]	1.00 [1.00, 2.00]	0.97
Total stent length (mm), median [IQR]	38.0 [25.0, 50.8]	33.0 [28.0, 52.0]	38.0 [24.0, 50.0]	0.76
Physiological characteristics				
Pre-PCI Pd/Pa*, median [IQR]	0.85 [0.75, 0.90]	0.86 [0.81, 0.91]	0.83 [0.72, 0.89]	0.11
Pre-PCI CFR*, median [IQR]	2.03 [1.47, 2.61]	2.11 [1.49, 2.60]	1.99 [1.31, 2.60]	0.43
Pre-PCI IMR*, median [IQR]	22.9 [16.6, 31.8]	24.0 [18.0, 33.5]	21.7 [16.0, 31.3]	0.31
Pre-PCI FFR*, median [IQR]	0.62±0.14	0.65±0.12	0.58±0.15	0.04
Final post PCI FFR*, mean ± SD	0.85±0.07	0.86±0.08	0.85±0.07	0.27
Normalised delta FFR*	59.2±21.6	59.4±20.8	58.9±22.7	0.91
Final post-PCI FFR ≤0.80 (%), n (%)	27 (23.7)	13 (21.3)	14 (26.4)	0.68
Final post-PCI FFR ≥0.80 (%), n (%)	88 (77.2)	48 (78.7)	40 (75.5)	0.85
Final post-PCI FFR ≥0.90 (%), n (%)	32 (28.1)	22 (36.1)	10 (18.9)	0.07
PPG, median [IQR]	0.66 [0.55, 0.78]	0.64 [0.56, 0.79]	0.68 [0.54, 0.79]	0.65
Residual PPG*	0.07±0.04	0.06±0.04	0.07±0.04	0.06

Categorical variables are expressed as number and percentage. Continuous variables are indicated as median (interquartile range). BMI, body mass index; CABG, coronary artery bypass graft; CCS, Canadian cardiovascular society; CFR, coronary flow reserve; FFR, fractional flow reserve; IMR, index of microvascular resistance; IVUS, intravascular ultrasound; LAD, left anterior descending artery; LCX, left circumflex artery; Pa, aortic pressure; PCI, percutaneous coronary intervention; Pd, distal coronary pressure; PDA, posterior descending artery; PLA, posterior lateral artery; PPG, pullback pressure gradient MI, myocardial infarction; NSTE-ACS, non-ST elevation acute coronary syndrome; RCA, right coronary artery; QCA, quantitative coronary angiography; OCT, optical coherence tomography. Normalised delta FFR was normalised by pre-PCI FFR ([final post-PCI FFR minus pre-PCI FFR divided by one minus pre-PCI FFR] by a factor of one hundred). Pre-PCI Pd/Pa*: N=110 (PIOS =60, Control=50); Pre-PCI CFR*: N=107 (PIOS =58, Control=49); Pre-PCI IMR*: N=104 (PIOS =56, Control=48); Pre-PCI FFR*: N=111 (PIOS =61, Control=50); Final post-PCI FFR*: N=114 (PIOS 61, Control 53); Normalised delta FFR*: N=111 (PIOS =61, Control=50); Residual PPG*: N=94 (PIOS =52, Control=42)

Table 2. Comparison of functional characteristics between randomized groups stratified PPG

Variables	PIOS			Controls			p-value***
	Focal CAD	Diffuse CAD	p-value*	Focal CAD	Diffuse CAD	p-value**	
Number, (%)	18 (29.5)	43 (70.5)		20 (37.7)	33 (62.3)		
Vessel (%)			<0.001			<0.001	<0.001
LAD, n (%)	2 (11.1)	36 (83.7)		6 (30.0)	28 (84.8)		
LCx, n (%)	10 (55.6)	2 (4.7)		3 (15.0)	2 (6.1)		
RCA, n (%)	7 (33.3)	3 (11.6)		11 (55.0)	3 (9.1)		
Baseline coronary physiology							
Pd/Pa, median [IQR]	0.93 [0.83, 0.95]	0.85 [0.81, 0.88]	0.01	0.76 [0.69, 0.91]	0.85 [0.76, 0.89]	0.77	0.048
CFR, median [IQR]	2.00 [1.78, 2.21]	2.25 [1.42, 2.69]	0.33	1.71 [1.21, 2.012	2.24 [1.66 2.71]	0.07	0.19
IMR, median [IQR]	25.1 [19.9, 37.5]	23.9 [17.8, 32.0]	0.55	24.1 [18.6, 31.8]	20.8 [15.8, 28.5]	0.42	0.59
FFR, mean ± SD	0.69±0.13	0.63±0.11	0.048	0.55±0.15	0.61±0.15	0.17	0.02
PPG, median [IQR]	0.81 [0.78, 0.82]	0.58 [0.53, 0.66]	<0.001	0.81 [0.78, 0.82]	0.59 [0.48, 0.66]	<0.001	<0.001
Immediately after stenting							
Stent post-dilatation, n (%)	18 (100.0)	43 (100.0)	1	18 (90.5)	33 (100.0)	0.27	0.02
Intravascular imaging, n (%)	1 (5.6)	9 (20.9)	0.26	0 (0)	12 (36.4)	0.006	0.004
Pd/Pa, median [IQR]	0.98 [0.97, 1.01]	0.90 [0.88, 0.92]	<0.001	0.98 [0.93, 1.00]	0.92 [0.89, 0.94]	0.001	<0.001
CFR, median [IQR]	4.44 [2.39, 5.81]	2.71 [1.97, 4.00]	0.01	3.28 [2.44, 5.41]	2.74 [2.41, 4.13]	0.25	0.04
IMR, median [IQR]	16.1 [13.2, 23.1]	18.9 [13.1, 26.3]	0.31	13.1 [10.7, 19.5]	17.3 [13.1, 22.7]	0.06	0.07
FFR, mean ± SD	0.93±0.05	0.80±0.09	<0.001	0.87±0.07	0.83±0.07	0.09	<0.001
1st PIOS treatments							
1st PIOS treatments performed, n (%)	1 (5.6)	18 (41.9)	0.006	-	-		-
Additional stent post-dilatation, n (%)	1 (5.6)	11 (25.6)	0.09	-	-		-
Additional lesion treated PCI, n (%)	0 (0)	8 (18.6)	0.09	-	-		-
Additional intravascular imagings, n (%)	0 (0.0)	1 (2.3)	1	-	-		-
Pd/Pa, median [IQR]	0.98 [0.97, 1.01]	0.90 [0.89, 0.93]	<0.001				-

128

CFR, median [IQR]	4.44 [2.59, 5.81]	3.46 [2.01, 4.14]	0.07	-	-		-
IMR, median [IQR]	16.1 [13.2, 18.7]	17.1 [13.1, 25.2]	0.52				-
FFR, mean ± SD	0.93±0.05	0.83±0.07	<0.001	-	-		-
2nd PIOS treatments							
2nd PIOS treatments performed, n (%)	0 (0)	2 (4.7)	1	-	-		-
Additional stent post-dilatation, n (%)	0 (0)	2 (4.7)	1	-	-		-
Additional lesion treated, n (%)	0 (0)	2 (4.7)	1	-	-		-
Additional intravascular imaging, n (%)	0 (0)	2 (4.7)	1	-		-	-
Pd/Pa, median [IQR]	0.98 [0.97, 1.01]	0.91 [0.90, 0.93]	<0.001	-	-		-
CFR, median [IQR]	4.44 [2.59, 5.81]	3.23 [2.01, 4.11]	0.051	-	-		-
IMR, median [IQR]	16.1 [13.2, 18.7]	17.6 [13.1, 25.2]	0.49	-	-		-
FFR, mean ± SD	0.93±0.05	0.83±0.07	<0.001	-	-		-
Final coronary physiology							
Number of stents per patients, median [IQR]	1.00 [1.00, 1.00]	1.00 [1.00, 2.00]	0.14	1.00 [1.00, 2.00]	1.00 [1.00, 2.00]	0.28	0.34
Total stent length (mm), median [IQR]	32.0 [25.0, 36.8]	38.0 [28.0, 56.0]	0.12	38.0 [30.3, 48.0]	38.0 [24.0, 56.0]	0.93	0.47
Pd/Pa, median [IQR]	0.98 [0.97, 1.01]	0.91 [0.90, 0.93]	<0.001	0.98 [0.93, 1.00]	0.92 [0.89, 0.94]	0.001	<0.001
CFR, median [IQR]	4.44 [2.59, 6.14]	3.23 [2.01, 4.11]	0.051	3.28 [2.44, 5.41]	2.74 [2.41, 4.13]	0.25	0.18
IMR, median [IQR]	16.1 [13.2, 18.7]	17.6 [13.01 25.2]	0.53	13.1 [10.7, 19.5]	17.3 [13.1, 22.7]	0.07	0.17
FFR, mean ± SD	0.93±0.05	0.83±0.07	<0.001	0.87±0.07	0.83±0.07	0.057	<0.001
Delta Pd/Pa, median [IQR]	0.06 [0.04, 0.15]	0.06 [0.03, 0.10]	0.82	0.20 [0.07, 0.28]	0.06 [0.04, 0.19]	0.079	0.09
Delta CFR, median [IQR]	2.36 [0.79, 3.18]	0.63 [-0.05, 1.92]	0.01	1.60 [0.78, 2.90]	1.04 [0.20, 1.97]	0.11	0.03
Delta IMR, median [IQR]	-8.23 [-13.2, -3.09]	-3.55 [-9.98, -0.28]	0.19	-11.3 [-15.1, -5.67]	-3.13 [-9.71, 1.26]	0.04	0.10
Normalised delta FFR (%), mean ± SD	76.5±15.5	52.2±18.5	<0.001	67.8±23.5	53.0±20.5	0.02	<0.001
FFR ≥ 0.90 (%), n (%)	14 (77.8)	8 (18.6)	<0.001	6 (30.0)	4 (12.1)	0.21	<0.001
FFR ≥ 0.80 (%), n (%)	0 (0.0)	13 (30.2)	0.02	5 (25.0)	9 (27.3)	0.79	0.07
Residual PPG	0.04±0.02	0.07±0.04	0.004	0.07±0.04	0.08±0.04	0.44	0.008

CFR, coronary flow reserve; FFR, fractional flow reserve; IMR, index of microvascular resistance; Pa, aortic pressure; Pd, distal coronary pressure; PPG, pullback pressure gradient. Normalised delta FFR was normalised by pre-PCI FFR ([final post-PCI FFR minus pre-PCI FFR divided by one minus pre-PCI FFR] by a factor of one hundred. Pre-PCI Pd/Pa*: N=110 (PIOS/Focal=18, PIOS/Diffuse=42, Control/Focal=20, Control/Diffuse=30); Pre-PCI CFR: N=107 (PIOS/Focal=17, PIOS/Diffuse=41, Control/Focal=18, Control/Diffuse=31); Pre-PCI IMR: N=104 (PIOS/Focal=18, PIOS/Diffuse=38, Control/Focal=16, Control/Diffuse=32) ; Pre-PCI FFR: N=111 (PIOS/Focal=18, PIOS/Diffuse=43, Control/Focal=20, Control/Diffuse=30) ; Immediately after stenting Pd/Pa: N=113 (PIOS/Focal=18, PIOS/Diffuse=42, Control/Focal=20, Control/Diffuse=33); Immediately after stenting CFR: N=112 (PIOS/Focal=18, PIOS/Diffuse=43, Control/Focal=20, Control/Diffuse=31); Immediately after stenting IMR: N=112 (PIOS/Focal=18, PIOS/Diffuse=43, Control/Focal=20, Control/Diffuse=31); Immediately after stenting FFR: N=113 (PIOS/Focal=18, PIOS/Diffuse=42, Control/Focal=20, Control/Diffuse=33); After 1st PIOS Pd/Pa: N=114 (PIOS/Focal=18, PIOS/Diffuse=43, Control/Focal=20, Control/Diffuse=33); After 1st PIOS CFR: N=109 (PIOS/Focal=18, PIOS/Diffuse=40, Control/Focal=20, Control/Diffuse=31); After 1st PIOS IMR: N=109 (PIOS/Focal=18, PIOS/Diffuse=40, Control/Focal=20, Control/Diffuse=31); After 1st PIOS FFR: N=114 (PIOS/Focal=18, PIOS/Diffuse=43, Control/Focal=20, Control/Diffuse=33); After 2nd PIOS Pd/Pa: N=114 (PIOS/Focal=18, PIOS/Diffuse=43, Control/Focal=20, Control/Diffuse=33); After 2nd PIOS CFR: N=109 (PIOS/Focal=18, PIOS/Diffuse=40, Control/Focal=20, Control/Diffuse=31); After 2nd PIOS IMR: N=109 (PIOS/Focal=18, PIOS/Diffuse=40, Control/Focal=20, Control/Diffuse=31); After 2nd PIOS FFR: N=114 (PIOS/Focal=18, PIOS/Diffuse=43, Control/Focal=20, Control/Diffuse=33); Final post-PCI Pd/Pa: N=114 (PIOS/Focal=18, PIOS/Diffuse=43, Control/Focal=20, Control/Diffuse=33); Final post-PCI CFR: N=109 (PIOS/Focal=18, PIOS/Diffuse=40, Control/Focal=20, Control/Diffuse=31); Final post-PCI IMR: N=109 (PIOS/Focal=18, PIOS/Diffuse=40, Control/Focal=20, Control/Diffuse=31); Final Post-PCI FFR: N=114 (PIOS/Focal=18, PIOS/Diffuse=43, Control/Focal=20, Control/Diffuse=33); Delta PdPa: N=110 (PIOS/Focal=18, PIOS/Diffuse=42, Control/Focal=20, Control/Diffuse=30); Delta CFR: N=103 (PIOS/Focal=17, PIOS/Diffuse=39, Control/Focal=18, Control/Diffuse=29); Delta IMR: N=103 (PIOS/Focal=17, PIOS/Diffuse=39, Control/Focal=18, Control/Diffuse=29); Normalised delta FFR: N=111 (PIOS/Focal=18,

PIOS/Diffuse=43, Control/Focal=20, Control/Diffuse=30) ; Residual PPG N=94 (PIOS/Focal=16, PIOS/Diffuse=36, Control/Focal=14, Control/Diffuse=28). *Focal CAD vs. Diffuse CAD among PIOS group. **Focal CAD vs. Diffuse CAD among the Controls group. ***Focal CAD PIOS vs. Diffuse CAD PIOS vs. Focal CAD Controls vs. Diffuse CAD Controls group.

Figure 1. Correlation between pullback pressure gradient (PPG) and final post-PCI fractional frow reserve (FFR) and normalised delta FFR
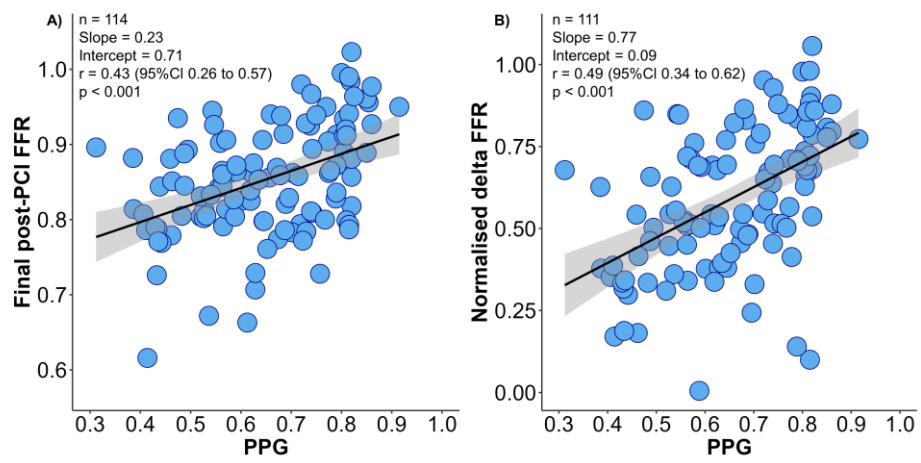
Figure 2. Use of physiology-guided optimisation stratified by focal and diffuse coronary artery disease.

Panel A shows the frequency of additional optimisation in overall population in the PIOS arm (gray colour). Panel B shows the frequency of additional optimisation in focal CAD and panel C shows the frequency of additional optimisation in diffuse CAD. CAD = coronary artery disease; PIOS = physiology-guided incremental optimisation strategy. *Comparison frequency of additional optimisation between focal and diffuse CAD.
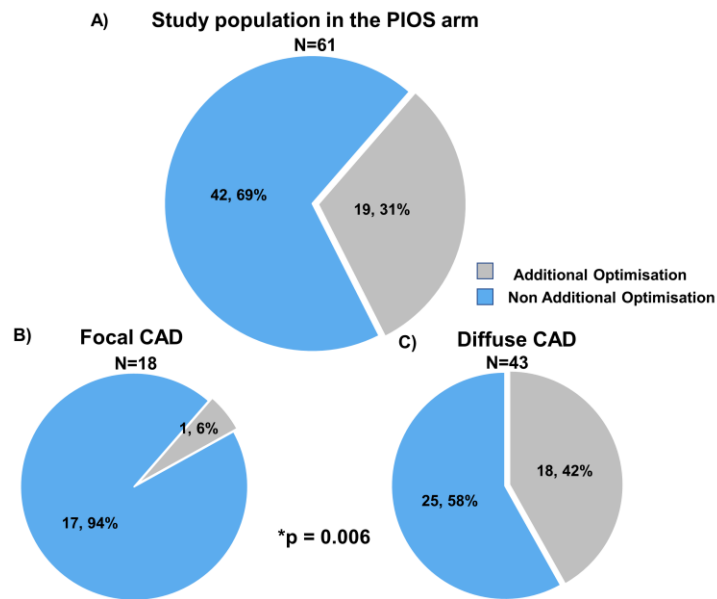
Figure 3. Interaction between pullback pressure gradient (PPG) and randomization arms. Interaction between PPG and randomization arms for final post-PCI FFR. The blue dots and line represent patients in the PIOS arm and the red dots and line represent the control arm. There was a significant interaction between randomization groups. FFR = fractional flow reserve; PCI = pecutaneous coronary intervention; PIOS = physiology-guided incremental optimisation strategy; PPG = pullback pressure gradient
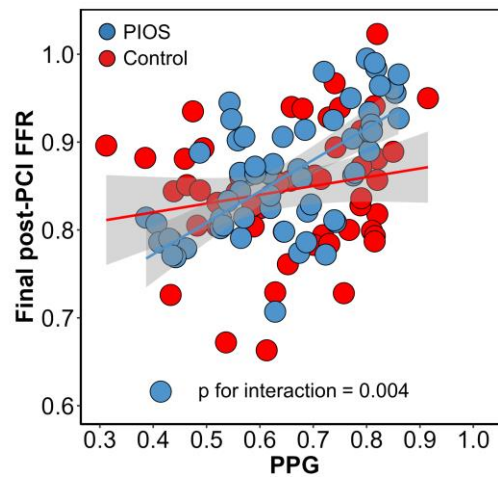
Figure 4. Residual pullback pressure gradient (PPG) and post-PCI fractional flow reserve (FFR).

Panel A shows the relationship between the residual PPG (x-axis) and final post-PCI FFR (y-axis). Residual PPG had significant correlation with final post-PCI FFR. Panel B demonstrates differences in residual FFR between the focal PIOS, diffuse PIOS, focal control, and diffuse control groups. *Focal CAD PIOS vs. Diffuse CAD PIOS vs. Focal CAD Controls vs. Diffuse CAD Controls group. Panel C shows ROC curve analysis for the capacity of Residual PPG for predicting final post-PCI FFR ≥ 0.90 AUC = area under curve; CAD = coronary artery disease; FFR = fractional flow reserve; PIOS = physiology-guided incremental optimisation strategy; PPG = pullback pressure gradient; ROC = receiver operating characteristic

135
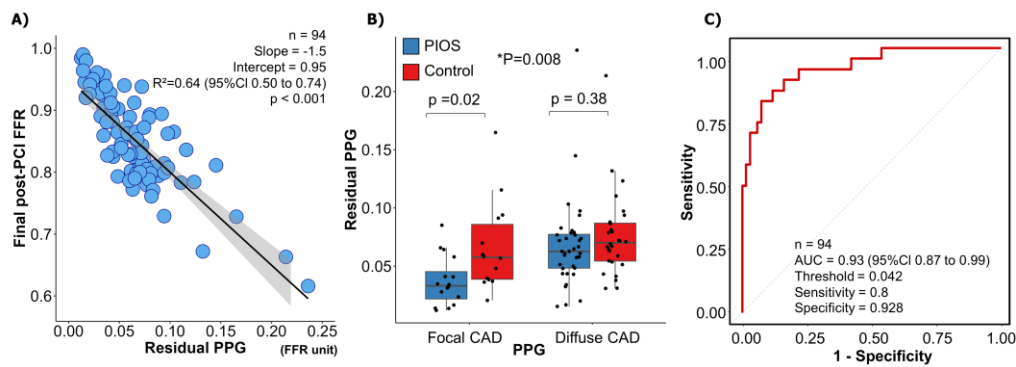
References

1.   Raber L, Mintz GS, Koskinas KC, et al. Clinical use of intracoronary imaging. Part 1: guidance and optimization of coronary interventions. An expert consensus document of the European Association of Percutaneous Cardiovascular Interventions. *European heart journal*. 2018;39(35):3281-3300. doi:10.1093/eurheartj/ehy285 [doi]

2.   Johnson TW, Raber L, Di Mario C, et al. Clinical use of intracoronary imaging. Part2: acute coronary syndromes, ambiguous coronary angiography findings, and guiding interventional decision-making: an expert consensus document of the European Association of Percutaneous Cardiovascular Interventions. *EuroIntervention*. Aug 29 2019;15(5):434-451. doi:10.4244/EIJY19M06_02

3.   Lee JM, Choi KH, Song YB, et al. Intravascular Imaging–Guided or Angiography-Guided Complex PCI. *New England Journal of Medicine*. 2023;doi:10.1056/NEJMoa2216607

4.   Johnson NP, Toth GG, Lai D, et al. Prognostic value of fractional flow reserve: linking physiologic severity to clinical outcomes. *J Am Coll Cardiol*. Oct 21 2014;64(16):1641-54. doi:10.1016/j.jacc.2014.07.973

5.   Collison D, Didagelos M, Aetesam-Ur-Rahman M, et al. Post-stenting fractional flow reserve vs coronary angiography for optimization of percutaneous coronary intervention (TARGET-FFR). *Eur Heart J*. Dec 1 2021;42(45):4656-4668. doi:10.1093/eurheartj/ehab449

6.   Rimac G, Fearon WF, De Bruyne B, et al. Clinical value of post-percutaneous coronary intervention fractional flow reserve value: A systematic review and meta-analysis. *Am Heart J*. Jan 2017;183:1-9. doi:10.1016/j.ahj.2016.10.005

7.   Hwang D, Koo BK, Zhang J, et al. Prognostic Implications of Fractional Flow Reserve After Coronary Stenting: A Systematic Review and Meta-analysis. *JAMA Netw Open*. Sep 1 2022;5(9):e2232842. doi:10.1001/jamanetworkopen.2022.32842

8.   Collet C, Sonck J, Vandeloo B, et al. Measurement of Hyperemic Pullback Pressure Gradients to Characterize Patterns of Coronary Atherosclerosis. *J Am Coll Cardiol*. Oct 8 2019;74(14):1772-1784. doi:10.1016/j.jacc.2019.07.072

9.   Layland J, Carrick D, Lee M, Oldroyd K, Berry C. Adenosine: physiology, pharmacology, and clinical applications. *JACC Cardiovasc Interv*. Jun 2014;7(6):581-91. doi:10.1016/j.jcin.2014.02.009

10.   Rajkumar CA, Shun-Shin M, Seligman H, et al. Placebo-Controlled Efficacy of Percutaneous Coronary Intervention for Focal and Diffuse Patterns of Stable Coronary Artery Disease. *Circ Cardiovasc Interv*. Aug 2021;14(8):e009891. doi:10.1161/CIRCINTERVENTIONS.120.009891

11.   Samady H, McDaniel M, Veledar E, et al. Baseline fractional flow reserve and stent diameter predict optimal post-stent fractional flow reserve and major adverse cardiac events after bare-metal stent deployment. *JACC Cardiovasc Interv*. Apr 2009;2(4):357-63. doi:10.1016/j.jcin.2009.01.008

12.   Piroth Z, Toth GG, Tonino PAL, et al. Prognostic Value of Fractional Flow Reserve Measured Immediately After Drug-Eluting Stent Implantation. *Circ Cardiovasc Interv*. Aug 2017;10(8)doi:10.1161/CIRCINTERVENTIONS.116.005233

13.   Mizukami T, Sonck J, Sakai K, et al. Procedural Outcomes After Percutaneous Coronary Interventions in Focal and Diffuse Coronary Artery Disease. *J Am Heart Assoc*. Nov 29 2022:e026960. doi:10.1161/JAHA.122.026960

14.   Erlinge D, Gotberg M. We need intracoronary physiology guidance before percutaneous coronary intervention, but do we need it post-stenting? *Eur Heart J*. Sep 4 2021;doi:10.1093/eurheartj/ehab525

15.   Pijls NH, Klauss V, Siebert U, et al. Coronary pressure measurement after stenting predicts adverse events at follow-up: a multicenter registry. *Circulation*. Jun 25 2002;105(25):2950-4. doi:10.1161/01.cir.0000020547.92091.76

16.   Fujimura T, Matsumura M, Witzenbichler B, et al. Stent Expansion Indexes to Predict Clinical Outcomes: An IVUS Substudy From ADAPT-DES. *JACC Cardiovasc Interv*. Aug 9 2021;14(15):1639-1650. doi:10.1016/j.jcin.2021.05.019

17.   Biscaglia S, Tebaldi M, Brugaletta S, et al. Prognostic Value of QFR Measured Immediately After Successful Stent Implantation: The International Multicenter Prospective HAWKEYE Study. *JACC Cardiovasc Interv*. Oct 28 2019;12(20):2079-2088. doi:10.1016/j.jcin.2019.06.003

18.   Lee JM, Choi G, Koo BK, et al. Identification of High-Risk Plaques Destined to Cause Acute Coronary Syndrome Using Coronary Computed Tomographic Angiography and Computational Fluid Dynamics. *JACC Cardiovasc Imaging*. Jun 2019;12(6):1032-1043. doi:10.1016/j.jcmg.2018.01.023

19.   Liu X, Xu C, Rao S, et al. Physiologically personalized coronary blood flow model to improve the estimation of noninvasive fractional flow reserve. *Med Phys*. Jan 2022;49(1):583-597. doi:10.1002/mp.15363

20.   Gao Z, Wang X, Sun S, et al. Learning physical properties in complex visual scenes: An intelligent machine for perceiving blood flow dynamics from static CT angiography imaging. *Neural Netw*. Mar 2020;123:82-93. doi:10.1016/j.neunet.2019.11.017

Part D.

Mechanisms of benefit of PPG-guided PCI

Chapter 7. Coronary Atherosclerosis Phenotypes in Focal and Diffuse Disease.

Sakai K, Mizukami T, Leipsic J, Belmonte M, Sonck J, Nørgaard BL, Otake H, Ko B, Koo BK, Maeng M, Jensen JM, Buytaert D, Munhoz D, Andreini D, Ohashi H, Shinke T, Taylor CA, Barbato E, Johnson NP, De Bruyne B, Collet C.

Patients with hemodynamic significant coronary artery disease

Focal CAD (High PPG)

High translesional gradient

PPG 0.86

Diffuse CAD (Low PPG)

Diffuse pressure losses

PPG 0.45
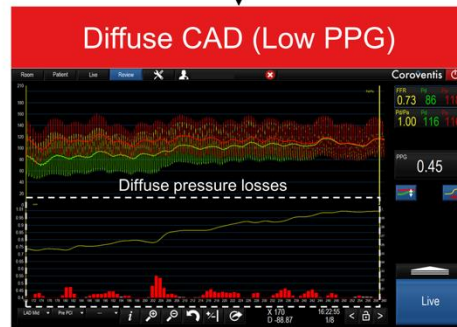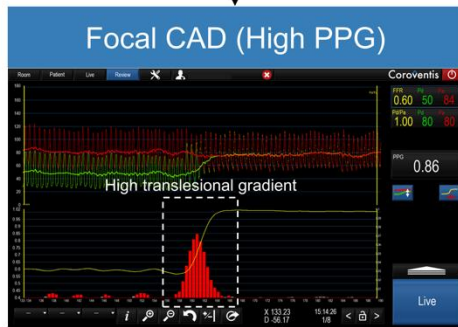
Invasive and non-invasive atherosclerosis phenotype

Focal CAD

Lipid-rich plaque with a large plaque burden

Thin-cap fibroatheroma

Diffuse CAD

High calcium score and calcium burden

Fibrocalcified plaque

FFR 1.0 0.8 0

142
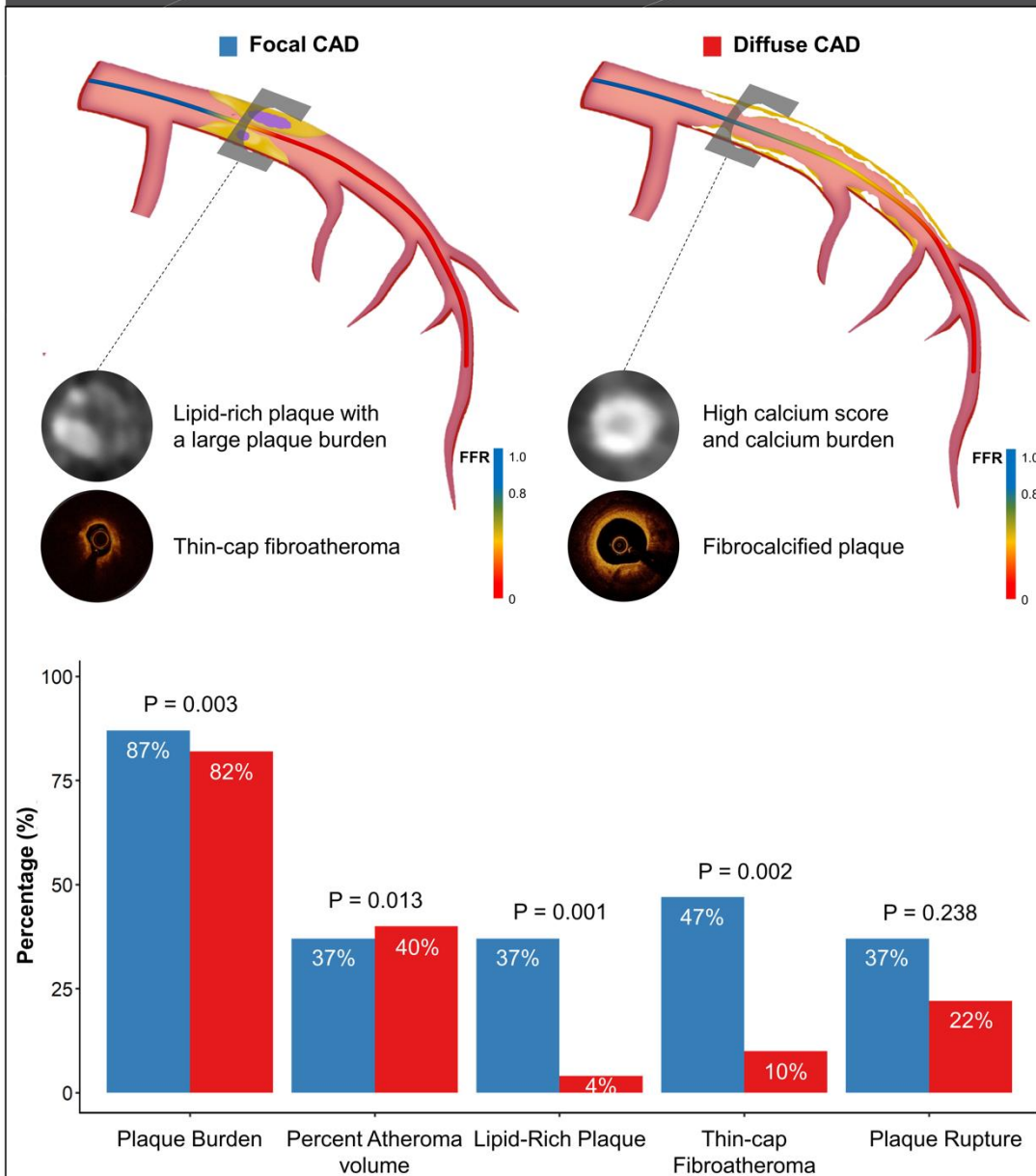
Abstract

Background: The interplay between coronary hemodynamics and plaque characteristics remains poorly understood.

Objectives: We aimed to compare atherosclerotic plaque phenotypes between focal and diffuse coronary artery disease (CAD) defined by coronary hemodynamics.

Methods: This was a multicenter, prospective, single-arm study conducted in five countries (NCT03782688). Patients with functionally significant lesions based on an invasive fractional flow reserve (FFR) ≤0.80 were included. Plaque analysis was performed using computed tomography angiography (CCTA) and optical coherence tomography (OCT). CAD patterns were assessed using motorized FFR pullbacks and quantified by pullback pressure gradients (PPG). Focal and diffuse CAD was defined according to the median PPG value.

Results: A total of 117 patients (120 vessels) were included. The median PPG was 0.66 [0.54, 0.75]. By CCTA analysis, plaque burden was higher in patients with focal CAD (87±8% focal versus 82±10% diffuse, p=0.003). Calcifications were significantly more prevalent in patients with diffuse CAD (Agatston score per vessel 51 [11, 204] focal versus 158 [52, 341] diffuse, p=0.024). By OCT analysis, patients with focal CAD had a significantly higher prevalence of circumferential lipid-rich plaque (37% focal versus 4% diffuse, p=0.001) and thin-cap fibroatheroma (TCFA 47% focal versus 10% diffuse, p=0.002). Focal disease defined by PPG predicted the presence of TCFA with an area under the curve (AUC) of 0.73 (95% CI 0.58 to 0.87).

Conclusions: Atherosclerotic plaque phenotypes associate with intracoronary hemodynamics. Focal CAD had a higher plaque burden and was predominantly lipid-rich with a high prevalence of TCFA, whereas calcifications were more prevalent in diffuse CAD.

Introduction

Coronary atherosclerosis can manifest as a broad range of plaque phenotypes. [1]Plaque differentiation and progression likely result from the interaction between multiple genetic and environmental factors, with the underlying inflammatory milieu playing an essential role. [2-4]Vessel hemodynamics – more specifically, endothelial wall shear stress (WSS) and tensile stress – have also been associated with specific plaque phenotypes. [5,6]However, the interplay between plaque morphology and local hemodynamics remains incompletely understood. [7]

Atherosclerosis can be characterized using invasive and non-invasive imaging methods that quantify volume, extension, and composition. Large plaque burden and lipid-rich plaques have been identified as predictors of adverse clinical events. [8-10]Similarly, the presence of thin-cap fibroatheroma (TCFA) has been associated with plaque rupture, clinically manifested as acute myocardial infarction. Conversely, calcifications are considered markers of plaque stability. [11]

It has been postulated that the presence of focal pressure gradients may influence plaque biology and its propensity to rupture. [12-14]The pullback pressure gradient (PPG) is a quantitative index to quantify coronary artery disease (CAD) patterns into focal or diffuse CAD based on intravascular hemodynamics. Large pressure gradients define focal disease, whereas the absence of focal gradients characterizes diffuse CAD. [15]We sought to investigate the pathophysiological interplay between physiological patterns and plaque characteristics using a combination of non-invasive and invasive imaging in patients with CAD.

Methods

Study population

The present study is a sub-analysis of the Precise PCI Plan (P3) study. The main results have been published previously. [16]Briefly, this multicenter, prospective, single-arm study was conducted in five countries (NCT03782688). Patients with stable CAD and invasive fractional flow reserve (FFR) $\leq$ 0.80 were eligible for inclusion. All patients had coronary computed tomography angiography (CCTA) with quantitative plaque analysis. Patients underwent an invasive procedure with motorized intracoronary pressure recordings for longitudinal vessel evaluation followed by optical coherence tomography (OCT). The P3 study validated a CCTA-based revascularization planning tool in predicting post-PCI FFR. The objective of this sub-study was to characterize atherosclerotic plaque phenotypes between focal and diffuse CAD defined by coronary hemodynamics using PPG. The study protocol was approved by the

investigational review board or ethics committee at each participating center. All patients signed informed consent before the study procedures.

Coronary computed tomography angiography

Coronary computed tomography angiography (CCTA) was performed using the latest-generation CT scanners. Imaging acquisition guidelines recommended nitrates before CT acquisition and beta-blockers for heart rates higher than 65 b.p.m. Calcium scores were calculated by the Agatston method at the vessel level. Absolute and relative plaque volumes were measured for each component as follows. [17,18]Plaque burden (PB) was defined as plaque area divided by vessel area at the minimal lumen area (MLA). Percent atheroma volume (PAV) was defined as plaque volume divided by vessel volume. [17]Plaque composition was assessed by applying specific thresholds as described previously. [19]Low attenuation plaque was defined as the presence of plaque with < 30 Hounsfield units (HU). [20]Positive remodeling was defined by a remodeling index > 1.1. [21,22]CCTA were analyzed using validated software (QAngio CT, Medis Medical Imaging, Netherlands) by a core laboratory (CoreAalst BV, Aalst, Belgium) blinded to the invasive data.

Invasive Procedure

Invasive coronary angiography was performed following a dedicated protocol. Intracoronary nitroglycerin (100-200 µg) was administered before angiography. At least two projections separated by at least 30 degrees were obtained. Coronary angiography was analyzed with 3D-quantitative coronary angiography (QCA) software (CAAS 8.2 Software, Pie Medical Imaging, Maastricht, Netherlands). The location of the lesions was determined by measuring the distance between the ostium of the vessel and the MLA. Resting pressure ratios and FFR were measured in the distal segment of the vessel. During intravenous adenosine infusion (140 µg/kg/min), FFR pullbacks at a speed of 1 mm/s were performed using a motorized device (Volcano R 100, San Diego, California) fixed to the pressure wire.[16] From the FFR pullback curves, PPG was calculated using commercially-available software (Coroflow v3.5, Coroventis Research AP, Uppsala, Sweden). The PPG calculation has been described in detail elsewhere. [15]Briefly, PPG combines two parameters extracted from FFR pullback curves: first, the maximal pressure gradient over 20% of the pullback, and second, the length of functional disease. PPG ranges from 0 (diffuse disease) to 1 (focal disease). For the present analysis, the median PPG value dichotomized focal versus diffuse CAD. Aortic pressure tracings without a dicrotic notch, ventricularization, drift more than 0.05 FFR units,

unstable hyperemic conditions during the pullback maneuver, and pullback curves with major artifacts were excluded.

Optical coherence tomography (OCT) pullbacks of 75 mm were acquired using a Dragonfly OPTIS Imaging Catheter (Abbott Vascular, St. Paul, Minnesota). An automated algorithm defined minimal lumen area (MLA). OCT pullbacks were performed before balloon pre-dilatation when feasible; cases in which OCT was performed after pre-dilatation were excluded from the OCT plaque analysis. Lipid-rich plaques (LRP) were defined as a low-signal region with a diffuse border of at least 90° with a length >1 mm. [23]Circumferential LRP was defined as lipid occupying 360°. A fibrous cap was defined as a signal-rich homogenous layer overlying a LRP. [24]The thinnest part of the fibrous cap was measured three times, and its average thickness was defined as the fibrous cap thickness. TCFA was defined as the presence of fibrous cap thickness <65 µm overlying LRP. [25]Plaque rupture was defined as intimal tearing, disruption, or dissection of the cap. Additional OCT definitions are shown in Supplemental Material Table S1. [26,27]OCT images were analyzed by the core laboratory using CAAS Intravascular version 2.1 (Pie Medical Imaging, Maastricht, Netherlands) blinded to the physiological data.

Statistical Analysis

Variables are expressed as mean ± standard deviation (SD) and median [interquartile range (IQR)] for normally and non-normally distributed data, respectively. Categorical variables are expressed as frequencies and percentages (%). Continuous variables were compared using the student's t-test (or Mann–Whitney tests as appropriate), and categorical variables were compared using the Chi-square (or Fisher's exact test as appropriate). Pearson correlation coefficient was used to assess the relationship between continuous variables. Univariable and multivariable regression analyses with logistic and generalized linear models were used to assess the association between CAD patterns defined by PPG (predictor variable) and plaque characteristics derived from CCTA and OCT (outcome variables). PPG and FFR were analyzed as continuous variables. Receiver operating characteristic (ROC) curve analyses were used to assess the capacity of PPG to predict adverse plaque characteristics. In patients with multivessel interrogation (n=3), the lowest PPG value was used to classify the case for the patient-level analysis. A p-value of 0.05 or less was considered to indicate statistical significance. All statistical analyses were performed using R statistical software version 4.1.2 (R Foundation for Statistical Computing, Vienna, Austria).

Results

Study Population

From February 2019 to December 2020, 259 patients were screened and 117 patients (120 vessels) were included. The study flowchart is shown in Supplemental Material Figure S1. CCTA plaque analysis was feasible for all cases, and OCT plaque analysis was feasible in 57% (68/120) of the cases.

Baseline characteristics

Clinical characteristics stratified by CAD pattern are shown in Table 1. Mean age tended to be lower in patients with focal CAD, most of the patients were male, and one-fifth had diabetes – all without differences between focal and diffuse disease. Procedural, morphological, and coronary physiology characteristics stratified CAD patterns are shown in Table 2. Diffuse CAD was more frequently observed in the left anterior descending (LAD) artery. The median PPG was 0.66 [IQR 0.54 to 0.75]. PPG distribution and its relationship with lesion severity are shown in Figure 1. Patients with focal versus diffuse disease CAD had greater lesion severity represented by lower MLA in QCA and lower FFR. A sensitivity analysis restricted to patients with single vessel interrogation is shown in Supplemental Material Table S2.

Plaque morphology based on CCTA stratified by CAD pattern

The mean plaque burden (at the MLA) was 85±9% and was significantly higher in patients with focal CAD. Conversely, PAV (vessel level) was higher in patients with diffuse CAD. Patients with diffuse CAD had a higher Agatston score, longer calcium length, and higher calcified plaque burden than focal CAD (Table 3 and Figure 2). Other plaque components based on CCTA stratified by the PPG are shown in Supplemental Material Table S3.

FFR was associated with plaque burden at the MLA (Supplemental Material Table S4). PPG was significantly associated with plaque burden at the MLA, non-calcified and calcified plaque burdens, low-attenuation plaque burden, PAV, and Agatston score (Table 4); the higher the PPG, the larger the plaque burden at the MLA, the greater the low-attenuation plaque burden and non-calcified plaque burden, and the lower the calcific plaque burden. PPG remained associated with plaque CCTA characteristics independent of FFR (Supplemental Material Table S5).

Plaque morphology based on OCT stratified by CAD patterns

Lipid-rich plaques (LRP) were present in 57% of cases, and circumferential LRP was significantly more prevalent in patients with focal CAD. Associations between PPG and OCT

plaque features are shown in Table 4 and Figure 3. PPG predicted the presence of circumferential LRP with an area under the curve (AUC) of 0.82 (95% CI 0.66 to 0.99). In vessels with focal CAD, fibrous caps overlying fibroatheromas were thinner (63 ± 9.9 μm focal versus 90.3 ± 25.2 μm diffuse, p=0.001) and TCFA more prevalent (47.4% focal versus 10.2% diffuse, p=0.002) than in vessels with diffuse disease. PPG and fibrous cap thickness were negatively correlated (r=-0.55; 95% CI: -0.74 to -0.28; p<0.001; Figure 3, panel A). PPG was associated with fibrous cap thickness independent of FFR and diabetes mellitus (Supplemental Material Table S6). High PPG predicted the presence of TCFA with an AUC of 0.73 (95% CI 0.58 to 0.87). Independent of FFR, PPG was significantly associated with the presence of circumferential LRP, TCFA, and plaque rupture (Supplemental Material Table S7). FFR was not associated with OCT plaque characteristics (Supplemental Material Table S8). Two case examples summarizing the association between plaque characteristics by CCTA and OCT and coronary physiology are shown in Figure 4. The central illustration summarizes the association between pathophysiology patterns of CAD defined by PPG and plaque characteristics based on invasive and non-invasive imaging.

Discussion

The present study describes the interplay between coronary hemodynamics and atherosclerotic plaque phenotypes. The main finding is the distinctive plaque features observed in patients with focal versus diffuse CAD. Atherosclerotic lesions in vessels with focal disease (high PPG) had a higher plaque burden and were predominantly lipid-rich with a high prevalence of TCFA, whereas calcifications were the hallmark of vessels with diffuse disease (low PPG). Furthermore, trans-lesion pressure gradients correlated inversely with fibrous cap thickness.

Previous studies have shown that low FFR, measured at the distal segment of the coronary artery, is associated with plaque characteristics, particularly the presence of plaques with a higher risk of rupture. [12,28]However, these studies are limited by the absence of longitudinal vessel hemodynamic information. PPG, derived from hyperemic pullback pressure curves, quantifies the longitudinal distribution of abnormal epicardial resistance, thus providing a second dimension to single-point FFR. [29]A unique feature of our methodology is the use of motorized pullback recordings, which increased the accuracy of the analysis and allowed for the standardization of the pressure-length relationship. [30]Trans-lesion pressure gradients concentrated on a short segment of the artery (i.e., high PPG) translate into increased plaque tensile and compressive stresses. [31]Focal disease, defined by coronary physiology with

PPG, was anatomically more severe and had a greater plaque burden, explaining the lower FFR measured at the distal coronary segment than vessels with diffuse disease. These localized pressure gradients also induce disturbance of laminar flow with eddies at the lesion exit, producing areas of low and oscillatory WSS, which can lead to plaque progression and inflammation, cap thinning and destabilization, and ultimately, plaque rupture when the physical forces exerted on the plaque exceeds its material strength. [31,32]In the present study, we observed that high PPG values were associated with plaque rupture and a negative relationship between PPG and cap thickness overlying fibroatheromas. In contrast, in vessels with a low PPG value, epicardial resistance is spread over a longer vessel segment. These findings expand our knowledge about the relationship between coronary physiology, quantified by FFR and PPG, and plaque characteristics assessed invasively using OCT and non-invasively through CCTA.

It can be hypothesized that lipidic plaque progression occurs rapidly with localized growth leading to focal stenosis, here captured as high PPG. Conversely, in the absence of focal pressure gradients, the prevalence of lipid-rich plaques was low, and low PPG values were mainly associated with coronary calcifications. Patients with diffuse pressure losses had higher calcium scores, calcium burden, and calcium volume derived from the quantitative CCTA analysis. Plaque calcification stabilizes CAD by decreasing fibrous cap stress. [11]Moreover, calcifications influence coronary artery interventions and are associated with fewer procedural successes and a higher rate of long-term complications after percutaneous coronary intervention (PCI). [33]Interestingly, the percent atheroma volume (PAV) was greater in diffuse disease. PAV and calcifications are also considered prognostic indicators, but instead of identifying plaque-related risk, they reflect the general burden of disease.

TCFA can be observed in a broad range of angiographic lesion severity; however, they are twice as common in severe stenosis than in non-severe stenosis. This finding is compatible with our study, where patients with focal disease (high PPG) had lower FFR and more TCFA. This is also consistent with the observation that acute coronary syndrome (ACS) occurred more frequently in cases with significant stenosis. [34]Interestingly, the association between PPG and TCFA was independent of FFR, highlighting the role of local hemodynamics on plaque characteristics. The presence of lipidic plaque and TFCA have been shown to predict the occurrence of ischemic events with a poor to moderate predictive capacity; however, the limited prediction of adverse events by these plaque impedes their use for revascularization decisions comparable to the invasive physiologic metrics of FFR and PPG. A prospective

natural-history study of coronary atherosclerosis with novel imaging and physiological techniques is warranted.

The PPG will allow for connecting coronary physiology patterns with plaque characteristics. Since the PPG is easily obtainable in practice after a manual 20-30 seconds FFR pullback maneuver, the present findings have several clinical implications. Beyond the classical evaluation of lesion significance with FFR, a pullback maneuver not only adds additional information on the likelihood of PCI success but also provides further stratification on patients' risk for adverse events. High PPG predicted the presence of circumferential lipid-rich plaques and TCFA with AUC of 0.82 and 0.73, respectively. This atherosclerotic phenotyping based on coronary physiology allows for the understanding of CAD as two entities: a focal disease with predominantly lipidic atherosclerotic and diffuse more stable atherosclerotic and hemodynamic pattern. Clinically, focal disease is more amenable to therapies like PCI, and based on the linked lipidic plaque phenotype; this patient subgroup might benefit from an intervention. [35,36]In contrast, diffuse disease, less appropriate for PCI and stable in nature, may benefit more from conservative management. The PPG may facilitate the standardization of the diagnosis of CAD patterns and be able to identify individuals with different responses to coronary interventions. A randomized clinical trial addressing the clinical benefit of a PPG-guided treatment strategy is warranted.

Limitations

The main limitation of the present study is that it represents a snapshot of the atherosclerosis process. Because of the lack of serial data, we could not assess the disease progression nor the clinical outcomes associated with focal and diffuse disease. In addition, OCT was not available for all patients, with a higher image attrition rate in patients with focal CAD mainly because of technical difficulties during image acquisition. Nonetheless, this was partly circumvented by the CCTA analysis available in the complete cohort. Furthermore, information on microcirculation, which has been associated with plaque characteristics, was not collected. [7]Moreover, we acknowledge that despite adjusting the association between plaque features and PPG by FFR, the absence of vessels with high FFR (FFR > 0.80) may have influenced the analysis. It is important to highlight that the patients included in this study had hemodynamically significant lesions defined as FFR ≤ 0.80. The extrapolation of these findings to patients with hemodynamically non-significant lesions requires further investigation. Finally, the present study is focused on the association between coronary hemodynamics and

plaque characteristics; the impact of these findings on clinical outcomes remains to be determined.

Conclusions

Atherosclerotic plaque phenotypes associate with intracoronary hemodynamics. Vessels with focal disease (high PPG) had a higher plaque burden and predominantly lipid-rich plaques with a high prevalence of TCFA, whereas, in vessels with diffuse disease (low PPG), the plaques were predominantly calcified. PPG was associated with cap thickness with thinner caps observed in lesions with higher focal pressure gradients.

These results relate invasive pathophysiology and plaque characteristics supporting the clinical utility of FFR and PPG for differentiating focal from diffuse disease. The data support the use and interpretation of PPG in relation to plaque composition but do not support the use of anatomic plaque characteristics by either CCTA or OCT as a basis for revascularization in the absence of reduced FFR. In addition, the absence of comparable plaque evaluation for non-hemodynamically significant lesions (FFR > 0.80) precludes extrapolating these findings to a less diseased population.

Table 1. Baseline clinical characteristics.

Variables	All	Focal CAD (PPG > 0.66)	Diffuse CAD (PPG ≤ 0.66)	p-value
Number of patients, n[*]	117	58	59	
Clinical characteristics				
Age, years (mean ± SD)	63.5 ± 9.3	61.9 ± 9.7	65.1 ± 8.7	0.062
Male, n (%)	93 (79.5)	44 (75.9)	49 (83.1)	0.368
BMI (kg/m^2, mean ± SD)	27.0 ± 3.4	26.9 ± 3.5	27.1 ± 3.3	0.771
Dyslipidemia, n (%)	91 (77.8)	44 (75.9)	47 (79.7)	0.662
Hypertension, n (%)	66 (56.4)	35 (60.3)	31 (52.5)	0.457
Diabetes mellitus, n (%)	26 (22.2)	11 (19.0)	15 (25.4)	0.506
Smoking, n (%)	24 (20.5)	13 (22.4)	11 (18.6)	0.653
Prior PCI, n (%)	6 (5.1)	2 (3.4)	4 (6.8)	0.679
PAD, n (%)	5 (4.3)	3 (5.2)	2 (3.4)	0.679
Stroke, n (%)	4 (3.4)	3 (5.2)	1 (1.7)	0.364
Creatinine, mg/dl (mean ± SD)	0.94 ± 0.2	0.93 ± 0.22	0.95 ± 0.18	0.546
Creatinine clearance, ml/min (mean ± SD)	80.1 ± 23.9	83.9 ± 26.4	76.4 ± 20.6	0.097
LVEF, % (mean ± SD)	60.3 ± 6.2	60.4 ± 5.2	60.2 ± 7.0	0.826
Clinical presentation, n (%)				0.041
Silent ischemia, n (%)**	29 (24.8)	10 (17.2)	19 (32.2)	
CCS I, n (%)	36 (30.8)	15 (25.9)	21 (35.6)	
CCS II, n (%)	41 (35.0)	25 (43.1)	16 (27.1)	
CCS III, n (%)	8 (6.8)	6 (10.3)	2 (3.4)	
CCS IV, n (%)	1 (0.9)	0 (0.0)	1 (1.7)	
Unstable angina, n (%)	2 (1.7)	2 (3.4)	0 (0.0)	

Agatston score per patient (median, IQR)	230 [81, 708]	147 [55, 453]	462 [141, 996]	0.025

* Three patients had two vessels assessed.

** Silent ischemia is defined as asymptomatic patients with a positive non-invasive test.

The lowest PPG was used to classify the patients as focal or diffuse CAD. BMI body mass index. CAD coronary artery disease. CCS Canadian cardiovascular society. IQR interquartile range. LVEF left ventricular ejection fraction. PAD peripheral artery disease. PCI percutaneous coronary intervention. PPG pullback pressure gradient. SD standard deviation.

Table 2. Imaging and hemodynamic vessel characteristics.

Variables	All	Focal CAD (PPG>0.66)	Diffuse CAD (PPG ≤0.66)	p-value
Number of vessels, n	120	60	60	
Vessels				<0.001
LAD, n (%)	92 (76.7)	35 (58.3)	57 (95.0)	
LCx, n (%)	13 (10.8)	11 (18.3)	2 (3.3)	
RCA, n (%)	15 (12.5)	14 (23.3)	1 (1.7)	
QCA analysis (mean ± SD)				
Minimum lumen diameter, mm	1.3 ± 0.43	1.1 ± 0.38	1.5 ± 0.40	<0.001
Reference lumen diameter, mm	2.7 ± 0.49	2.7 ± 0.49	2.7 ± 0.49	0.959
Percent diameter stenosis, %	51.6 ± 14.0	58.8 ± 11.4	44.5 ± 12.8	<0.001
Percent area stenosis, %	74.7 ± 14.4	81.9 ± 10.2	67.5 ± 14.6	<0.001
Location of the lesion¶, mm (mean ± SD)	40.6 ± 18.0	40.1 ± 19.5	41.0 ± 16.4	0.789
OCT analysis (mean ± SD)				
Number of vessels, n	68	19[*]	49[**]	
Lesion length, mm	29.8 ± 12.9	26.8 ± 11.5	31.0 ± 13.4	0.23
Minimum lumen area, mm^2	1.8 ± 0.76	1.4 ± 0.71	2.0 ± 0.74	0.007
Percent area stenosis, %	73.2 ± 11.1	83.7 ± 3.5	69.2 ± 10.4	<0.001
Physiological analysis (mean ± SD)				
Resting Pd/Pa	0.82 ± 0.14	0.77 ± 0.17	0.88 ± 0.06	<0.001
FFR	0.65 ± 0.14	0.59 ± 0.15	0.72 ± 0.09	<0.001
PPG	0.66 ± 0.13	0.77 ± 0.07	0.54 ± 0.08	<0.001

¶ Distance between the ostium and minimal lumen area assessed by quantitative coronary angiography. *41 vessels were excluded because pre-dilatation was performed before OCT acquisition to facilitate catheter advancement. **11 vessels were excluded because pre-dilatation was performed before OCT acquisition to facilitate catheter advancement.

CAD coronary artery disease. FFR fractional flow reserve. LAD left anterior descending. LCx left circumflex. OCT optical coherence tomography. Pa aortic pressure. Pd distal coronary pressure. PPG pullback pressure gradient. QCA quantitative coronary angiography. RCA right coronary artery. SD standard deviation.

Table 3. Plaque characteristics based on coronary computed tomography angiography (CCTA) and optical coherence tomography (OCT) in focal and diffuse coronary artery disease (CAD).

Variables	All	Focal CAD (PPG >0.66)	Diffuse CAD (PPG ≤0.66)	p-value
CCTA plaque analysis				
Number of vessels, n	120	60	60	
Lesion level (mean ± SD)				
Plaque burden at the MLA, %	84.7 ± 9.0	87.1 ± 7.5	82.3 ± 9.8	0.003
Remodeling index	0.93 ± 0.21	0.94 ± 0.19	0.93 ± 0.23	0.760
Non-calcified plaque burden, %	80.9 ± 17.0	84.4 ± 14.9	77.5 ± 18.3	0.027
Low-attenuation plaque burden, %	21.3 ± 15.4	22.7 ± 14.0	19.9 ± 16.7	0.319
Napkin-ring sign, n (%)	7 (5.8)	4 (6.7)	3 (5.0)	1.0
Calcified plaque burden, %	19.1 ± 17.0	15.7 ± 14.9	22.5 ± 18.3	0.027
Calcium length, mm	6.0 ± 6.5	4.1 ± 5.6	7.7 ± 6.8	0.011
Calcium arc, degrees*	45 [0, 150]	0 [0, 90]	55 [30, 180]	0.022
Spotty calcification, n (%)	30 (25.0)	19 (31.7)	11 (18.3)	0.139
Vessel level analysis (mean ± SD)				
Percent atheroma volume, %	38.5 ± 8.3	36.6 ± 8.5	40.3 ± 7.8	0.013
Non-calcified plaque burden, %	84.7 ± 13.7	86.5 ± 12.7	82.8 ± 14.4	0.147
Low-attenuation plaque burden, %	18.0 ± 12.1	17.9 ± 11.0	18.2 ± 13.1	0.888
Agatston score per vessel*	104 [31, 300]	51 [11, 204]	158 [52, 341]	0.024
OCT plaque analysis				

Number of vessels, n	68	19	49	
Lipid rich plaque (LRP), n (%)	39 (57.4%)	14 (73.7%)	25 (51.0%)	0.108
LRP > 180°, n (%)	30 (44.1%)	12 (63.2%)	18 (36.7%)	0.061
Circumferential LRP, n (%)	9 (13.2%)	7 (36.8%)	2 (4.1%)	0.001
Calcified plaque, n (%)	55 (80.9%)	13 (68.4%)	42 (85.7%)	0.166
Eruptive calcified nodule, n (%)	3 (4.4%)	0 (0.0%)	3 (6.1%)	0.554
Spotty calcium, n (%)	16 (23.5%)	3 (15.8%)	13 (26.5%)	0.526
Thin-cap fibroatheroma (TCFA), n (%)	14 (20.6%)	9 (47.4%)	5 (10.2%)	0.002
Plaque rupture, n (%)	18 (26.5%)	7 (36.8%)	11 (22.4%)	0.238
Thrombus, n (%)	13 (19.1%)	6 (31.6%)	7 (14.3%)	0.166
Micro channel, n (%)	25 (36.8%)	6 (31.6%)	19 (38.8%)	0.780
Macrophage accumulation, n (%)	18 (26.5%)	5 (26.3%)	13 (26.5%)	1.000
Cholesterol crystal, n (%)	22 (32.4%)	7 (36.8%)	15 (30.6%)	0.773
Layered plaque, n (%)	44 (64.7%)	14 (73.7%)	30 (61.2%)	0.405

* Values presented as median [IQR].

CAD coronary artery disease. CCTA coronary computed tomography angiography. IQR interquartile range. MLA minimal lumen area. OCT optical coherence tomography. PPG pullback pressure gradient. SD standard deviation.

Table 4. Univariable regression analysis of pullback pressure gradient (PPG) for the association of plaque characteristics based on coronary computed tomography angiography (CCTA) and optical coherence tomography (OCT).

Variables	Exp (β)	95% CI	p-value
CCTA plaque analysis*			
Plaque burden at MLA, %	2.06	0.90 to 3.23	<0.001
Remodeling index	0.01	-0.02 to 0.04	0.558
Non-calcified plaque burden (lesion level), %	3.60	1.39 to 5.82	0.002
Low-attenuation plaque burden (lesion level), %	2.27	0.22 to 4.33	0.032
Calcified plaque burden (lesion level), %	-3.60	-5.82 to -1.39	0.002
Percent atheroma volume (vessel level), %	-1.80	-2.88 to -0.71	0.002
Agatston score per vessel (vessel level)	-55.38	-105.63 to -5.13	0.034
OCT plaque analysis**			
Lipid rich plaque (LRP) > 180°, n (%)	1.72	1.14 to 2.71	0.013
Circumferential LRP, n (%)	3.01	1.57 to 6.93	0.003
Thin-cap fibroatheroma, n (%)	1.83	1.13 to 3.15	0.018
Plaque rupture, n (%)	1.61	1.04 to 2.58	0.040
Eruptive calcified nodule, n (%)	0.80	0.25 to 2.03	0.657
Spotty calcium, n (%)	0.73	0.44 to 1.17	0.212
Microchannels, n (%)	1.08	0.73 to 1.62	0.688
Macrophage accumulation, n (%)	1.06	0.68 to 1.63	0.806
Cholesterol crystals, n (%)	1.10	0.73 to 1.65	0.660
Layered plaque, n (%)	1.30	0.86 to 2.01	0.224

The explanatory variable was the PPG as a continuous variable. * Continuous variables. **Categorical variables.

CCTA coronary computed tomography angiography. CI confidence interval. MLA minimal lumen area. OCT optical coherence tomography. PPG pullback pressure gradient.

Figure 1. Distribution of pullback pressure gradient (PPG) and relationship with fractional flow reserve and diameter stenosis.

The bottom panel shows the distribution of PPG in the present cohort. The median value was 0.66 [IQR 0.54, 0.75]; values > 0.66 defined focal disease (blue shaded area), and PPG ≤ 0.66 represent diffuse coronary artery disease (red shaded area). The top left panel displays the relationship between PPG and minimal lumen area (MLA) derived from quantitative coronary angiography (QCA) analysis and the top right panel the relationship between PPG and fractional flow reserve (FFR). In the correlation plots, the box plots show the median and interquartile range (IQR) of MLA and FFR, respectively. The solid black line represents the line of best fit, and the dashed line is the confidence interval.
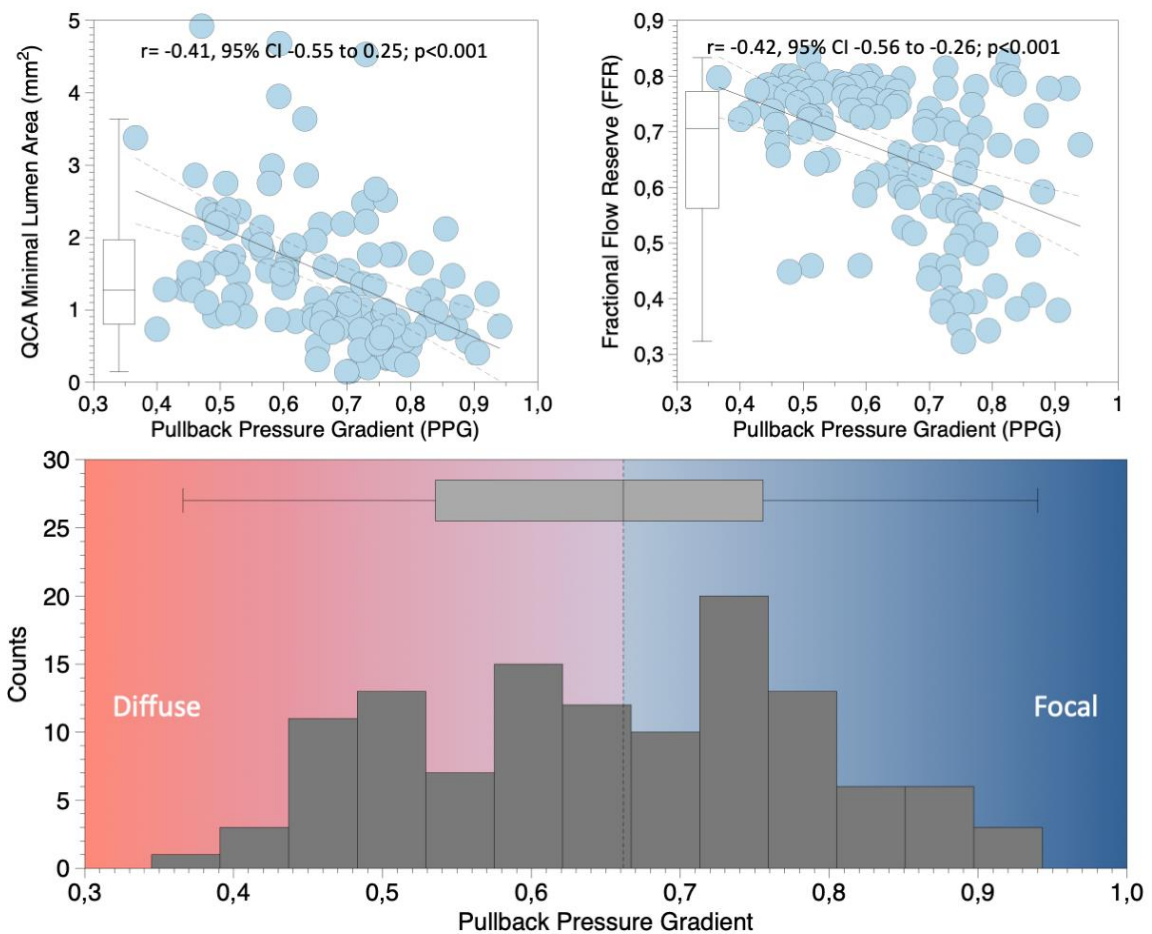
Figure 2. Plaque characteristics based on coronary computed tomography angiography (CCTA) in focal and diffuse disease.

The box plots show CCTA-derived plaque characteristics stratified coronary artery disease (CAD) pattern. Focal CAD is depicted in blue, whereas diffuse disease is in red. Panel A shows plaque burden at the minimal lumen area (MLA); panel B shows percent atheroma volume (vessel level); panel C shows calcified plaque burden; panel D shows non-calcified plaque burden; panel E shows low attenuation plaque burden and panel F shows Agatston score per vessel.
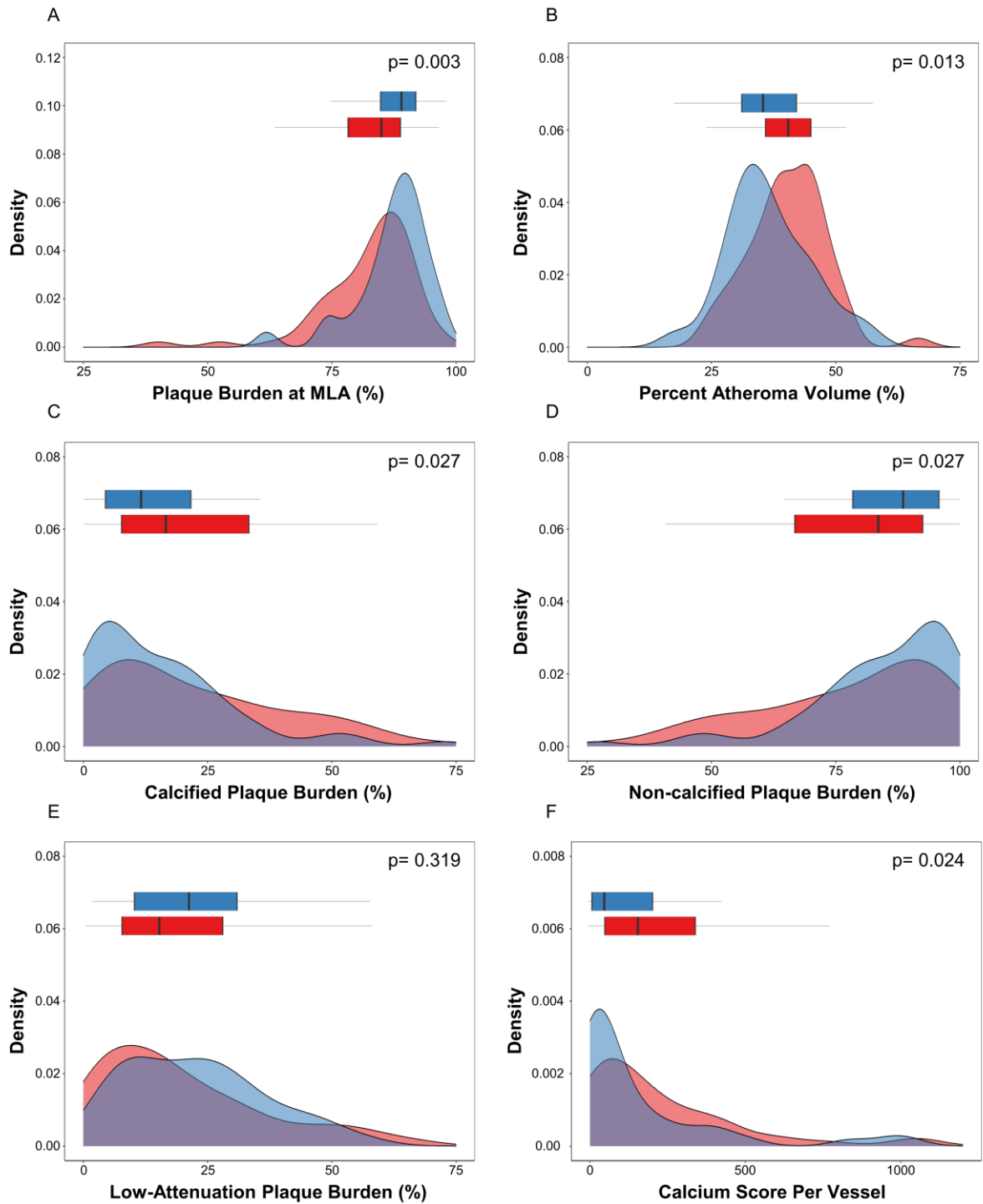
Figure 3. Plaque characteristics based on optical coherence tomography (OCT) in focal and diffuse disease.

Panel A shows the association between pullback pressure gradient (PPG) and fibrous cap thickness, whereas panel B shows the predictive capacity of the PPG for thin-cap fibroatheroma (TCFA). Panel C shows the association between PPG and maximal lipidic arc, while panel D displays the area under the curve for the prediction of circumferential lipid-rich plaque (LRP) based on PPG. Panel E shows the prevalence of OCT plaque features stratified by focal (blue bars) and diffuse disease (red bars).

CI confidence interval. AUC area under the curve.

A

r= -0.55 95% CI -0.74 to -0.28
p-value<0.001

B

AUC: 0.73 (95%CI: 0.58 to 0.87)
Sensitivity: 0.714
Specificity: 0.759
Best PPG Cut-off: 0.65

C

r= 0.54 95% CI 0.28 to 0.73
p-value<0.001

D

AUC: 0.82 (95%CI: 0.66 to 0.99)
Sensitivity: 0.889
Specificity: 0.746
Best PPG Cut-off: 0.65

E
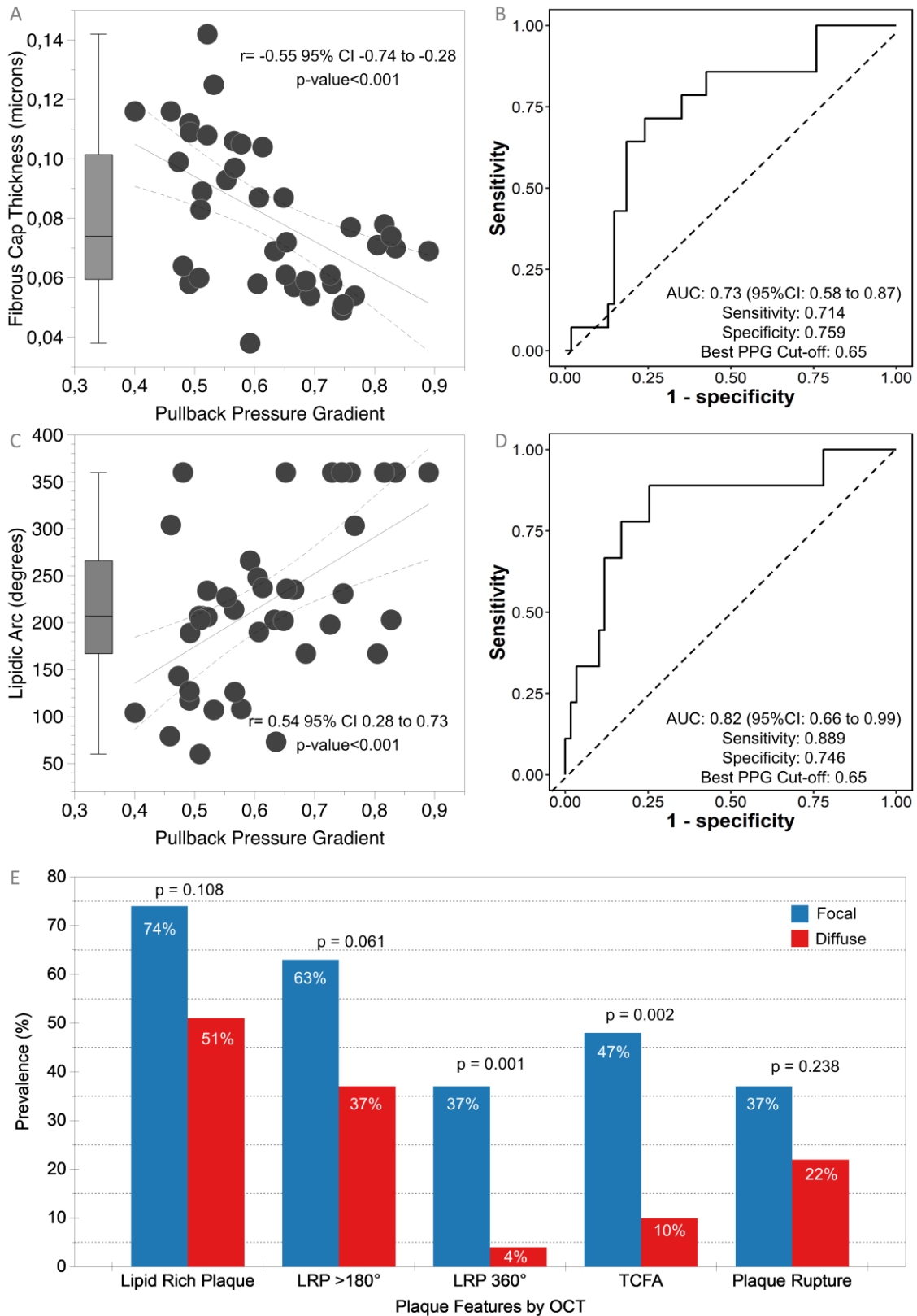
Figure 4. Case examples of focal and diffuse coronary artery disease (CAD).

The left panel shows a case with focal CAD (high PPG), while the right panel shows a patient with diffuse CAD. Panels a and a' show coronary angiography and the white arrowheads identify the lesions. Panels b and b' show coronary computed tomography angiography straight multiplanar reconstructions of the vessel, and panels c and c' and d and d' show the cross-section without and with tissue characterization, respectively. Panels e and e' present the FFR pullback tracings with the corresponding FFR and PPG values. The red bars depict the location and magnitude of pressure drops along the coronary vessel. Panels f through k show cross-sectional and longitudinal optical coherence tomography images, respectively. The star (*) shows plaque rupture, the two stars (**) depict circumferential lipid-rich plaque, the arrowhead thin-cap fibroatheroma, and the white cross (✝) shows circumferential calcified plaque.

FFR fractional flow reserve. PPG pullback pressure gradient.

Central Illustration. Association between CAD patterns and plaque characteristics based on invasive and non-invasive imaging.

We included patients with hemodynamic significant coronary artery disease (CAD) based on FFR ≤ 0.80 with plaque characterization based on coronary computed tomography angiography (CCTA) and optical coherence tomography (OCT). Based on the pullback pressure gradient (PPG) index, patients were divided into those with focal (PPG > 0.66), or diffuse CAD (PPG ≤ 0.66). Vessels with focal CAD (blue bars) had a higher plaque burden and predominantly lipid-rich plaque with a high prevalence of TCFA, whereas calcifications were the hallmark of vessels with diffuse disease (red bars).

Focal CAD

Diffuse CAD
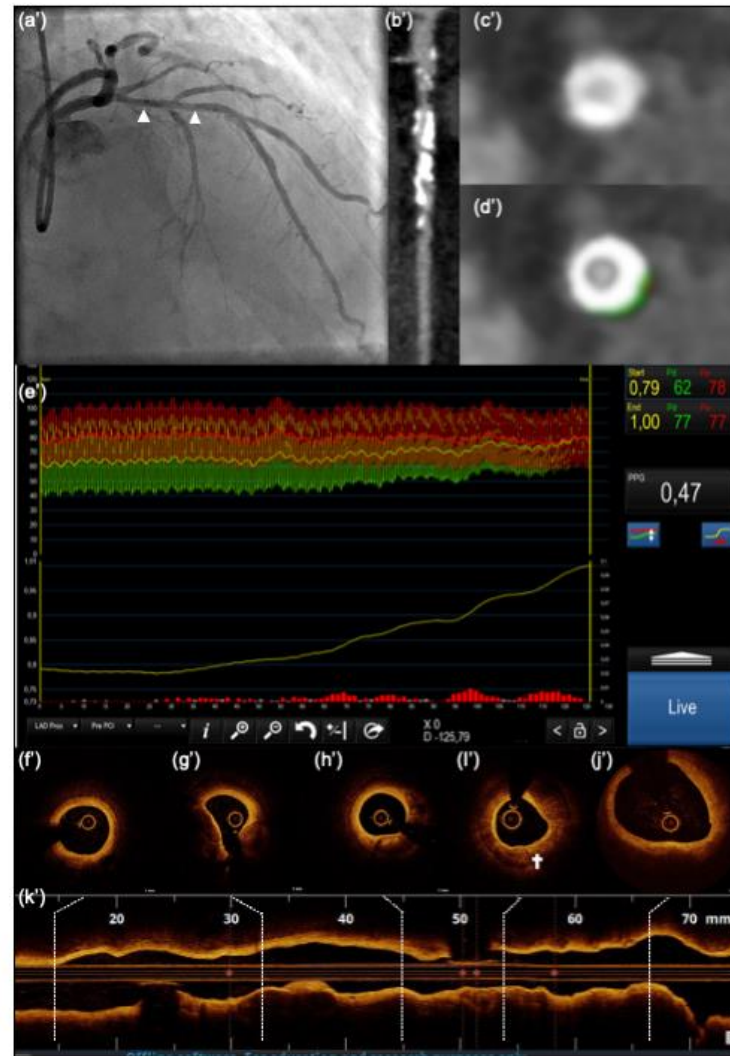
References

1.   Libby P. The changing landscape of atherosclerosis. *Nature*. Apr 2021;592(7855):524-533. doi:10.1038/s41586-021-03392-8

2.   Aherrahrou R, Guo L, Nagraj VP, et al. Genetic Regulation of Atherosclerosis-Relevant Phenotypes in Human Vascular Smooth Muscle Cells. *Circulation Research*. 2020;127(12):1552-1565. doi:10.1161/circresaha.120.317415

3.   Geovanini GR, Libby P. Atherosclerosis and inflammation: overview and updates. *Clin Sci (Lond)*. Jun 29 2018;132(12):1243-1252. doi:10.1042/CS20180306

4.   Wolf D, Ley K. Immunity and Inflammation in Atherosclerosis. *Circulation Research*. 2019;124(2):315-327. doi:10.1161/circresaha.118.313591

5.   Wentzel JJ, Janssen E, Vos J, et al. Extension of increased atherosclerotic wall thickness into high shear stress regions is associated with loss of compensatory remodeling. *Circulation*. Jul 8 2003;108(1):17-23. doi:10.1161/01.CIR.0000078637.21322.D3

6.   Kwak BR, Back M, Bochaton-Piallat ML, et al. Biomechanical factors in atherosclerosis: mechanisms and clinical implications. *Eur Heart J*. Nov 14 2014;35(43):3013-20, 3020a-3020d. doi:10.1093/eurheartj/ehu353

7.   Yang S, Koo BK, Narula J. Interactions Between Morphological Plaque Characteristics and Coronary Physiology: From Pathophysiological Basis to Clinical Implications. *JACC Cardiovasc Imaging*. Jun 2022;15(6):1139-1151. doi:10.1016/j.jcmg.2021.10.009

8.   Stone GW, Maehara A, Lansky AJ, et al. A prospective natural-history study of coronary atherosclerosis. *N Engl J Med*. Jan 20 2011;364(3):226-35. doi:10.1056/NEJMoa1002358

9.   Prati F, Romagnoli E, Gatto L, et al. Relationship between coronary plaque morphology of the left anterior descending artery and 12 months clinical outcome: the CLIMA study. *Eur Heart J*. Jan 14 2020;41(3):383-391. doi:10.1093/eurheartj/ehz520

10.   Waksman R, Di Mario C, Torguson R, et al. Identification of patients and plaques vulnerable to future coronary events with near-infrared spectroscopy intravascular ultrasound imaging: a prospective, cohort study. *The Lancet*. 2019;394(10209):1629-1637. doi:10.1016/s0140-6736(19)31794-5

11.   Huang H, Virmani R, Younis H, Burke AP, Kamm RD, Lee RT. The impact of calcification on the biomechanical stability of atherosclerotic plaques. *Circulation*. Feb 27 2001;103(8):1051-6. doi:10.1161/01.cir.103.8.1051

12.   Matsuo Y, Higashioka D, Ino Y, et al. Association of Hemodynamic Severity With Plaque Vulnerability and Complexity of Coronary Artery Stenosis: A Combined Optical Coherence Tomography and Fractional Flow Reserve Study. *JACC Cardiovasc Imaging*. Jun 2019;12(6):1103-1105. doi:10.1016/j.jcmg.2018.11.023

13.   Lee JM, Choi G, Koo BK, et al. Identification of High-Risk Plaques Destined to Cause Acute Coronary Syndrome Using Coronary Computed Tomographic Angiography and Computational Fluid Dynamics. *JACC Cardiovasc Imaging*. Jun 2019;12(6):1032-1043. doi:10.1016/j.jcmg.2018.01.023

14.   Pagnoni M, Meier D, Candreva A, et al. Future culprit detection based on angiography-derived FFR. *Catheter Cardiovasc Interv*. Sep 2021;98(3):E388-E394. doi:10.1002/ccd.29736

15.   Collet C, Sonck J, Vandeloo B, et al. Measurement of Hyperemic Pullback Pressure Gradients to Characterize Patterns of Coronary Atherosclerosis. *Journal of the American College of Cardiology*. 2019;74(14):1772-1784. doi:10.1016/j.jacc.2019.07.072

16.   Sonck J, Nagumo S, Norgaard Bjarne L, et al. Clinical Validation of a Virtual Planner for Coronary Interventions Based on Coronary CT Angiography. *JACC: Cardiovascular Imaging*. 2022/07/01 2022;15(7):1242-1255. doi:10.1016/j.jcmg.2022.02.003

17.   Williams MC, Kwiecinski J, Doris M, et al. Low-Attenuation Noncalcified Plaque on Coronary Computed Tomography Angiography Predicts Myocardial Infarction: Results From the Multicenter SCOT-HEART Trial (Scottish Computed Tomography of the HEART). *Circulation*. May 5 2020;141(18):1452-1462. doi:10.1161/CIRCULATIONAHA.119.044720

18.   Monizzi G, Sonck J, Nagumo S, et al. Quantification of calcium burden by coronary CT angiography compared to optical coherence tomography. *Int J Cardiovasc Imaging*. Dec 2020;36(12):2393-2402. doi:10.1007/s10554-020-01839-z

19.   Matsumoto H, Watanabe S, Kyo E, et al. Standardized volumetric plaque quantification and characterization from coronary CT angiography: a head-to-head comparison with invasive intravascular ultrasound. *Eur Radiol*. Nov 2019;29(11):6129-6139. doi:10.1007/s00330-019-06219-3

20.   Dey D, Diaz Zamudio M, Schuhbaeck A, et al. Relationship Between Quantitative Adverse Plaque Features From Coronary Computed Tomography Angiography and Downstream Impaired Myocardial Flow Reserve by 13N-Ammonia Positron Emission Tomography: A Pilot Study. *Circ Cardiovasc Imaging*. Oct 2015;8(10):e003255. doi:10.1161/CIRCIMAGING.115.003255

21.   Achenbach S, Ropers D, Hoffmann U, et al. Assessment of coronary remodeling in stenotic and nonstenotic coronary atherosclerotic lesions by multidetector spiral computed tomography. *J Am Coll Cardiol*. Mar 3 2004;43(5):842-7. doi:10.1016/j.jacc.2003.09.053

22.   Park HB, Heo R, B OH, et al. Atherosclerotic plaque characteristics by CT angiography identify coronary lesions that cause ischemia: a direct comparison to fractional flow reserve. *JACC Cardiovasc Imaging*. Jan 2015;8(1):1-10. doi:10.1016/j.jcmg.2014.11.002

23.   Tearney GJ, Regar E, Akasaka T, et al. Consensus standards for acquisition, measurement, and reporting of intravascular optical coherence tomography studies: a report from the International Working Group for Intravascular Optical Coherence Tomography Standardization and Validation. *J Am Coll Cardiol*. Mar 20 2012;59(12):1058-72. doi:10.1016/j.jacc.2011.09.079

24.   Hoshino M, Yonetsu T, Usui E, et al. Clinical Significance of the Presence or Absence of Lipid-Rich Plaque Underneath Intact Fibrous Cap Plaque in Acute Coronary Syndrome. *J Am Heart Assoc*. May 7 2019;8(9):e011820. doi:10.1161/jaha.118.011820

25.   Miyamoto Y, Okura H, Kume T, et al. Plaque characteristics of thin-cap fibroatheroma evaluated by OCT and IVUS. *JACC Cardiovasc Imaging*. Jun 2011;4(6):638-46. doi:10.1016/j.jcmg.2011.03.014

26.   Sugiyama T, Yamamoto E, Fracassi F, et al. Calcified Plaques in Patients With Acute Coronary Syndromes. *JACC Cardiovasc Interv*. Mar 25 2019;12(6):531-540. doi:10.1016/j.jcin.2018.12.013

27.   Nakajima A, Araki M, Minami Y, et al. Layered Plaque Characteristics and Layer Burden in Acute Coronary Syndromes. *Am J Cardiol*. Feb 1 2022;164:27-33. doi:10.1016/j.amjcard.2021.10.026

28.   Driessen RS, de Waard GA, Stuijfzand WJ, et al. Adverse Plaque Characteristics Relate More Strongly With Hyperemic Fractional Flow Reserve and Instantaneous Wave-Free Ratio Than With Resting Instantaneous Wave-Free Ratio. *JACC: Cardiovascular Imaging*. 2020;13(3):746-756. doi:10.1016/j.jcmg.2019.06.013

29.   Ando H, Takashima H, Suzuki A, et al. Impact of lesion characteristics on the prediction of optimal poststent fractional flow reserve. *Am Heart J*. Dec 2016;182:119-124. doi:10.1016/j.ahj.2016.09.015

30.   Sonck J, Collet C, Mizukami T, et al. Motorized fractional flow reserve pullback: Accuracy and reproducibility. *Catheter Cardiovasc Interv*. Sep 1 2020;96(3):E230-E237. doi:10.1002/ccd.28733

31.   Li ZY, Taviani V, Tang T, et al. The mechanical triggers of plaque rupture: shear stress vs pressure gradient. *Br J Radiol*. Jan 2009;82 Spec No 1:S39-45. doi:10.1259/bjr/15036781

32.   Chatzizisis YS, Coskun AU, Jonas M, Edelman ER, Feldman CL, Stone PH. Role of endothelial shear stress in the natural history of coronary atherosclerosis and vascular remodeling: molecular, cellular, and vascular behavior. *J Am Coll Cardiol*. Jun 26 2007;49(25):2379-93. doi:10.1016/j.jacc.2007.02.059

33.   Genereux P, Madhavan MV, Mintz GS, et al. Ischemic outcomes after coronary intervention of calcified vessels in acute coronary syndromes. Pooled analysis from the HORIZONS-AMI (Harmonizing Outcomes With Revascularization and Stents in Acute Myocardial Infarction) and ACUITY (Acute Catheterization and Urgent Intervention Triage Strategy) TRIALS. *J Am Coll Cardiol*. May 13 2014;63(18):1845-54. doi:10.1016/j.jacc.2014.01.034

34.   Motoyama S, Ito H, Sarai M, et al. Plaque Characterization by Coronary Computed Tomography Angiography and the Likelihood of Acute Coronary Events in Mid-Term Follow-Up. *J Am Coll Cardiol*. Jul 28 2015;66(4):337-46. doi:10.1016/j.jacc.2015.05.069

35.   Chaitman BR, Alexander KP, Cyr DD, et al. Myocardial Infarction in the ISCHEMIA Trial: Impact of Different Definitions on Incidence, Prognosis, and Treatment Comparisons. *Circulation*. Feb 23 2021;143(8):790-804. doi:10.1161/CIRCULATIONAHA.120.047987

36.   Yang S, Koo BK, Hwang D, et al. High-Risk Morphological and Physiological Coronary Disease Attributes as Outcome Markers After Medical Treatment and Revascularization. *JACC Cardiovasc Imaging*. Oct 2021;14(10):1977-1989. doi:10.1016/j.jcmg.2021.04.004

Chapter 8. Influence of intracoronary hemodynamic forces on atherosclerotic plaque phenotypes

Candreva A, Gallo D, Munhoz D, Rizzini ML, Mizukami T, Seki R, Sakai K, Sonck J, Mazzi V, Ko B, Nørgaard BL, Jensen JM, Maeng M, Otake H, Koo BK, Shinke T, Aben JP, Andreini D, Gallinoro E, Stähli BE, Templin C, Chiastra C, De Bruyne B, Morbiducci U, Collet C.

Central illustration – Interplay between wall shear stress and intracoronary pressure patterns and their association with plaque phenotypes.
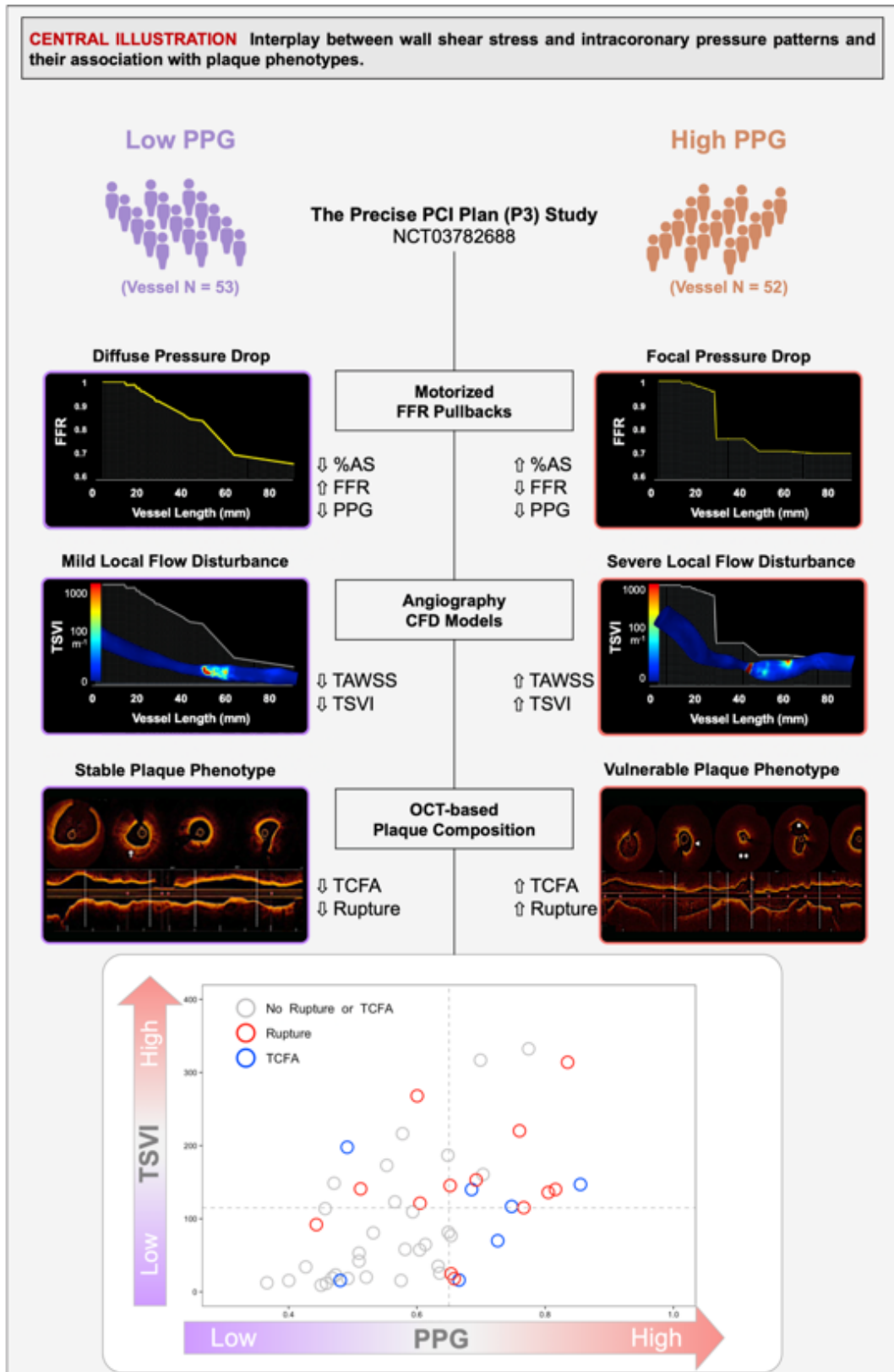
Abstract

Background and aims: Coronary hemodynamics impact coronary plaque progression and destabilization. The aim of the present study was to establish the association between focal vs. diffuse intracoronary pressure gradients and wall shear stress (WSS) patterns with atherosclerotic plaque composition.

Methods: Prospective, international, single-arm study of patients with chronic coronary syndromes and hemodynamic significant lesions (fractional flow reserve [FFR] $\leq$ 0.80). Motorized FFR pullback pressure gradient (PPG), optical coherence tomography (OCT), and time-average WSS (TAWSS) and topological shear variation index (TSVI) derived from three-dimensional angiography were obtained.

Results: One hundred five vessels (median FFR 0.70 [Interquartile range (IQR) 0.56-0.77]) had combined PPG and WSS analyses. TSVI was correlated with PPG (r = 0.47, [95% Confidence Interval (95% CI) 0.30-0.65], p < 0.001). Vessels with a focal CAD (PPG above the median value of 0.67) had significantly higher TAWSS (14.8 [IQR 8.6-24.3] *vs.* 7.03 [4.8-11.7] Pa, p < 0.001) and TSVI (163.9 [117.6-249.2] *vs.* 76.8 [23.1-140.9] m^{-1}, p < 0.001). In the 51 vessels with baseline OCT, TSVI was associated with plaque rupture (OR 1.01 [1.00-1.02], p = 0.024), PPG with the extension of lipids (OR 7.78 [6.19-9.77], p = 0.003), with the presence of thin-cap fibroatheroma (OR 2.85 [1.11-7.83], p = 0.024) and plaque rupture (OR 4.94 [1.82 to 13.47], p = 0.002).

Conclusions: Focal and diffuse coronary artery disease, defined using coronary physiology, are associated with differential WSS profiles. Pullback pressure gradients and WSS profiles are associated with atherosclerotic plaque phenotypes. Focal disease (as identified by high PPG) and high TSVI are associated with high-risk plaque features.

Introduction

An elevated translesional pressure gradient is considered the main biomechanical hallmark of atherosclerotic disease,[1] and clinically has been associated with plaque destabilization and adverse clinical events.[2] The recent introduction of pullback pressure gradient (PPG) allowed to quantify the distribution of intracoronary pressure decay [3,4] promising standardization in the diagnosis of focal *vs.* diffuse coronary artery disease (CAD) and favoring the identification of vulnerable coronary lesions.[5]

Besides pressure gradients, the shear action exerted at the blood-endothelium interface, quantifiable in terms of wall shear stress (WSS), is associated with coronary plaque nucleation, progression and destabilization.[6] WSS characterization based on computational fluid dynamics (CFD) simulations applied to three-dimensional (3D) coronary vessel models identifies vascular segments with dysfunctional endothelial function [7] or vulnerable plaques.[8-12] Furthermore, WSS calculation predictive of plaque rupture can now be made based on conventional coronary angiography, potentially facilitating its use in clinical practice.[13]

I   n the present investigation longitudinal invasive pressure assessment, WSS profiles obtained from angiography-derived CFD simulations, and atherosclerotic plaque phenotype identification based on intracoronary optical coherence tomography (OCT) were combined to explore possible links between focal *vs.* diffuse intracoronary pressure gradients, WSS and atherosclerotic plaque features.

Methods

The workflow of the study is graphically illustrated in Figure 1.

Study design

The P3 study was an investigator-initiated, multicenter, prospective, single-arm study of patients electively referred to invasive coronary angiography (ICA). The study aimed to validate the accuracy of coronary computed tomography angiography-derived fractional flow reserve (FFR_{CT}) planner for post-percutaneous coronary intervention (PCI) invasive FFR prediction. Patients were included in the P3 study if invasive distal FFR demonstrated a significant flow impairment (FFR $\leq$ 0.80). The design and results of the P3 Study are presented extensively elsewhere.[14,15] Patients undergoing motorized FFR pullbacks, angiography-derived WSS and OCT were included.

The registered study protocol (NCT03782688) was approved by the investigational review board or ethics committee at each participating center, and all enrolled patients provided

written informed consent before study procedures. The P3 study was sponsored by the Cardiac Research Institute Aalst (Aalst, Belgium), with unrestricted grants from HeartFlow (Redwood City, CA, USA) and CardioPath (University of Naples, Naples, Italy).

Pullback Pressure Gradient

Motorized FFR pressure pullback tracings were acquired using a pullback device (Volcano R100, Volcano Corporation, San Diego, USA) at a speed of 1 mm per second and were used for quantitative invasive translesional pressure gradients before and after PCI. Technically, from the FFR pullback pressure curves the PPG (a non-dimensional pullback FFR-based quantity ranging from 0 "diffuse disease" to 1 "focal disease") [3] was calculated with commercial software (CoroFlow v3.5, Coroventis Research, Uppsala, Sweden). Functional descriptors based on hyperemic pressure pullbacks included PPG, maximal pressure gradient over 20 mm (MaxPPG$_{20mm}$), and length of functional disease, and are detailed in the Supplemental Methods. [3]

Quantitative coronary angiography

Individual coronary vessel geometries were reconstructed based on 3D quantitative coronary angiography (3D-QCA) using two angiographic end-diastolic frames at least 30 degrees apart (CAAS Workstation WSS software, Pie Medical Imaging, Maastricht, The Netherlands). Automatic lumen contour detection was enabled, and manually corrected only if needed. 3D vascular models were reconstructed from vessel ostium to pressure sensor position. Vessels presenting ostial lesions identified in terms of minimal lumen area (MLA) located at ≤ 20 mm distance from the ostium or presenting side branches with diameter ≥ 2.0 mm were excluded from the analysis.

The *lesion* was quantified as percentage area stenosis (%AS) and defined as the coronary segment including the MLA, delimited proximally and distally by the intersection of the 3D-QCA diameter function line with the interpolated reference line. [16] The mid lesion segment included the MLA section and its length was proximally and distally delimited on the 3D-QCA reference diameter function line using a threshold value set at 60% of the hydraulic diameter of the MLA section relative severity value (Supplemental Figure S1). The rationale for the choice of this threshold lies on the supposition of a Gaussian stenosis distribution profile, wherein the relative severity is maximal and equal to 100% at the MLA, while the proximal and distal cross-sections at a relative severity of 60% subdivide the lesion segment into three sub-segments of equal length.

175

Blood flow simulations and wall shear stress

Realistic CFD simulations of coronary hemodynamics were carried out on the reconstructed 3D vascular geometries using a finite element-based code (CAAS Workstation WSS software, Pie Medical Imaging, Maastricht, The Netherlands). Using CFD data, the WSS distribution on the luminal surface was quantified along the cardiac cycle. In details, two WSS-based quantities, namely the time-averaged wall shear stress (TAWSS) and the recently proposed topological shear variation index (TSVI, a measure of the variability of the WSS contraction/expansion action exerted on the endothelium along the cardiac cycle), were computed as extensively reported in previous studies.[13,17-19] TAWSS and TSVI data reported in the following text refer uniquely to their values averaged over the mid segment of the lesion. Details on CFD settings and vessel segmentation for 3D anatomical reconstructions are reported in the Supplemental Methods.

Optical coherence tomography

OCT pullbacks of 75 mm length were acquired using Dragonfly OPTIS Imaging Catheter (Abbott Vascular, St. Paul, MN, USA). OCT acquisitions performed after lesion pre-dilatation were excluded from the present analysis. OCT-based plaque composition analysis was performed at the lesion level as extensively detailed elsewhere.[20]

Statistical analysis

The statistical analysis was performed on a per-vessel basis. The median PPG value was used to define groups with focal or diffuse disease. Median TAWSS and TSVI values were adopted to define "high or low TAWSS" and "high or low TSVI" sub-groups.

Normality of distribution was assessed with the Shapiro–Wilk test. Continuous variables with normal distribution are presented as mean ± standard deviation (SD) and non-normally distributed variables as median and inter-quartile range [IQR]. Categorical variables are presented as percentage. The Chi-squared test was used for comparing categorical variables, the Student's t test (or Mann-Whitney test as appropriate) for continuous ones. Linear relationship between continuous variables was assessed using correlation coefficients. Uni- and multivariate generalized linear models were used to perform regression analyses on continuous OCT variables and PPG- or WSS-based quantities. The logistic generalized linear model was used in case of categorical OCT variables. Odd ratios (OR) per unit increase in the independent variable and their 95% confidence interval (95% CI) were obtained from the exponential of the standardized correlation coefficients. A p-value < 0.050 was considered

significant. The discriminatory capacity for high-risk plaque features of %AS, PPG, TAWSS and TSVI were assessed using C-statistics. Receiving operator characteristic (ROC) curves were compared in terms of area under the curve (AUC) and using the DeLong method.[21]

All analyses were performed using R (Version 1.2.5033, R Foundation for Statistical Computing, Vienna, Austria) and MATLAB (Version R2022, MathWorks, Natick, MA, USA).

Results

Of 120 vessels (117 patients) with PPG tracings, 105 (87.5%) underwent 3D vessel reconstruction and WSS analysis. Of those, 51 (42.5%) had OCT pullbacks performed before any intracoronary intervention, Supplemental Figure S2.

Baseline characteristics

Baseline patient characteristics and results from the analysis of WSS and PPG data are reported in Table 1. Median FFR and mean PPG were 0.70 [IQR 0.56-0.77] and 0.66 ± 0.13, respectively. Vessels in the high PPG group exhibited significantly higher %AS, and significantly lower FFR. The hemodynamics in vessels presenting with high PPG (focal CAD) was characterized by a two-fold increase in the TAWSS and TSVI values.

Association of CAD patterns and wall shear stress profiles

There was an association between WSS profiles and CAD patterns, Figure 2. After adjustment for other lesion features such as %AS and lesion length, the independent association with PPG was retained only for TSVI. Results from the uni- and multivariate analysis for the association between CAD patterns and WSS profiles are presented in Table 2.

Association of coronary plaque features with wall shear stress

A summary of the investigated pre-PCI OCT-based plaque characteristics are displayed in Table 3 and Supplemental Table S1. The relationship between pressure gradients and WSS with plaque phenotype is summarized in Figure 3. Fibrocalcific plaque was the most common observed plaque phenotype (60.8%). Thin cap fibroatheroma (TCFA) and plaque rupture were more prevalent among high PPG than among low PPG vessels. TAWSS was associated with macrophage plaque infiltration. TSVI was associated with plaque rupture and cholesterol crystals. Other associations between WSS and OCT plaque features are presented in Table 4. The predicted capacity for identification of high risk plaque features by %AS, WSS and PPG are shown in the Supplemental Figure S3.

Association of coronary plaque features with intracoronary pressure gradients

PPG was associated with the extension of the lipid circumferential infiltration, thin-cap fibroatheroma and plaque rupture, and inversely associated to the fibrous cap thickness. Other associations between PPG and OCT plaque features are presented in Table 4. PPG was associated with fibrous cap thickness independently from TAWSS and TSVI (Supplemental Table S2-S3).

When combining CAD and WSS patterns, vessels presenting high PPG presented thinner fibrous caps, higher prevalence of TCFA and plaque rupture in both low and high TAWSS and TSVI conditions, see Supplemental Table S4-S5.

The main results of the study are summarized in the Central Illustration.

Discussion

In this study, we addressed the inter-relationship between intravascular hemodynamic forces exerted by the blood and plaque composition. The main findings of the study are: (i) higher values of TAWSS (depicting the WSS magnitude averaged along the cardiac cycle) and TSVI (a measure of the contraction/expansion variability exerted by the shear forces on the endothelium along the cardiac cycle) were found in vessels presenting a focal rather than diffuse disease; (ii) focal disease and elevated shear forces were associated with high-risk plaque phenotypes at the OCT evaluation; (iii) vessels with a diffuse pattern of disease based on coronary physiology showed milder local flow disturbances and less frequently presented plaque vulnerability features.

Wall shear stress and pressure gradients

High pressure gradients across epicardial lesions have been recognized as independent predictors of cardiovascular events.[22] In simple cases, as per Hagen-Poiseuille theory, pressure gradients and WSS are in direct linear relationship in cylindric conduits.[23] Still, the nature of such a relationship becomes more intricate in coronary arteries, mainly because of anatomical complexity and flow pulsatility. However, because of their effect on coronary flow rate, pressure gradients reflect on the shear forces acting at the level of the blood-endothelium interface.[24] The existence of such a link was confirmed by a sub-analysis from the Fractional Flow Reserve Versus Angiography for Multivessel Evaluation II (FAME II) trial, where Kumar et al. suggested that in flow-impairing lesions high TAWSS values were predictive of lesion destabilization and clinically overt MI.[8] Moreover, high TAWSS and mostly high TSVI identified lesions with negative FFR leading to future adverse events,[9] and showed incremental

power for MI prediction on top of lesion anatomical severity and translesional pressure gradients.[13]

In the present analysis, in addition to time-averaged magnitude of WSS (TAWSS), also the time-dependent variability in the contraction-expansion action exerted by the shear forces on the endothelium was quantified by TSVI. Focal lesions (high PPG) were anatomically more severe than in vessels with diffuse disease (low PPG) (percentage AS = 83.73% *vs* 72.86%, p < 0.001). This more pronounced anatomical severity reflected not only on a more pronounced flow impairment in the focal pressure drop group with lower FFR values (0.57 vs. 0.75, p < 0.001), but also in deranged WSS profiles at the lesion level. In fact, vessels with a focal disease presented elevated TAWSS and TSVI (14.78 Pa and 163.93 m^{-1}) values, exceedingly above the known values associated with adverse coronary events (5-7 Pa for TAWSS and 40.5 m^{-1} for TSVI).[13,25] On the other hand, lesions with diffuse pressure losses presented with lower TAWSS and TSVI values (7.03 Pa and 76.82 m^{-1}), and in half of cases with TAWSS values within the physiological range (i.e., 1-7 Pa).[25] These findings suggested a more stable endothelial shear stress profile in lesions with diffuse disease defined by longitudinal intracoronary pressure assessment.

Wall shear stress and plaque composition

Links between adverse endothelial shear stress patterns and plaque progression have been described *post-mortem* and *in vivo*.[7,19,26] Less well characterized is the relationship between WSS patterns and plaque composition. Extensive preclinical experience related WSS with the development of lipid-rich, inflamed or thin-capped (vulnerable) plaques.[27,28] In humans, lower WSS areas have been associated with larger plaque burden, predicting adverse clinical events.[29] Notably, as plaques grow sufficiently to encroach into the lumen, translesional pressure gradients increase and low WSS areas at the throat of the stenoses turn into high WSS areas, altering the hemodynamic microenvironment and increasing the risk of plaque destabilization and rupture.[8,30] Focal intracoronary pressure gradients were previously associated with higher plaque burden and increased lipidic plaque components, while a diffuse intravascular pressure decay was associated with an increased calcific plaque component.[5] In a prospective study based on virtual histology intravascular ultrasound (VH-IVUS), WSS patterns were associated with adverse alterations in plaque composition (rather than plaque size), pointing towards the need for a wider intracoronary flow patterns description to capture the complexity of plaque evolution.[31] In the present study, OCT-defined plaque rupture was

associated with TSVI. TSVI has also been linked to the development of long-term restenosis after carotid endarterectomy,[18] to the longitudinal coronary vessel wall thickening,[19] and the longitudinal risk of MI.[13] These studies demonstrated that TSVI represents a different hemodynamic signal to the endothelium with respect to TAWSS and relates to high-risk features previously link with adverse events.[17,18]

This is consistent with the findings of the present study, where TSVI (rather than TAWSS) showed an association with OCT plaque characteristics. In fact, TAWSS associated significantly with macrophage infiltration, while TSVI with plaque rupture, cholesterol crystals and inversely with the thickness of the calcium component of the plaque. Finally, focal disease presented with larger lipid components and thinner fibrotic caps, often (subclinically) ruptured. These findings confirm that coronary lesions with a focal pressure gradient pattern present also adverse WSS features, which might synergically interplay favoring plaque destabilization and rupture. On the contrary, diffusely diseased vessels exhibited lower TAWSS and TSVI and a more favorable plaque phenotype, with lower TCFA or plaque rupture prevalence.

Making sense of the 'alphabet soup' of hemodynamic quantities in focal and diffuse flow-limiting lesions

The observed results suggest a differential interplay between translesional pressure gradients, WSS and plaque composition. Lesions generating an abrupt local increase in epicardial resistance (high PPG, i.e. high focal pressure gradients) elicit more marked flow disturbances, captured by high TAWSS values, and alter the physiological topology of the WSS field, as documented by high TSVI values. Conceptually, while an interaction of pressure gradients with TAWSS was expected (see e.g. the above-mentioned simple fluid mechanics paradigm of Hagen-Poiseuille theory), an interaction with TSVI is not a foregone conclusion: the obtained results cannot be easily justifiable on the basis of very simple fluid mechanics examples, as they come up from the hemodynamic richness within coronary vessels presenting with severe lesions and in general in the presence of marked flow disturbances in arteries.

Nonetheless, the clustering of hemodynamic factors (focal pressure gradients and adverse WSS profiles) may result in a worsening of the endothelial function, unphysiological intra- and intercellular tensions, and the widening in the intercellular gaps.[32] This favors further plaque infiltration while the shearing of the fibrotic cap increases, and with it the risk of plaque destabilization and plaque rupture when humoral forces exceed the plaque strength.[6,33] For this reason, the presence of high translesional focal pressure gradients combined with adverse

plaque features may permit a refined plaque risk stratification, where pre-emptive strategies with sealing effect on those vulnerable plaques might be tested.[34] On the other hand, flow-impairing lesions with a diffuse pressure drop pattern might accommodate better local blood flow disturbances, resulting in a less vulnerable plaque phenotype.

Limitations

Some limitations merit consideration. First, the uncertainty inherent in the reconstruction of vascular geometries from angiographic images as well as the idealizations introduced in modelling coronary flows with CFD might have influenced the calculation of the considered WSS-based quantities. However, previous sensitivity studies [25,35] suggest that the generalization of the results can be affected only modestly. Second, given the relatively small sample size, a larger population is required to confirm the presented findings. In the OCT sub-analysis, only patients with native OCT lesion crossings were considered, excluding any crossings after lesion manipulation. This selection ensured a genuine evaluation of native lesions. Nonetheless, the here investigated dataset is the first cohort combining motorized pressure recordings along the epicardial vessel and high resolution OCT imaging acquisitions. Third, the report is restricted to the description of the association between CAD patterns and WSS profiles, the clinical implications of these findings requires further investigation.

Conclusions

The present investigation related intracoronary pressure gradients with angiography-based WSS analysis from CFD simulations and plaque composition in vessels presenting flow-impairing lesions in the elective setting of a chronic coronary syndrome. The findings of this study support the hypotheses that: (i) the hemodynamic profile identified by pressure gradient and the WSS-based quantities TAWSS and TSVI is different in patients presenting with focal and diffuse CAD; (ii) the different hemodynamic profiles characterizing focal and diffuse CAD are associated with different atherosclerotic plaque phenotype. Taken together, these findings point towards a central role of adverse WSS features in the destabilization mechanisms of coronary lesions presenting a focal pressure drop pattern.

Table 1. Clinical and anatomo-functional baseline characteristics

	Overall (Patient n = 103)	Low PPG (Patient n = 52)	High PPG (Patient n = 51)	p-value (two-sided)
Age, years (mean ± SD)	63.85 ± 9.17	64.92 ± 8.64	62.72 ± 9.65	0.226
Male, n (%)	85 (82.5)	44 (84.6)	41 (80.4)	0.613
BMI, kg/m2 (mean ± SD)	26.8 ± 3.23	26.67 ± 3.44	26.67 ± 3.04	0.681
Dyslipidemia, n (%)	78 (75.7)	39 (75.0)	39 (76.5)	1.000
Hypertension, n (%)	57 (55.3)	27 (51.9)	30 (58.8)	0.554
Diabetes mellitus, n (%)	22 (21.4)	12 (23.1)	10 (19.6)	0.811
- under insulin, n (%)	4 (3.9)	4 (7.7)	0 (0.0)	0.118
Current smoker, n (%)	20 (19.4)	11 (21.2)	9 (17.6)	0.804
Coronary artery disease, n (%)	4 (3.9)	2 (3.8)	2 (3.9)	1.000
Peripheral artery disease, n (%)	5 (4.9)	2 (3.8)	3 (5.9)	0.678
Clinical Presentation				
Silent ischemia, n (%)	24 (23.3)	16 (30.8)	8 (15.7)	
Stable angina CCS I, n (%)	33 (32.0)	19 (36.5)	14 (27.5)	
Stable angina CCS II, n (%)	36 (35.0)	14 (26.9)	22 (43.1)	
Stable angina CCS III, n (%)	7 (6.8)	2 (3.8)	5 (9.8)	0.091
Stable angina CCS IV, n (%)	1 (1.0)	1 (1.9)	0 (0.0)	
Unstable angina, n (%)	2 (1.9)	0 (0.0)	2 (3.9)	
Creatinine Clearance, mL/min (mean ± SD)	78.94 ± 22.65	74.80 ± 18.12	83.16 ± 25.99	0.061
LVEF, % (mean ± SD)	60.14 ± 6.11	60.16 ± 7.09	60.12 ± 4.98	0.978
Anatomical and functional characteristics				
	Overall (Vessel N = 105)	Low PPG (Vessel N = 53)	High PPG (Vessel N = 52)	p-value (two-sided)
LAD, n (%)	76 (72.4)	51 (96.2)	25 (48.1)	
LCX, n (%)	12 (11.4)	1 (1.9)	11 (21.1)	< 0.001
RCA, n (%)	17 (16.2)	1 (1.9)	16 (30.8)	
%AS (mean ± SD)	78.24 ± 11.64	72.86 ± 10.53	83.73 ± 10.12	<0.001
Anatomical lesion length, mm (mean ± SD)	19.48 ± 10.57	20.45 ± 10.46	18.49 ± 10.70	0.345
FFR (median [IQR])	0.70 [0.56-0.77]	0.75 [0.68-0.78]	0.57 [0.45-0.70]	<0.001

PPG (mean ± SD)	0.66 ± 0.13	0.55 ± 0.08	0.77 ± 0.06	<0.001
MaxPPG20mm (mean ± SD)	0.27 ± 0.16	0.17 ± 0.08	0.38 ± 0.14	<0.001
Vessel percentage with functional disease (mean ± SD)	0.35 ± 0.20	0.39 ± 0.22	0.31 ± 0.17	0.057
TAWSS, Pa (median [IQR])	9.93 [5.75-16.35]	7.03 [4.80-11.67]	14.78 [8.62-24.34]	<0.001
TSVI, m^{-1} (median [IQR])	123.13 [58.39-198.03]	76.82 [23.10-140.95]	163.93 [117.56-249.22]	<0.001

Results for categorical variables are presented as count and percentage. Results for continuous variables are presented as mean ± standard deviation (SD) or as median and interquartile range (IQR). %AS = percentage area stenosis; BMI=body mass index; CCS=Canadian cardiovascular society; FFR = fractional flow reserve; LVEF=left ventricle ejection fraction; MaxPPG$_{20mm}$= maximum pressure gradients over 20 mm; PPG=pullback pressure gradient; TAWSS = time-averaged wall shear stress measured at the mid lesion segment (*throat*); TSVI = topological shear variation index measured at the mid lesion segment (*throat*).

Table 2. Uni- and multivariate analyses for the association with the PPG (Vessel N = 105).

	Univariate models		Multivariate model With TAWSS		Multivariate model With TSVI	
	OR (95% LCI to UCI)	*p-value*	OR (95% LCI to UCI)	*p-value*	OR (95% LCI to UCI)	*p-value*
- Lesion length	0.9997 (0.9973 to 1.0021)	0.797	0.9983 (0.9963 to 1.0002)	0.082	0.9984 (0.9965 to 1.0004)	0.118
- %AS	1.0063 (1.0045 to 1.0081)	<0.0001	1.0056 (1.0035 to 1.0077)	<0.0001	1.0052 (1.0030 to 1.0074)	<0.0001
- TAWSS	1.0046 (1.0026 to 1.0065)	<0.0001	1.0020 (0.9999 to 1.0040)	0.059	-	-
- TSVI	1.0006 (1.0004 to 1.0008)	<0.0001	-	-	1.0003 (1.0000 to 1.0005)	0.030

The PPG is assumed as continuous quantitative variable. Univariate models: PPG *vs*. anatomical lesion length, PPG *vs*. percentage area stenosis (%AS); PPG *vs*. TAWSS or TSVI. Multivariate models: PPG *vs*. anatomical lesion length + %AS + TAWSS or TSVI. OR = odds ratio of the univariate or multivariate analysis; 95% LCI to UCI = 95% lower and upper confidence intervals. %AS = percentage area stenosis; TAWSS = time-averaged wall shear stress measured at the mid lesion segment (*throat*); TSVI = topological shear variation index measured at the mid lesion segment (*throat*).

Table 3. Optical coherence tomography (OCT) plaque analysis before PCI (Vessel N = 51).

	Total (Vessel N = 51)	Low PPG (Vessel N = 38)	High PPG (Vessel N = 13)	p-value (two-sided)
Lipid-rich plaque, n (%)	29 (56.9)	20 (52.6)	9 (69.2)	0.297
Lipid-rich plaque ≥ 180°, n (%)	21 (41.2)	14 (36.8)	7 (53.8)	0.282
Lipidic arc, degree (°) (median [IQR])	205 [143 – 237]	203 [126 – 235]	267 [182 – 360]	0.107
Calcific plaque, n (%)	42 (82.4)	31 (81.6)	11 (84.6)	0.804
Calcium thickness, mm (median [IQR])	0.89 [0.73 – 1.16]	0.89 [0.73 – 1.20]	0.90 (0.68 – 1.16)	0.933
Calcium arc, degree (°) (median [IQR])	140 [86 – 308]	139 [80 – 308]	206 [94 – 360]	0.107
Fibrocalcific plaque, n (%)	31 (60.8)	25 (65.8)	6 (46.2)	0.211
Fibrous cap thickness, µm (median [IQR])	77.0 (61.0 – 99.0)	91.0 (66.5 – 105.5)	61.0 (54.0 – 71.0)	0.005
TCFA, n (%)	11 (21.6)	5 (13.2)	6 (46.2)	0.013
Plaque rupture, n (%)	13 (25.5)	7 (18.4)	6 (46.2)	0.048
Macrophage, n (%)	14 (27.5)	10 (26.3)	4 (30.8)	0.756
Cholesterol crystals, n (%)	21 (41.2)	14 (36.8)	7 (53.8)	0.282

Frequencies of coronary plaque features independently adjudicated from optical coherence tomography (OCT) acquisition before any percutaneous coronary intervention (PCI). Results for categorical variables are presented as count and percentage. Results for continuous variables are presented as median and interquartile range (IQR). TCFA = Thin-cap fibrous atheroma.

Table 4. Association between TAWSS, TSVI or PPG and OCT plaque phenotypes (Vessel N = 51).

OCT-based plaque feature	TAWSS Mid		TSVI Mid		PPG	
	OR (95% LCI to UCI)	*p-value*	OR (95% LCI to UCI)	*p-value*	OR (95% LCI to UCI)	*p-value*
Lipid-rich plaque ≥ 180°	0.935 (0.846 to 1.033)	0.176	1.002 (0.994 to 1.010)	0.702	3.171 (1.021 to 9.845)	0.046
Lipidic arc	0.153 (0.004 to 5.677)	0.296	1.195 (0.830 to 1.720)	0.327	7.776 (6.186 to 9.773)	0.003
Calcific plaque	1.111 (0.925 to 1.334)	0.251	1.004 (0.995 to 1.014)	0.373	1.052 (0.422 to 2.625)	0.911
Calcium thickness	0.988 (0.973 to 1.002)	0.094	0.998 (0.997 to 0.999)	0.032	0.548 (0.195 to 1.541)	0.247
Calcium arc	0.990 (0.962 to 1.019)	0.611	1.000 (0.998 to 1.002)	0.756	2.021 (0.378 to 10.796)	0.401
Fibrocalcific plaque	0.967 (0.865 to 1.081)	0.540	0.994 (0.986 to 1.002)	0.135	0.309 (0.094 to 1.009)	0.052
Fibrous cap thickness	1.000 (0.999 to 1.001)	0.964	1.000 (0.999 to 1.000)	0.562	0.898 (0.845 to 0.954)	0.001
TCFA	0.999 (0.873 to 1.146)	0.999	1.000 (0.993 to 1.008)	0.907	2.847 (1.112 to 7.825)	0.029
Plaque rupture	1.043 (0.913 to 1.192)	0.523	1.012 (1.001 to 1.024)	0.024	4.943 (1.815 to 13.465)	0.002
Macrophage	1.154 (1.021 to 1.304)	0.018	1.010 (0.999 to 1.020)	0.061	1.008 (0.339 to 2.995)	0.988
Cholesterol crystals	1.131 (0.980 to 1.304)	0.084	1.008 (1.000 to 1.015)	0.041	1.293 (0.378 to 4.430)	0.676

OR = Odds ratio of the univariate analysis; 95% LCI to UCI = 95% lower and upper confidence intervals. PPG = pullback pressure gradients; TAWSS = time-averaged wall shear stress measured at the mid lesion segment (throat); TCFA Thin-cap fibrous atheroma; TSVI = topological shear variation index measured at the mid lesion segment (throat).

Figure 1 – Study workflow.

The present sub-analysis of the Precise PCI Plan (P3) study investigated coronary lesions with a pathological fractional flow reserve (FFR ≤ 0.80) with motorized pullback pressure gradient (PPG). From the PPG, lesions were classified as presenting a focal functional pattern (PPG above the median value) or as presenting a diffuse functional pattern (PPG below the median value). Next, angiography-based three-dimensional vessel reconstructions were obtained from two angiographic projections and used to run computational fluid dynamics (CFD) simulations with the measurement of time-averaged wall shear stress (TAWSS) and topological shear variation index (TSVI) at the level of the throat of the lesion. In parallel, pre-PCI optical coherence tomography (OCT) acquisitions of each lesion were independently assessed for the adjudication of plaque composition and vulnerability features. Finally, association between functional parameters (derived from the PPG and WSS analyses) and anatomical parameters (derived from the quantitative angiography and the OCT analyses) was statistically investigated. TCFA = thin-cap fibrous atheroma; MF = macrophage infiltration.

Flow-impairing coronary
lesion (FFR ≤ 0.80)
with motorized pullback
pressure gradient (PPG)
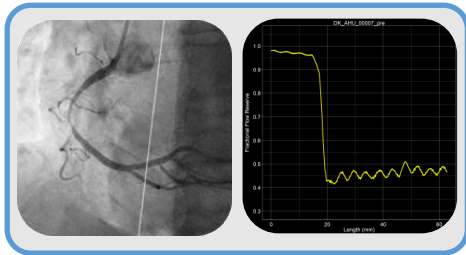
HIGH vs. LOW PPG
Focal vs. diffuse functional pattern

Angiography-based wall shear stress (WSS)

Pre-PCI optical coherence tomography (OCT)
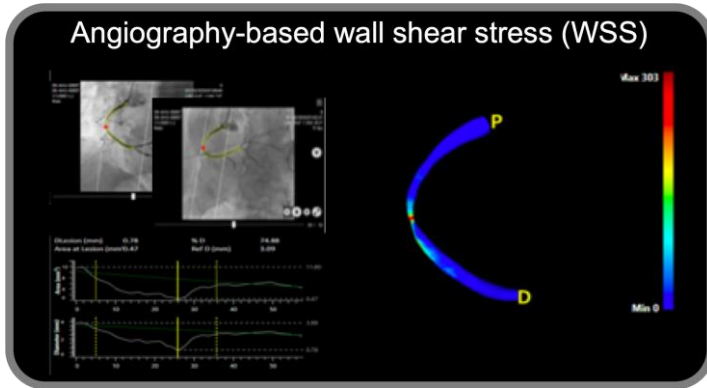
TAWSS (in Pa)
Time-averaged wall shear stress

TSVI (in m^{-1})
Topological shear variation index

Statistical Analysis
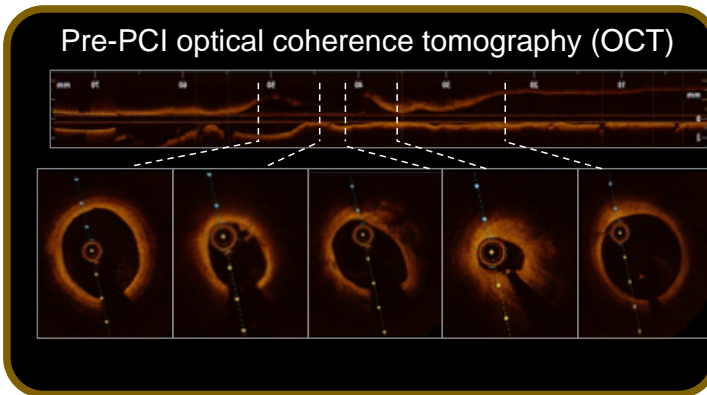
Plaque composition
Fibrotic, lipidic, calcific components

Vulnerability features
TCFA, MF, Rupture

188

Figure 2 – Linear correlation between intracoronary pressure gradients and translesional shear forces.
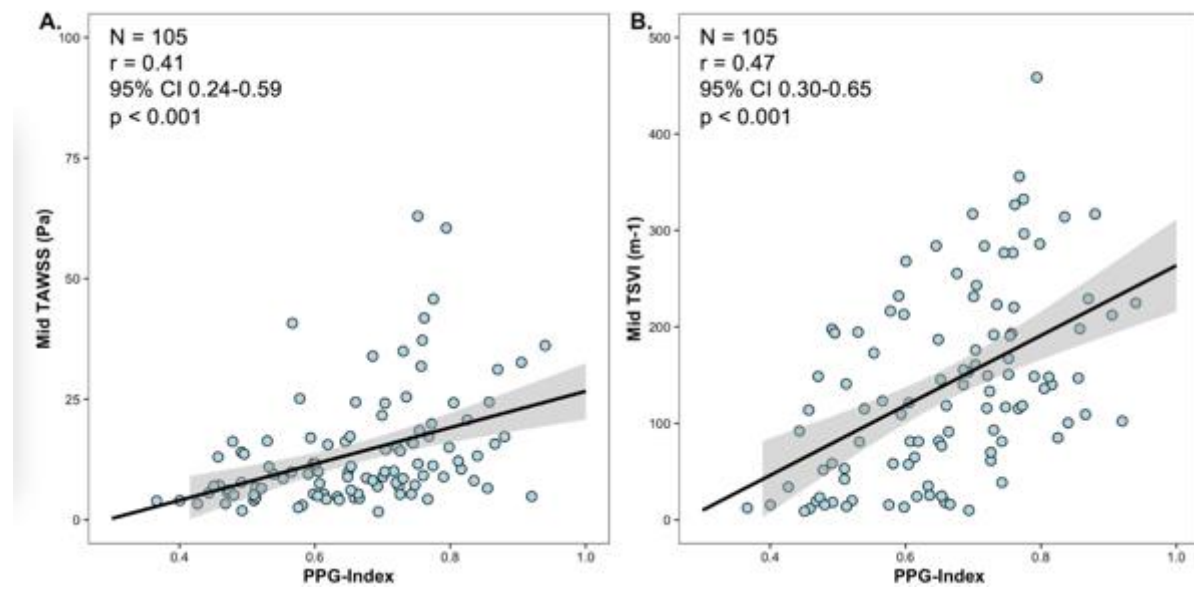
X-axis "PPG-Index" = pullback pressure gradient index. Panel A) Y-axis "Mid TAWSS" = time-averaged wall shear stress measured at the mid lesion segment (*throat*). Panel B) Y-axis "Mid TSVI" = topological shear variation index measured at the mid lesion segment (*throat*).

Figure 3 – Interplay between intracoronary hemodynamics and plaque composition.
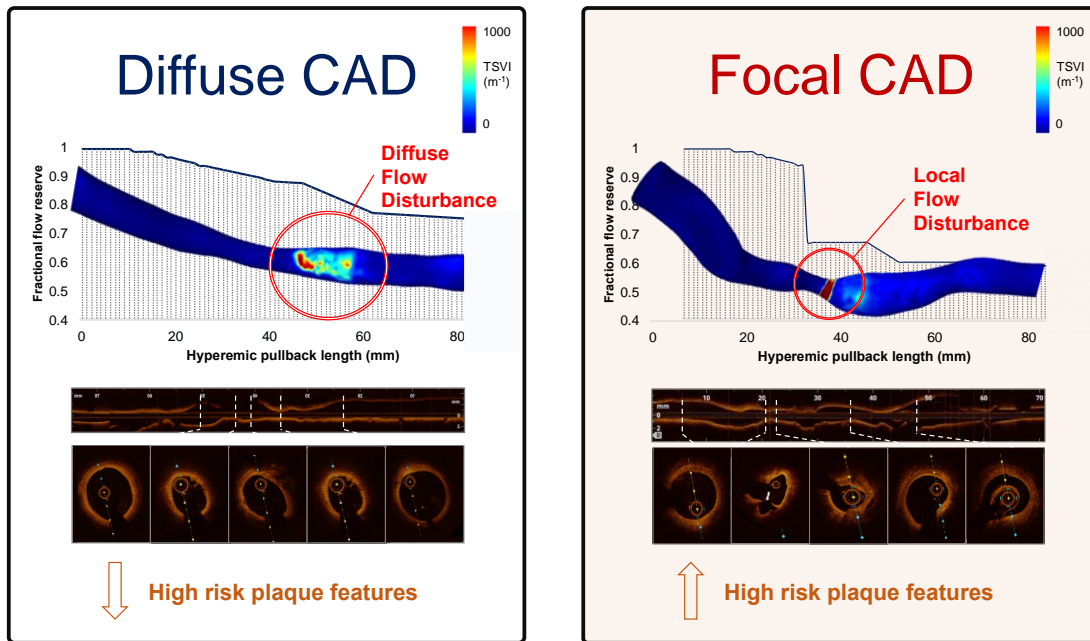
Lesions with a diffuse pressure drop (left panel "diffuse CAD") presented milder local flow disturbances and less frequently high risk plaque phenotypes. Conversely, lesions presenting a focal pressure drop (right panel "focal CAD") had increased local flow disturbances and were associated with the presence of macrophage infiltration, plaque rupture (white arrow) and cholesterol crystals at the pre-PCI optical coherence tomography assessment. PPG = pullback pressure gradient.

References

1.   Kwak BR, Back M, Bochaton-Piallat ML, et al. Biomechanical factors in atherosclerosis: mechanisms and clinical implications. *Eur Heart J*. Nov 14 2014;35(43):3013-20, 3020a-3020d. doi:10.1093/eurheartj/ehu353

2.   Pijls NH, Fearon WF, Tonino PA, et al. Fractional flow reserve versus angiography for guiding percutaneous coronary intervention in patients with multivessel coronary artery disease: 2-year follow-up of the FAME (Fractional Flow Reserve Versus Angiography for Multivessel Evaluation) study. *J Am Coll Cardiol*. Jul 13 2010;56(3):177-84. doi:10.1016/j.jacc.2010.04.012

3.   Collet C, Sonck J, Vandeloo B, et al. Measurement of Hyperemic Pullback Pressure Gradients to Characterize Patterns of Coronary Atherosclerosis. *Journal of the American College of Cardiology*. 2019;74(14):1772-1784. doi:10.1016/j.jacc.2019.07.072

4.   Candreva A, Mizukami T, Sonck J, et al. Hyperemic hemodynamic characteristics of serial coronary lesions assessed by pullback pressure gradients. *Catheterization and cardiovascular interventions : official journal of the Society for Cardiac Angiography & Interventions*. Nov 1 2021;98(5):E647-E654. doi:10.1002/ccd.29868

5.   Sakai K, Mizukami T, Leipsic J, et al. Coronary Atherosclerosis Phenotypes in Focal and Diffuse Disease. *JACC Cardiovasc Imaging*. Jul 6 2023;doi:10.1016/j.jcmg.2023.05.018

6.   Chatzizisis YS, Coskun AU, Jonas M, Edelman ER, Feldman CL, Stone PH. Role of endothelial shear stress in the natural history of coronary atherosclerosis and vascular remodeling: molecular, cellular, and vascular behavior. *J Am Coll Cardiol*. Jun 26 2007;49(25):2379-93. doi:10.1016/j.jacc.2007.02.059

7.   Kumar A, Hung OY, Piccinelli M, et al. Low Coronary Wall Shear Stress Is Associated With Severe Endothelial Dysfunction in Patients With Nonobstructive Coronary Artery Disease. *JACC Cardiovascular interventions*. Oct 22 2018;11(20):2072-2080. doi:10.1016/j.jcin.2018.07.004

8.   Kumar A, Thompson EW, Lefieux A, et al. High Coronary Shear Stress in Patients With Coronary Artery Disease Predicts Myocardial Infarction. *J Am Coll Cardiol*. Oct 16 2018;72(16):1926-1935. doi:10.1016/j.jacc.2018.07.075

9.   Tufaro V SH, Torii R, Koo BK, Kitslaar P, Ramasamy A, Mathur A, Jones DA, Bajaj R, Erdoğan E, Lansky A, Zhang J, Konstantinou K, Little CD, Rakhit R, Karamasis GV, Baumbach A, Bourantas CV. Wall shear stress estimated by 3D-QCA can predict cardiovascular events in lesions with borderline negative fractional flow reserve. *Atherosclerosis*. 2021;(02.018)

10.   Bajraktari A, Bytyci I, Henein MY. High Coronary Wall Shear Stress Worsens Plaque Vulnerability: A Systematic Review and Meta-Analysis. *Angiology*. Sep 2021;72(8):706-714. doi:10.1177/0003319721991722

11.   Samady H, Molony DS, Coskun AU, Varshney AS, De Bruyne B, Stone PH. Risk stratification of coronary plaques using physiologic characteristics by CCTA: Focus on shear stress. *J Cardiovasc Comput Tomogr*. Sep - Oct 2020;14(5):386-393. doi:10.1016/j.jcct.2019.11.012

12.   Lee SE, Sung JM, Andreini D, et al. Differences in Progression to Obstructive Lesions per High-Risk Plaque Features and Plaque Volumes With CCTA. *JACC Cardiovasc Imaging*. Jun 2020;13(6):1409-1417. doi:10.1016/j.jcmg.2019.09.011

13.   Candreva A, Pagnoni M, Rizzini ML, et al. Risk of myocardial infarction based on endothelial shear stress analysis using coronary angiography. *Atherosclerosis*. Feb 2022;342:28-35. doi:10.1016/j.atherosclerosis.2021.11.010

14.	Nagumo S, Collet C, Norgaard BL, et al. Rationale and design of the precise percutaneous coronary intervention plan (P3) study: Prospective evaluation of a virtual computed tomography-based percutaneous intervention planner. *Clin Cardiol*. Apr 2021;44(4):446-454. doi:10.1002/clc.23551

15.	Sonck J, Nagumo S, Norgaard BL, et al. Clinical Validation of a Virtual Planner for Coronary Interventions Based on Coronary CT Angiography. *JACC Cardiovasc Imaging*. Jul 2022;15(7):1242-1255. doi:10.1016/j.jcmg.2022.02.003

16.	Suzuki N, Asano T, Nakazawa G, et al. Clinical expert consensus document on quantitative coronary angiography from the Japanese Association of Cardiovascular Intervention and Therapeutics. *Cardiovasc Interv Ther*. Apr 2020;35(2):105-116. doi:10.1007/s12928-020-00653-7

17.	Mazzi V, Gallo D, Calo K, et al. A Eulerian method to analyze wall shear stress fixed points and manifolds in cardiovascular flows. *Biomech Model Mechanobiol*. Oct 2020;19(5):1403-1423. doi:10.1007/s10237-019-01278-3

18.	Morbiducci U, Mazzi V, Domanin M, et al. Wall Shear Stress Topological Skeleton Independently Predicts Long-Term Restenosis After Carotid Bifurcation Endarterectomy. *Ann Biomed Eng*. Dec 2020;48(12):2936-2949. doi:10.1007/s10439-020-02607-9

19.	Mazzi V, De Nisco G, Hoogendoorn A, et al. Early Atherosclerotic Changes in Coronary Arteries are Associated with Endothelium Shear Stress Contraction/Expansion Variability. *Ann Biomed Eng*. Sep 2021;49(9):2606-2621. doi:10.1007/s10439-021-02829-5

20.	Jang IK, Tearney GJ, MacNeill B, et al. In vivo characterization of coronary atherosclerotic plaque by use of optical coherence tomography. *Circulation*. Mar 29 2005;111(12):1551-5. doi:10.1161/01.Cir.0000159354.43778.69

21.	DeLong ER DDaC-PD. Comparing the Areas under Two or More Correlated Receiver Operating Characteristic Curves: A Nonparametric Approach. *Biometrics*. 1988;Vol. 44, No. 3 (Sep., 1988), pp. 837-845

22.	De Bruyne B, Pijls NH, Kalesan B, et al. Fractional flow reserve-guided PCI versus medical therapy in stable coronary disease. *N Engl J Med*. Sep 13 2012;367(11):991-1001. doi:10.1056/NEJMoa1205361

23.	S P Sutera a, Skalak R. The History of Poiseuille's Law. *Annual Review of Fluid Mechanics*. 1993;25(1):1-20. doi:10.1146/annurev.fl.25.010193.000245

24.	Candreva A, Nisco GD, Rizzini ML, et al. Current and Future Applications of Computational Fluid Dynamics in Coronary Artery Disease. *RCM*. 2022-11-19 2022;23(11)doi:10.31083/j.rcm2311377

25.	Gijsen F, Katagiri Y, Barlis P, et al. Expert recommendations on the assessment of wall shear stress in human coronary arteries: existing methodologies, technical considerations, and clinical applications. *Eur Heart J*. Nov 1 2019;40(41):3421-3433. doi:10.1093/eurheartj/ehz551

26.	Moore JE, Jr., Xu C, Glagov S, Zarins CK, Ku DN. Fluid wall shear stress measurements in a model of the human abdominal aorta: oscillatory behavior and relationship to atherosclerosis. *Atherosclerosis*. Oct 1994;110(2):225-40. doi:10.1016/0021-9150(94)90207-0

27.	Chatzizisis YS, Jonas M, Coskun AU, et al. Prediction of the localization of high-risk coronary atherosclerotic plaques on the basis of low endothelial shear stress: an intravascular ultrasound and histopathology natural history study. *Circulation*. Feb 26 2008;117(8):993-1002. doi:10.1161/CIRCULATIONAHA.107.695254

28.	Cheng C, Tempel D, van Haperen R, et al. Atherosclerotic lesion size and vulnerability are determined by patterns of fluid shear stress. *Circulation*. Jun 13 2006;113(23):2744-53. doi:10.1161/CIRCULATIONAHA.105.590018

29.   Stone PH, Saito S, Takahashi S, et al. Prediction of progression of coronary artery disease and clinical outcomes using vascular profiling of endothelial shear stress and arterial plaque characteristics: the PREDICTION Study. *Circulation*. Jul 10 2012;126(2):172-81. doi:10.1161/CIRCULATIONAHA.112.096438

30.   Wentzel JJ, Chatzizisis YS, Gijsen FJ, Giannoglou GD, Feldman CL, Stone PH. Endothelial shear stress in the evolution of coronary atherosclerotic plaque and vascular remodelling: current understanding and remaining questions. *Cardiovasc Res*. Nov 1 2012;96(2):234-43. doi:10.1093/cvr/cvs217

31.   Kok AM, Molony DS, Timmins LH, et al. The influence of multidirectional shear stress on plaque progression and composition changes in human coronary arteries. *EuroIntervention : journal of EuroPCR in collaboration with the Working Group on Interventional Cardiology of the European Society of Cardiology*. Oct 20 2019;15(8):692-699. doi:10.4244/EIJ-D-18-00529

32.   Melchior B, Frangos JA. Shear-induced endothelial cell-cell junction inclination. *Am J Physiol Cell Physiol*. Sep 2010;299(3):C621-9. doi:10.1152/ajpcell.00156.2010

33.   Koskinas KC, Chatzizisis YS, Baker AB, Edelman ER, Stone PH, Feldman CL. The role of low endothelial shear stress in the conversion of atherosclerotic lesions from stable to unstable plaque. *Curr Opin Cardiol*. Nov 2009;24(6):580-90. doi:10.1097/HCO.0b013e328331630b

34.   Costopoulos C, Timmins LH, Huang Y, et al. Impact of combined plaque structural stress and wall shear stress on coronary plaque progression, regression, and changes in composition. *Eur Heart J*. May 7 2019;40(18):1411-1422. doi:10.1093/eurheartj/ehz132

35.   Lodi Rizzini M, Gallo D, De Nisco G, et al. Does the inflow velocity profile influence physiologically relevant flow patterns in computational hemodynamic models of left anterior descending coronary artery? *Med Eng Phys*. Aug 2020;82:58-69. doi:10.1016/j.medengphy.2020.07.001
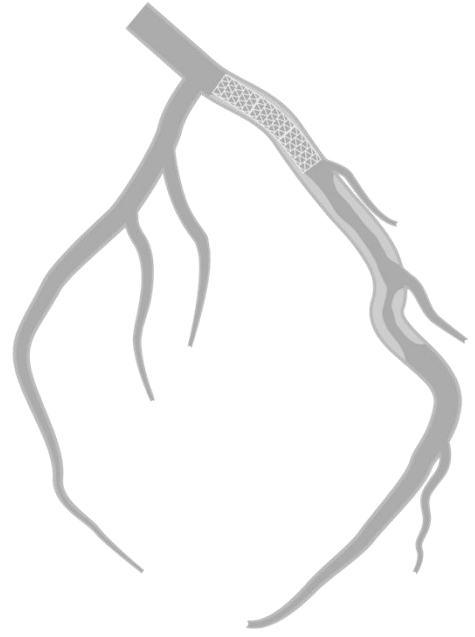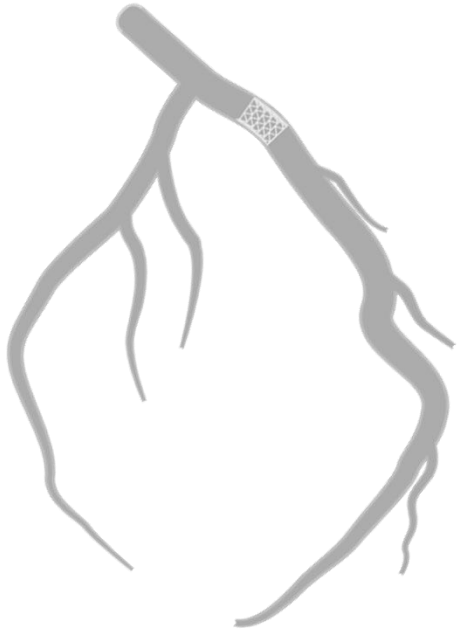
Chapter 9. Procedural Outcomes after PCI in Focal and Diffuse CAD

Mizukami T, Sonck J, Sakai K, Ko B, Maeng M, Otake H, Koo BK, Nagumo S, Nørgaard BL, Leipsic J, Shinke T, Munhoz D, Mileva N, Belmonte M, Ohashi H, Barbato E, Johnson NP, De Bruyne B, Collet C.

Abstract

Background: Coronary artery disease (CAD) patterns play an essential role in the decision-making process about revascularisation. The pullback pressure gradient (PPG) quantifies CAD patterns as either focal or diffuse based on fractional flow reserve (FFR) pullbacks. The objective of this study was to evaluate the impact of CAD patterns on acute PCI results considered surrogates of clinical outcomes.

Methods: Prospective, multicenter study of patients with hemodynamically significant CAD undergoing PCI. Motorized FFR pullbacks and optical coherence tomography (OCT) were performed before and after PCI. Post-PCI FFR greater than 0.90 was considered an optimal result. Focal disease was defined as PPG >0.73.

Results: Overall, 113 patients (116 vessels) were included. Patients with focal disease (PPG >0.73) were younger than those with diffuse CAD (61.4±9.9 vs. 65.1±8.7 years, p-value=0.042). PCI in vessels with high PPG (focal CAD) was associated with higher post-PCI FFR (0.91±0.07 focal vs. 0.86±0.05 diffuse, p<0.001) and larger minimal stent areas (MSA) (6.3±2.3 mm^2 focal vs. 5.3±1.8 mm^2 diffuse, p-value=0.015) than diffuse CAD. The PPG was associated with the change in FFR with PCI (R^2 = 0.51, p <0.001). The PPG significantly improved the capacity to predict optimal functional PCI results compared to the angiographic assessment of CAD patterns (AUC$_{PPG}$ 0.81, 95% CI 0.73 to 0.88 vs. AUC$_{angio}$ 0.51, 95% CI 0.42 to 0.60; p-value <0.001).

Conclusion: PCI in vessels with focal disease defined by the coronary physiology resulted in greater improvement in epicardial conductance and larger MSA compared to diffuse disease. PPG, but not angiographically defined CAD patterns, distinguished patients attaining superior procedural outcomes.

Introduction

The success of percutaneous coronary intervention (PCI) is assessed immediately after stent implantation using angiography or intravascular imaging. Large stent luminal areas with adequate stent expansion have been associated with improved prognosis. [1,2]Coronary physiology can also be used to assess PCI results by measuring post-PCI fractional flow reserve (FFR). Improvement in FFR after PCI has been associated with angina relief. [3,4]Furthermore, both minimal stent area (MSA) and post-PCI FFR have been identified as independent predictors of target vessel failure. [5,6]

Characterizing coronary artery disease (CAD) patterns plays a central role in the management of patients with stable CAD as treatment options may be more suited for a particular disease phenotype. The pattern of CAD, i.e., focal or diffuse, has been shown to influence revascularization treatment decisions. Diffuse disease is considered a marker of poor prognosis with limited treatment options and is one of the underlying mechanisms of persistent angina after PCI. [7]In contrast, PCI in focal CAD improves myocardial perfusion and relieves angina. [8]While results of PCI may be logically influenced by CAD patterns, the impact of diffuse or focal CAD on the efficacy and safety of PCI still remains poorly understood. One of the reasons is the lack of a reproducible metric standardizing the diagnosis of focal and diffuse CAD.

Pathophysiological patterns of CAD can be distinguished into focal and diffuse using hyperaemic intracoronary pressure pullbacks recordings. The pullback pressure gradient (PPG) provides a novel index based on FFR pullback curves that quantify CAD patterns. PPG values close to 1 represent focal disease, while PPG approaching 0 characterize diffuse disease. [9]PCI, a focal therapy for CAD, might be of its highest benefit in vessels with high PPG. We investigated the effect of PCI in patients with focal and diffuse CAD defined by the PPG in terms of procedural outcomes considered surrogates of adverse events.

Methods

The data that support the findings of this study are available from the corresponding author upon reasonable request.

Study design

This substudy is a pre-defined analysis of the *Precise PCI Plan (P3)*, whose study design and main results have been reported elsewhere. [10]Briefly, the P3 study was a prospective, investigator-initiated, multicenter study of patients with stable CAD referred for PCI. Patients with a significant epicardial lesion based on an FFR ≤0.80 were considered for

inclusion. Patients underwent an invasive protocol using motorized FFR pullbacks recordings, and optical coherence tomography (OCT) was performed both before and after PCI. Patients with severely calcified vessels, bifurcation or ostial lesions, left main disease, severe vessel tortuosity, previous revascularization, and atrial fibrillation were excluded. [11]The study protocol was approved by the institutional review board or ethics committee at each participating center. All patients signed informed consent. Invasive anatomical and functional data were analyzed by a core laboratory (CoreAalst BV, Aalst, Belgium). The protocol was registered under NCT03782688. The study was sponsored by the Cardiac Research Institute Aalst (Aalst, Belgium).

To test the hypothesis that PCI offers the greatest benefit to patients with focal CAD, we divided the population into PPG tertiles and considered the highest third as focal disease. The intermediate and lower PPG tertiles comprising patients with diffuse and combined (focal and diffuse) CAD were considered diffuse disease.

The study objective was to compare the success of PCI in focal and diffuse CAD defined functionally by measuring post-PCI FFR and morphologically assessing MSA.

Fractional Flow Reserve Pullbacks

FFR measurements were performed adhering to published standards. [12]The pressure wire sensor was positioned in a distal coronary segment >2 mm in diameter by visual estimation. A continuous intravenous adenosine infusion was given at a dose of 140 mcg/kg/min via a peripheral or central vein for at least 2 minutes. A pullback device (Volcano R 100, San Diego, California), adapted to grip the coronary pressure wire (PressureWire X, Abbott Vascular, St. Paul, MN, USA), was set to pull back the pressure wire at a speed of 1 mm/s during continuous recording. If drift >0.03 was observed, the hyperaemic pullback was repeated. To account for baseline disease severity, functional gain (defined as the difference between post- and pre-PCI FFR divided by 1 minus pre-PCI FFR) assessed the physiologic improvement from PCI. Post-PCI FFR greater than 0.90 was considered an optimal result. [13]

Characterization of CAD patterns

The PPG calculation has been described in detail elsewhere. [9]In brief, PPG is calculated by combining two parameters extracted from FFR pullback curves: the maximal pressure gradient over 20% of the pullback duration; and the relative length of functional disease. PPG values close to 1 represent focal disease, and close to 0 indicate diffuse CAD. PPG was calculated offline from FFR pullbacks using a commercially available console (Coroflow v3.5, Coroventis Research, Uppsala, Sweden).

In addition, coronary angiograms were analyzed blinded to the clinical and physiological data to determine the anatomical pattern of CAD, adjudicated visually as focal or diffuse by two independent observers (HO and KS). Based on angiography, focal lesions were defined as lesions ≤20 mm in length. [9]

Optical Coherence Tomography analysis

OCT pullbacks of 75 mm were acquired using the Dragonfly OPTIS Imaging Catheter (Abbott Vascular, St. Paul, MN, USA) and performed before and after PCI. An automated algorithm defined minimal lumen area (MLA) and MSA. Cases in which OCT was performed after pre-dilatation were excluded from analyses necessitating MLA information. Stent expansion was defined as the ratio between MSA and average reference lumen areas. OCT images were analyzed using CAAS Intravascular version 2.1 (Pie Medical Imaging, Maastricht, The Netherlands).

Procedure and Clinical Outcomes

PCI was guided by FFR and OCT, including both physiology and imaging for stent optimization. Optimal procedural results were defined as MSA > 5.5 mm^2 and post-PCI FFR >0.90. Latest-generation drug-eluting stents (DES) were implanted. Cardiac biomarkers and an electrocardiogram were collected 6 to 24 h after the procedure. To allow for comparison among different troponin assays, values were normalized to the assay-specific 99th percentile upper reference limit (URL). Clinical follow-up was collected at 1-year. Prognostically relevant major periprocedural myocardial injury was defined as post-PCI troponin >5× 99th percentile URL.[14] Periprocedural myocardial infarction was defined according to the fourth universal definition of myocardial infarction (MI), [15]Target vessel failure (TVF) was defined as cardiac death, target vessel myocardial infarction (TVMI) and ischemia driven target vessel revascularization (IDTVR), as independently adjudicated by a clinical events committee.

Statistical analysis

Continuous variables with normal distribution are presented as mean ± standard deviation and non-normally distributed variables as median [interquartile range]. Categorical variables are presented as counts and percentages. T-tests or Mann-Whitney U tests were used to compare groups according to the distribution of the variables. Pearson correlation coefficients assessed the relationship between variables. The agreement between angiography and physiology regarding CAD patterns (focal vs. diffuse) was assessed using Cohen's Kappa. The area under the receiving operating characteristic (ROC) curve (AUC) quantified the predictive capacity of PPG for MSA (cutoff 5.5 mm^2) and post-PCI FFR (cutoff 0.90). The De

Long method was used to compare AUC. Multiple linear regression models adjusted by (vessel type, lesion length, FFR, and PPG) were used to assess the independent predictors of post-PCI FFRUnadjusted logistic regression analysis examined the association between the PPG and TVF. For the outcome analysis, patients with more than one treated vessel were classified according to the lowest PPG value. All analyses were performed using R statistical software (R Foundation for Statistical Computing, Vienna, Austria).

Results

From February 2019 to December 2020, 113 patients (116 vessels) were included from five centers in five countries. The mean age was 63.9±9.2 years, 80% were men, and 23% were diabetics. Most patients (98%) presented with stable CAD. The study flowchart is shown in Figure 1. Patient characteristics in the overall population and stratified by CAD patterns are shown in Table 1. Mean PPG was 0.66±0.30 (median 0.66, IQR [0.55, 0.75]). Physiological pattern was dichotomised as focal and diffuse CAD based on the highest PPG tertiles (threshold 0.73). Patients with diffuse disease were older (61.4±9.9 years vs. 65.1±8.7 years, p-value=0.042) and tended to have reduced renal function (creatinine clearance 85.5±27.6 ml/min vs. 76.5±21.1 ml/min; p-value=0.066) compared to patients with focal CAD. Other baseline clinical characteristics were similar between patients with focal and diffuse CAD (Table 1).

The LAD was more frequently associated with the presence of diffuse disease (Table 2). Mean diameter stenosis was higher in focal compared to diffuse disease (59.9±11.2% vs. 47.3±13.7%, p-value<0.001). Similarly, patients with focal CAD had more severe hyperaemic pressure loss (FFR 0.58±0.15 vs. 0.70±0.11, p-value<0.001). Baseline angiographic, OCT, and functional characteristics stratified by focal and diffuse CAD are shown in Table 2. On average, patients received 1.25±0.5 stents with no differences between disease phenotypes. Total stent length was longer for vessels with diffuse CAD (29.7±13.2 mm focal vs. 37.2±15.8 mm diffuse, p=0.012), whereas mean stent diameter did not differ (3.25±0.95 focal mm vs. 3.03±0.42 mm diffuse, p-value=0.081). There were no differences between groups in rates of pre-or post-dilatation (Table 3).

Post-PCI Intravascular Imaging Findings by CAD Pattern

Overall, the mean MSA was 5.65±2.03 mm^2 (Supplemental material Figure S1), but focal disease was associated with larger MSA compared to diffuse CAD (6.3±2.3 mm^2 vs. 5.3±1.8 mm^2, p-value=0.015). Moreover, analyzing both as continuous variables, there was a significant and weak correlation between the PPG and MSA (r = 0.25, 95% CI 0.06 to 0.42,

p=0.012). Likewise, acute lumen area gain was higher in patients with focal CAD (5.6±2.1 mm^2 vs. 3.5±1.6 mm^2, p-value<0.001; and r=0.46, 95% CI 0.24 to 0.64, p<0.001; Figure 2). Stent expansion was similar between focal and diffuse disease (84±13% vs. 79±19%, p=0.254). Post-PCI stent edge dissections were more frequently observed in patients with diffuse disease (5.4% [2/37] focal vs. 15.4% [10/65] diffuse, p=0.10); however, this finding did not reach the statistical threshold for significance.

Post-PCI Physiologic findings by CAD Pattern

Mean post-PCI FFR was 0.88±0.06 (Supplemental material Figure S2), but focal disease achieved significantly higher post-PCI FFR than cases with diffuse CAD (0.91±0.07 vs. 0.86±0.05, p<0.001, Figure 3). There was a significant and modest correlation between the pre-PCI PPG and post-PCI FFR (r = 0.51, 95% CI 0.37 to 0.64, p<0.001). PPG predicted post-PCI FFR >0.90 with an AUC of 0.81 (95% CI 0.73 to 0.88, best PPG cutoff of 0.60). A higher proportion of patients with focal CAD achieved a post-PCI FFR >0.90 compared to diffuse disease (57% focal vs. 23% diffuse, p-value=0.001). In multivariable analysis, PPG and the LAD emerged as independent predictors of post-PCI FFR (Supplementary Material Table S1). Functional gain was also significantly higher in patients with focal versus diffuse disease (0.33±0.14 vs. 0.17±0.12, p<0.001). The change in FFR with PCI was largely determined by the PPG (R^2 = 0.51, p <0.001). Changes in lumen area with PCI correlated with changes in FFR (r = 0.39, 95% CI 0.15 to 0.58, p=0.002). PCI in cases of diffuse CAD was associated with smaller improvements in both FFR and MSA. PCI in vessels with focal disease resulted in higher post-PCI FFR and larger MSA. Patients with diffuse CAD had a higher rate of clustered morphological and functional suboptimal results (Figure 4).

Comparison between angiographic and functional patterns of CAD

Based on angiography, 67% (78/116) of the patients exhibited focal CAD. The agreement between anatomy and physiology for the CAD pattern was slight (Cohen's Kappa 0.15, 95% CI 0.01 to 0.29). Compared to the angiographic assessment of CAD patterns, the PPG significantly improved the capacity to predict optimal functional PCI results (AUC$_{PPG}$ 0.81, 95% CI 0.73 to 0.88 vs. AUC$_{angio}$ 0.51, 95% CI 0.42 to 0.60; p-value <0.001; Supplemental material Figure S3). Case examples of focal and diffuse disease are shown in Figure 5.

Clinical outcomes in patients with focal and diffuse CAD

After 12 months, the TVF rate was 16.8% and did not differ between patients with focal and diffuse disease (OR 0.85, 95% CI 0.58 to 1.24; Table 4). Post-procedural troponin values

were higher in patients with diffuse compared to focal CAD (normalized post-PCI troponin 0.99 [0.36, 3.66] focal vs 2.59 [1.03, 11.46] diffuse, p=0.037; Supplemental Material Figure S4). The rate of peri-procedural MI, according to the 4th universal definition, was comparable between patients with focal and diffuse CAD (19% diffuse vs. 10% focal, p=0.35).

Discussion

The pressure pullback gradient (PPG) – a novel metric that characterizes CAD patterns – identified patients in whom PCI resulted in superior procedural success. PCI in vessels with high PPG (focal disease) was associated with higher functional gain, higher post-PCI FFR, and larger MSA compared to vessels with low PPG (diffuse disease). The main determinant of functional improvement with PCI was the CAD pattern at baseline. Furthermore, CAD patterns based on coronary physiology increase the predictive capacity for optimal functional PCI results compared to the angiographic assessment alone.

Revascularization is considered appropriate when guided by the presence of ischemia. [16]Similarly important is the evaluation of CAD patterns (focal or diffuse). Coronary physiology with longitudinal vessel assessment can distinguish focal vs. diffuse CAD. Pullback maneuvers can be performed during resting and hyperemic conditions to inform about the functional pattern of disease. The main added value of PPG over other pullback technologies (e.g., instantaneous wave-free ratio) is the quantification of the CAD pattern on a scale from 0 to 1, which may facilitate interpretation and its use for clinical decision-making. PPG is the first physiologic metric to quantify atherosclerosis distribution and leverages intracoronary pressure gradients unmasked during hyperaemic conditions. Characterizing disease patterns using coronary physiology reclassifies up to one-third of patients compared to invasive angiography. [9]The presence of large, focal pressure gradients is the hallmark of focal CAD with high PPG values; conversely, their absence results in low PPG and typifies diffuse disease. In this way, PPG adds a second dimension to classical FFR measurements by providing information about the distribution of epicardial resistance. Thus, PPG appears useful after the hemodynamic significance of the total epicardial vessel has been established to further understand the appropriateness of PCI.

Minimal stent area (MSA) and post-PCI FFR carry prognostic information following PCI. [2,5]Post-PCI MSA is a strong predictor of DES failure. Small MSA is associated with DES restenosis, stent thrombosis, and target lesion revascularisation. [2,6,17]MSA has been used as a surrogate endpoint in clinical trials. In practice, intravascular imaging has been recommended to safely achieve the largest stent lumen possible. [18]Likewise, low post-PCI FFR has been

associated with adverse clinical outcomes in several randomized and observational studies. [5,19]Low post-PCI FFR has been associated with an increased risk of target vessel revascularization, myocardial infarction, and cardiac death. [19-21]Similar to MSA, post-PCI FFR has been proposed as a target for PCI optimization. [4]The present study provided a unique opportunity to assess changes in morphological and physiological parameters. Sub-optimal PCI results based on intravascular imaging (MSA ≤ 5.5 mm^2) and physiology (post-PCI FFR ≤ 0.90) were observed in 40% and 55% of patients, respectively. Furthermore, the presence of both suboptimal imaging and functional findings were observed in 44% of the cases, and suboptimal PCI criteria were clustered in patients with diffuse CAD (58% diffuse vs. 19% focal, p-value<0.001). Nonetheless, it should be highlighted that in the present study, there was no difference in clinical outcomes between patients with focal and diffuse disease defined by the PPG.

The associations among CAD patterns quantified by PPG, MSA, and post-PCI FFR were also observed when PPG was used as a continuous variable, suggesting that PPG should be interpreted as a continuous metric rather than using a dichotomous approach. The mechanisms underlying the association between low PPG and suboptimal PCI results relate to both the stented and non-stented segments. In diffusely diseased vessels, lumen reduction due to atherosclerosis leads to smaller MSA.[22,23] On the other hand, the main contributor to low post-PCI FFR was the presence of pressure losses proximal and distal to treated lesions. [8,24]Of note, the rate of stent edge dissections was higher in vessels with low PPG. This has been related to diffuse atherosclerosis present at stent edges. [7]OCT detection of stent edge dissections has also been identified as a major predictor of major adverse clinical outcomes at mid and long-term follow-up. [6]

Peri-procedural MI is one of the shortcomings of PCI. In the ISCHEMIA study, PCI-related MI (i.e., type 4a according to the 4th universal definition) significantly influenced the results of the study, offsetting the reduction in spontaneous MI observed with an invasive strategy. [25,26] Consequently, strategies aiming at reducing peri-procedural PCI risk could translate into patient benefit. Compared to focal CAD, PCI in diffusely diseased vessels usually requires longer and more stents, thereby increasing the risk of side branch(es) occlusion and stent-induced dissection. In the present study, patients with diffuse disease, defined by a PPG < 0.60, had significantly higher troponin levels after PCI and had a trend towards higher rates of major peri-procedural injury (35% vs. 18%, p=0.09) which in turn have been associated with adverse long-term outcomes. [14]However, there was no difference in the rate of peri-procedural

MI (defined by the 4th universal definition) between patients with focal and diffuse CAD. It can be hypothesized that a strategy of thoughtful PCI in vessels with high PPG while deferring PCI in vessels with diffuse disease may increase procedural safety by reducing PCI-related myocardial injury.

Despite the long-standing awareness of the adverse scenario that diffuse CAD poses for PCI, differentiation of CAD patterns in clinical practice remains suboptimal, partly related to the lack of standardized criteria. Coronary pressure pullbacks have been used since the early days of interventional cardiology because they help in depicting the distribution of epicardial resistance and select an optimal interventional strategy. [27] The advent of PPG quantifies the stratification of patients with hemodynamically significant lesions into focal or diffuse CAD using a scale from 0 to 1. PPG is an objective, operator-independent method that can be obtained with high reproducibility after manual FFR pullback maneuvers.[28] This additional level of disease discrimination opens the door for personalized management of patients with CAD. Based on the results of the present study, patients with high PPG appear to derive the greatest benefit from PCI. Long-term follow-up in a larger population is required to assess whether patients with focal disease have an improved prognosis after PCI compared to those with diffuse CAD. This is currently being investigated in the PPG Global registry (NCT04789317), where approximately 1,000 subjects undergoing PCI will be assessed by the PPG and will be followed clinically for three years.

Limitations

First, a relatively small number of patients was included; this resulted in limited statistical powered to assess differences in clinical outcomes between focal and diffuse CAD. Nonetheless, we evaluated post-PCI FFR and MSA, two surrogate markers of adverse events after PCI. Second, motorized FFR pullbacks were used for the PPG calculation, which is unpractical for daily practice. However, the PPG can be similarly derived from manual FFR pullbacks with excellent reproducibility.[28] Third, the definition of focal CAD was based on the highest tertile of the PPG distribution rather than a threshold derived from clinical endpoints. The investigation of a PPG cutoff and the clinical impact of focal and diffuse CAD in a larger population is currently ongoing in the PPG Global study (NCT04789317).

Conclusion

PCI in patients with focal CAD defined by the PPG resulted in greater improvement in FFR and larger MSA compared to patients with diffuse disease. Optimal PCI results (high post-PCI FFR and large MSA) were clustered in patients with focal disease. By identifying patients

attaining superior procedural outcomes before PCI, the PPG may be useful in enhancing patients' selection for revascularization. Further randomized clinical trials are required to investigate the value of a PPG-guided PCI strategy.

Table 1. Patient characteristics

Variables	Overall	Diffuse CAD	Focal CAD	p-value[*]
Number of patients	**113**	**74**	**39**	
Age (yrs), mean ± SD	**63.9±9.2**	**65.1±8.7**	**61.4±9.9**	**0.042**
Sex (Male), n (%)	**90 (79.6%)**	**62 (81.6%)**	**28 (75.7%)**	**0.629**
Weight (kg), mean ± SD	**80.7 ± 13.2**	**79.6 ± 13.0**	**83.0 ± 13.3**	**0.207**
Height (cm), mean ± SD	**172.8 ± 9.2**	**172.5 ± 9.8**	**173.3 ± 7.7**	**0.661**
BMI, mean ± SD	**27.0 ± 3.4**	**26.7 ± 3.2**	**27.5 ± 3.7**	**0.203**
Dyslipidemia, n (%)	**88 (77.9%)**	**60 (78.9%)**	**28 (75.7%)**	**0.879**
Hypertension, n (%)	**65 (57.5%)**	**40 (52.6%)**	**25 (67.6%)**	**0.192**
Diabetes mellites, n (%)	**26 (23.0%)**	**18 (23.7%)**	**8 (21.6%)**	**0.995**
Current smoker, n (%)	**24 (21.2%)**	**16 (21.1%)**	**8 (21.6%)**	**1.000**
Prior PCI, n (%)	**6 (5.3%)**	**4 (5.3%)**	**2 (5.4%)**	**1.000**
Peripheral artery disease, n (%)	**5 (4.4%)**	**3 (3.9%)**	**2 (5.4%)**	**1.000**

Previous stroke, n (%)	4 (3.5%)	4 (5.3%)	0 (0.0%)	0.380
Clinical presentation, n (%)				0.144
Silent ischemia	27 (23.9%)	22 (28.9%)	5 (13.5%)	
Stable angina CCS I	35 (31.0%)	26 (34.2%)	9 (24.3%)	
Stable angina CCS II	41 (36.3%)	23 (30.3%)	18 (48.6%)	
Stable angina CCS III	7 (6.2%)	3 (3.9%)	4 (10.8%)	
Stable angina CCS IV	1 (0.9%)	1 (1.3%)	0 (0.0%)	
Unstable angina	2 (1.8%)	1 (1.3%)	1 (2.7%)	
Creatinine (mg/dl), mean ± SD	0.94 ± 0.20	0.94 ± 0.19	0.94 ± 0.22	0.975
Creatinine Clearance, mean ± SD	79.4 ± 23.6	76.5 ± 21.1	85.5 ± 27.6	0.066
Left ventricular ejection fraction (%), mean ± SD	60.1 ± 6.1	60.3 ± 6.5	59.8 ± 5.3	0.735

* For the comparison between focal and diffuse. Continuous variables were compared using T-tests and categorical variables using chi-square.

Table 2. Baseline angiographic, OCT, and functional characteristics stratified by disease pattern.

Variables	Overall	Diffuse CAD	Focal CAD	p-value[*]
Number of vessels	**116**	**77**	**39**	
Vessel (%)				**<0.001**
LAD	**87 (75.0%)**	**69 (89.6%)**	**18 (46.2%)**	
LCX	**13 (11.2%)**	**4 (5.2%)**	**9 (23.1%)**	
RCA	**16 (13.8%)**	**4 (5.2%)**	**12 (30.8%)**	
Baseline QCA				
Lesion length (mm), mean ± SD	**23.7±12.9**	**25.6±13.4**	**19.9±11.3**	**0.026**
Reference lumen diameter (mm), mean ± SD	**2.7±0.5**	**2.7±0.5**	**2.7±0.5**	**0.928**
Reference lumen area (mm², mean ± SD	**6.0±2.2**	**6.0±2.3**	**5.9±2.1**	**0.887**
Minimal lumen diameter (mm), mean ± SD	**1.31±0.44**	**1.43±0.43**	**1.1±0.4**	**<0.001**

Minimal lumen area (mm²), mean ± SD	**1.5±1.0**	**1.7±1.06**	**1.0±0.7**	**<0.001**
Diameter stenosis (%), mean ± SD	**51.5±14.2**	**47.3±13.7**	**59.9±11.2**	**<0.001**
Baseline OCT				
Number of vessels	**103**	**71**	**32**	
Distal reference lumen area (mm²), mean ± SD	**5.6±2.4**	**5.4±2.4**	**6.1±2.5**	**0.182**
Proximal reference lumen area (mm²), mean ± SD	**8.2±3.5**	**8.1±3.5**	**8.4±3.4**	**0.700**
Lesion length (mm)	**30.8±3.9**	**32.4±14.1**	**27.2±12.9**	**0.084**
Minimal lumen area (mm²), mean ± SD**	**1.7±0.7**	**1.9±0.8**	**1.4±0.6**	**0.020**
Baseline Physiology				
FFR, mean ± SD	**0.66±0.13**	**0.70±0.11**	**0.58±0.2**	**<0.001**
PPG, mean ± SD	**0.66±0.13**	**0.58±0.09**	**0.80±0.06**	**<0.001**

* For the comparison between focal and diffuse. Continuous variables were compared using T-tests and categorical variables using chi-square. ** Available for 67 vessels (55 diffuse and 12 focal) before pre-dilation.

Table 3. Procedural characteristics stratified by disease pattern.

Variables	Overall	Diffuse CAD	Focal CAD	p-value[*]
Number of vessels	116	77	39	
Procedural characteristics				
Number of stents, mean ± SD	1.3±0.5	1.3±0.6	1.2±0.4	0.290
Total stent length (mm), mean ± SD	34.7±15.4	37.2±159	29.7±13.2	0.012
Stent diameter (mm), mean ± SD	3.1±0.7	3.03±0.42	3.25 ± 0.95	0.081
Pre-dilatation, n (%)	102 (87.9%)	67 (87.0%)	35 (89.7%)	0.901
Post-dilatation, n (%)	106 (91.4%)	69 (89.6%)	37 (94.9%)	0.546
Post-PCI QCA				
Reference lumen diameter (mm), mean ± SD	2.87±0.48	2.85±0.47	2.91±0.49	0.501
Minimal stent diameter (mm), mean ± SD	2.79±0.46	2.74±0.42	2.87±0.52	0.160
Residual diameter stenosis (%), mean ± SD	2.49±10.51	3.19±10.09	1.10±11.31	0.313
Post-PCI OCT				
Number of vessels	102	65	37	
Minimal stent area (mm^2), mean ± SD	5.64±2.04	5.27±1.79	6.29±2.30	0.015
Distal reference lumen area (mm^2), mean ± SD	5.70±2.30	5.33±2.21	6.35±2.34	0.030
Proximal reference lumen area (mm^2), mean ± SD	8.58±3.34	8.52±3.51	8.71±3.05	0.782
Stent expansion, mean ± SD	0.81±0.17	0.79±0.19	0.84±0.13	0.254
Edge dissection, n (%)	12 (11.8%)	10 (15.4%)	2 (5.4%)	0.236
Number of vessels	60	48	12	
Acute lumen gain, mean ± SD	3.90±1.93	3.47±1.63	5.63±2.12	<0.001
Post-PCI Physiology				

Fractional flow reserve, mean ± SD	0.88±0.06	0.86±0.05	0.91±0.07	<0.001
Relative functional gain, % ± SD	0.61±0.24	0.52±0.22	0.79±0.16	<0.001

* For the comparison between focal and diffuse. Continuous variables were compared using T-tests and categorical variables using chi-square.

Table 4. Clinical outcomes at one-year follow-up.

Variables	Overall	Diffuse CAD	Focal CAD	p-value[*]
Number of patients	113	74	39	
Target Vessel Failure	19 (16.8%)	14 (18.9%)	5 (12.8%)	0.576
Cardiac death	0 (0%)	0 (0%)	0 (0%)	NA
Myocardial infarction	18 (15.9%)	14 (18.9%)	4 (10.3%)	0.354
Spontaneous myocardial infarction	1 (0.9%)	1 (1.4%)	0 (0.0%)	1.000
Periprocedural myocardial infarction	18 (15.9%)	14 (18.9%)	4 (10.3%)	0.354
Major periprocedural injury	33 (29.2%)	26 (35.1%)	7 (17.9%)	0.091
Urgent target vessel revascularization	1 (0.9%)	0 (0.0%)	1 (2.6%)	0.744
Stent thrombosis	0 (0%)	0 (0%)	0 (0%)	NA

* For comparing focal and diffuse using chi-square.

Figure 1. Study Flowchart.
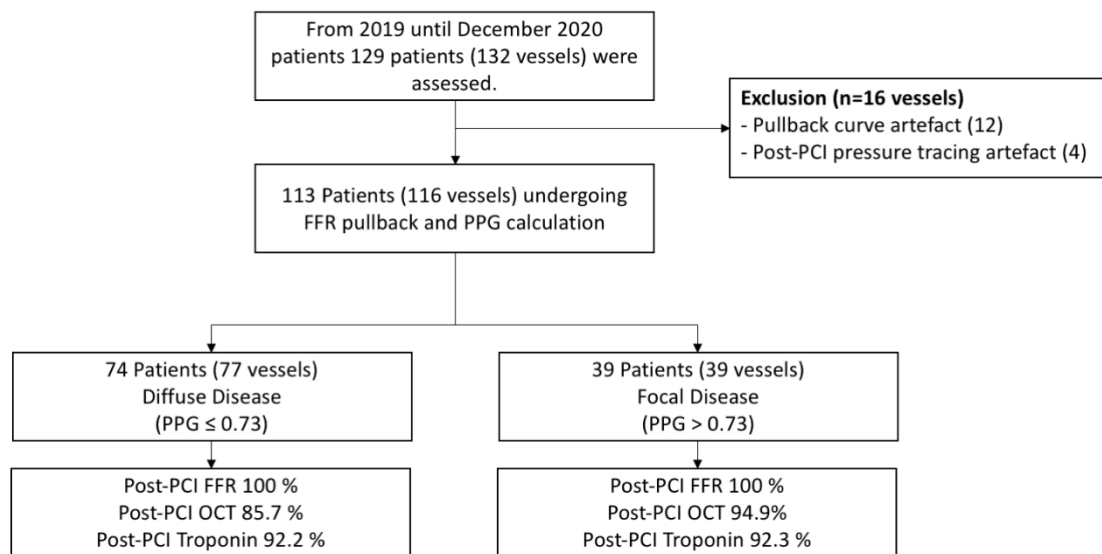
Figure 2. Relationships between pullback pressure gradient (PPG) and morphological lesions characteristics before and after PCI.
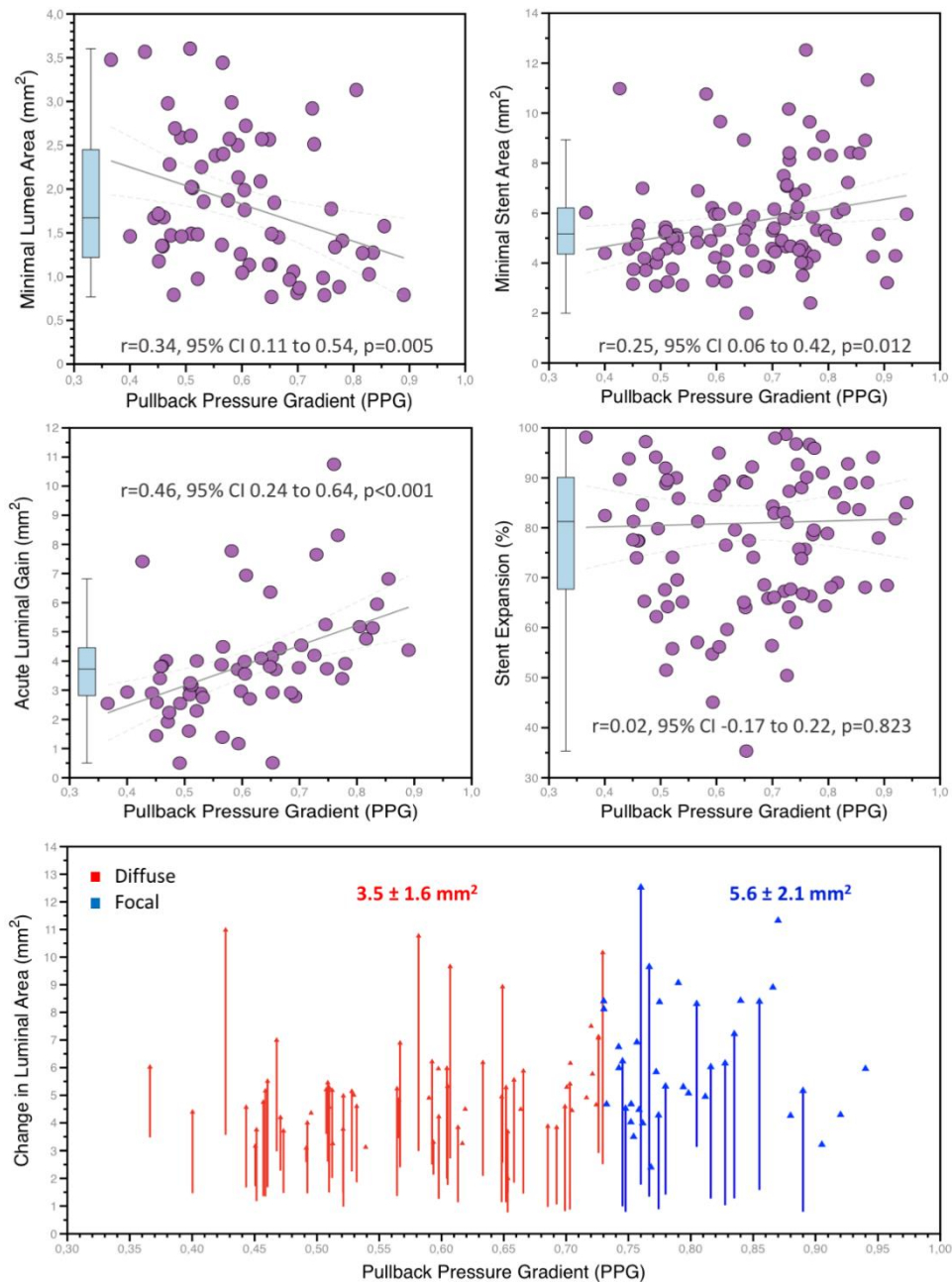
The top row shows the relationship between the PPG (x-axes) and minimal lumen area (left), and minimal stent area (right). The mid-row shows the relationship between PPG and acute luminal gain obtained (minimal stent area minus minimal lumen area) on the left side and stent

expansion on the right side. The bottom panel shows the lumen area change with PCI stratified by PPG (x-axis). The red arrows identify patients with diffuse disease, whereas the blue arrows focal disease.

MSA Minimal stent area. PPG Pullback pressure gradient. PCI percutaneous coronary intervention.

Figure 3. Relationships between pullback pressure gradient (PPG), post-PCI, and delta FFR.
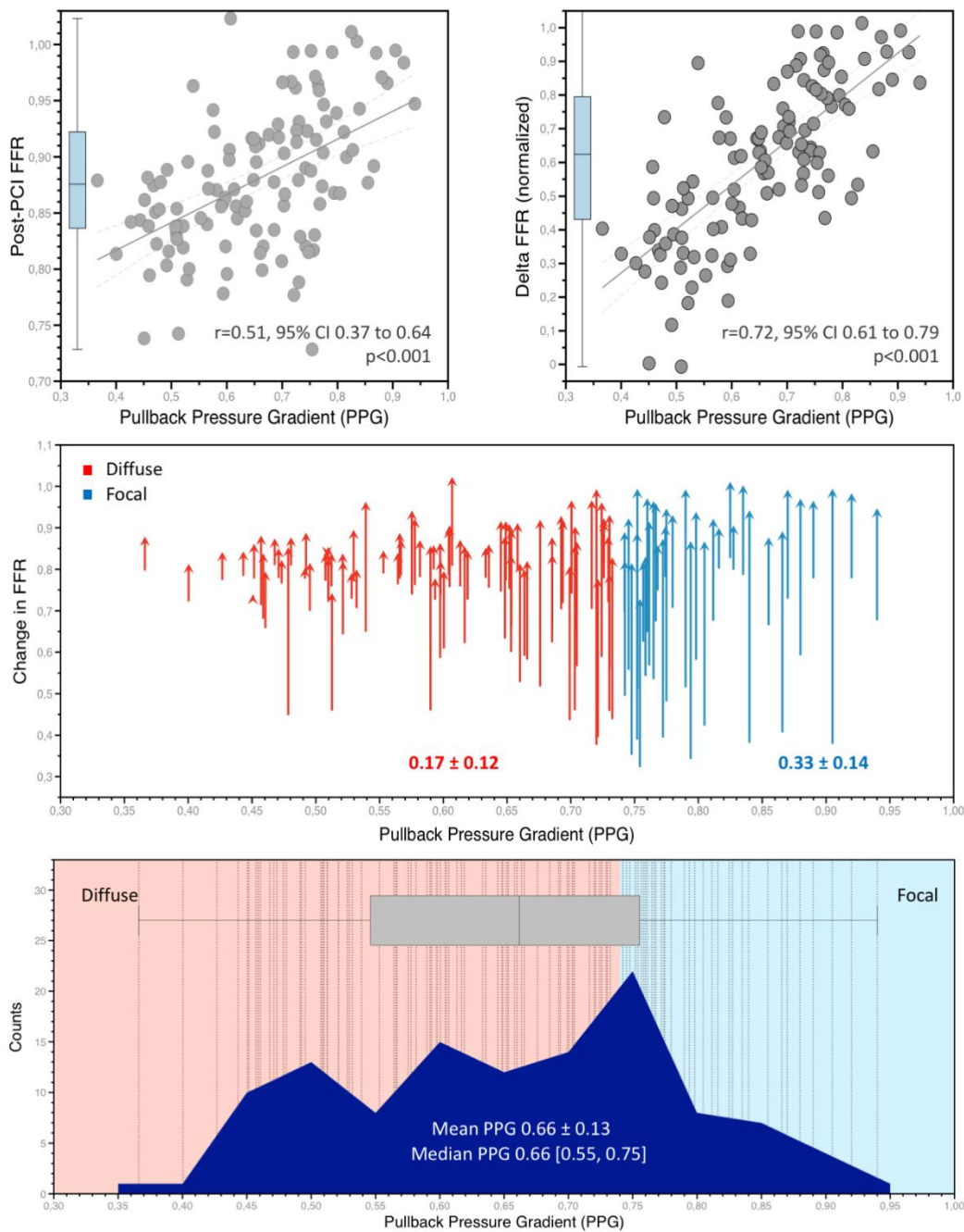
The top row shows the correlations between the PPG (x-axes) and post-PCI FFR (left), and delta FFR (right). In the mid panel, the changes in FFR stratified by the PPG are presented. The red arrows categorize patients with diffuse disease, whereas the blue arrows focal disease. The bottom panel shows the distribution of the PPG. The red shaded area points to PPG values

considered diffuse CAD, whereas the blue shade is focal CAD. The dashed vertical lines show each vessel analyzed.

CAD Coronary artery disease. FFR Fractional flow reserve. MSA Minimal stent area. PPG Pullback pressure gradient.

Figure 4. Proportions of patients attaining optimal anatomical and functional outcomes stratified by CAD patterns.
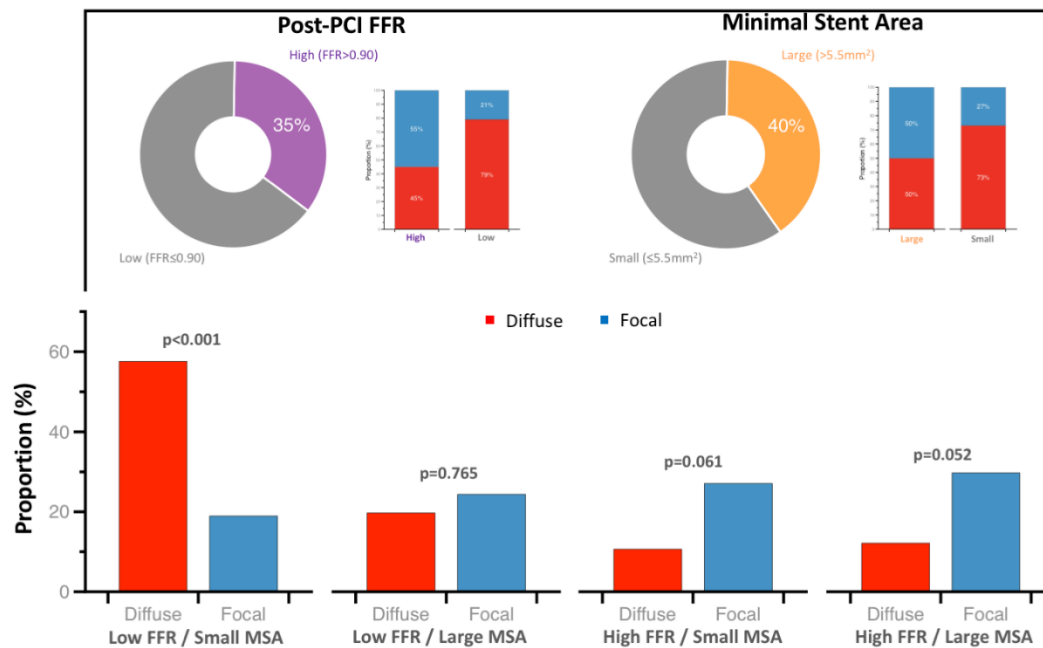
In the top row, the pie charts show the proportion of patients achieving high post-PCI FFR (defined as ≥ 0.90) and high MSA (> 5.5 mm^2). The stacked bars next to the pie charts show the proportion of patients with focal and diffuse CAD having high or low post-PCI FFR (right) and large or small minimal stent areas (right). At the bottom, the proportion of patients with focal and diffuse CAD in the different morphological and functional PCI outcomes combination are shown. A significantly higher proportion of patients with diffuse disease had small MSA and low post-PCI FFR.

CAD Coronary artery disease. FFR Fractional flow reserve. MSA Minimal stent area. PPG Pullback pressure gradient.

Figure 5. Case examples of focal and diffuse CAD.
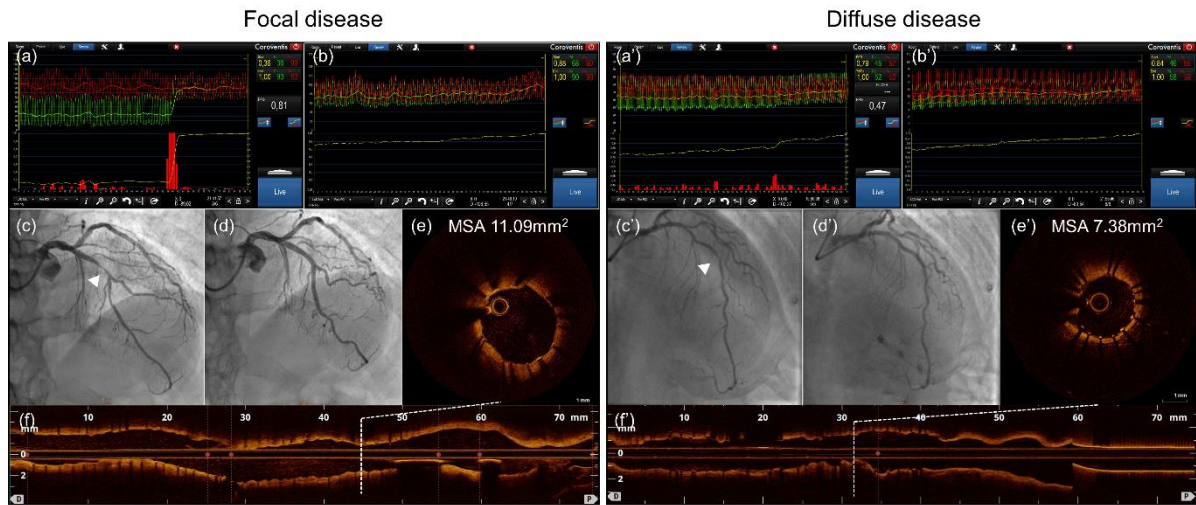
Left panel: Functional focal CAD, Right panel: Functional diffuse CAD.

(a) and (a'): pre-PCI FFR pullbacks. (b) and (b'): post-PCI FFR and FFR pullbacks. (c) and (c'): pre-PCI coronary angiography, white arrowheads show target lesions. (d) and (d'): post-PCI angiographies. (e) and (e'): post-PCI OCT with a cross-sectional view at MSA. (f) and (f'): post-PCI OCT longitudinal view indicating the position of the MSA.

CAD Coronary artery disease. PPG pullback pressure gradient, FFR fractional flow reserve, PCI percutaneous coronary intervention, MSA minimum stent area, OCT optical coherence tomography.

References

1.   Kang SJ, Ahn JM, Song H, et al. Comprehensive intravascular ultrasound assessment of stent area and its impact on restenosis and adverse cardiac events in 403 patients with unprotected left main disease. *Circulation Cardiovascular interventions*. Dec 1 2011;4(6):562-9. doi:10.1161/circinterventions.111.964643

2.   Song HG, Kang SJ, Ahn JM, et al. Intravascular ultrasound assessment of optimal stent area to prevent in-stent restenosis after zotarolimus-, everolimus-, and sirolimus-eluting stent implantation. *Catheter Cardiovasc Interv*. May 1 2014;83(6):873-8. doi:10.1002/ccd.24560

3.   Fournier S, Ciccarelli G, Toth GG, et al. Association of Improvement in Fractional Flow Reserve With Outcomes, Including Symptomatic Relief, After Percutaneous Coronary Intervention. *JAMA Cardiol*. Apr 1 2019;4(4):370-374. doi:10.1001/jamacardio.2019.0175

4.   Collison D, Didagelos M, Aetesam-Ur-Rahman M, et al. Post-stenting fractional flow reserve vs coronary angiography for optimisation of percutaneous coronary intervention: TARGET-FFR trial. *European heart journal*. Jul 19 2021;doi:10.1093/eurheartj/ehab449

5.   Piroth Z, Toth GG, Tonino PAL, et al. Prognostic Value of Fractional Flow Reserve Measured Immediately After Drug-Eluting Stent Implantation. *Circ Cardiovasc Interv*. Aug 2017;10(8)doi:10.1161/circinterventions.116.005233

6.   Prati F, Romagnoli E, Burzotta F, et al. Clinical Impact of OCT Findings During PCI: The CLI-OPCI II Study. *JACC Cardiovasc Imaging*. Nov 2015;8(11):1297-305. doi:10.1016/j.jcmg.2015.08.013

7.   Crea F, Bairey Merz CN, Beltrame JF, et al. Mechanisms and diagnostic evaluation of persistent or recurrent angina following percutaneous coronary revascularization. *European heart journal*. Jan 4 2019;doi:10.1093/eurheartj/ehy857

8.   Ando H, Takashima H, Suzuki A, et al. Impact of lesion characteristics on the prediction of optimal poststent fractional flow reserve. *American heart journal*. Dec 2016;182:119-124. doi:10.1016/j.ahj.2016.09.015

9.   Collet C, Sonck J, Vandeloo B, et al. Measurement of Hyperemic Pullback Pressure Gradients to Characterize Patterns of Coronary Atherosclerosis. *Journal of the American College of Cardiology*. 2019;74(14):1772-1784. doi:10.1016/j.jacc.2019.07.072

10.   Nagumo S, Collet C, Norgaard BL, et al. Rationale and design of the precise percutaneous coronary intervention plan (P3) study: Prospective evaluation of a virtual computed tomography-based percutaneous intervention planner. *Clin Cardiol*. Mar 3 2021;doi:10.1002/clc.23551

11.   Sianos G, Morel MA, Kappetein AP, et al. The SYNTAX Score: an angiographic tool grading the complexity of coronary artery disease. *EuroIntervention : journal of EuroPCR in collaboration with the Working Group on Interventional Cardiology of the European Society of Cardiology*. Aug 2005;1(2):219-27.

12.   Toth GG, Johnson NP, Jeremias A, et al. Standardization of Fractional Flow Reserve Measurements. *J Am Coll Cardiol*. Aug 16 2016;68(7):742-53. doi:10.1016/j.jacc.2016.05.067

13.   Rimac G, Fearon WF, De Bruyne B, et al. Clinical value of post-percutaneous coronary intervention fractional flow reserve value: A systematic review and meta-analysis. *American heart journal*. Jan 2017;183:1-9. doi:10.1016/j.ahj.2016.10.005

14.   Bulluck H, Paradies V, Barbato E, et al. Prognostically relevant periprocedural myocardial injury and infarction associated with percutaneous coronary interventions: a Consensus Document of the ESC Working Group on Cellular Biology of the Heart and European Association of Percutaneous Cardiovascular Interventions (EAPCI). *Eur Heart J*. Jul 15 2021;42(27):2630-2642. doi:10.1093/eurheartj/ehab271

15.   Taylor CA, Fonte TA, Min JK. Computational fluid dynamics applied to cardiac computed tomography for noninvasive quantification of fractional flow reserve: scientific basis. *J Am Coll Cardiol*. Jun 4 2013;61(22):2233-41. doi:10.1016/j.jacc.2012.11.083

16.   Patel MR, Calhoon JH, Dehmer GJ, et al. ACC/AATS/AHA/ASE/ASNC/SCAI/SCCT/STS 2017 Appropriate Use Criteria for Coronary Revascularization in Patients With Stable Ischemic Heart Disease: A Report of the American College of Cardiology Appropriate Use Criteria Task Force, American Association for Thoracic Surgery, American Heart Association, American Society of Echocardiography, American Society of Nuclear Cardiology, Society for Cardiovascular Angiography and Interventions, Society of Cardiovascular Computed Tomography, and Society of Thoracic Surgeons. *Journal of the American College of Cardiology*. May 2 2017;69(17):2212-2241. doi:10.1016/j.jacc.2017.02.001

17.   Soeda T, Uemura S, Park SJ, et al. Incidence and Clinical Significance of Poststent Optical Coherence Tomography Findings: One-Year Follow-Up Study From a Multicenter Registry. *Circulation*. Sep 15 2015;132(11):1020-9. doi:10.1161/circulationaha.114.014704

18.   Ali Z, Landmesser U, Karimi Galougahi K, et al. Optical coherence tomography-guided coronary stent implantation compared to angiography: a multicentre randomised trial in PCI - design and rationale of ILUMIEN IV: OPTIMAL PCI. *EuroIntervention : journal of EuroPCR in collaboration with the Working Group on Interventional Cardiology of the European Society of Cardiology*. Jan 20 2021;16(13):1092-1099. doi:10.4244/eij-d-20-00501

19.   Agarwal SK, Kasula S, Hacioglu Y, Ahmed Z, Uretsky BF, Hakeem A. Utilizing Post-Intervention Fractional Flow Reserve to Optimize Acute Results and the Relationship to Long-Term Outcomes. *JACC Cardiovascular interventions*. May 23 2016;9(10):1022-31. doi:10.1016/j.jcin.2016.01.046

20.   Diletti R, Masdjedi K, Daemen J, et al. Impact of Poststenting Fractional Flow Reserve on Long-Term Clinical Outcomes: The FFR-SEARCH Study. *Circulation Cardiovascular interventions*. Mar 2021;14(3):e009681. doi:10.1161/circinterventions.120.009681

21.   Li SJ, Ge Z, Kan J, et al. Cutoff Value and Long-Term Prediction of Clinical Events by FFR Measured Immediately After Implantation of a Drug-Eluting Stent in Patients With Coronary Artery Disease: 1- to 3-Year Results From the DKCRUSH VII Registry Study. *JACC Cardiovasc Interv*. May 22 2017;10(10):986-995. doi:10.1016/j.jcin.2017.02.012

22.   Schoenhagen P, Ziada KM, Vince DG, Nissen SE, Tuzcu EM. Arterial remodeling and coronary artery disease: the concept of "dilated" versus "obstructive" coronary atherosclerosis. *Journal of the American College of Cardiology*. Aug 2001;38(2):297-306. doi:10.1016/s0735-1097(01)01374-2

23.   Seiler C, Kirkeeide RL, Gould KL. Basic structure-function relations of the epicardial coronary vascular tree. Basis of quantitative coronary arteriography for diffuse coronary artery disease. *Circulation*. Jun 1992;85(6):1987-2003. doi:10.1161/01.cir.85.6.1987

24.   Wolfrum M, De Maria GL, Benenati S, et al. What are the causes of a suboptimal FFR after coronary stent deployment? Insights from a consecutive series using OCT imaging. *EuroIntervention*. Dec 20 2018;14(12):e1324-e1331. doi:10.4244/eij-d-18-00071

25.   Maron DJ, Hochman JS, Reynolds HR, et al. Initial Invasive or Conservative Strategy for Stable Coronary Disease. *N Engl J Med*. Apr 9 2020;382(15):1395-1407. doi:10.1056/NEJMoa1915922

26.   Chaitman BR, Reynolds HR, Maron DJ, Hochman JS. Response by Chaitman et al to Letter Regarding Article, "Myocardial Infarction in the ISCHEMIA Trial: Impact of Different Definitions on Incidence, Prognosis, and Treatment Comparisons". *Circulation*. Jul 13 2021;144(2):e14-e15. doi:10.1161/circulationaha.121.055296

27.	Grüntzig AR, Senning A, Siegenthaler WE. Nonoperative dilatation of coronary-artery stenosis: percutaneous transluminal coronary angioplasty. *N Engl J Med*. Jul 12 1979;301(2):61-8. doi:10.1056/nejm197907123010201

28.	Sonck J, Mizukami T, Johnson NP, et al. Development, validation, and reproducibility of the pullback pressure gradient (PPG) derived from manual fractional flow reserve pullbacks. *Catheter Cardiovasc Interv*. Mar 2 2022;doi:10.1002/ccd.30064

Chapter 10. Differential Improvement in Angina and Health-Related Quality of Life After PCI in Focal and Diffuse Coronary Artery Disease

Collet C, Collison D, Mizukami T, McCartney P, Sonck J, Ford T, Munhoz D, Berry C, De Bruyne B, Oldroyd K.

Patients with hemodynamic significant coronary artery disease

Manual FFR Pullbacks with PPG

Focal CAD (PPG ≥ 0.66)

Diffuse CAD (PPG < 0.66)

Physiological assessment after PCI

High	Post-PCI FFR	Low
High	Delta FFR	Low
High	Post-PCI CFR	Low

Patient reported outcomes after PCI

Angina free   Residual angina

27%
73%

48%
52%

p-value = 0.02

Focal CAD

Diffuse CAD

224
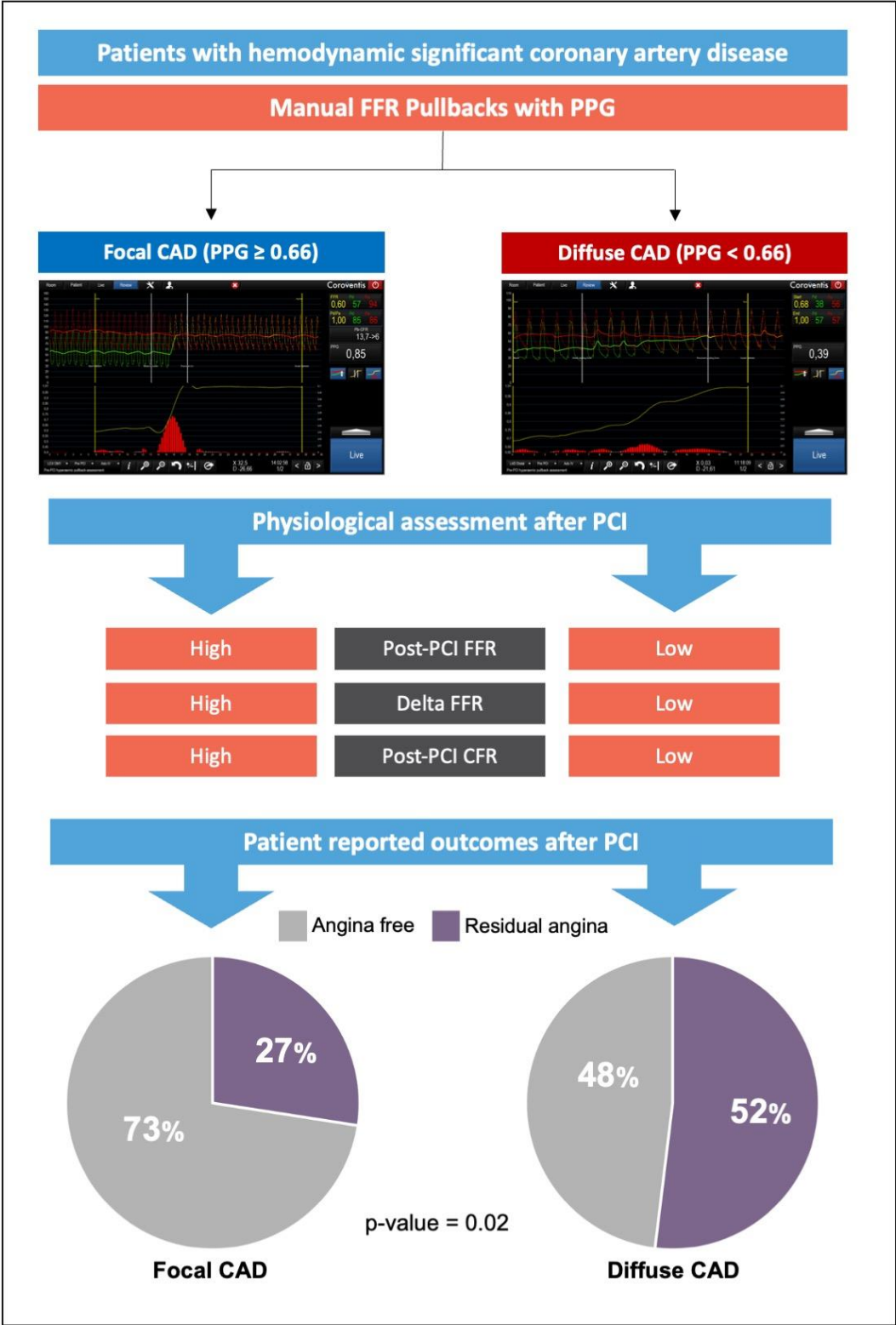
Abstract

Background: Increase in fractional flow reserve (FFR) following percutaneous coronary interventions (PCI) is associated with improvement in angina. Coronary artery disease (CAD) patterns (focal vs. diffuse) influence the FFR change after stenting and may predict angina relief. The objective was to investigate the differential improvement in patient-reported outcomes after PCI in focal and diffuse CAD as defined by the pullback pressure gradient (PPG).

Methods: This is a sub-analysis of the TARGET-FFR randomized clinical trial (NCT03259815). The 7-item Seattle Angina Questionnaire (SAQ-7) was administered at baseline and three months after PCI. The PPG index was calculated from manual pre-PCI FFR pullbacks. The median PPG value was used to define focal and diffuse CAD. Residual angina was defined as an SAQ score less than 100.

Results: One hundred and three patients were analyzed. There were no differences in baseline characteristics between patients with focal and diffuse CAD. Focal disease had larger increase in FFR with PCI than diffuse disease (0.30 ± 0.14 vs. 0.19 ± 0.12, $p<0.001$). Patients who underwent PCI to focal CAD had significantly higher SAQ-7 summary scores at follow-up than those with diffuse CAD (87.1 ± 20.3 vs. 75.6 ± 24.4, mean difference 11.5 [95%CI 2.8 to 20.3], $p=0.01$). Following PCI, residual angina was present in 39.8% but was significantly lower among those with treated focal CAD (27.5% vs. 51.9%, p-value=0.020).

Conclusion: Residual angina after PCI was almost twice as common in patients with a low PPG, whereas patients with focal disease reported greater improvement in angina and quality of life. The baseline pattern of CAD can predict the likelihood of angina relief.

Introduction

Ischemia relating to obstructive epicardial coronary artery disease (CAD) is a common cause of angina pectoris. The frequency and severity of anginal symptoms have been associated with cardiovascular mortality. [1]Revascularization, either through percutaneous coronary interventions (PCI) or coronary artery bypass grafting (CABG), can effectively reduce angina. [2]Nevertheless, approximately one in four patients remain symptomatic after PCI. [3]Residual angina impairs quality of life and portends a worse prognosis. [4]

The magnitude of change in fractional flow reserve (FFR) with PCI predicts improvements in angina. [5]Moreover, large gains in FFR following PCI are associated with freedom from angina. [6]The baseline CAD pattern influences the degree of FFR change achievable through stenting. PCI to focal CAD frequently yields high post-PCI FFR values, whereas more modest improvements can be expected when treating diffuse disease. [7]The likelihood of successful angina relief from PCI can therefore be anticipated by the baseline pattern of CAD. Nevertheless, the definition of diffuse CAD is not standardized and most often relies only on visual assessment, limiting its reliability and reproducibility. [8][9][10][11]

We recently showed that a pressure pullback maneuver could quantify the longitudinal distribution of epicardial resistance. The pullback pressure gradient (PPG) is a novel metric that complements FFR and quantitatively defines CAD patterns ('focality' or diffuseness) on a scale from 0 to 1. [12]

In the present study, we sought to investigate the differential effects of PCI in focal and diffuse CAD as defined by the pre-procedural PPG on patient-reported outcomes.

Methods

Study design

This study is a sub-analysis of the TARGET-FFR (Trial of Angiography vs. pressure-Ratio-Guided Enhancement Techniques–Fractional Flow Reserve) randomized clinical trial. Briefly, TARGET-FFR was a prospective, single-center, randomized, controlled, parallel-group, blinded clinical trial conducted at the Golden Jubilee National Hospital in Glasgow, UK, and registered at ClinicalTrials.gov (NCT03259815). [5][13] All patients signed informed consent before their PCI. Following angiographically successful PCI for either stable angina, medically stabilized non-ST-elevation myocardial infarction (NSTEMI), eligible patients were randomized to an FFR pullback-guided PCI optimization strategy (PIOS) or a control group. Coronary physiology data were analyzed by a core laboratory (CoreAalst BV, Aalst, Belgium). There was no significant difference between groups in the primary endpoint of the proportion

of patients with final post-PCI FFR ≥0.90 (PIOS *minus* control 10%, 95% confidence interval -1.84 to 21.91, p=0.099).

The objective of the present analysis was to compare the effectiveness of PCI in terms of angina relief and quality of life improvement in focal and diffuse CAD as defined by the PPG. For this purpose, patients with both pre-PCI FFR pullbacks (required for PPG calculation) and follow-up patient-reported outcome measure (PROM) questionnaires were eligible for inclusion. A list of the inclusion and exclusion criteria is shown in Supplemental Material Table S1.

Angina and quality of life assessments

The 7-item Seattle Angina Questionnaire (SAQ-7) and EuroQol five-level EQ-5D questionnaire (EQ-5D-5L) were administered at baseline and three months after PCI. The questionnaires were administered by telephone or mail by a research nurse blinded to the physiology results. The SAQ-7 addresses three domains, i.e., angina frequency, physical limitation, and quality of life, which are combined in a summary score. Higher scores indicate better health status. A score of 100 in the angina frequency domain denotes freedom from angina. [14,15] The EQ-5D-5L consists of five dimensions (i.e., mobility, self-care, usual activities, pain & discomfort, anxiety & depression), each of which has five severity levels in each dimension; level 1 indicates no problem, and level 5 extreme problems. The EQ-5D-5L is then summarized as a country-specific weighted health index (0 to 1), with higher values representing worse health status.

Procedure

Details of the coronary physiology measurements and PCI procedures have been published previously. [5] FFR measurements were performed using the PressureWire X Guidewire (Abbott Laboratories, IL, USA). Following administration of a 200 ug bolus of intracoronary nitrate, the pressure wire sensor was positioned at the tip of the guide catheter and equalized with the aortic pressure. The pressure wire was then advanced to position the sensor in the distal third of the vessel. Hyperemia was induced by adenosine infusion into an antecubital vein at a rate of 140 µg/kg/min. Coronary flow reserve (CFR) was assessed using the bolus thermodilution technique. FFR pullback maneuvers were performed manually at a constant speed for over 20 to 30 seconds. The specifics of the PCI procedure, including the use of intracoronary imaging, were at the operator's discretion. Following angiographically successful PCI, a blinded coronary physiology assessment was repeated. Patients randomized to the PIOS group with post-PCI FFR <0.90 were eligible for additional intervention based on

an assessment of the post-PCI FFR pullback. In the control group, post-PCI FFR and pullback information were acquired but concealed from the operator. Final coronary physiology results were not disclosed to patients.

Pressure Pullback Gradient

The PPG index was calculated post hoc from the manual pre-PCI FFR pullback recordings using a commercially available console (Coroflow v3.5, Coroventis Research AP, Uppsala, Sweden). The PPG combines two parameters extracted from FFR pullback curves, i.e., the maximal pressure gradient over 20% of the pullback duration and the length of functional disease, to provide a value from 0 to 1. PPG values close to 1.0 represent focal disease and approaching 0 diffuse CAD. [12]The following exclusion criteria were applied to the recordings: absence of a dicrotic notch from the pressure waveforms; ventricularization; drift of more than 0.05 FFR units on the pullback to the guide catheter; unstable hyperemic conditions during the pullback maneuver; pullback duration less than 15 seconds, and pullback curves with major artifacts. To adjust for baseline disease severity, delta FFR was normalized by pre-PCI FFR (i.e., post-PCI FFR *minus* pre-PCI FFR divided by 1 minus pre-PCI FFR).

Statistical Analysis

Data are expressed as mean ± SD and median [interquartile range] for normally and non-normally distributed data, respectively. Categorical variables are expressed as frequencies and percentages (%). Continuous variables were compared using the Student's t-test (or Mann–Whitney tests as appropriate), and categorical variables were compared using the Chi-square or Fisher's exact test as appropriate. The median value of the PPG was used to differentiate focal from diffuse CAD. SAQ-7 and EQ-5D-5L scores are reported stratified by CAD patterns. The SAQ summary score was the primary outcome. The SAQ summary score and scores from its component domains were used as continuous variables and compared between patients with diffuse and focal CAD. In addition, SAQ scores were categorized into daily or weekly, monthly, or none for the angina frequency domain and as poor or fair, good or excellent health status for the physical limitation and quality of life domains. We also estimated the probability of being angina-free as a function of baseline angina frequency. For this analysis, the model for the SAQ Angina Frequency score was augmented by the inclusion of two-way interaction terms: CAD pattern, and baseline SAQ score, to estimate the probability of being angina-free (i.e., SAQ angina frequency score equal to 100) at follow-up. [16]The predictors of residual angina were assessed using univariate and multivariate regression analyses. Variables included age, diabetes mellitus, pre-PCI FFR, and the PPG. A 2-sided p-value of 0.05 or less was

considered to indicate statistical significance. All statistical analyses were performed using R statistical software (R Foundation for Statistical Computing, Vienna, Austria).

Results

Between 22 February 2018 and 22 November 2019, 721 patients were screened, and 260 were randomized; amongst these, 190 patients had pre-PCI FFR pullback. After excluding pullback recordings of inadequate quality and patients without health-status questionnaires at follow-up, 103 patients (51 with focal and 52 with diffuse disease) were included in the present analysis. The study flowchart is shown in Figure 1. The median PPG was 0.66 [IQR 0.55 to 77]. There were no differences in baseline clinical characteristics between patients with focal and diffuse CAD (Table 1).

Procedural outcomes

Patients with focal disease (PPG ≥ 0.66) had more angiographically severe lesions than diffuse disease (percentage diameter stenosis 65.2±16.4% vs. 57.6±14.2%, p=0.013). However, the functional severity of the disease was similar between focal and diffuse disease (FFR 0.59±0.16 vs. 0.64±0.11, p-value=0.118). Focal CAD was treated with shorter and fewer stents than diffuse disease (37.4±19.2 mm vs. 47.7±22.6 mm, p=0.015 and 1.3±0.5 stents per vessel vs. 1.6±0.8 stents per vessel, p-value=0.022; Table 2).

Patients with focal disease attained higher post-PCI FFR compared to diffuse disease (0.89±0.07 vs. 0.83±0.07, p<0.001) and greater change in FFR after PCI (0.30±0.14 units vs. 0.19±0.12 units, p<0.001). As a continuous variable, the PPG showed significant correlations with post-PCI FFR and delta FFR (Figure 2). Improvement in coronary flow reserve (CFR) was also significantly higher in patients with focal CAD (delta CFR 2.1±1.5 vs. 0.9±1.7, p=0.001).

Patient-reported outcomes

Baseline

At baseline, there were no differences in angina frequency, physical limitation, or quality of life between patients with focal or diffuse CAD. FFR was associated with baseline angina in symptomatic patients (p-value=0.037). Clinical and procedural characteristics stratified by angina status at baseline are shown in the Supplemental Material Table S2. The mean baseline SAQ summary score was 66.1±26.0 in focal CAD and 57.6±25.6 in diffuse disease (p=0.099). Overall, 44.7% of participants had daily or weekly angina, 26.2% had monthly angina, and 29.1% had no angina before PCI, and there were no differences between focal and diffuse disease.

Follow-up after PCI

After PCI, residual angina was present in 39.8% of patients and was significantly lower in patients with focal CAD (27.5% focal vs. 51.9% diffuse, p-value=0.020). Patients with focal CAD reported less angina, less physical limitation, and better quality of life than patients with diffuse CAD (Table 3 and Figure 3). The SAQ summary score for patients with focal CAD was significantly higher than diffuse CAD (87.1±20.3 vs. 75.6±24.4, mean difference 11.5 [95% CI 2.8 to 20.3] SAQ points, p=0.010). Similar magnitudes of benefit were observed in the individual SAQ domains. Levels of daily or weekly, and monthly angina were significantly lower in patients with focal CAD (Figure 4). Among patients with angina at baseline, PPG predicted post-PCI angina-free status with an AUC of 0.65 (95% CI 0.52 to 0.78), best PPG cut-off of 0.68 (Supplemental Material Figure S1). The predictive capacity of the PPG for freedom from angina at follow-up adjusted by other clinical and procedural characteristics is shown in Supplemental Material Table S3. There was a higher probability of being free from angina in patients with focal than in diffuse CAD. The difference was larger among patients who had angina at baseline but was minimal among those who were asymptomatic before PCI (Figure 5).

Health-related quality of life

At baseline, there were no differences in mobility, self-care, usual activities, pain, and discomfort between patients with focal and diffuse CAD (Table 4). At baseline, the EQ-5D-5L index was similar between focal and diffuse disease (0.80 ± 0.21 vs. 0.75 ± 0.21, p=0.251). After PCI, patients with focal disease reported higher mobility, self-care, usual activities, and pain and discomfort compared to patients with diffuse CAD. There were no differences in the level of anxiety and depression after PCI between patients with focal and diffuse CAD (Supplemental Material Figure S2). The EQ-5D-5L index was significantly higher in patients with focal CAD treated with PCI than in diffuse disease (0.9 ± 0.2 vs. 0.8±0.3, p=0.004).

Discussion

This study presents a novel approach for stratifying patients with hemodynamically significant CAD into focal and diffuse disease. These two phenotypes are differentially associated with the likelihood of symptom relief post-PCI. We found that patients with focal CAD (PPG closer to one) treated with PCI had a more favorable prognosis in terms of angina relief and improvement in quality of life. In contrast, more than half of patients with diffuse disease (PPG closer to zero) remained symptomatic after PCI. We also found that PPG was not

associated with anginal symptoms at baseline, indicating that the severity of angina is associated with flow-limiting CAD rather than its distribution.

PCI reduces epicardial resistance, and the resultant increase in myocardial perfusion ameliorates anginal symptoms. [4]In the present study, PCI was more effective in cases with focal pressure gradients resulting in higher post-PCI FFR and a greater change in FFR than in cases with diffuse disease. The PPG determined 27% of the change in coronary flow with PCI. In other words, the improvement in myocardial perfusion achieved by PCI was partly determined by the baseline CAD pattern. This finding highlights the importance of integrating CAD patterns to define the appropriateness of PCI. The quantitative and continuous nature of PPG allows the determination of cut-offs to predict improvements in angina which may prove useful in clinical practice to predict the expected benefit of the intervention.

Structural and functional alterations of coronary circulation have been proposed as causes of persistent angina after PCI. [17]In the present study, we investigated the impact of diffuse CAD on patient-reported outcomes, as defined by PPG. After PCI, we found diffuse CAD was associated with significantly more residual angina. In the International Study of Comparative Health Effectiveness with Medical and Invasive Approaches (ISCHEMIA) trial, patients randomized to the invasive strategy had greater improvement in angina than those assigned to the conservative strategy. The benefit of the invasive strategy was captured by a difference in SAQ Summary scores of 2.9 points (84.7 ± 16 invasive arm vs. 81.8 ± 17 conservative arm at three months). [2]In the present study, the difference in SAQ Summary score between patients with focal and diffuse was 11.5 points at the same follow-up period. The benefit of revascularization was three times higher in patients with focal CAD than in diffuse disease. Moreover, the proportion of symptomatic patients was comparable between ISCHEMIA (65%) and the present study (71%). In symptomatic participants, the observed difference in the probability of being from angina between focal and diffuse CAD was greater, similar to the larger effect on patient-reported outcomes observed between the invasive vs. conservative strategy in ISCHEMIA.[2]

The Objective Randomised Blinded Investigation With Optimal Medical Therapy of Angioplasty in Stable Angina (ORBITA) trial investigated the impact of CAD patterns derived from visual assessment of focal disease on the resting instantaneous wave-free ratio (iFR) pullback curve. This approach identified patients with focal CAD that benefited from PCI in terms of ischemia reduction assessed by stress echocardiography; however, there was no relationship between CAD patterns and patient-reported outcomes. [18]Several reasons may

explain the discrepancy with the present report. First, assessing CAD patterns in hyperemic conditions magnifies focal pressure losses allowing the assessment of focal pressure gradients with less signal-to-noise ratio. Several reports have suggested that resting coronary flow conditions might be insufficient to elicit pressure gradients, particularly in focal stenosis. A second element relates to the definition of focal CAD in the iFR pullback curve. Focal disease was based on the presence of a focal pressure gradient only. This approach disregards pressure losses proximal and distal to the focal gradient, which are equally important for evaluating the absolute improvement in myocardial perfusion after PCI contributing to the resolution of angina. The PPG formula assesses both the magnitude of focal pressure drops and the diffuseness of the disease, providing a comprehensive approach that correlates with symptom improvement.

Utilizing pressure pullbacks to assess CAD patterns is an example of personalized medicine to determine the appropriateness of PCI. The PPG quantifies CAD patterns, enhancing clinical decision-making and reducing the uncertainty associated with a visual interpretation of the pullback curve. In clinical practice, this technique adds 30 to 40 seconds to the classical FFR measurement and can be performed in a reproducible manner with standard pressure wires. [19]Based on the result of this study, patients with high PPG are ideal candidates for PCI and are expected to achieve near-complete resolution of their symptoms with improved quality of life. Conversely, the best treatment strategy for patients with diffuse disease requires further study. An additional consideration when deciding between treatment options for patients with diffuse disease is the higher rate of device-related adverse events observed after PCI. [2010] In this study, patients with low PPG required longer and more stents during PCI. Consequently, decision-making in diffuse CAD must be individualized. In our view, most patients with low PPG can be treated with optimal medical therapy. [11]A randomized clinical trial evaluating treatment options for patients with diffuse disease is warranted; the availability of PPG may serve as a method to standardize selection criteria.

Limitations

The present study has several limitations. First, it is a single-center RCT of moderate size. Attrition from the original sample size resulted from the lack of pre-PCI FFR pullback evaluation in 27% of the patients. Second, this is a post hoc analysis of an RCT; therefore, prospective validation is required to confirm these findings. Third, patient-reported outcomes were collected at a 3-month follow-up interval. Although the effect of PCI is certainly discernible within this time frame, a longer-term follow-up would be required to understand

the durability of the findings better. Fourth, the PPG calculation was performed offline; thus, the clinical outcomes after a PPG-guided PCI strategy require further investigation. Fifth, we used the median PPG to distinguish focal from diffuse CAD for this analysis. Despite the AUC analysis suggesting a PPG threshold for symptom improvement, we believe that PPG should be interpreted as a continuous variable with lower values associated with lower PCI clinical success rates and higher values related to nearly complete resolution of angina. The ongoing PPG Global registry (NCT04789317) will include approximately 1000 patients with the collection of clinical and patient-reported outcomes and will further inform about PPG cut-offs for clinical decision-making.

Conclusion

Residual angina after PCI was frequent and predominantly observed in patients with diffuse CAD as defined by the pre-PCI PPG. Patients with focal disease reported greater improvement in angina and quality of life with PCI. The PPG identified patients most likely to benefit from PCI in terms of angina relief. Therefore, the distribution of the epicardial resistance should be factored into the clinical decision-making process about the appropriateness and the modality of revascularization. A randomized clinical trial assessing the clinical and economic impact of a PPG-guided PCI strategy is warranted.

Table 1. Clinical characteristics stratified by coronary artery disease patterns.

Variables	Overall	Focal (PPG ≥ 0.66)	Diffuse (PPG < 0.66)	p-value
Number of patients, n	103	51	52	
Gender Female, n (%)	14 (13.6)	5 (9.8)	9 (17.3)	0.410
Age years, mean (SD)	60.61 (8.11)	60.24 (7.25)	60.98 (8.93)	0.643
BMI, mean (SD)	29.39 (4.62)	28.96 (4.57)	29.81 (4.67)	0.351
Family history of CAD, n (%)	70 (68.0)	36 (70.6)	34 (65.4)	0.723
Smoking, n (%)	70 (68.0)	37 (72.5)	33 (63.5)	0.437
Hypertension, n (%)	45 (43.7)	22 (43.1)	23 (44.2)	1.000
Dyslipidemia, n (%)	58 (56.3)	31 (60.8)	27 (51.9)	0.479
Diabetes, n (%)	21 (20.4)	8 (15.7)	13 (25.0)	0.353
Insulin-dependent, n (%)	2 (9.5)	1 (12.5)	1 (7.7)	1.000
Renal insufficiency, n (%)	2 (1.9)	1 (2.0)	1 (1.9)	1.000
Previous PCI, n (%)	47 (45.6)	18 (35.3)	29 (55.8)	0.059
Angina, n (%)	88 (85.4)	42 (82.4)	46 (88.5)	0.549
CCS Class, n (%)				0.148
CCS 1	23 (26.1)	15 (35.7)	8 (17.4)	
CCS 2	41 (46.6)	17 (40.5)	24 (52.2)	
CCS 3	24 (27.3)	10 (23.8)	14 (30.4)	
Medications				
Any antiplatelet, n (%)	102 (99.0)	50 (98.0)	52 (100.0)	0.992
DAPT, n (%)	79 (76.7)	41 (80.4)	38 (73.1)	0.519
Statins, n (%)	99 (96.1)	49 (96.1)	50 (96.2)	1.000
Beta-blocker, n (%)	96 (93.2)	48 (94.1)	48 (92.3)	1.000
ACEI, n (%)	76 (73.8)	37 (72.5)	39 (75.0)	0.953
ARB, n (%)	8 (7.8)	4 (7.8)	4 (7.7)	1.000
Calcium channel blocker, n (%)	20 (19.4)	8 (15.7)	12 (23.1)	0.485
Nitrates, n (%)	29 (28.2)	10 (19.6)	19 (36.5)	0.091
GTN spray use	55 (53.4)	23 (45.1)	32 (61.5)	0.140
Frequency of GTN use, n (%)				0.394
Daily	9 (16.4)	3 (13.0)	6 (18.8)	
Weekly	32 (58.2)	12 (52.2)	20 (62.5)	
Monthly	14 (25.5)	8 (34.8)	6 (18.8)	

Diuretics, n (%)	10 (9.7)	4 (7.8)	6 (11.5)	0.764
Oral anticoagulation, n (%)	7 (6.8)	3 (5.9)	4 (7.7)	1.000

Table 2. Procedural characteristics stratified by coronary artery disease patterns.

Variables	Overall	Focal (PPG ≥ 0.66)	Diffuse (PPG < 0.66)	p-value
Number	103	51	52	
Diameter stenosis (%), mean ± SD	61.4 ± 15.7	65.2 ± 16.4	57.6 ± 14.3	0.013
Lesion length, mean ± SD	11.6 ± 5.3	10.9 ± 4.9	12.3 ± 5.6	0.157
AHA/ACC Lesion type, n (%)				0.195
A	18 (17.5)	8 (15.7)	10 (19.2)	
B	39 (37.9)	24 (47.1)	15 (28.8)	
B2	41 (39.8)	18 (35.3)	23 (44.2)	
C	5 (4.9)	1 (2.0)	4 (7.7)	
SYNTAX score, mean ± SD	11.60 ± 8.20	9.21 ± 7.49	13.94 ± 8.26	0.003
Jeopardy score, mean ± SD	5.18 ± 3.06	4.92 ± 3.08	5.44 ± 3.05	0.399
Pd/Pa, mean ± SD	0.81 ± 0.14	0.80 ± 0.16	0.81 ± 0.12	0.665
FFR, mean ± SD	0.61 ± 0.14	0.59 ± 0.16	0.64 ± 0.11	0.118
CFR, mean ± SD	2.14 ± 0.95	1.83 ± 0.58	2.42 ± 1.13	0.002
PPG, mean ± SD	0.65 ± 0.14	0.77 ± 0.06)	0.54 ± 0.09	<0.001
Pre-dilatation, n (%)	103 (100.0)	51 (100.0)	52 (100.0)	NA
Post-dilatation, n (%)	101 (98.1)	49 (96.1)	52 (100.0)	0.467
Intravascular imaging, n (%)	20 (19.4)	4 (7.8)	16 (30.8)	0.007
PIOS, n (%)	53 (51.5)	26 (51.0)	27 (51.9)	1.000
Number of stents (per vessel), mean ± SD	1.49 ± 0.67	1.33 ± 0.52	1.63 ± 0.77	0.022
Stent diameter, mean ± SD	3.20 ± 0.41	3.23 ± 0.44	3.17 ± 0.38	0.443
Total stent length (mm), mean ± SD	42.61±21.51	37.43±19.20	47.69±22.61	0.015
Residual diameter stenosis, mean ± SD	14.82 ± 9.13	14.78 ± 9.54	14.86 ± 8.80	0.962
Residual SYNTAX score, mean ± SD	2.16 ± 4.02	2.76 ± 4.84	1.57 ± 2.92	0.146
Post-PCI Pd/Pa, mean ± SD	0.93 ± 0.05	0.96 ± 0.05	0.91 ± 0.04	<0.001
Post-PCI FFR, mean ± SD	0.86 ± 0.08	0.89 ± 0.07	0.83 ± 0.07	<0.001
Post-PCI CFR, mean ± SD	3.60 ± 1.83	3.88 ± 1.66	3.30 ± 1.97	0.118

Delta FFR, mean ± SD	0.25 ± 0.14	0.30 ± 0.14	0.19 ± 0.12	<0.001
Delta FFR normalized (%), mean ± SD	61 ± 22	71 ± 19	50 ± 20	<0.001
Delta CFR, mean ± SD	1.45 ± 1.70	2.06 ± 1.50	0.89 ± 1.71	0.001
Delta CFR normalized, mean ± SD	0.88 ± 1.03	1.29 ± 1.09	0.50 ± 0.82	<0.001

AHA American Heart Association. ACC American College of Cardiology. CFR Coronary flow reserve. FFR Fractional Flow Reserve. Pa Aortic pressure. Pd Distal pressure. PPG Pullback pressure gradient.

Table 3. Seattle Angina Questionnaire at baseline and follow-up stratified by coronary artery disease patterns.

Variables	Overall	Focal (PPG ≥ 0.66)	Diffuse (PPG < 0.66)	p-value
n	103	51	52	
Baseline SAQ-7				
Physical limitation score, mean ± SD	67.8 ± 27.6	73.3 ± 27.9	62.8 ± 26.6	0.061
Angina frequency, mean ± SD	69.5 ± 27.6	73.5 ± 26.9	65.6 ± 28.0	0.145
Quality of life, mean ± SD	48.2 ± 31.5	52.2 ± 31.8	44.2 ± 31.0	0.200
Summary score, mean ± SD	61.79±26.02	66.1 ± 26.0	57.6 ± 25.6	0.099
Physical Limitation				0.127
Poor or Fair, n (%)	24 (25.3)	10 (22.2)	14 (28.0)	
Good, n (%)	24 (25.3)	8 (17.8)	16 (32.0)	
Excellent, n (%)	47 (49.5)	27 (60.0)	20 (40.0)	
Angina frequency				0.511
Daily or weekly, n (%)	46 (44.7)	20 (39.2)	26 (50.0)	
Monthly, n (%)	27 (26.2)	14 (27.5)	13 (25.0)	
None, n (%)	30 (29.1)	17 (33.3)	13 (25.0)	
Quality of life				0.232
Poor or Fair, n (%)	53 (51.5)	22 (43.1)	31 (59.6)	
Good, n (%)	20 (19.4)	11 (21.6)	9 (17.3)	
Excellent, n (%)	30 (29.1)	18 (35.3)	12 (23.1)	
Follow-up SAQ-7				
Physical limitation score, mean ± SD	79.9 ± 26.8	85.0± 24.4	74.0 ± 28.4	0.049
Angina frequency, mean ± SD	85.5 ± 22.6	91.8±17.1	79.4 ± 25.7	0.005
Quality of life, mean ± SD	78.3 ± 28.3	84.3 ± 24.5	72.4 ± 30.8	0.032
Summary score, mean ± SD	81.3 ± 23.1	87.1 ± 20.3	75.6 ± 24.4	0.010
Physical Limitation				0.242

Poor or Fair, n (%)	12 (13.0)	4 (8.2)	8 (18.6)	
Good, n (%)	13 (14.1)	6 (12.2)	7 (16.3)	
Excellent, n (%)	67 (72.8)	39 (79.6)	28 (65.1)	
Angina frequency				0.008
Daily or weekly, n (%)	20 (19.4)	4 (7.8)	16 (30.8)	
Monthly, n (%)	21 (20.4)	10 (19.6)	11 (21.2)	
None, n (%)	62 (60.2)	37 (72.5)	25 (48.1)	
Quality of life				0.211
Poor or Fair, n (%)	14 (13.6)	4 (7.8)	10 (19.2)	
Good, n (%)	15 (14.6)	7 (13.7)	8 (15.4)	
Excellent, n (%)	74 (71.8)	40 (78.4)	34 (65.4)	
Residual Angina, n (%)	41 (39.8)	14 (27.5)	27 (51.9)	0.020

PPG Pullback pressure gradient. SAQ Seattle Angina Questionnaire

Table 4. EuroQOL five-level questionnaire at baseline and follow-up stratified by coronary artery disease patterns.

Variables	Overall	Focal (PPG ≥ 0.66)	Diffuse (PPG < 0.66)	p-value
Baseline EQ-5D-5L				
Mobility score, mean ± SD	1.8 ± 1.1	1.6 ± 1.1	1.9 ± 1.0	0.175
Self-care score, mean ± SD	1.3 ± 0.6	1.2 ±0.5	1.4 ± 0.6	0.177
Usual activities score, mean ± SD	2.2 ± 1.1	2.2 ± 1.2	2.3 ± 1.1	0.699
Pain score, mean ± SD	2.1 ± 1.0	1.9 ± 0.9	2.2 ± 1.03	0.125
Anxiety and depression score, mean ± SD	1.83 (0.95)	1.7 ± 0.9	2.0 ± 1.00	0.169
Visual Analogue Scale, mean ± SD	69.0 ± 19.5	69.0 ± 20.2	68.9 ± 18.9	0.984
EQ-5D-5L index, mean ± SD	0.78 ± 0.21	0.80 ± 0.21	0.75 ± 0.21	0.251
Follow-up EQ-5D-5L				
Mobility score, mean ± SD	1.62 ± 1.0	1.4 ± 0.8	1.9 ± 1.2	0.014
Self-care score, mean ± SD	1.4 ± 0.7	1.2 ± 0.6	1.5 ± 0.8	0.015
Usual activities score, mean ± SD	1.8 ± 1.0	1.5 ± 0.9	2.0 ± 1.1	0.027
Pain score, mean ± SD	1.7 ± 1.0	1.4 ± 0.7	2.1 ± 1.1	<0.001
Anxiety and depression score, mean ± SD	1.7 ± 1.0	1.5 ± 0.8	1.9 ± 1.2	0.076
Visual Analogue Scale, mean ± SD	75.7 ± 20.9	79.8 ±19.1	71.7 ± 21.9	0.048
EQ-5D-5L index, mean ± SD	0.8 ± 0.2	0.9 ± 0.2	0.8 ± 0.3	0.004

PPG Pullback pressure gradient.

Figure 1. Study flowchart

The total number of patients included in the TARGET-FFR (Trial of Angiography vs. pressure-Ratio-Guided Enhancement Techniques–Fractional Flow Reserve) randomized clinical trial and in the present analysis. Focal coronary artery disease was defined as a pullback pressure gradients (PPG) value ≥ 0.66 and diffuse CAD as PPG < 0.66.

CAD Coronary artery disease. FU Follow-up. PCI percutaneous coronary intervention. PPG Pullback pressure gradient. SAQ Seattle angina questionnaire.

260 patients with hemodynamically significant lesions undergoing PCI

70 patients without pre-PCI FFR pullbacks
• Pre-PCI FFR pullback was not performed (n = 66)
• FFR pullback performed after pre-dilatation (n = 4)

190 patients with FFR pullbacks before PCI

37 patients without adequate pullback curves for PPG analysis
• Pullback time ≤ 15 sec (n = 19)
• Drift > 0.05 FFR units (n = 18)

153 patients with PPG calculation

18 PPG analyses excluded
•Major pullback curve artefacts (n = 15)
•Pressure curve ventricularization during pullback (n = 2)
•Pullback end not identified (n = 1)

76 patients with focal CAD

77 patients with diffuse CAD

14 PPG analyses excluded
•Major pullback curve artefacts (n = 12)
•Unstable Hyperemia (n = 1)
•Pressure curve ventricularization during pullback (n = 1)

58 patients with focal CAD

63 patients with diffuse CAD

7 patients without follow-up SAQ-7

11 patients without follow-up SAQ-7

51 patients with focal CAD and SAQ-7 at follow-up
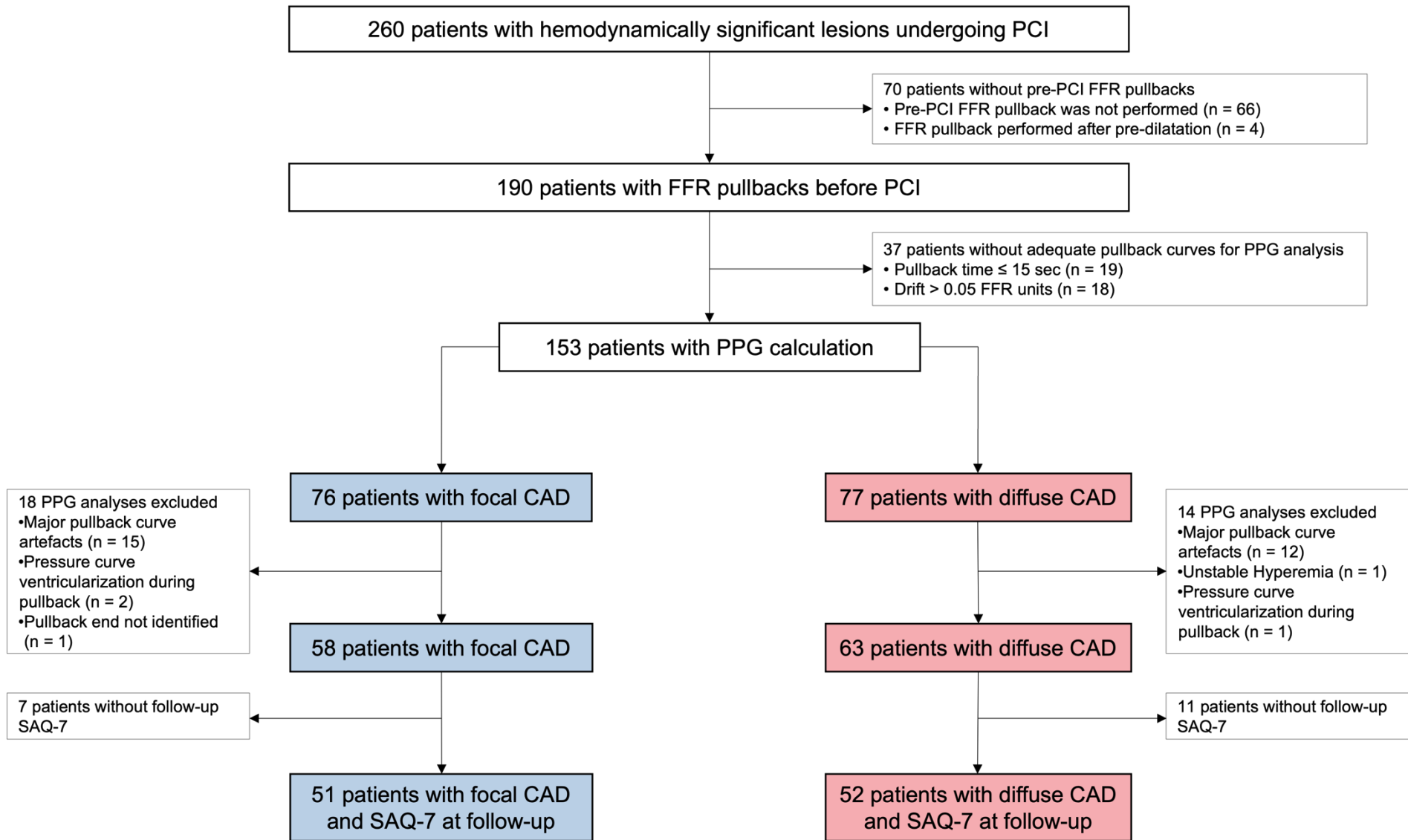
52 patients with diffuse CAD and SAQ-7 at follow-up

Figure 2. Distribution of the pullback pressure gradient (PPG) and its correlation with pre-PCI FFR, post-PCI FFR, and delta FFR.

The bottom panel shows the distribution of pullback pressure gradient (PPG) values; the horizontal gray box plot shows the median value (0.66), range, and interquartile range. The top panel shows the correlation between the PPG (x-axes) and, from left to right, pre-PCI FFR, post-PCI FFR, an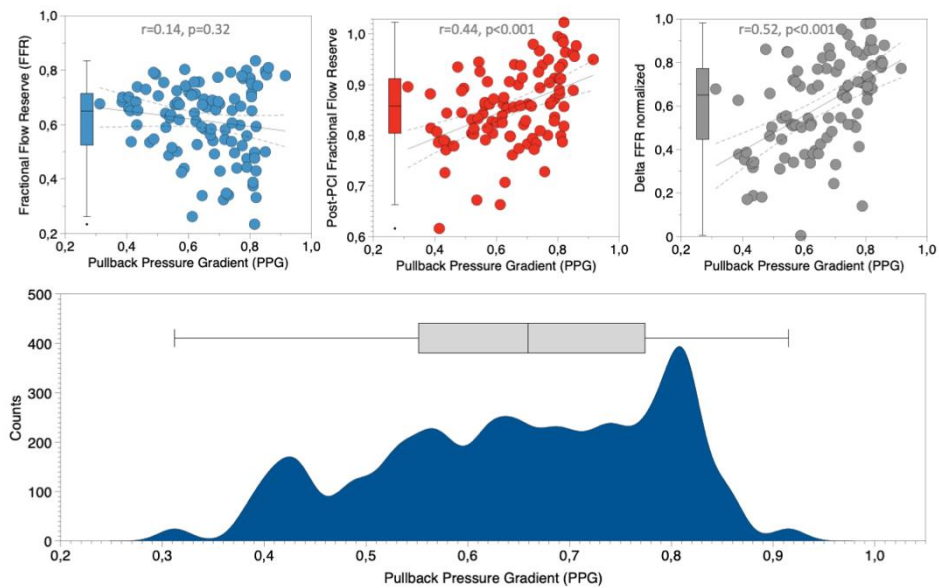d delta FFR. The PPG was significantly correlated with post-PCI FFR and delta   FFR.

Figure 3. Distribution of Seattle angina questionnaire scores at baseline (left) and follow-up (right) stratified by CAD patterns.

The top panels show the Seattle Angina Questionnaire (SAQ) angina frequency score at baseline (left) and follow-up (right). The mid panels show the SAQ physical limitation score at baseline (left) and follow-up (right). The bottom panels show the SAQ quality of life score at baseline (left) and follow-up (right). Patients with focal disease (PPG ≥ 0.66) are represented in blue and diffuse disease in red. The area of each color depicts the frequency of the score's interval, and the height of the bar represents the score's density. The blue and red lines with diamonds represent the means and standard deviation of each score stratified by the CAD pattern. At baseline, there were no differences in the angina frequency, physical limitation, and quality of life domains between focal and diffuse disease. At follow-up, patients with focal disease reported significantly higher scores in the angina frequency, physical limitation, and quality of life domains; p values < 0.05 for all.
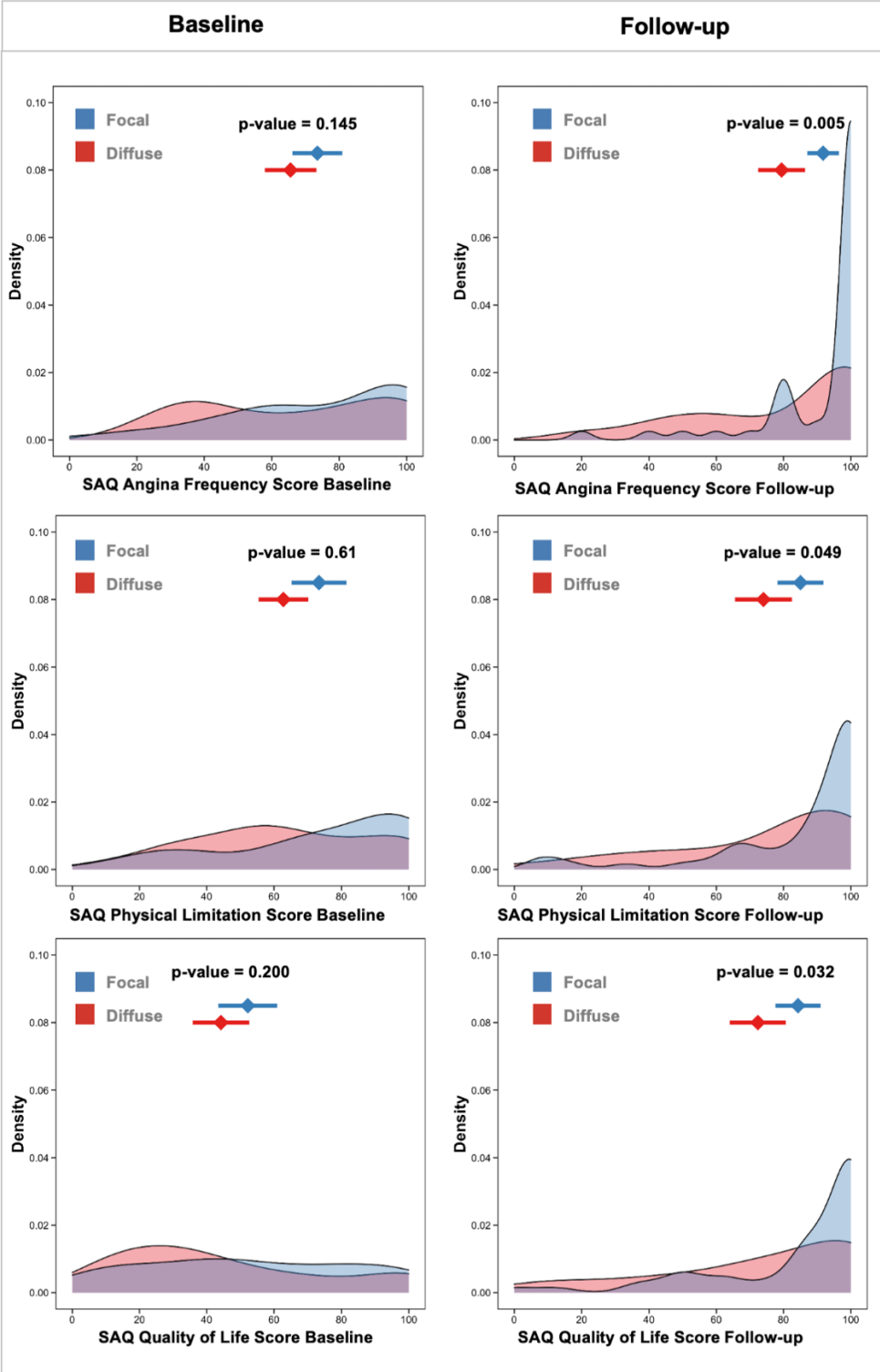
Figure 4. Rate of freedom from angina after PCI stratified by CAD patterns.

The pie charts show the proportions of angina-free (SAQ Angina Frequency score = 100) and residual angina (SAQ Angina Frequency score < 100) patients with diffuse (left) and focal CAD (right). There were significantly more patients free from angina after PCI if the baseline CAD pattern was focal (PPG ≥ 0.66). The bottom panel shows a Sankey diagram depicting the changes in angina frequency (daily or weekly, monthly or none) from baseline to follow-up stratified by diffuse (left) and focal CAD (right).
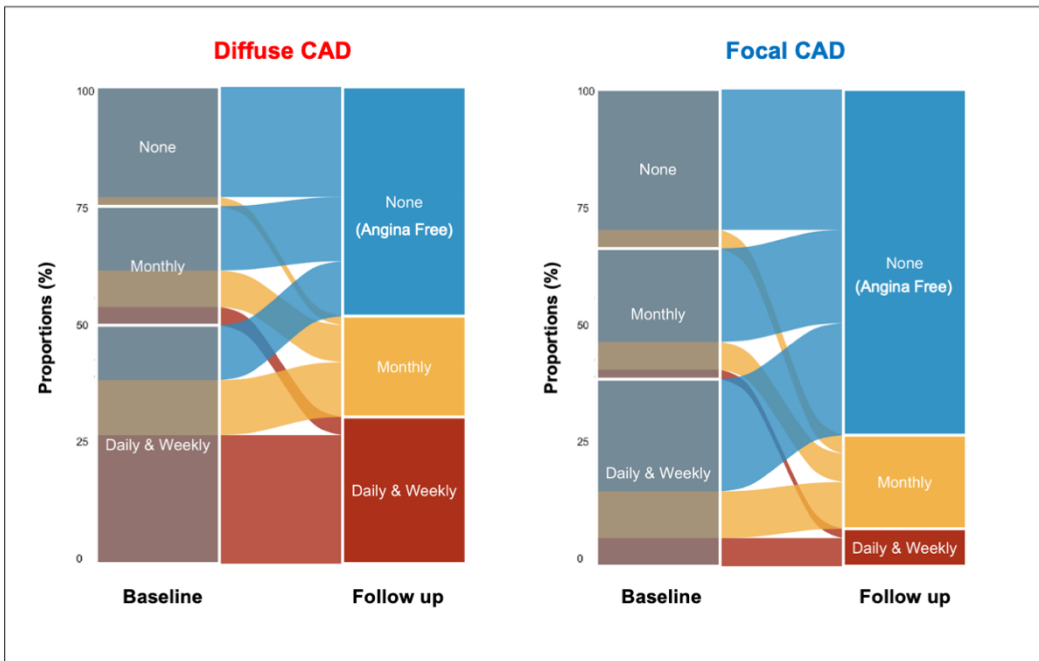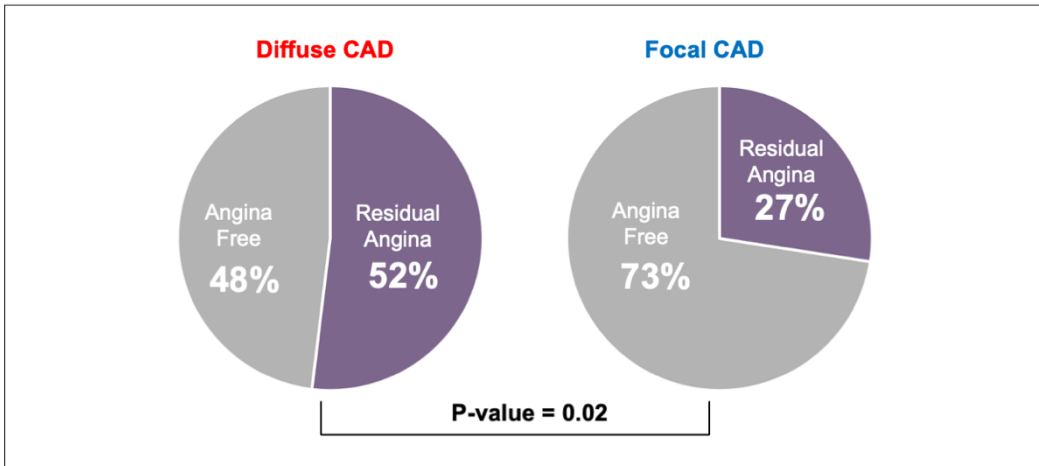
247

Figure 5. Effect of coronary artery disease pattern and results of PCI as a function of patients' baseline SAQ Angina Frequency score.

Probability of being angina-free (SAQ Angina Frequency score = 100) at three months after PCI if baseline coronary artery disease pattern was focal (blue) or diffuse (red) as a function of patients' baseline SAQ Angina Frequency score. Shading represents 95% confidence intervals.
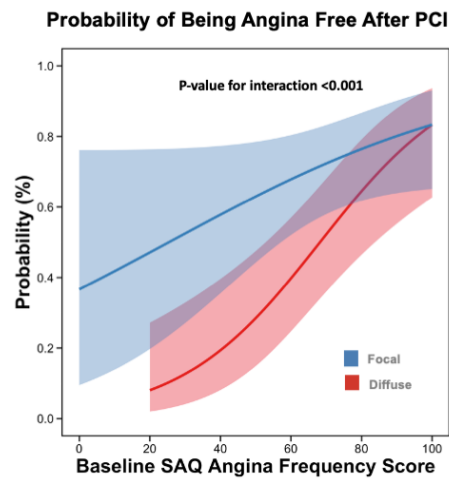
References

1.   Mozaffarian D, Bryson CL, Spertus JA, McDonell MB, Fihn SD. Anginal symptoms consistently predict total mortality among outpatients with coronary artery disease. *Am Heart J*. Dec 2003;146(6):1015-22. doi:10.1016/s0002-8703(03)00436-8

2.   Spertus JA, Jones PG, Maron DJ, et al. Health-Status Outcomes with Invasive or Conservative Care in Coronary Disease. *N Engl J Med*. Apr 9 2020;382(15):1408-1419. doi:10.1056/NEJMoa1916370

3.   Venkitachalam L, Kip KE, Mulukutla SR, et al. Temporal trends in patient-reported angina at 1 year after percutaneous coronary revascularization in the stent era: a report from the National Heart, Lung, and Blood Institute-sponsored 1997-2006 dynamic registry. *Circ Cardiovasc Qual Outcomes*. Nov 2009;2(6):607-15. doi:10.1161/circoutcomes.109.869131

4.   Shaw LJ, Berman DS, Maron DJ, et al. Optimal medical therapy with or without percutaneous coronary intervention to reduce ischemic burden: results from the Clinical Outcomes Utilizing Revascularization and Aggressive Drug Evaluation (COURAGE) trial nuclear   substudy.   *Circulation*.   Mar   11   2008;117(10):1283-91. doi:10.1161/circulationaha.107.743963

5.   Collison D, Didagelos M, Aetesam-Ur-Rahman M, et al. Post-stenting fractional flow reserve vs coronary angiography for optimisation of percutaneous coronary intervention: TARGET-FFR trial. *Eur Heart J*. Jul 19 2021;doi:10.1093/eurheartj/ehab449

6.   Fournier S, Ciccarelli G, Toth GG, et al. Association of Improvement in Fractional Flow Reserve With Outcomes, Including Symptomatic Relief, After Percutaneous Coronary Intervention. *JAMA Cardiol*. Apr 1 2019;4(4):370-374. doi:10.1001/jamacardio.2019.0175

7.   Ando H, Takashima H, Suzuki A, et al. Impact of lesion characteristics on the prediction of optimal poststent fractional flow reserve. *Am Heart J*. Dec 2016;182:119-124. doi:10.1016/j.ahj.2016.09.015

8.   Sianos G, Morel MA, Kappetein AP, et al. The SYNTAX Score: an angiographic tool grading the complexity of coronary artery disease. *EuroIntervention*. Aug 2005;1(2):219-27.

9.   Patel MR, Jeremias A, Maehara A, et al. 1-Year Outcomes of Blinded Physiological Assessment of Residual Ischemia After Successful PCI: DEFINE PCI Trial. *JACC Cardiovasc Interv*. Jan 10 2022;15(1):52-61. doi:10.1016/j.jcin.2021.09.042

10.   Di Sciascio G, Patti G, Nasso G, Manzoli A, D'Ambrosio A, Abbate A. Early and long-term results of stenting of diffuse coronary artery disease. *Am J Cardiol*. Dec 1 2000;86(11):1166-70.

11.   van Beek KAJ, van Steenbergen GJ, Vervaat FE, et al. Single center experience in the treatment of hemodynamically significant diffuse coronary artery disease of the left anterior descending. *Int J Cardiol*. Jan 26 2022;doi:10.1016/j.ijcard.2022.01.048

12.   Collet C, Sonck J, Vandeloo B, et al. Measurement of Hyperemic Pullback Pressure Gradients to Characterize Patterns of Coronary Atherosclerosis. *Journal of the American College of Cardiology*. 2019;74(14):1772-1784. doi:10.1016/j.jacc.2019.07.072

13.   Collison D, McClure JD, Berry C, Oldroyd KG. A randomized controlled trial of a physiology-guided percutaneous coronary intervention optimization strategy: Rationale and design   of   the   TARGET FFR   study.   *Clin   Cardiol*.   May   2020;43(5):414-422. doi:10.1002/clc.23342

14.   Spertus JA, Winder JA, Dewhurst TA, et al. Development and evaluation of the Seattle Angina Questionnaire: a new functional status measure for coronary artery disease. *J Am Coll Cardiol*. Feb 1995;25(2):333-41. doi:10.1016/0735-1097(94)00397-9

15.   Chan PS, Jones PG, Arnold SA, Spertus JA. Development and validation of a short version of the Seattle angina questionnaire. *Circ Cardiovasc Qual Outcomes*. Sep 2014;7(5):640-7. doi:10.1161/circoutcomes.114.000967

16.   Thomas M, Jones PG, Arnold SV, Spertus JA. Interpretation of the Seattle Angina Questionnaire as an Outcome Measure in Clinical Trials and Clinical Care: A Review. *JAMA Cardiol*. May 1 2021;6(5):593-599. doi:10.1001/jamacardio.2020.7478

17.   Crea F, Bairey Merz CN, Beltrame JF, et al. Mechanisms and diagnostic evaluation of persistent or recurrent angina following percutaneous coronary revascularization. *Eur Heart J*. Jan 4 2019;doi:10.1093/eurheartj/ehy857

18.   Rajkumar CA, Shun-Shin M, Seligman H, et al. Placebo-Controlled Efficacy of Percutaneous Coronary Intervention for Focal and Diffuse Patterns of Stable Coronary Artery Disease. *Circ Cardiovasc Interv*. Aug 3 2021:Circinterventions120009891. doi:10.1161/circinterventions.120.009891

19.   Sonck J, Mizukami T, Johnson NP, et al. Development, validation, and reproducibility of the pullback pressure gradient (PPG) derived from manual fractional flow reserve pullbacks. *Catheter Cardiovasc Interv*. Apr 2022;99(5):1518-1525. doi:10.1002/ccd.30064

20.   Quadri G, D'Ascenzo F, Bollati M, et al. Diffuse coronary disease: short- and long-term outcome after percutaneous coronary intervention. *Acta Cardiol*. Apr 2013;68(2):151-60. doi:10.1080/ac.68.2.2967272

0.95

FFR

Length
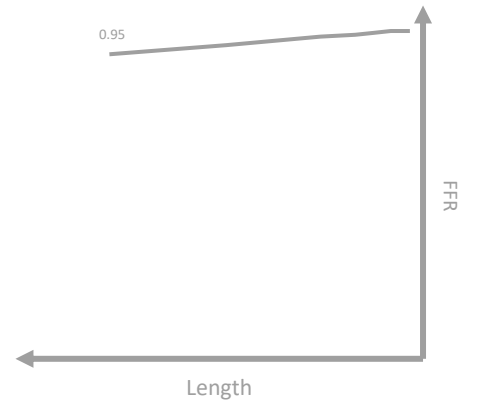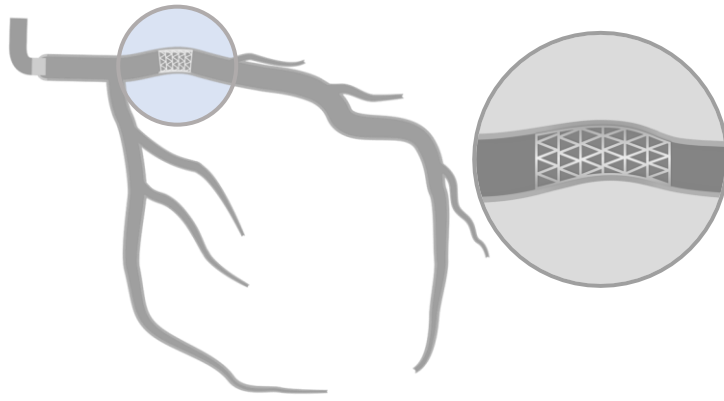
Part E.

Validation of PPG as predictor of PCI outcomes

0.95

FFR

Length
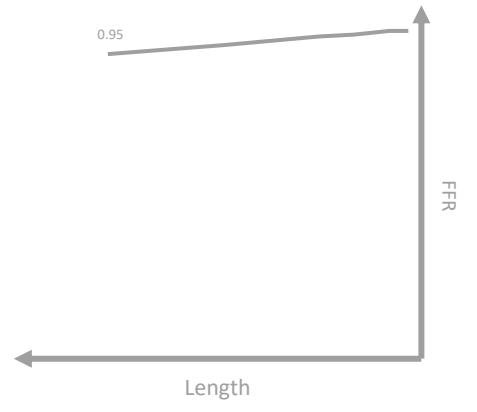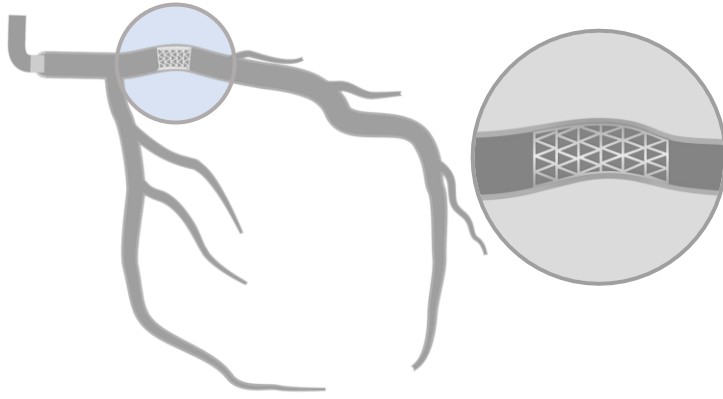
Chapter 11. Rationale and Design of the Pullback Pressure Gradient (PPG) Global Registry

Munhoz D, Collet C, Mizukami T, Yong A, Leone AM, Eftekhari A, Ko B, da Costa BR, Berry C, Collison D, Perera D, Christiansen EH, Rivero F, Zimmermann FM, Ando H, Matsuo H, Nakayama M, Escaned J, Sonck J, Sakai K, Adjedj J, Desta L, van Nunen LX, West NEJ, Fournier S, Storozhenko T, Amano T, Engstrøm T, Johnson T, Shinke T, Biscaglia S, Fearon WF, Ali Z, De Bruyne B, Johnson NP.
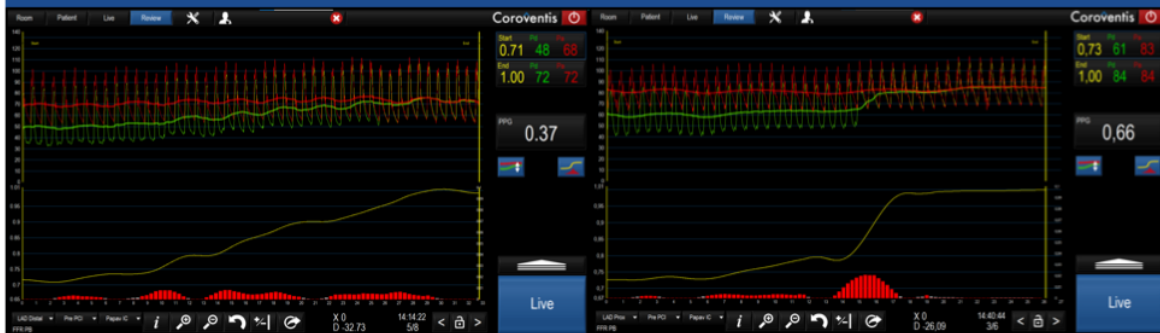
Abstract

Introduction: Diffuse disease has been identified as one of the main reasons leading to low post-PCI fractional flow reserve (FFR) and residual angina after PCI. Coronary pressure pullbacks allow for the evaluation of hemodynamic coronary artery disease (CAD) patterns. The pullback pressure gradient (PPG) is a novel metric that quantifies the distribution and magnitude of pressure losses along the coronary artery in a focal-to-diffuse continuum.

Aim: The primary objective is to determine the predictive capacity of the PPG for post-PCI FFR.

Methods: This prospective, large-scale, controlled, investigator-initiated, multicenter study is enrolling patients with at least one lesion in a major epicardial vessel with a distal FFR ≤ 0.80 intended to be treated by PCI. The study will include 982 subjects. A standardized physiological assessment will be performed pre-PCI, including the online calculation of PPG from FFR pullbacks performed manually. PPG quantifies the CAD pattern by combining several parameters from the FFR pullback curve. Post-PCI physiology will be recorded using a standardized protocol with FFR pullbacks. We hypothesize that PPG will predict optimal PCI results (post-PCI FFR ≥ 0.88) with an area under the ROC curve (AUC) ≥ 0.80. Secondary objectives include patient-reported and clinical outcomes in patients with focal vs. diffuse CAD defined by the PPG. Clinical follow-up will be collected for up to 36 months, and an independent clinical event committee will adjudicate events.

Results: Recruitment is ongoing and is expected to be completed in the second half of 2023.

Conclusion: This international, large-scale, prospective study with pre-specified powered hypotheses will determine the ability of the pre-procedural PPG index to predict optimal revascularization assessed by post-PCI FFR. In addition, it will evaluate the impact of PPG on treatment decisions and the predictive performance of PPG for angina relief and clinical outcomes. ClinicalTrials.gov Identifier: NCT04789317

Introduction

Assessing the distribution of flow-limiting atherosclerosis along a coronary artery adds a second dimension to evaluating lesion significance. Ascertainment of the hemodynamic pattern of coronary artery disease (CAD) - either as focal or diffuse - carries therapeutic implications. Coronary angiography has historically been used to assess CAD patterns. However, insights from intracoronary pressure pullbacks and intravascular imaging have underlined that coronary angiography underestimates the burden of atherosclerosis and can misjudge the distribution of disease.[1,2] Moreover, CAD patterns have been shown to influence treatment decisions concerning myocardial revascularization; diffuse CAD has been identified as one mechanism associated with persistent angina after percutaneous coronary intervention (PCI).[3,4]

Fractional flow reserve (FFR) is a hyperemic intracoronary pressure measurement that correlates with myocardial ischemia by providing a metric of peak flow reduction.[5] It has proven superior to an angiographic-based strategy when selecting lesions for PCI for predicting death, myocardial infarction or urgent revascularization[6] as well as for cost effectiveness[7]. Nevertheless, the distal FFR value (also referred to as spot or single point FFR) results from cumulative pressure loss along the entire vessel due to focal or diffuse atherosclerotic disease and, frequently, a combination of both.[1,8] Diffuse CAD is associated with a lower FFR after PCI[9,10] and a higher incidence of clinical events.[11] Currently, definitions of diffuse CAD are heterogenous, commonly based on visual assessment, and therefore subject to high interobserver variability.[8,12]

Intracoronary pressure losses along the vessel reflect the interplay between epicardial atherosclerotic burden and coronary flow. A pullback maneuver reveals the distribution and magnitude of these pressure losses. This pattern can be quantified along a focal-to-diffuse continuum using a novel metric: the pullback pressure gradient (PPG).[8] PPG quantifies the CAD pattern by combining two parameters: the maximal pressure gradient in the pullback and the amount of functional disease along the vessel.

A pre-intervention evaluation of the pressure pullback pattern may help predict the post-PCI FFR and thus individualize revascularization decisions. [13]When measured immediately after PCI, a low residual FFR has been identified as an independent predictor of future vessel-related adverse events.[14-16] Likewise, the magnitude of improvement in FFR after

PCI has been associated with angina relief, linking the clinical benefit of PCI to a reduction of pressure gradients and improvements in epicardial conductance.[10,17-19]

The PPG Global study will determine the capacity of PPG to predict optimal functional revascularization assessed by FFR after PCI. It will also explore the implications for clinical decision-making, its association with angina improvement at one year, and clinical outcomes up to three years.

Methods

Study design

This prospective, investigator-initiated, multicenter, international, large-scale study with pre-specified powered hypotheses, registered at clinicaltrials.gov as NCT04789317, is enrolling subjects with at least one lesion in a major epicardial vessel with a distal FFR ≤ 0.80 intended to be treated with PCI. Table 1 provides inclusion and exclusion criteria. Briefly, subjects must be 18 years or older at the time of inclusion with stable CAD or a non-culprit vessel after an acute coronary syndrome (ACS). Aorto-ostial lesions are excluded, given the challenges of maintaining a suitable guide catheter position during pressure wire pullback. A total of 25 centers with experience in coronary physiology are recruiting patients in Europe, the United Kingdom, Japan, the USA, and Australia (Table S1). The trial follows the Declaration of Helsinki and all applicable local regulations. Every subject must give written informed consent before enrollment, and every site must receive approval from its local institutional review board before recruitment begins. Figure 1 details the flow of patients included in the PPG Global registry.

Primary and secondary endpoints

The primary endpoint is the predictive capacity of the PPG index for post-PCI FFR evaluated by area under the curve (AUC) from receiver operator characteristic (ROC) analysis.

Secondary endpoints include the following:

Impact of the PPG on treatment decisions assessed by the rate of deferral from planned PCI to either coronary artery bypass grafting (CABG) or medical therapy;

Relationship between the baseline PPG and improvement in angina symptoms one year after PCI assessed by the Seattle Angina Questionnaire (SAQ-7) both in the overall population and in patients with symptoms at baseline;

Relationship between baseline PPG and health-related quality of life improvement assessed by the SAQ-7;

Proportion of patients with focal and diffuse disease free from angina after PCI (defined by the SAQ-7 angina frequency domain) both in the overall population and in patients with symptoms at baseline;

Proportion of patients with focal and diffuse disease with post-PCI FFR ≥ 0.90 or > 0.80;

Rates of TVF defined as a composite of cardiac death, target-vessel myocardial infarction, and ischemia-driven target vessel revascularization between patients with focal and diffuse disease at one, two and three years;

Rates of the individual components of TVF, including peri-procedural MI, in patients with focal and diffuse disease defined by PPG;

Impact of intracoronary imaging guidance during PCI on TVF stratified by focal and diffuse disease defined by the PPG index.

In addition, subanalysis addressing the association between microvascular assessment, PPG and PRO, comparison of PPG derive in resting and hyperemic conditions, impact of analysis of serial lesions the post-PCI FFR predcition by the PPG and a comparison between stable and ACS patient are planned.

Clinical event definitions

Cardiovascular death represents a death resulting from cardiovascular or undetermined causes. Myocardial infarction (MI) includes both spontaneous and periprocedural. Spontaneous MI represents an infarct after the first 48 hours following PCI or CABG and unrelated to the revascularization procedure.[20] Periprocedural MI occurs within the first 48 hours following PCI or CABG. The criteria for peri-procedural MI are shown in Supplemental material Table S2.[21,22] Target-vessel MI is defined as an MI in the vessel that underwent FFR and PPG measurement during the index procedure. Target vessel revascularization (TVR) is defined as repeat PCI or CABG of any segment of a target vessel, including the target lesion. Target lesion revascularization is defined as a reintervention up to 5 mm proximally or distally to the index lesion. Revascularization is considered ischemia-driven if associated with any of the following: 1) positive non-invasive stress test or invasive FFR ≤ 0.80; 2) angiographic diameter stenosis ≥50% by core laboratory quantitative coronary angiography (QCA) with ischemic clinical symptoms or angiography-derived FFR ≤ 0.80; or 3) angiographic diameter stenosis ≥70% by core laboratory QCA without angina. Completeness of revascularization will

be quantified by the residual SYNTAX score (rSS) with complete revascularization indicating an rSS of 0.[23]

Catheterization laboratory protocol

Vascular access and size of the guiding catheter are left to the operator's discretion. All subjects will receive 100 to 200 μg of intracoronary nitroglycerin at the beginning of the procedure. An 0.014" coronary wire with a distal pressure sensor (PressureWire X, Abbott Vascular, Santa Clara, CA, USA) will be introduced into the target vessel after pressure equalization at the tip of the guiding catheter.[24] The pressure wire will be positioned in the distal coronary artery in a segment ≥ 2mm and at least 15 mm beyond the most distal stenosis by visual estimation; its position recorded by contrast angiography. Resting full cycle ratio (RFR) and FFR will be measured at the distal wire position. Hyperemia can be induced by various pharmacologic agents (e.g., Adenosine, Papaverine, Nicorandil, ATP, etc.) according to local practice. The most commonly used hyperemic agents are intra-coronary (IC), Papaverine, Adenosine IV, and Nicorandil IC. It's important to note that IC Adenosine cannot be used for PPG assessment because the hyperemic time is not long enough to perform a pullback maneuver. The operator will then record 3 items of the initial strategy in a dedicated pre-PPG questionnaire: (1) the segment to be treated, (2) the number of stents, and (3) the total stent length. Subsequently and during maximal hyperemia, a manual pullback will be performed at a steady speed over 20 to 30 seconds. All operators will be trained via movies on how to perform the manual pullback maneuver.[13] PPG will be calculated online using CoroFlow software (version 3.5.1, Coroventis Research, Uppsala, Sweden). After the calculation of the PPG, the operator will answer a dedicated post-PPG questionnaire with the same three questions regarding the treatment plan. After the calculation of PPG, deferral of PCI to either CABG or medical therapy is permitted. Measurement of the microvascular function (coronary flow reserve [CFR] and index of microvascular resistance [IMR]) pre- and post-PCI will be performed optionally in selected centers. PCI will be performed at the operator's discretion; the use of intravascular imaging for PCI guidance will be encouraged. After PCI, RFR and distal FFR will again be assessed with the pressure wire in the same position as before the PCI. Finally, an FFR pullback will be repeated, with markers placed at the distal and proximal stent edges to allow for coregistration with residual pressure gradients and stent position. The quality of the pressure pullback tracings and compliance with the physiology protocol were controlled by the core laboratory, which provided feedback to the investigators on the adequacy of the tracings during the first ten cases in every site.

Calculation of the PPG

The formula for PPG has been described and modified previously.[13] Its equation combines two equally-weighted parameters:

PPG

$$= \frac{\frac{\text{Maximal Pressure Gradient over 20\% pullback duration}}{\text{Vessel FFR gradient}} + (1 - \text{proportion of pullback time with FFR deterioration})}{2}$$

The *maximal pressure gradient over 20% of the pullback duration* calculates the pressure drop over a fixed time window lasting 20% of the total pullback duration. Likewise, the *proportion of pullback time with FFR deterioration* uses an FFR threshold of 0.0015 units per time. The adapted formula has been incorporated into a commercial console and allows for calculation of the PPG after a manual pullback manuever (CoroFlow, Coroventis Research, Uppsala, Sweden). Figure 2 shows the diffuse to focal functional CAD spectrum.

The Seven Items Seattle Angina Questionnaire

The 7-items Seattle Angina Questionnaire (SAQ-7) is a shortened version of a commonly-used tool to measure health status by quantifying anginal symptoms, functional limitations due to angina, and the impact of angina on quality of life. The SAQ-7 summary score and scores from its individual domains will be used to quantify angina frequency, physical limitation and quality of life. In addition, angina frequency scores will be categorized into daily or weekly (≤ 60), monthly (>60, < 100), or none ($= 100$), and for the domains of physical limitation and quality into poor or fair (< 50), good (≥ 50, < 75), or excellent (≥ 75) categories.[25]

Clinical decision and treatment

While an FFR ≤ 0.80 is considered abnormal and revascularization deemed appropriate, there is no guidance on a PPG threshold; therefore, no threshold was provided to operators regarding the PPG value. As the first clinical decision is registered before the pullback, this clinical decision resembles a strategy without access to the PPG value or the pullback curve pattern, as is common in clinical practice. Based on prior work, we hypothesize that PCI of lesions in vessels with low PPG (representing more diffuse disease) will lead to low post-PCI FFR, less angina relief, and more frequent target vessel failure (TVF).

Clinical Follow-up

Patients will be followed up to 36 months. Follow-up can occur either by a clinical visit or by telephone contact. During the first-year follow-up interview, an SAQ-7 will be re-

administered, and clinical status will be collected at 12, 24, and 36 months. Documentation of hospital records will be reviewed for all subjects admitted for major adverse coronary events (cardiac death, periprocedural and spontaneous myocardial infarction, target vessel revascularization, and stent thrombosis). Based on the documentation provided by the local site, clinical endpoints will be adjudicated by an independent clinical events committee (CEC).

Statistical analysis and Sample size

We hypothesize that PPG will predict optimal revascularization defined as post-PCI FFR $\geq$ 0.88 with an expected area under the ROC curve (AUC) of 0.80.[14] Under the assumptions of power of 90%, 2.5% two-sided alpha, a sample size of 128 patients will be required. The study will also be powered for the key major secondary objective of the impact of PPG on treatment decisions expecting a 20% change in revascularization decisions from the initial intention to perform PCI to either CABG or medical therapy. Considering a width of the 95% confidence interval of 5%, a sample size of 982 patients will be required to detect this change.

The analysis cohort for the primary outcome will consist only of patients who received PCI. For the primary objective, we will calculate the area under the receiver operating characteristic (AUC) curve, adjusted by vessel type and pre-PCI FFR, and its 95% bias-corrected bootstrapped confidence interval (CI) as a measure of PPG discrimination of patients achieving optimal revascularization (post-PCI FFR $\geq$ 0.88). If this interval excludes 0.60 and contains $\geq$ 0.80, the study will have met its primary endpoint. We will then calculate sensitivity, specificity, positive and negative likelihood ratios to identify the most appropriate baseline PPG cut-off(s) to identify patients who will likely achieve optimal revascularization. We will use two different linear regression models to predict patients' post-PCI FFR one using baseline PPG dichotomized according to the selected cut-off, and one using baseline PPG on a continuous scale as predictor, with both models including vessel type and pre-PCI FFR as additional predictors. Discrimination based on AUC, likelihood ratios associated with identified cut-off(s) of baseline PPG, calibration of predicted post-PCI FFR from dichotomized baseline PPG, and calibration of predicted post-PCI FFR from baseline PPG will be internally validated in the temporally defined derivation cohort based on 500 bootstrap samples with replacement (primary validation), and then validated in the temporally defined validation cohort (secondary validation).[26] Calibration is defined as the agreement between observed and predicted values and will be assessed using calibration plots, ratio of predicted to observed

post-PCI FFR, and calibration-in-the-large.[27] Therefore, this analysis will provide a PPG threshold for the prediction of optimal revascularization based on post-PCI FFR. For the secondary endpoints, the definition of focal and diffuse coronary artery disease will be based on the baseline PPG threshold derived from the AUC analysis.[4] Patients reported-outcomes will be evaluated by comparing focal and diffuse disease using linear regression models adjusted by outcomes' baseline values and medication use. Clinical outcomes between patients with focal and diffuse disease will be assessed using adjusted multivariable logistic regression and Cox regression analyses.

Study limitations

Because of the nonrandomized, observational, and nonblinded design, certain limitations apply. The primary objective will be assessed using the AUC method using a post-PCI FFR cut-off of 0.88.[14] However, after starting this study a large pooled analysis indicated an optimal post-PCI FFR threshold of 0.86 to predict target vessel failure, very similar to the 0.88 prospectively chosen in this registry.[28] Clinical thresholds for PPG have not yet been fully determined; therefore, there is no guidance regarding treatment decisions based on the PPG value at the current stage.

Role of the funding source and study oversight

The PPG Global Registry is an investigator-initiated trial sponsored by the Cardiac Research Institute Aalst with an unrestricted grant from Abbott Vascular. The grant giver will not be involved in the study design, data collection, and data analysis. A core laboratory (CoreAalst BV, Aalst, Belgium) will analyze imaging and physiological data. An independent CEC will adjudicate all endpoints, blinded to the physiological data.

Results

Recruitment is ongoing, and the primary endpoint is anticipated in the second half of 2023. Figure 3 shows two case examples from the PPG global registry with FFR pullback before and after PCI in focal and diffuse CAD.

Discussion

Studies in which the indication of PCI has been set on the grounds of intracoronary physiology have shown that, after an angiographically successful procedure, approximately one-fourth of patients show residual flow-limiting epicardial vessel disease.[15,29,30] The main reasons for low FFR after PCI relate to residual atherosclerotic disease or suboptimal stent deployment.[31] By anticipating the impact of residual disease after PCI, PPG provides a tool to

predict post-PCI FFR and angina improvement, thereby allowing personalized revascularization decisions. PPG pullback augments the single value distal FFR evaluation by quantifying the CAD pattern and identifying focal pressure gradients amenable to PCI. The present study will determine PPG's predictive capacity for post-PCI physiology. In addition, the change in treatment decision after systematic longitudinal vessel investigation with hyperemic manual pullbacks will be defined. Furthermore, the impact of focal and diffuse disease quantified based on intracoronary hemodynamics on patient-reported and clinical outcomes will be assessed at mid-term follow-up.

The field of coronary physiology continues to evolve, and longitudinal pressure evaluation obtained by manual pullback manuevers has been shown to have clinical implications and predict the interventions' results.[4] Pullback maneuvers can be performed in resting or hyperemic conditions to define the disease as focal or diffuse. In addition to PPG Global, a randomized clinical trial, Distal Evaluation of Functional Performance With Intravascular Sensors to Assess the Narrowing Effect: Guided Physiologic Stenting (DEFINE-GPS NCT04451044), which uses co-registration of instantaneous- wave-free period (iFR) with angiography, is also utilizing systematic pullback evaluations to plan and guide PCI. These trials will shed light of the effects of PCI in focal vs. diffuse CAD.

Conclusion

This international, large-scale, controlled, prospective study with pre-specified powered hypotheses will determine the ability of the PPG index to predict post-PCI FFR. In addition, it will evaluate the impact of PPG on treatment decision-making and the predictive performance of PPG for angina relief and clinical outcomes. A subsequent randomized clinical trial will be required to assess the clinical benefit of a PPG-guided PCI strategy.

Table 1. Inclusion and exclusion criteria

Inclusion criteria	Exclusion criteria

1. Age >18 years
 	
2. Provide written informed consent (IC)
 	
3. Angiographic lesion amenable to PCI
 	
4. Invasive FFR ≤0.80
	8.1 Angiographic exclusion criteria:
	
	  1. Aorto-ostial lesions.
	
	  2. Severe vessel tortuosity*.
	
	  3. Vessel rewiring is deemed 'difficult' by the operator.
	
	  4. Bifurcation with planned two-stent strategy.
	
	8.2 Concomitant contra-indications
	
	  1. NYHA class III or IV, or last known left ventricular ejection fraction <30%
	  2. Acute STEMI
	  3. NSTEMI culprit vessels
	  4. Uncontrolled or recurrent ventricular tachycardia
	  5. Prior myocardial infarction in the treated vessel
	  6. History of any haemorrhagic stroke
	  7. Active liver disease or hepatic dysfunction, defined as AST or ALT > 3 times the upper limit of normal
	  8. Severe renal dysfunction, defined as an eGFR <30 mL/min/1.73 m^2
	
	8.3 Other exclusion criteria
	
	  9. Known pregnancy or breastfeeding at the time of randomization.

* Tortuosity is defined as one or more bends of 90° or more, or three or more bends of 45° to 90° proximal of the diseased segment.

Figure 1 Study Flowchart

Detailed flow of the study, with first and second clinical decisions registered in dedicated questionnaires. The second (or adapted) clinical decision is registered after FFR pullbacks with PPG calculation. PCI or deferral is at the operator's discretion. Patients will be followed up to three years.

ACS: Acute coronary syndrome; FFR: Fractional flow reserve; SAQ-7: 7-point Seattle Angina Questionnaire; PCI: Percutaneous coronary intervention; PPG: Pullback pressure gradient.; OMT: Optimized Medical Therapy; CABG: Coronary artery bypass graft

Stable patients with significant coronary artery disease (FFR ≤ 0.80) and intention to perform PCI

Initial strategy based on angiography and distal point physiology

FFR Pullback with Pullback Pressure Gradient (PPG)

Adapted Treatment Decision

OMT

PCI

CABG

Primary objective
Predictive capacity of PPG for Post-PCI FFR

Secondary objectives
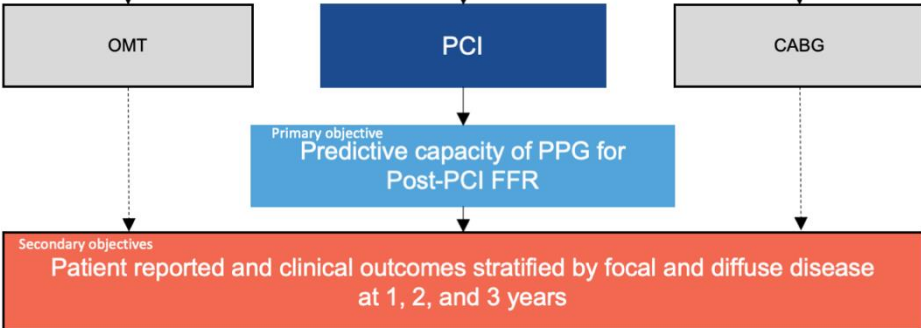Patient reported and clinical outcomes stratified by focal and diffuse disease at 1, 2, and 3 years

Figure 2 Diffuse to Focal functional CAD spectrum

Fractional flow reserve (FFR) pullbacks with a pullback pressure gradient (PPG) ordered from panel A showing diffuse (low PPG) to panel F depicting focal disease (high PPG).

Figure 3 Case examples

Panel A shows the pre-PCI FFR pullback of a mid-LAD lesion with a distal FFR of 0.73 and a PPG of 0.66 (calculated with the average of two components of a maximal pressure gradient within 20% of the pullback length of 76% and 43% of disease length). The dashed box, for illustration purposes, shows the location of the maximal pressure gradient detected in the pullback curve. Panel B shows the baseline angiography, and panel C shows the post-PCI angiographic results (the white dashed line indicates the position of the stent). Panel D shows the post-PCI FFR pullback with a distal FFR of 0.86. Panel E shows another case with diffuse disease; the pre-PCI FFR was 0.71 with a PPG 0.37. Panel F and G show the pre- and post-PCI angiography (the white dashed line indicates the position of the stent). Panel H shows a post-PCI FFR of 0.69 with residual diffuse disease.

LAD: Left anterior descending artery; FFR: Fractional flow reserve; PG: Pressure gradient; PPG: Pullback pressure gradient.
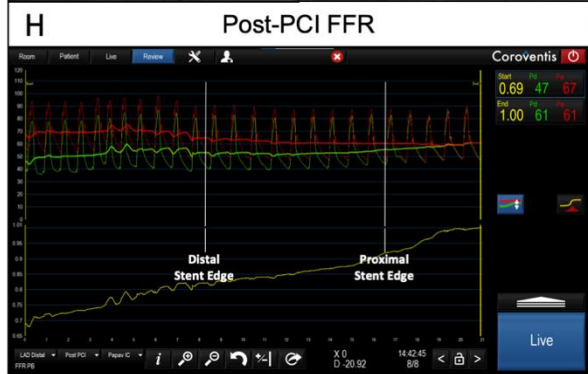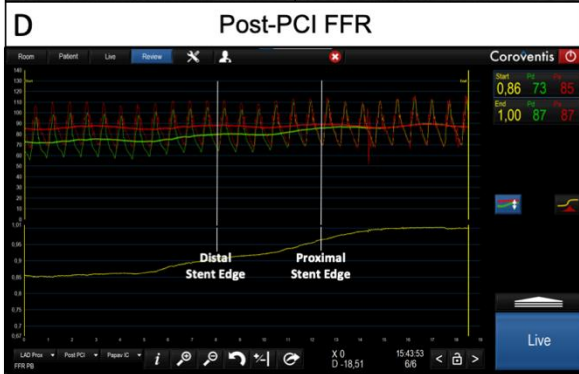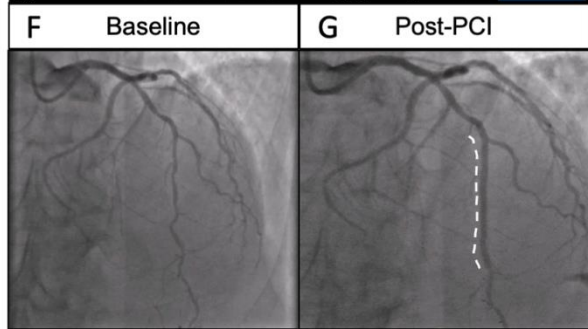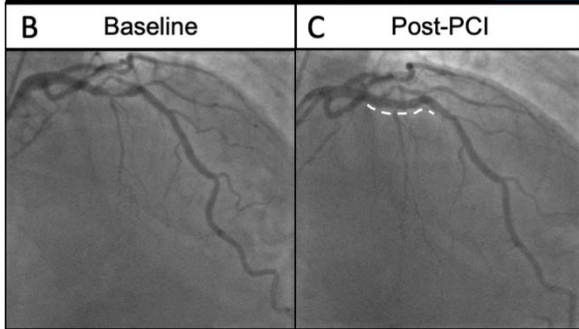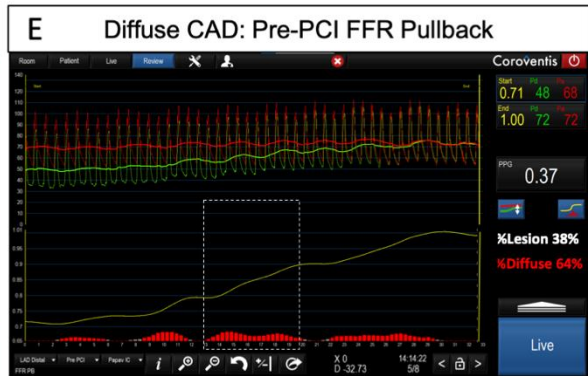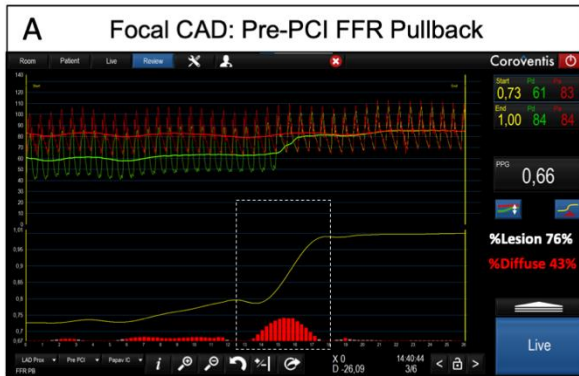
A — Focal CAD: Pre-PCI FFR Pullback

B — Baseline

C — Post-PCI

D — Post-PCI FFR

E — Diffuse CAD: Pre-PCI FFR Pullback

F — Baseline

G — Post-PCI

H — Post-PCI FFR

References

1.   De Bruyne B, Hersbach F, Pijls NH, et al. Abnormal epicardial coronary resistance in patients with diffuse atherosclerosis but "Normal" coronary angiography. *Circulation*. Nov 2001;104(20):2401-6. doi:10.1161/hc4501.099316

2.   Mintz GS, Painter JA, Pichard AD, et al. Atherosclerosis in angiographically "normal" coronary artery reference segments: an intravascular ultrasound study with clinical correlations. *J Am Coll Cardiol*. Jun 1995;25(7):1479-85. doi:10.1016/0735-1097(95)00088-l

3.   Crea F, Bairey Merz CN, Beltrame JF, et al. Mechanisms and diagnostic evaluation of persistent or recurrent angina following percutaneous coronary revascularization. *Eur Heart J*. 08 01 2019;40(29):2455-2462. doi:10.1093/eurheartj/ehy857

4.   Collet C, Collison D, Mizukami T, et al. Differential Improvement in Angina and Health-Related Quality of Life After PCI in Focal and Diffuse Coronary Artery Disease. *JACC Cardiovasc Interv*. Dec 26 2022;15(24):2506-2518. doi:10.1016/j.jcin.2022.09.048

5.   Pijls NH, De Bruyne B, Peels K, et al. Measurement of fractional flow reserve to assess the functional severity of coronary-artery stenoses. *The New England journal of medicine*. Jun 27 1996;334(26):1703-8. doi:10.1056/nejm199606273342604

6.   Tonino PA, De Bruyne B, Pijls NH, et al. Fractional flow reserve versus angiography for guiding percutaneous coronary intervention. *N Engl J Med*. Jan 2009;360(3):213-24. doi:10.1056/NEJMoa0807611

7.   Fearon WF, Shilane D, Pijls NH, et al. Cost-effectiveness of percutaneous coronary intervention in patients with stable coronary artery disease and abnormal fractional flow reserve. *Circulation*. Sep 17 2013;128(12):1335-40. doi:10.1161/CIRCULATIONAHA.113.003059

8.   Collet C, Sonck J, Vandeloo B, et al. Measurement of Hyperemic Pullback Pressure Gradients to Characterize Patterns of Coronary Atherosclerosis. *J Am Coll Cardiol*. 10 2019;74(14):1772-1784. doi:10.1016/j.jacc.2019.07.072

9.   Baranauskas A, Peace A, Kibarskis A, et al. FFR result post PCI is suboptimal in long diffuse coronary artery disease. *EuroIntervention*. Dec 2016;12(12):1473-1480. doi:10.4244/EIJ-D-15-00514

10.   Mizukami T, Sonck J, Sakai K, et al. Procedural Outcomes After Percutaneous Coronary Interventions in Focal and Diffuse Coronary Artery Disease. *J Am Heart Assoc*. Dec 06 2022;11(23):e026960. doi:10.1161/JAHA.122.026960

11.   Di Sciascio G, Patti G, Nasso G, Manzoli A, D'Ambrosio A, Abbate A. Early and long-term results of stenting of diffuse coronary artery disease. *Am J Cardiol*. Dec 01 2000;86(11):1166-70. doi:10.1016/s0002-9149(00)01197-8

12.   Sianos G, Morel MA, Kappetein AP, et al. The SYNTAX Score: an angiographic tool grading the complexity of coronary artery disease. *EuroIntervention*. Aug 2005;1(2):219-27.

13.   Sonck J, Mizukami T, Johnson NP, et al. Development, validation, and reproducibility of the pullback pressure gradient (PPG) derived from manual fractional flow reserve pullbacks. *Catheter Cardiovasc Interv*. Mar 02 2022;doi:10.1002/ccd.30064

14.   Piroth Z, Toth GG, Tonino PAL, et al. Prognostic Value of Fractional Flow Reserve Measured Immediately After Drug-Eluting Stent Implantation. *Circ Cardiovasc Interv*. Aug 2017;10(8)doi:10.1161/CIRCINTERVENTIONS.116.005233

15.   Pijls NH, Klauss V, Siebert U, et al. Coronary pressure measurement after stenting predicts adverse events at follow-up: a multicenter registry. *Circulation*. Jun 25 2002;105(25):2950-4. doi:10.1161/01.cir.0000020547.92091.76

16.   Li SJ, Ge Z, Kan J, et al. Cutoff Value and Long-Term Prediction of Clinical Events by FFR Measured Immediately After Implantation of a Drug-Eluting Stent in Patients With Coronary Artery Disease: 1- to 3-Year Results From the DKCRUSH VII Registry Study. *JACC Cardiovasc Interv*. 05 22 2017;10(10):986-995. doi:10.1016/j.jcin.2017.02.012

17.   Fournier S, Ciccarelli G, Toth GG, et al. Association of Improvement in Fractional Flow Reserve With Outcomes, Including Symptomatic Relief, After Percutaneous Coronary Intervention. *JAMA Cardiol*. 04 01 2019;4(4):370-374. doi:10.1001/jamacardio.2019.0175

18.   Nishi T, Piroth Z, De Bruyne B, et al. Fractional Flow Reserve and Quality-of-Life Improvement After Percutaneous Coronary Intervention in Patients With Stable Coronary Artery Disease. *Circulation*. Oct 23 2018;138(17):1797-1804. doi:10.1161/CIRCULATIONAHA.118.035263

19.   Collison D, Didagelos M, Aetesam-Ur-Rahman M, et al. Post-stenting fractional flow reserve vs coronary angiography for optimisation of percutaneous coronary intervention: TARGET-FFR trial. *Eur Heart J*. Jul 19 2021;doi:10.1093/eurheartj/ehab449

20.   Thygesen K, Alpert JS, Jaffe AS, et al. Fourth Universal Definition of Myocardial Infarction (2018). *Journal of the American College of Cardiology*. Oct 30 2018;72(18):2231-2264. doi:10.1016/j.jacc.2018.08.1038

21.   Garcia-Garcia HM, McFadden EP, Farb A, et al. Standardized End Point Definitions for Coronary Intervention Trials: The Academic Research Consortium-2 Consensus Document. *Eur Heart J*. Jun 2018;39(23):2192-2207. doi:10.1093/eurheartj/ehy223

22.   Thygesen K, Alpert JS, Jaffe AS, et al. Fourth Universal Definition of Myocardial Infarction (2018). *Circulation*. Nov 2018;138(20):e618-e651. doi:10.1161/CIR.0000000000000617

23.   Généreux P, Palmerini T, Caixeta A, et al. Quantification and impact of untreated coronary artery disease after percutaneous coronary intervention: the residual SYNTAX (Synergy Between PCI with Taxus and Cardiac Surgery) score. *J Am Coll Cardiol*. Jun 12 2012;59(24):2165-74. doi:10.1016/j.jacc.2012.03.010

24.   Toth GG, Johnson NP, Jeremias A, et al. Standardization of Fractional Flow Reserve Measurements. *J Am Coll Cardiol*. Aug 16 2016;68(7):742-53. doi:10.1016/j.jacc.2016.05.067

25.   Chan PS, Jones PG, Arnold SA, Spertus JA. Development and validation of a short version of the Seattle angina questionnaire. *Circ Cardiovasc Qual Outcomes*. Sep 2014;7(5):640-7. doi:10.1161/CIRCOUTCOMES.114.000967

26.   Leligdowicz A, Conroy AL, Hawkes M, et al. Risk-stratification of febrile African children at risk of sepsis using sTREM-1 as basis for a rapid triage test. *Nat Commun*. Nov 25 2021;12(1):6832. doi:10.1038/s41467-021-27215-6

27.   Steyerberg EW, Vergouwe Y. Towards better clinical prediction models: seven steps for development and an ABCD for validation. *Eur Heart J*. Aug 01 2014;35(29):1925-31. doi:10.1093/eurheartj/ehu207

28.   Hwang D, Koo BK, Zhang J, et al. Prognostic Implications of Fractional Flow Reserve After Coronary Stenting: A Systematic Review and Meta-analysis. *JAMA Netw Open*. Sep 01 2022;5(9):e2232842. doi:10.1001/jamanetworkopen.2022.32842

29.   Jeremias A, Davies JE, Maehara A, et al. Blinded Physiological Assessment of Residual Ischemia After Successful Angiographic Percutaneous Coronary Intervention: The DEFINE PCI Study. *JACC Cardiovasc Interv*. 10 28 2019;12(20):1991-2001. doi:10.1016/j.jcin.2019.05.054

30.   Agarwal SK, Kasula S, Hacioglu Y, Ahmed Z, Uretsky BF, Hakeem A. Utilizing Post-Intervention Fractional Flow Reserve to Optimize Acute Results and the Relationship to Long-Term Outcomes. *JACC Cardiovasc Interv*. 05 2016;9(10):1022-31. doi:10.1016/j.jcin.2016.01.046

31.   Samady H, McDaniel M, Veledar E, et al. Baseline fractional flow reserve and stent diameter predict optimal post-stent fractional flow reserve and major adverse cardiac events after bare-metal stent deployment. *JACC Cardiovasc Interv*. Apr 2009;2(4):357-63. doi:10.1016/j.jcin.2009.01.008

0.95

FFR

Length
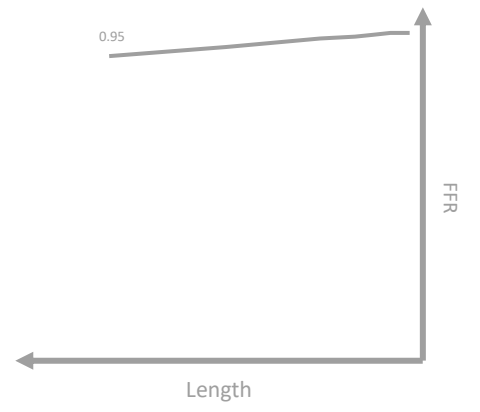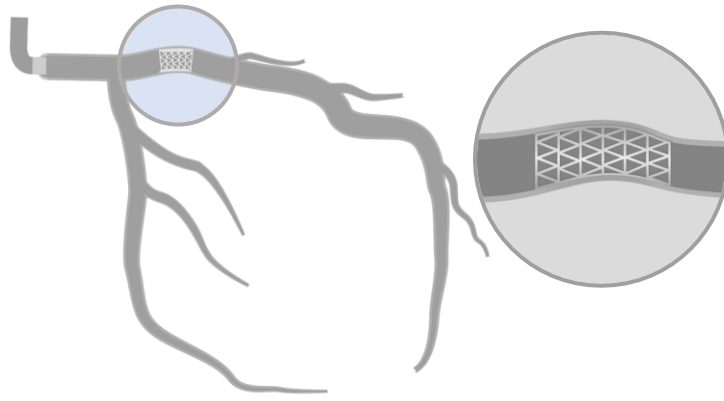
Chapter 12. Discordance in CAD Pattern between resting and hyperemic conditions

Nakayama M, Sakai K, Munhoz D, Ohashi H, Collet C, Johnson NP, Matsuo H.

A 70-year-old man with known hypertension, hyperlipidemia, current smoker, and history of percutaneous coronary intervention (PCI)presented with stable angina Canadian Cardiovascular Society class I under maximal medical therapy. Coronary computed tomography angiography showed severe focal stenosis with a minimum lumen area of 2.1 mm_2 in the distal right coronary artery (Figures 1A and 1B). Coronary angiography confirmed the coronary computed tomography angiography findings with angiography-derived fractional flow reserve (FFR, Pie Medical Imaging) of 0.42 (Figures 1C and 1D). The resting full-cycle flow ratio was 0.91, FFR was 0.68, and coronary flow reserve was 2.7 (Figure 2). The patient was included in the PPG Global Registry (Pullback Pressure Gradient [PPG] Registry; NCT04789317). The FFR manual pullback assessment showed a focal pressure stepup with a PPG of 0.91, indicating focal coronary artery disease (Figure 2).[1] He underwent PCI with one everolimus-eluting stent 4.0 mm 20 mm in the distal right coronary artery. The post-resting full-cycle flow ratio remained unchanged at 0.92, whereas FFR and coronary flow reserve increased to 0.96 and 3.7, respectively (Figure 2). The post-FFR pullback assessment showed a flat curve profile without residual pressure losses in the curve (Figure 3). Discordance between hyperemic and non-hyperemic pressure ratio remains a matter of debate. In the present case, the large focal pressure gradient was only unmasked during hyperemia. Focal coronary artery disease may be one of the underlying factors explaining the discrepancy between FFR and nonhyperemicpressure ratio.

Figure 1. Pre-PCI Examinations

(A) Coronary computed tomography angiography showed a noncalcified, severe plaque in the distal right coronary artery (arrowheads). (B) Three-dimensional luminal and plaque reconstruction (QAngio Cath Lab, Medis Medical Imaging) showed a plaque burden of 92% and with low Hounsfield units describing lipid composition. (C) Coronary angiography showed a severe focal lesion with diameter stenosis of 87% (arrow). (D) Angiography-derived fractional flow reserve was 0.42. D¼ distal; P¼ proximal; PCI¼ percutaneous coronary intervention.
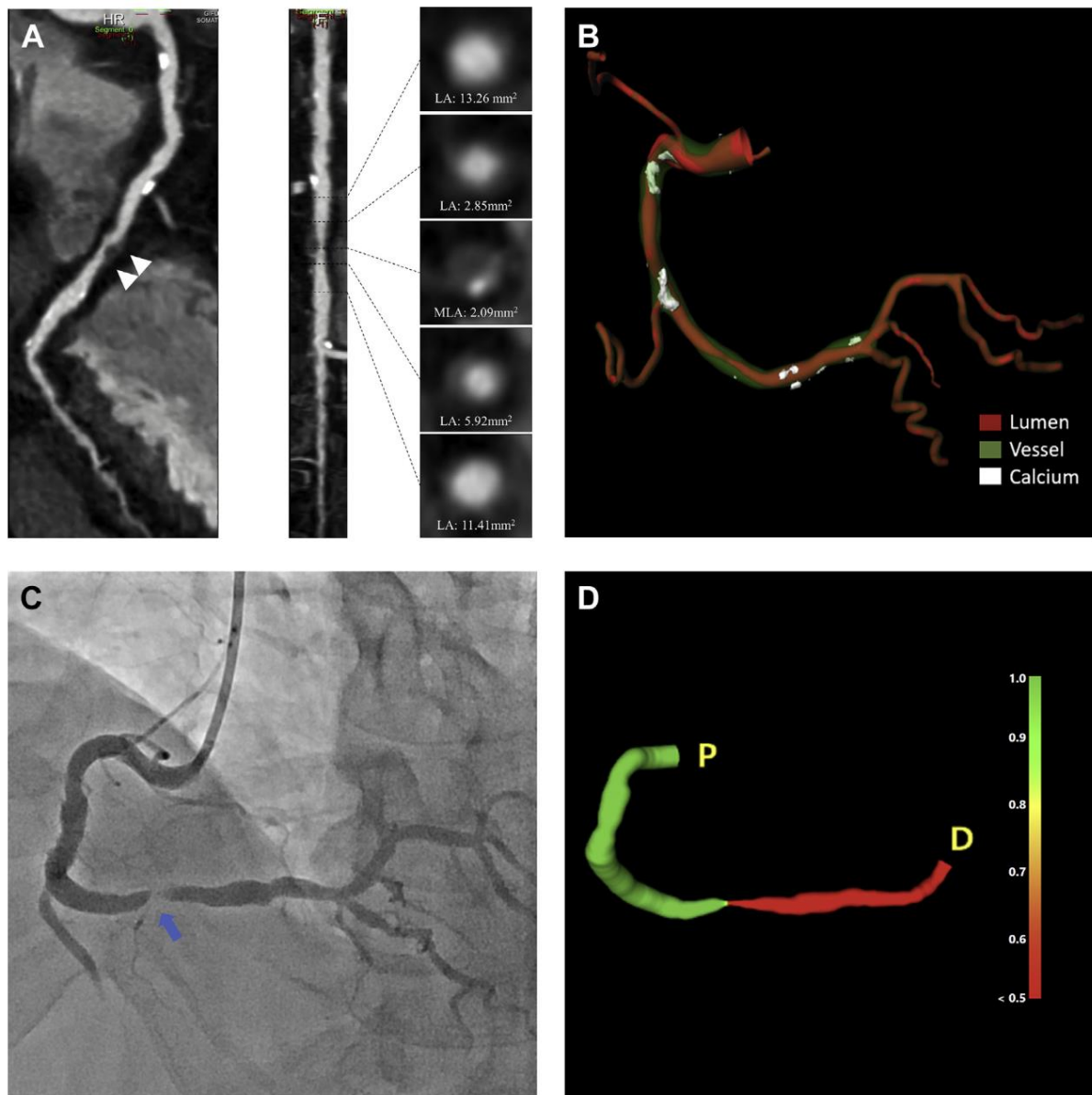
Figure 2. Physiological Assessment

The top panel shows the resting pressure ratio (RFR), hyperemic pressure ratio (FFR), and coronary flow reserve (CFR) measurements before percutaneous coronary intervention (PCI). The middle panel shows the FFR pullback with the pullback pressure gradient (PPG) calculation. The red bars represent the magnitude and location of the pressure losses. The bottom panel shows RFR, FFR, and CFR measurements after PCI.

280
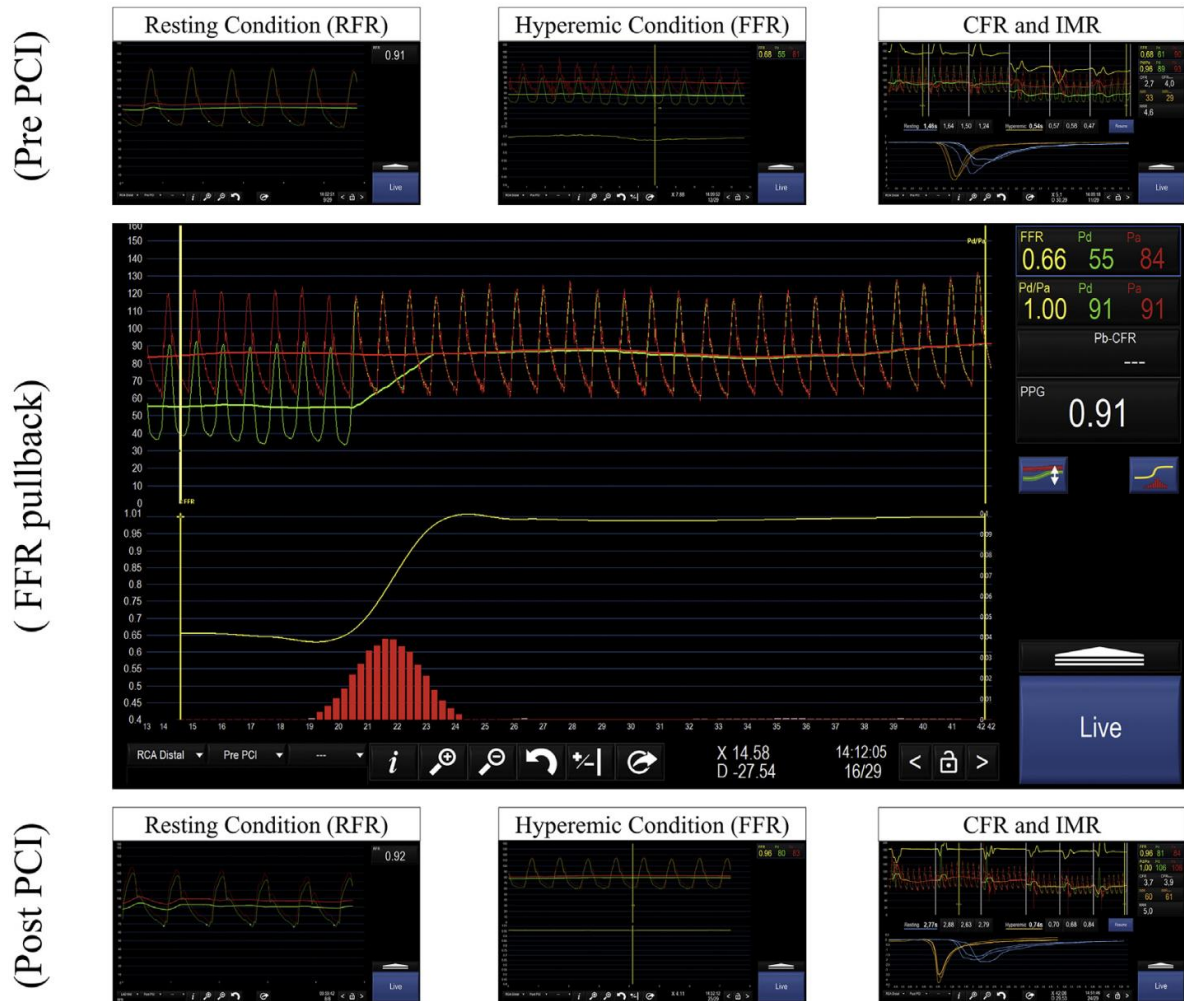
Figure 3 FFR Pullback Curves Pre- and Post-PCI

Comparison of fractional flow reserve (FFR) pullback curves between pre- and post-PCI. The FFR and FFR pullback curve significantly improve with percutaneous coronary intervention (PCI).
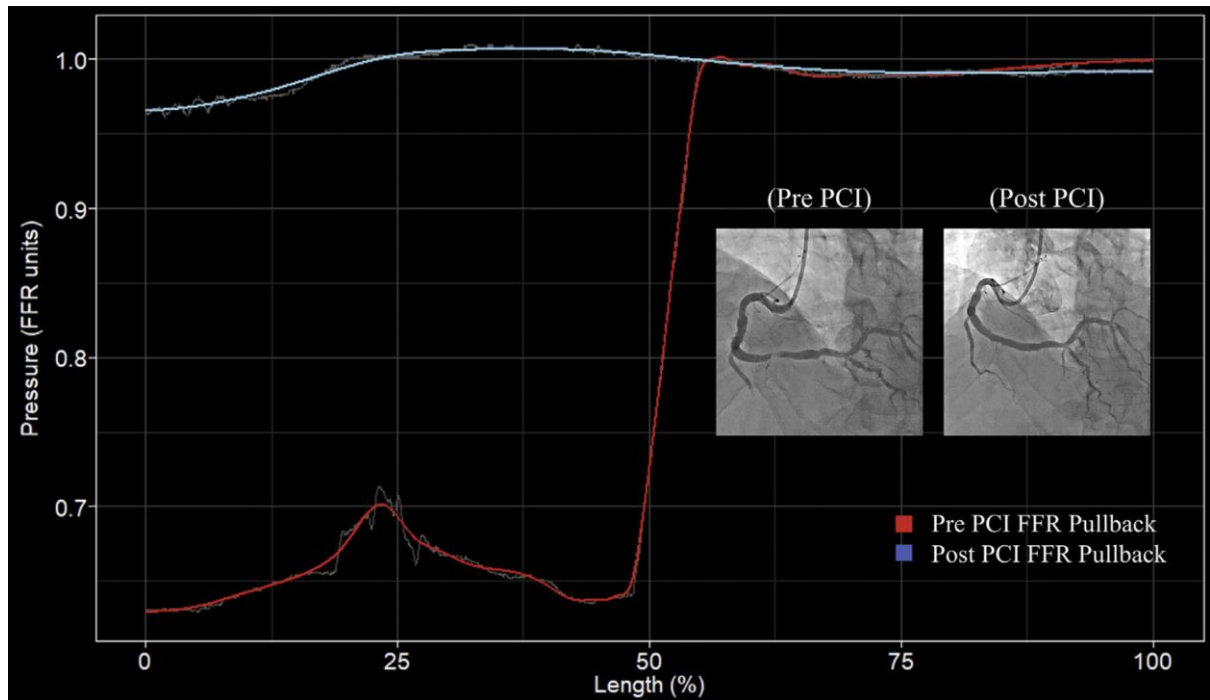
Reference

1. Collet C, Sonck J, Vandeloo B, et al. Measurement of hyperemic pullback pressure gradients to characterize patterns of coronary atherosclerosis. J Am Coll Cardiol. 2019;74:1772–1784.

0.95

FFR

Length
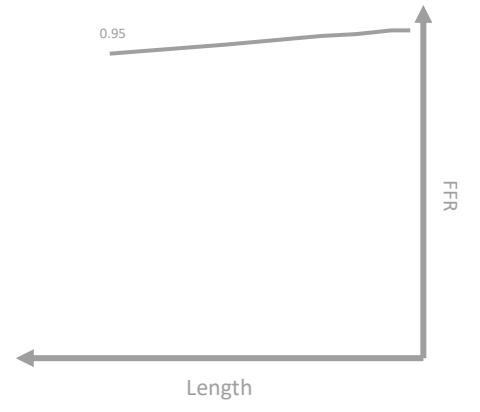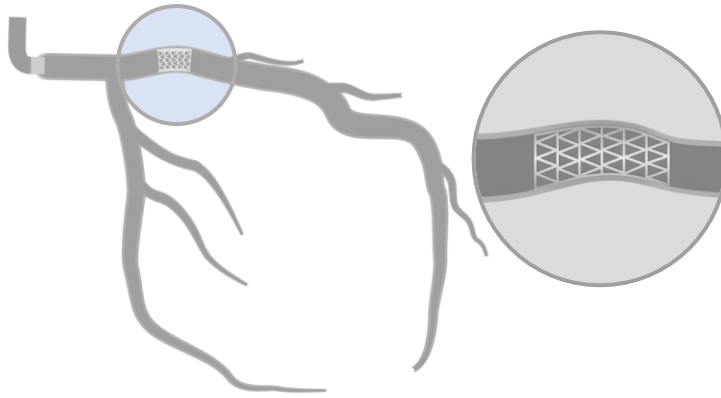
Chapter 13. Influence of Pathophysiological Patterns of Coronary Artery Disease on Immediate Percutaneous Coronary Intervention Outcomes

Collet C, Munhoz D, Mizukami T, Sonck J, Matsuo H, Shinke T, Ando H, Ko B, Biscaglia S, Rivero F, Engstrøm T, Arslani K, Leone AM, van Nunen L, Fearon W, Christiansen E, Fournier S, Desta L, Yong A, Adjedj J, Escaned J, Nakayama M, Eftekhari A, Zimmermann F, Sakai K, Storozhenko T, da Costa B, Campo G, West N, De Potter T, Heggermont W, Buytaert D, Bartunek J, Berry C, Collison D, Johnson T, Amano T, Perera D, Jeremias A, Ali Z, Pijls N, De Bruyne B and Johnson NP

Abstract

Background: Diffuse coronary artery disease (CAD) impacts the safety and efficacy of percutaneous coronary intervention (PCI). Pathophysiological CAD patterns can be quantified using fractional flow reserve (FFR) pullbacks incorporating the pullback pressure gradient (PPG) calculation. This study aimed to establish the capacity of PPG to predict optimal revascularisation and procedural outcomes.

Methods: This prospective, investigator-initiated, single-arm, multicentre study enrolled patients with at least one epicardial lesion with an FFR ≤ 0.80 scheduled for PCI. Manual FFR pullbacks were employed to calculate PPG. The primary outcome of optimal revascularisation was defined as a post-PCI FFR ≥ 0.88.

Results: 993 patients with 1044 vessels were included. The mean FFR was 0.68 ± 0.12, PPG 0.62 ± 0.17, and post-PCI FFR 0.87 ± 0.07. PPG was significantly correlated with the change in FFR after PCI (r=0.65, 95% CI 0.61-0.69, p<0.001) and demonstrated excellent predicted capacity for optimal revascularisation (AUC 0.82, 95% CI 0.79-0.84, p<0.001). Conversely, FFR alone did not predict revascularisation outcomes (AUC 0.54, 95% CI 0.50-0.57). PPG influenced treatment decisions in 14% of patients, redirecting them from PCI to alternative treatment modalities. Periprocedural myocardial infarction occurred more frequently in patients with low PPG (<0.62) compared to those with focal disease (OR 1.71, 95% CI: 1.00-2.97).

Conclusions: Pathophysiological CAD patterns distinctly affect the safety and effectiveness of PCI. The PPG showed an excellent predictive capacity for optimal revascularisation and demonstrated added value compared to a FFR measurement.

Clinical Trial Registration: https://classic.clinicaltrials.gov/ct2/show/NCT04789317

Structured Graphical Abstract. PPG, revascularization outcomes and treatment decision.
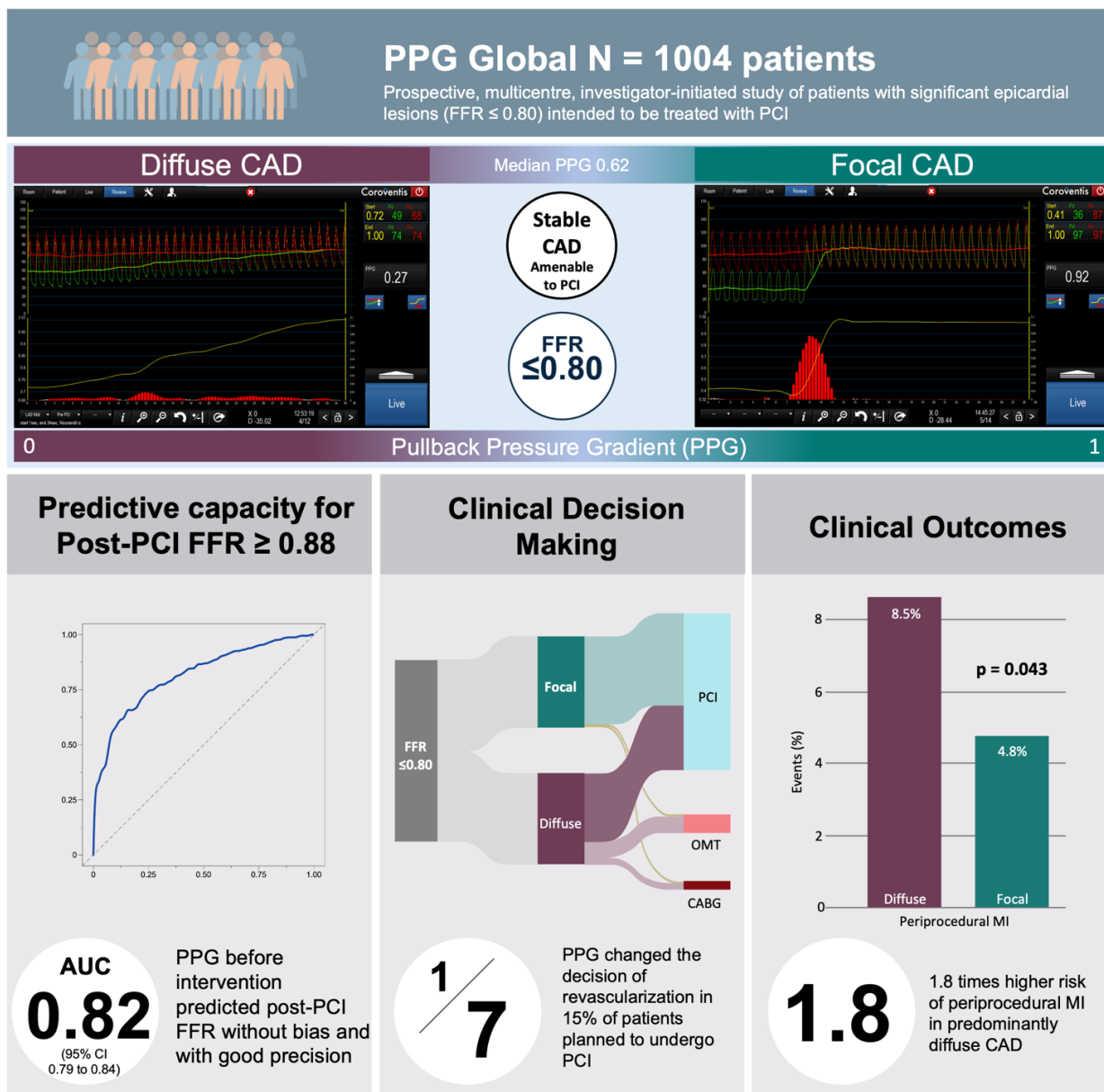
Non-standard Abbreviations and Acronyms

ACS: Acute coronary syndrome.

AUC: Area under the receiver operating characteristic curve.

CABG: Coronary artery bypass graft surgery.

CAD: Coronary artery disease.

CCS: Canadian cardiovascular society grading of angina pectoris.

CEC: Clinical events committee.

CFR: Coronary flow reserve.

FFR: Fractional flow reserve.

LAD: Left anterior descending artery.

LCX: Left circumflex.

LR: Likelihood ratio.

MI: Myocardial infarction.

MT: Medical therapy.

NHPR: non-hyperaemic pressure ratios.

PCI: Percutaneous coronary intervention.

PPG: Pullback pressure gradient.

QCA: Quantitative coronary angiography.

RCA: Right coronary artery.

SAQ-7: Seven-item Seattle angina questionnaire.

TVF: Target vessel failure.

ULN: Upper limit of normal.

Clinical Perspective

What is new?

• The Pullback Pressure Gradient (PPG) standardises the assessment of pathophysiological coronary artery disease (CAD) patterns.

• PPG helps guide revascularisation decisions by assessing the presence and severity of diffuse disease.

• The PPG value, derived after an FFR pullback, provides additional information to FFR forecasting revascularisation results.

What are the clinical implications?

• PPG identifies patients more likely to benefit from PCI.

• Patients with focal CAD experience greater FFR improvement and lower periprocedural myocardial infarction compared to those with diffuse CAD.

• A randomised clinical trial is warranted to assess the benefit of a PPG-guided PCI strategy.

Introduction

In stable patients with obstructive coronary artery disease (CAD), the primary goal of revascularisation is to improve myocardial blood flow. However, a sizable proportion of patients remains with a low fractional flow reserve (FFR) despite angiographically successful percutaneous coronary intervention (PCI). Low FFR after PCI is associated with a worse prognosis.[1] Furthermore, the magnitude of FFR improvement after PCI tracks directly with angina relief.[2] Therefore, the ability to predict the potential benefits of PCI in terms of final vessel physiology carries substantial diagnostic and therapeutic implications.

FFR measurement captures total pressure loss along the coronary artery. An adjunct pullback manoeuvre spatially localises pressure gradients and allows recognition of diffuse atherosclerotic patterns. The pullback pressure gradient (PPG) has emerged as an objective metric for characterising pressure loss patterns on a continuous scale ranging from 0 = diffuse to 1 = focal.[3] PPG may allow for the prediction of improvement in blood flow with PCI before intervention. Initial studies indicated that PCI might be more effective in patients with focal disease.[4,5]

Accordingly, the present study aimed to assess the potential of PPG to predict optimal revascularisation (defined as post-PCI FFR ≥ 0.88) and to investigate its influence on treatment decisions and procedural outcomes. The overarching hypothesis was that PCI would be more effective in vessels with high PPG, indicative of focal disease.

Methods

PPG Global was a prospective, investigator-initiated, multicentre, international, and single-arm study identified at clinicaltrials.gov as NCT04789317. Its design and rationale have been published previously.[6] Patients aged 18 years and older, who had stable CAD or had experienced an acute coronary syndrome (ACS) with non-culprit lesions, were candidates for inclusion in the study. Eligible patients had an epicardial angiographic stenosis intended to be treated with PCI. For inclusion, lesions had to be defined as haemodynamically significant, based on FFR ≤ 0.80. Patients with acute myocardial infarction, ejection fraction < 30%, estimated glomerular filtration rate < 30 mL/min/1.73 m^2, aorto-ostial lesions, severe vessel tortuosity, and planned two-stent bifurcation PCI were excluded. Every participant gave written informed consent, and every site received approval from its local institutional review board. **Supplemental Material Tables S1 and S2** detail the study leadership and committee

composition and participating sites. An independent clinical events committee (CEC) adjudicated adverse events, blinded to the invasive data. An external core laboratory centralised data collection and analysed imaging and physiological data. The study was sponsored by the Cardiovascular Research Institute (CRI) Aalst with an unrestricted grant from Abbott Vascular. The data that support the findings of this study are available from the corresponding author upon reasonable request.

Invasive Physiology Procedure

Coronary angiography was acquired in two views at least 30 degrees apart after injecting 100 to 200 μg of intracoronary nitroglycerin. A coronary wire equipped with a distal pressure sensor (PressureWire X, Abbott Vascular, Santa Clara, CA, USA) was introduced into the target vessel after pressure equalisation at the tip of the guiding catheter. The pressure wire was positioned in the distal coronary artery in a segment ≥ 2 mm and at least 15 mm beyond the most distal stenosis by visual estimation. Wire position was recorded during a contrast injection. A standardised physiological assessment was performed, including measurements of non-hyperaemic pressure ratios (NHPR), distal FFR, and a manual pullback during hyperaemia induced by a pharmacologic agent that ensured sufficient hyperaemic plateau (**Supplemental Table S3**). During study initiation, operators received training on the pullback manoeuvre, which involved the manual withdrawal of the pressure wire at a constant speed during 20 to 30 seconds. When the pressure sensor reached the catheter tip, the pullback recording was stopped, and PPG was calculated onsite using CoroFlow software v3.5.1 (Coroventis Research AB, Uppsala, Sweden). The calculation of the PPG involves the integration of two parameters derived from the FFR pullback curves, specifically the maximal pressure gradient observed over 20% of the pullback duration and the extent of functional disease. This integration of these parameters results in a numerical value ranging from 0 to 1. PPG values nearing 1.0 are indicative of focal disease, while values approaching 0 signify diffuse CAD.[3] FFR Pullbacks after PCI were analysed to derive the residual PPG defined as the maximal focal pressure gradients in FFR units in 20% of the pullback duration.[7]

Before performing the PPG assessment, operators answered a dedicated questionnaire about the anticipated PCI strategy to assess the impact of the PPG on decision-making. Based on the PPG value, operators could opt for medical therapy or coronary artery bypass graft (CABG) surgery instead of PCI. The change in decision-making to CABG or medical therapy after a comprehensive physiological assessment with FFR and PPG was left at the operator's

discretion. In cases undergoing PCI, the procedure was performed according to the operator's discretion with encouraged use of everolimus-eluting stents (Xience drug-eluting stent, Abbott Vascular). Following PCI, NHPR and FFR were measured at the same anatomical location as before PCI, and a post-PCI FFR pullback was repeated with visual co-registration of the stent position on the pressure tracing. Physicians were allowed to optimise PCI based on post-PCI physiology. Additional measurements of coronary flow reserve (CFR) before and after PCI were encouraged.

Core Laboratory Analysis

All angiographic and physiologic data underwent centralised, independent review at the CoreAalst core laboratory. Quantitative coronary angiography (QCA) was performed via two views using three-dimensional (3D) QCA with CAAS 8.2 software (Pie Medical Imaging, Maastricht, the Netherlands). Offline evaluation of physiology tracings was conducted using CoroFlow software (Coroventis Research AB, Uppsala, Sweden). The physiology core laboratory assessed each recording for quality following predefined criteria, including an examination of the aortic and coronary pressure tracings for any signs of waveform distortion or loss, aortic pressure ventricularisation, and the presence of limiting arrhythmias. A binary decision was made for each tracing, determining its suitability for inclusion.

Hyperaemic pullback curves were scrutinised for artifacts and the extent of pressure drift, and any drift less than 0.05 was considered acceptable and algorithmically corrected. All tracings were reviewed by an experienced physician specialising in physiology measurements. During the initial cases conducted at each site, prompt feedback was provided to ensure high quality of the physiologic data. Additionally, weekly case review meetings were conducted throughout the study's execution for continued education.

Patient symptoms and clinical outcomes

Patient symptoms before PCI were collected using the 7-item Seattle Angina Questionnaire (SAQ-7) containing three domains: angina frequency, physical limitation, and quality of life. Higher scores indicate better health status.[8] A score of 100 in the angina frequency domain denoted freedom from angina and scores lower than 60 defined severe angina. The SAQ-7 questionnaire will be re-administered after one year.

Target vessel failure (TVF) was defined as cardiac death, target-vessel myocardial infarction (MI) and ischaemia-driven target vessel revascularisation. Periprocedural

myocardial infarction was defined according to the Fourth Universal Definition of Myocardial Infarction.[9] Troponin measurements were collected from 4 to 24 hours after PCI. Results are reported here as a normalised ratio between the value and its established normal threshold specific to each local troponin assay, expressed as multiples beyond the upper limit of normal (ULN) and specifically categorised as ≥ 5-times ULN, ≥ 35-times ULN, and ≥ 70-times ULN. In this report, we present in-hospital clinical outcomes; clinical follow-up will be performed for up to 3 years. An independent clinical events committee adjudicated adverse events, blinded to the invasive data.

Objectives

The primary objective was to determine the predictive capacity of PPG for optimal functional revascularisation defined as post-PCI FFR ≥ 0.88.[10] The key secondary endpoints addressed the influence of PPG on clinical decision-making in patients intended to be treated with PCI and assessed the impact of PPG on clinical outcomes.

Statistical Analysis

Analyses were performed using R version 4.3.1 (R Foundation for Statistical Computing, Vienna, Austria) employing standard statistical techniques; applicable tests were two-tailed, and $p<0.05$ was considered statistically significant.

The median PPG value of 0.62 was used for the main analysis to categorise vessels in predominantly focal and diffuse disease. For the primary objective, i.e., to evaluate the predictive capability of PPG to achieve a post-PCI FFR of ≥ 0.88, this cut-off was predefined and was based on previous randomized clinical trials assessing the prognostic capacity of post-PCI FFR for clinical outcomes.[10] Sensitivity analyses with different post-PCI FFR cut-offs were performed. The area under the receiver operating characteristic curve (AUC) method adjusted for epicardial vessel and baseline FFR was used to assess the predictive capacity of PPG to predict post-PCI FFR. The optimal PPG cut-off was derived from the Youden's index. Additionally, PPG cut-offs were explored using the positive (LR+) and negative (LR-) likelihood ratios. We also report the results after dividing the cohort according to the PPG cut-off, at a LR+ of 5 and a LR- of 0.40 for achieving optimal revascularisation.[11] For group comparisons, we used a univariate mixed-effects logistic regression model, where the dependent variable is PPG dichotomized as focal (PPG ≥0.62) or diffuse (PPG<0.62), and the independent variable is the angiographic, physiological, or procedural characteristic. We used

a mixed-effects model with a random intercept at the patient level to account for clustering of vessels within patients. Additionally, to determine the capability of PPG to predict the post-PCI FFR value (on a continuous scale), linear regression models were built using PPG, epicardial vessel, and pre-PCI FFR as variables. For the development of the prediction model for post-PCI FFR, calibration of the predicted post-PCI FFR from PPG was internally trained in a derivation cohort (n = 524: 60%) and then evaluated in a validation cohort (n = 367: 40%); cohorts were selected using random sampling.

Results

Patient demographics and procedural data

Between December 2020 and September 2023, 1004 patients (1057 vessels) were enrolled. Invasive physiological assessments were performed in 1057/1057 (100%) and 880/890 (99%) vessels pre- and post-PCI, respectively (**Figure 1**). **Table 1** shows baseline clinical characteristics in the overall population and stratified by CAD pattern. Mean age was 68 ± 10 years, 24% were female, and 29% of the patients had diabetes. Clinical presentation was predominantly stable angina (89%). Patients with focal disease reported greater physical limitation, experienced angina more frequently, and reported a lower quality of life compared to patients with diffuse disease (**Supplemental Table S4**). Twenty-four percent of patients reported severe angina without difference between focal and diffuse patterns (25% vs. 22%, p=0.359).

Table 2 shows angiographic, physiologic, and procedural characteristics. The LAD was the most frequently assessed vessel (73%). In the overall population, mean diameter stenosis and reference vessel diameter were $50 \pm 14\%$ and 2.7 ± 0.6 mm; vessels with focal disease had more severe stenosis and larger reference size compared to diffuse disease. Vessels with diffuse disease were treated with more, smaller diameter, and longer stents than vessels with focal CAD (p<0.001 for all).

Baseline FFR was lower in vessels with focal disease. Overall, FFR increased from 0.68 ± 0.12 to 0.87 ± 0.07. PPG exhibited significant and moderate correlations with both post-PCI FFR and the change in FFR (**Figure 2**). PPG showed a weak correlation with pre-PCI FFR (**Supplemental Figure S1**). **Supplemental Material Figure S2** shows the correlations between PPG and angiographic parameters. PCI of vessels with focal disease achieved greater FFR improvements compared to diffusely diseased vessels ($\Delta = 0.26 \pm 0.14$ vs. $\Delta = 0.13 \pm 0.08$, p<0.001) and higher final FFR (0.89 ± 0.07 vs. 0.84 ± 0.06, p<0.001). PPG also correlated

with changes in CFR after PCI, with a larger improvement in CFR observed in focal disease (**Supplemental Material Figures S3 and S4**).

PPG showed an excellent capacity to predict post-PCI FFR ≥ 0.88 with an AUC of 0.82 (95% CI 0.79 to 0.84), and an optimal PPG cut-off was 0.73 (**Figure 3**). **Figure 4** shows case examples of focal and diffuse disease before and after PCI. The predictive capacity stratified by different post-PCI FFR cut-offs is shown in the **Supplemental Material Table S5.** PPG cut-offs at a LR+ of 5 and a LR- of 0.40 were 0.73 and 0.50, respectively (**Supplemental Material Table S6)**. Post-PCI FFR and changes in FFR stratified by these cut-offs are shown in the **Supplemental Material Figure S5**. Conversely, FFR alone did not predict revascularisation outcomes (AUC 0.54, 95% CI 0.50-0.57). Suboptimal FFR (<0.88) after an angiographically successful PCI occurred in 471 vessels (53.5%) and was significantly higher in patients with diffuse disease (37.1% vs 74.0%, p<0.001, **Supplemental Material Figure S6**). In the post-PCI FFR pullback evaluation, the mean residual PPG was 0.06 ± 0.03 and was lower after PCI in vessels with focal disease (0.05 ± 0.03 FFR units in focal disease vs 0.07 ± 0.04 FFR units in diffuse disease, p<0.001; **Supplemental Material Figure S7**). Residual PPG was not associated with adverse events (**Supplemental Material Table S7).**

The model based on PPG, vessel type and baseline FFR to predict the absolute post-PCI FFR value showed a mean difference of 0 ± 0.05 FFR units compared to invasive post-PCI FFR (**Figure 3**). Clinical, angiographic and functional characteristics were well balanced between the training and validation cohorts (**Supplemental Material Table S8**). Prediction of post-PCI FFR remained unchanged in different clinical presentations (stable CAD vs. ACS) and in the presence of serial lesions (**Supplemental Material Figure S9**).

Clinical decision-making

In the overall cohort of patients intended to be treated by PCI, PPG altered treatment decisions in 138 patients (13.9%), leading to CABG referral in 50 (5.0%) and medical management in 88 (8.9%). Changes in treatment decisions occurred more frequently after detection of diffuse disease with PPG (4% in focal vs 25% in diffuse, p<0.001). PPG was 0.65 ± 0.15 in the PCI cohort vs. 0.51 ± 0.13 in patients referred to CABG vs. 0.48 ± 0.11 in patients managed medically (p<0.001; **Supplemental Material Figure S9**). While PPG was similar in patients referred to CABG or deferred to medical therapy (p = 0.139), FFR was lower in patients referred to surgical revascularisation (p <0.001).

In-hospital clinical outcomes after PCI

A total of 855 patients (455 with focal and 400 with diffuse disease) underwent PCI. The clinical characteristics stratified by disease pattern are shown in the **Supplemental Material Table S9.** The rate of in-hospital TVF was similar between patients with focal vs diffuse disease (6.2% vs 9.8%, p=0.056; **Figure 5**). Target-vessel MI was significantly higher in patients with diffuse disease (OR 1.71, 95% CI 1.00 to 2.97); this was driven entirely by a higher incidence of periprocedural MI (5.9% vs 9.8%, p=0.040). **Supplemental Table S10** shows the rate of each component of TVF stratified by PPG. Baseline characteristics, and procedural and clinical outcomes stratified by PPG tertiles are shown in the **Supplemental Material Tables S11 and S12.**

Discussion

This prospective, large-scale, multicentre study of the pullback pressure gradient (PPG) offers several insights into the clinical relevance of applying coronary physiology in a novel way to differentiate focal from diffuse disease. First, PPG discriminates between patients who will have optimal functional revascularisation from those who will have a suboptimal FFR after PCI, FFR alone did not predict revascularisation outcomes; second, patients with predominantly focal disease defined by PPG (>0.62) achieved higher final FFR values after PCI compared to those with diffuse disease; third, PPG before intervention predicted post-PCI FFR accurately; fourth, the measurement of PPG in patients already planned to undergo PCI changed the revascularisation decision in one out of seven patients and, finally, PCI of vessels with focal disease was associated with a lower rate of periprocedural myocardial infarction than with diffuse disease.

Pressure-derived epicardial physiology

Coronary physiology has been mainly utilised to define haemodynamic lesion severity. Measurement of one distal FFR value provides information on the perfusion of the underlying myocardial territory expressed on a scale from 0 to 1. A pullback manoeuvre complements this evaluation by adding the spatial distribution of abnormal epicardial resistance, which PPG quantifies, and it is also expressed on a scale from 0 to 1. Hence, FFR assesses the severity of epicardial resistance, while PPG portrays its spatial distribution. The two indices, both derived from intracoronary pressure measurements, are therefore highly complementary. PPG, in

addition to FFR, adds a second dimension to epicardial coronary physiology. FFR helps decide the need for revascularisation, while PPG offers insight into the potential outcomes of PCI.

From a practical standpoint, obtaining PPG can be seamlessly integrated into the same measurement procedure as FFR by performing a manual pullback. The extra time required to gather this additional information is approximately 30 seconds, and the results have been shown to be highly reproducible.[12] In the present study, PPG values spanned from 0.25 to 0.95, with a median of 0.62, which was used to distinguish focal from diffuse CAD in this analysis. In addition, we utilised likelihood ratios to derive additional PPG cut-offs and demonstrated that physiological and clinical outcomes were progressively improved in patients with PPG > 0.73 and worse in cases with PPG < 0.50. Nonetheless, despite the AUC and likelihood ratio analyses suggesting PPG thresholds were associated with procedural outcomes, we believe that PPG should be interpreted as a continuous metric with lower values associated with lower PCI clinical success rates and higher values associated with higher blood flow improvement and related to nearly complete resolution of angina.[3,5] The long-term follow-up of this cohort with the collection of clinical and patient-reported outcomes will further inform about PPG cut-offs for clinical decision-making.

Clinical utility of PPG

In patients with haemodynamically significant stenoses, PPG identified the subset of patients in whom PCI will yield its most favourable outcomes. Vessels with high PPG achieved higher post-PCI FFR and larger delta FFR. The pattern of CAD, as quantified by PPG, significantly influenced the change in FFR after PCI ($R^2 = 0.42$). In other words, the improvement in blood flow after PCI was partly determined by the baseline pathophysiological disease pattern. This holds prognostic significance since a low post-PCI FFR independently predicts clinical prognosis. In the FAME studies, patients with post-PCI FFR <0.88 had significantly higher rates of adverse events compared to those with higher post-PCI FFR.[10,13] Nevertheless, it is essential to acknowledge that post-PCI FFR remains a surrogate marker, necessitating clinical follow-up to establish its association with an increased risk of adverse events. The present findings are in line with previous studies in which PCI of haemodynamic focal disease resulted in larger FFR improvement, higher FFR, reduced ischaemia, and less angina compared to vessels with diffuse disease.[4,5,14] In the longer term, studies using angiography-derived FFR have shown that the risk of TVF after angiographically successful PCI is determined by the physiological distribution of coronary atherosclerosis before PCI. In

the study by Shin et al. Patients with low angiography-derived PPG, indicative of diffuse disease, had a significantly higher risk of TVF compared to those with predominant focal disease.[15] This segregation of CAD phenotypes using physiology before intervention may facilitate better patient selection and improve outcomes with revascularisation.[1,16]

After PCI, the residual PPG was higher in vessels with baseline diffuse disease, confirming previous observations and suggesting the potential for further improvement in epicardial vessel conductance after PCI in diffuse disease.[7] The use of coronary physiology, targeting residual pressure gradients for PCI optimization, is currently being investigated in the INSIGHTFUL-FFR (NCT05437900) and Distal Evaluation of Functional Performance With Intravascular Sensors to Assess the Narrowing Effect: Guided Physiologic Stenting (DEFINE GPS NCT04451044) randomized clinical trials.

Forecasting post-PCI results and patient selection

The expansion of coronary physiology toward predicting PCI results will likely influence the contemporary management of CAD. The present study demonstrated an excellent predictive capacity of the PPG for optimal post-PCI physiology, with a PPG cut-off of 0.73. PPG cut-offs predictive of symptom improvement and clinical outcomes will be derived from long-term data collection. Post-PCI FFR can be forecast using several tools, e.g., the PCI planner derived from coronary CT angiography, angiography-derived software, and invasively with an instantaneous wave-free ratio system.[17-19] All of these approaches are based on the potential physiologic effects of stent implantation.[20] In the present study, the PPG predicted the absolute post-PCI FFR value without bias and with an acceptable precision (mean difference of 0 with SD of 0.05 FFR units compared to invasively measured FFR); however, there was a trend to higher differences between the predicted and measured in lower post-PCI FFR values. Vessel-level prediction of outcomes may avoid unnecessary procedures when the expected benefit of the intervention is low and may also be useful in the consenting and shared decision-making process. In this study, we observed that in patients with haemodynamically significant disease intended to be treated by PCI, knowledge of PPG changed the initial clinical decision in one out of seven patients. Patients referred for CABG or managed medically had a significantly lower PPG than those treated with PCI. Interestingly, patients referred to surgery had lower FFR and higher symptom burden than those managed medically, even with comparable PPG values. In patients with diffuse disease, van Beek and colleagues found no discernible difference in clinical outcomes between those treated with CABG and those

managed medically over a two-year follow-up.[21] Another study indicated investigating outcomes of CABG showed a significantly lower patency rate of the internal mammary artery in cases with baseline diffuse functional disease.[22] Phenotypically, plaque composition in patients with diffuse disease appears to be more stable, being atherosclerosis primarily of a calcific nature.[23] The current study additionally demonstrates that at baseline, patients with diffuse disease had less angina burden and a better quality of life compared to those with focal disease. Collectively, these findings suggest that medical therapy may be an acceptable initial strategy for managing patients with diffuse disease, reserving revascularisation for individuals with persistent symptoms despite medical therapy. However, it is essential to acknowledge that determining the optimal approach for treating diffuse coronary artery disease (CAD) requires further investigation. The introduction of PPG holds promise for standardising its diagnosis and facilitating future trials in this domain.

Considering clinical translation, the results of this study indicate that in patients with CAD scheduled for invasive management, PPG guidance may optimise revascularisation decisions, improve the benefit-risk ratio for periprocedural myocardial infarction, and improve clinical outcomes. Therefore, a randomised clinical trial is warranted to compare the safety and effectiveness of a PPG-guided PCI approach.

Limitations

The present study has several limitations. First, the inclusion criteria were based on the decision of the operator to perform PCI; therefore, these results do not apply to patients with extensive, diffuse multivessel disease. Second, the study was not powered to detect differences in clinical outcomes, and thus, these findings should be interpreted as hypothesis-generating Moreover, the differences in clinical outcomes were sensitive to the PPG cut-off used. Third, no PPG threshold was offered at the start of the study to guide clinical decision-making. A PPG cut-off should be derived from patient-reported or clinical outcomes; follow-up of this cohort is planned for up to 3 years to address this question. Fourth, we used FFR after PCI as a metric of optimal revascularisation. Although this definition is supported by many studies, it does not address other morphological aspects of PCI that can also be used to define optimal PCI, such as stent expansion, also linked to prognosis.[24] Fifth, operators were trained to perform manual pullbacks with the recommendation of manual wire withdrawal at a constant speed for 20 to 30 seconds; however, we must recognize that variable pullback speed may influence the

pullback morphology and PPG value. Finally, an extended follow-up period is essential to assess the benefit of the alterations in patient management prompted by the PPG.

Conclusion

Pathophysiological CAD patterns, i.e., focal or diffuse, distinctly affect the safety and effectiveness of PCI. Intervention in focal disease, characterised by high PPG values, was associated with improved haemodynamic outcomes and reduced myocardial infarction compared to vessels with low PPG values. In cases with haemodynamically significant lesions, quantifying the PPG index prior to intervention makes it possible to predict which patients will achieve optimal revascularisation based on coronary physiology. Further investigation through a randomized trial is warranted to explore the potential advantages of a PPG-guided PCI strategy.

Table 1. Baseline and clinical characteristics stratified by PPG

Variable	Overall	Focal	Diffuse	p-value
Number of patients	993	470	523	
Age (years), mean ± SD	67.7 ± 10.2	67.7 ± 10.4	67.6 ± 10.1	0.873
Gender (male), n (%)	757 (76.2)	347 (73.8)	410 (78.4)	0.107
BMI, kg/m^2 (%), mean ± SD	27.0 ± 8.9	26.7 ± 8.4	27.4 ± 9.3	0.221
Dyslipidaemia, n (%)	727 (73.2)	343 (73.0)	384 (73.4)	0.932
Hypertension, n (%)	694 (69.9)	322 (68.5)	372 (71.1)	0.407
Diabetes mellitus, n (%)	292 (29.4)	136 (28.9)	156 (29.8)	0.812
Current smoking, n (%)	164 (16.5)	85 (18.1)	79 (15.1)	0.239
Prior PCI for nontarget vessel, n (%)	277 (27.9)	121 (25.7)	156 (29.9)	0.167
Prior PCI for target vessel, n (%)	118 (11.9)	47 (10.0)	71 (13.6)	0.099
Prior MI, n (%)	197 (19.8)	82 (17.4)	115 (22.0)	0.087
Peripheral artery disease, n (%)	61 (6.1)	26 (5.5)	35 (6.7)	0.530
Clinical presentation, n (%)				0.156
NSTEMI	57 (5.8)	20 (4.3)	37 (7.1)	
Unstable angina	53 (5.3)	25 (5.3)	28 (5.4)	
Stable angina	881 (88.9)	425 (90.4)	456 (87.5)	
Symptom (Stable angina), n (%)*				0.003
Asymptomatic	119 (12.0)	43 (9.1)	76 (14.6)	
Silent ischaemia***	141 (14.2)	55 (11.7)	86 (16.5)	
CCS I	304 (30.7)	162 (34.5)	142 (27.3)	
CCS II	223 (22.5)	112 (23.8)	111 (21.3)	
CCS III	76 (7.7)	43 (9.1)	33 (6.3)	
CCS IV	18 (1.8)	10 (2.1)	8 (1.5)	
LVEF (%), mean ± SD	58.3 ± 9.5	59.3 ± 9.4	57.4 ± 9.5	0.001

For patients with multivessel interrogation, the lowest PPG was used for the patient-level analysis.

* As assessed by the treating physician.

** Define as s positive functional non-invasive test in an asymptomatic patient.

BMI = Body Mass Index; PCI = Percutaneous coronary intervention; MI = Myocardial infarction; NSTEMI = Non-ST elevation myocardial infarction; CCS = Canadian Cardiovascular Society Angina Score; LVEF = Left ventricular ejection fraction

Table 2. Angiographic, physiological, and procedural characteristics stratified by PPG.

Variable	Overall	Focal	Diffuse	p-value
Number of vessels	1044	515	529	
Vessel (%)				
LAD	756 (72.5)	283 (55.0)	473 (89.6)	Ref.
LCX	123 (11.8)	105 (20.4)	18 (3.4)	<0.001
RCA	164 (15.7)	127 (24.7)	37 (7.0)	<0.001
Serial lesions*, n (%)	212 (20.3)	83 (16.1)	129 (24.5)	<0.001
Minimal lumen diameter (mm), mean ± SD	1.49 ± 0.51	1.38 ± 0.55	1.59 ± 0.45	<0.001
Diameter stenosis (%), mean ± SD	50.1 ± 14.1	56.5 ± 13.0	44.0 ± 12.3	<0.001
Reference vessel diameter (mm), mean ± SD	2.65 ± 0.57	2.75 ± 0.60	2.55 ± 0.53	<0.001
Lesion length (mm), median [IQR]	17.4 [11.6, 26.2]	16.7 [11.1, 25.2]	17.8 [12.1, 27.6]	0.029
FFR, mean ± SD	0.68 ± 0.12	0.63 ± 0.13	0.72 ± 0.08	<0.001
PPG, mean ± SD	0.62 ± 0.16	0.76 ± 0.09	0.49 ± 0.08	<0.001
Vessels undergoing PCI, n (%)	890 (85.2)	494 (95.9)	396 (74.9)	<0.001
Number of stents, mean ± SD	1.14 ± 0.37	1.08 ± 0.29	1.21 ± 0.44	<0.001
Stent length (mm), mean ± SD	32.4 ± 16.6	28.6 ± 13.7	37.3 ± 18.7	<0.001
Stent diameter (mm), mean ± SD	3.04 ± 0.44	3.09 ± 0.48	2.97 ± 0.38	<0.001
Intracoronary imaging PCI (%), n (%)	395 (44.4)	234 (47.4)	161 (40.7)	0.046
Pre dilatation (%), n (%)	780 (87.7)	429 (87.0)	351 (88.6)	0.465
Post dilatation (%), n (%)	662 (74.5)	347 (70.4)	315 (79.7)	0.002
Post-PCI FFR, mean ± SD	0.87 ± 0.07	0.89 ± 0.07	0.84 ± 0.06	<0.001
Delta FFR, mean ± SD	0.20 ± 0.13	0.26 ± 0.14	0.13 ± 0.08	<0.001
Delta FFR (%), mean ± SD	58 ± 23	69 ± 19	44 ± 19	<0.001
Pre-PCI CFR, mean ± SD[δ]	2.39 ± 1.29	2.22 ± 1.31	2.55 ± 1.26	0.044
Post-PCI CFR, mean ± SD[ε]	3.19 ± 1.93	3.47 ± 2.06	2.78 ± 1.63	0.015
Delta CFR, mean ± SD[φ]	0.77 ± 1.84	1.18 ± 1.94	0.19 ± 1.52	<0.001

* Serial lesions were site-reported based on angiography alone.

[δ] 254 vessels were available. [ε] 188 vessels were available. [φ] 170 vessels were available.

LAD = Left anterior descending artery; LCX = Left circumflex artery; RCA = Right coronary artery; FFR = Fractional flow reserve; PPG = Pullback pressure gradient; CABG = Coronary artery bypass graft sugery; OMT = Optimal medical therapy; PCI = Percutaneous coronary intervention;

Figure 1. Study Flow chart.

FFR = fractional flow reserve; PPG = pullback pressure gradient; PCI = percutaneous coronary intervention.


```
┌─────────────────────────────────────────────────────────────────────────────┐
│ 1056 screened patients with significant coronary artery disease and intention │
│                           to perform PCI                                       │
└─────────────────────────────────────────────────────────────────────────────┘
                                                 ┌──────────────────────────────────┐
                                                 │ 52 screening failures:             │
                                                 │ - 46 with FFR > 0.80               │
                                                 │ - 5 with eGFR < 30 mL/min/1.73 m²  │
                                                 │ - 1 patient with graft as target   │
                                                 │   vessel                           │
                                                 └──────────────────────────────────┘
┌─────────────────────────────────────────────────────────────────────────────┐
│ 1004 patients (1057 vessels) with initial PCI strategy based on angiography    │
│                        and distal point FFR                                    │
└─────────────────────────────────────────────────────────────────────────────┘
                                                 ┌──────────────────────────────────┐
                                                 │ 11 patients (13 vessels) excluded: │
                                                 │ - 1 vessels: Pre-PCI FFR Pullback  │
                                                 │   < 15 seconds                     │
                                                 │ - 7 vessels: Pullback curve        │
                                                 │   artefact                         │
                                                 │ - 4 vessels: Ventricularization    │
                                                 │ - 1 vessels: Missing tracings      │
                                                 └──────────────────────────────────┘
┌─────────────────────────────────────────────────────────────────────────────┐
│  993 patients (1044 vessels) with adapted treatment decision after PPG         │
└─────────────────────────────────────────────────────────────────────────────┘
                                                 ┌──────────────────────────────────┐
                                                 │ 138 patients (164 vessels)         │
                                                 │ deferred from PCI:                 │
                                                 │ - 88 pts (100 vessels) to OMT      │
                                                 │ - 50 pts (54 vessels) to CABG      │
                                                 │ 10 vessel: Post-PCI FFR not        │
                                                 │ measured                           │
                                                 │ 1 vessel: Post-PCI FFR with        │
                                                 │ ventricularization                 │
                                                 └──────────────────────────────────┘
┌─────────────────────────────────────────────────────────────────────────────┐
│  855 patients (880 vessels) underwent PCI with post-PCI FFR measurement        │
└─────────────────────────────────────────────────────────────────────────────┘
```
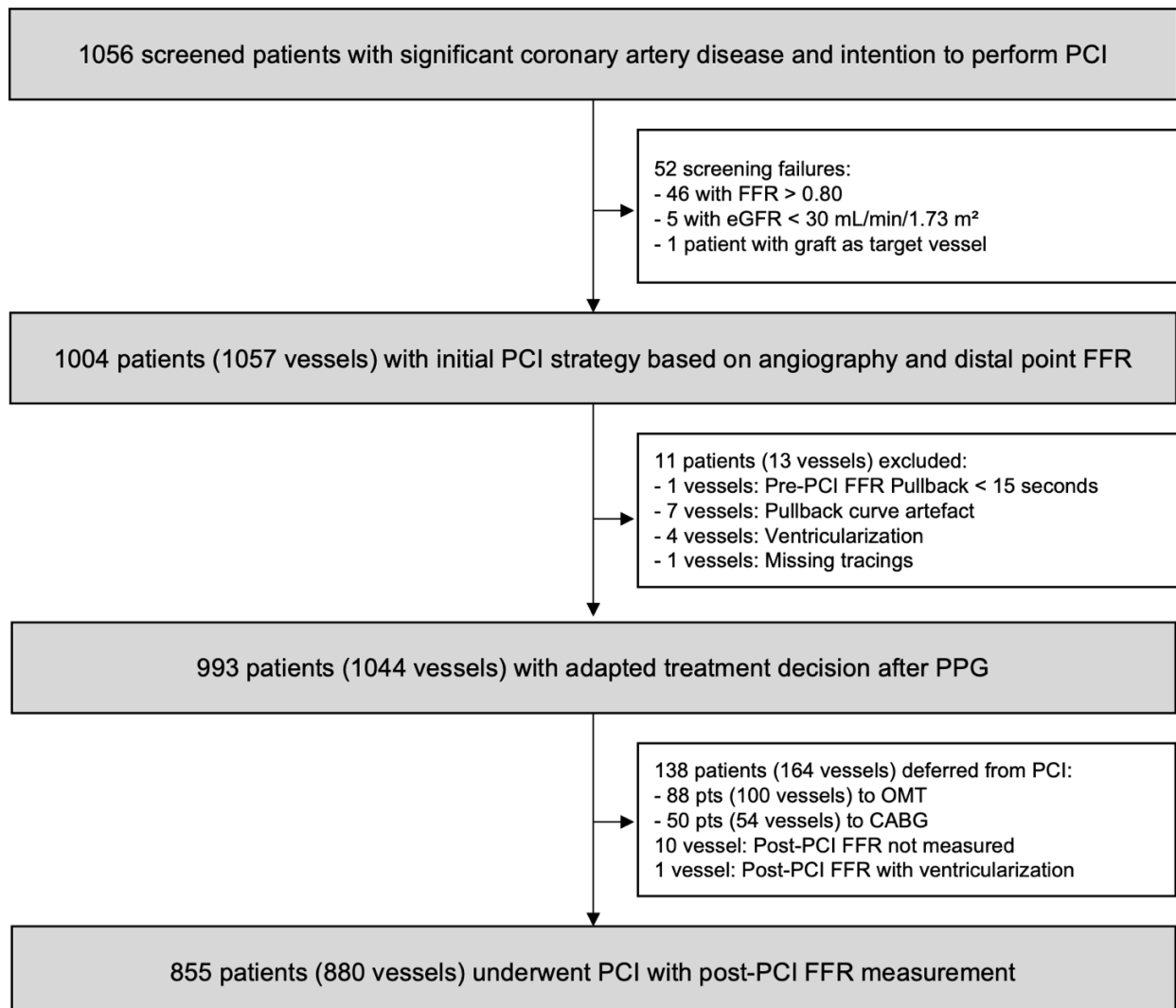
Figure 2. Correlation between PPG and FFR before and after PCI.

Panel A shows the relationship between PPG and post-PCI FFR. Panel B shows the relationship between PPG and delta FFR (%) ((post-PCI FFR – pre-PCI FFR)/ (1 – pre-PCI FFR)). Panel C shows the relationship between PPG and change in FFR after PCI; the triangles indicate the FFR at baseline, and the circles the post-PCI FFR. The length of the lines displays the change in FFR. The blue lines indicate PCI, where FFR post-PCI was higher than 0.88, and the red lines where post-PCI FFR was less than 0.88.
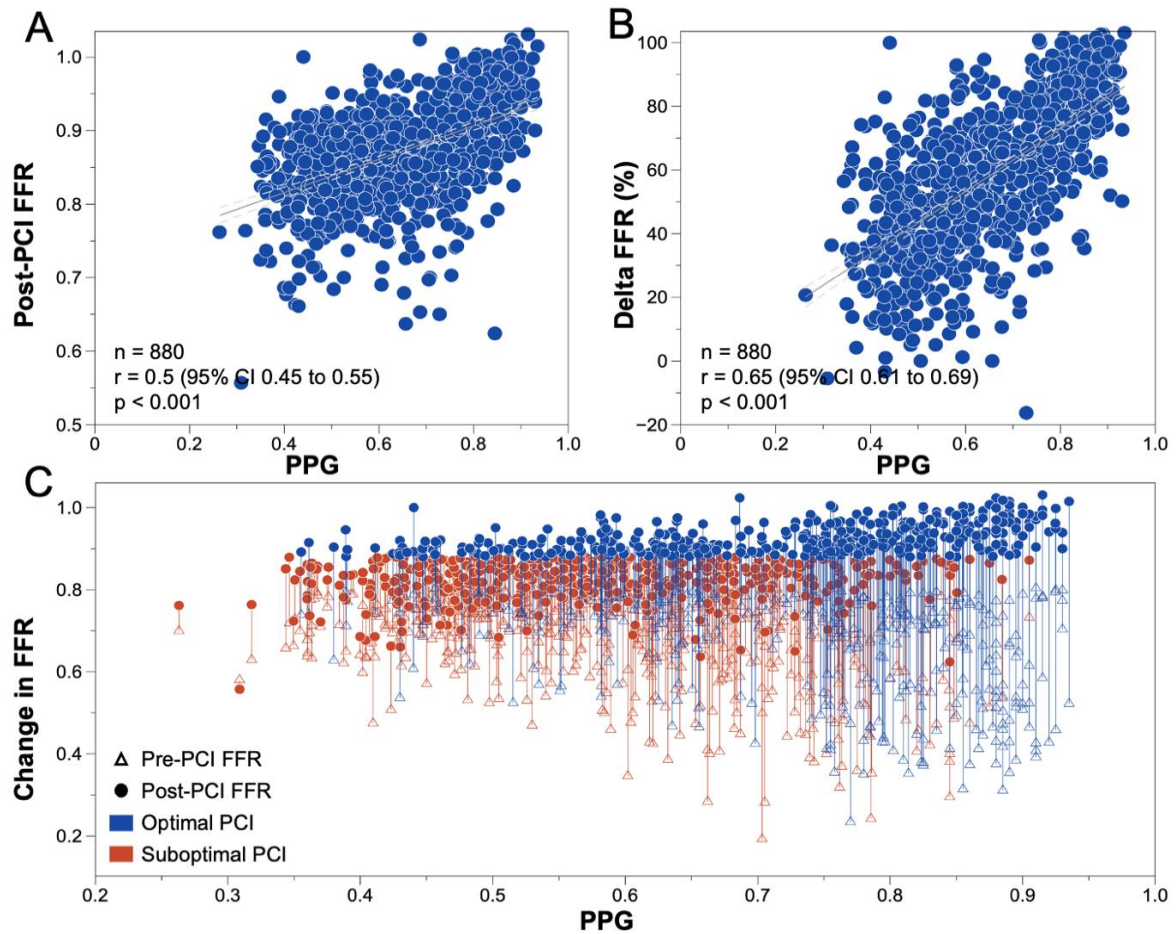
Figure 3. Predictive capacity of PPG for post-PCI FFR.

The left panel shows the predictive capacity of PPG (pullback pressure gradient) for predicting an FFR after PCI $\geq$ 0.88. The right panel shows the mean difference between the prediction of FFR in the validation cohort derived from the PPG regression analysis and measured post-PCI FFR.
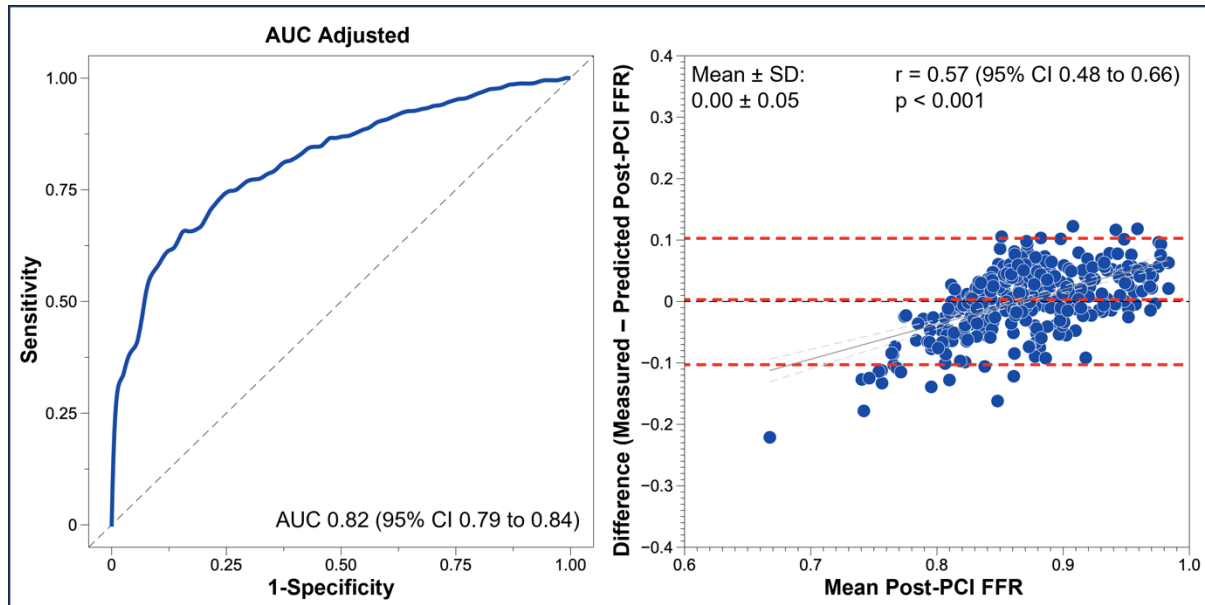
Figure 4. Case examples of focal and diffuse coronary artery disease.

Panels A shows an angiogram of a left anterior descending (LAD) artery with a lesion in the mid segment; panel B shows the fractional flow reserve (FFR) with a pullback before percutaneous coronary interventions (PCI). This case had a FFR 0.77 with a pullback pressure gradient (PPG) of 0.81. Panel C shows the angiogram after PCI and panel D the post-PCI FFR of 0.90. Panel E shows an angiogram of an LAD with a lesion in the mid segment, panel F shows a FFR of 0.55 with a PPG of 0.42, pointing at diffuse coronary artery disease. Panel G shows the post-PCI angiogram and panel H the post-PCI FFR of 0.66.

Focal coronary artery disease
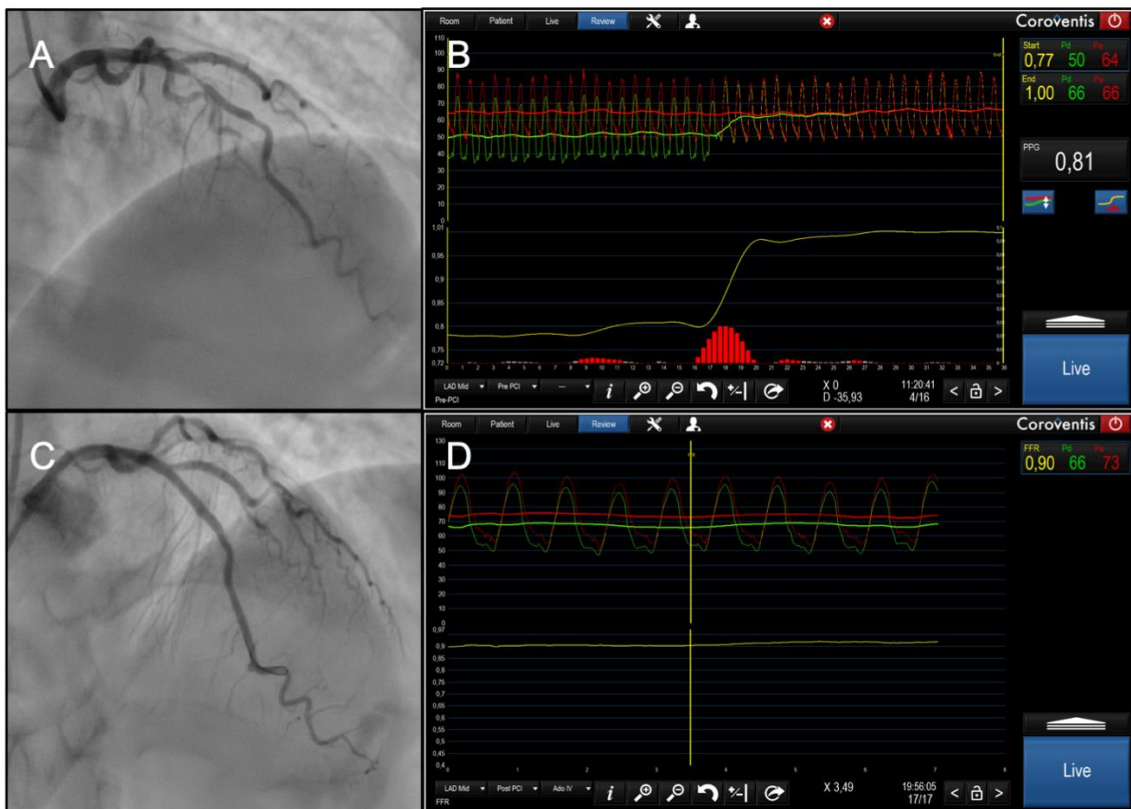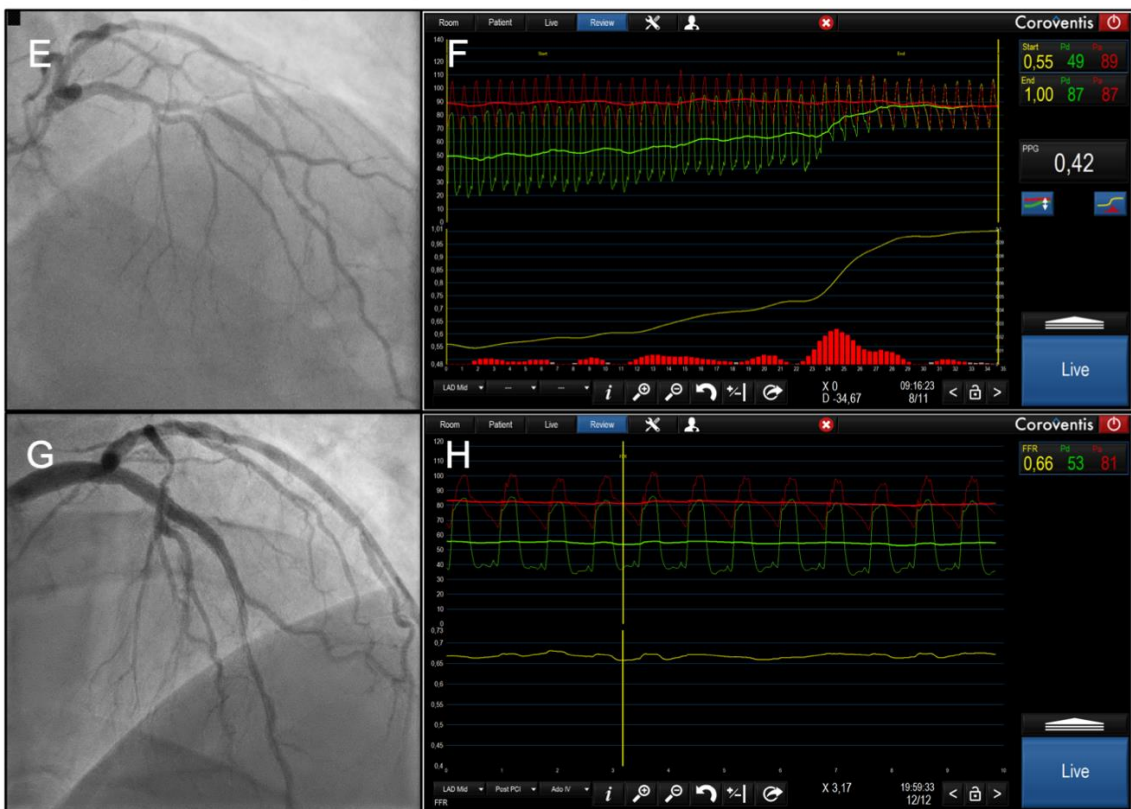

Diffuse coronary artery disease

Figure 5. In-hospital clinical outcomes after PCI in patients with predominantly focal or diffuse disease based on pullback pressure gradient (PPG).

Patients were stratified based on the median PPG value of 0.62 into predominantly focal or diffuse disease. Panel A shows the incidence of target vessel failure (TVF) and its components. Panel B shows the rate of target-vessel myocardial infarction (MI) stratified by periprocedural or spontaneous MI. The incidence of peri-procedural myocardial infarction was significantly higher in patients with diffuse disease.
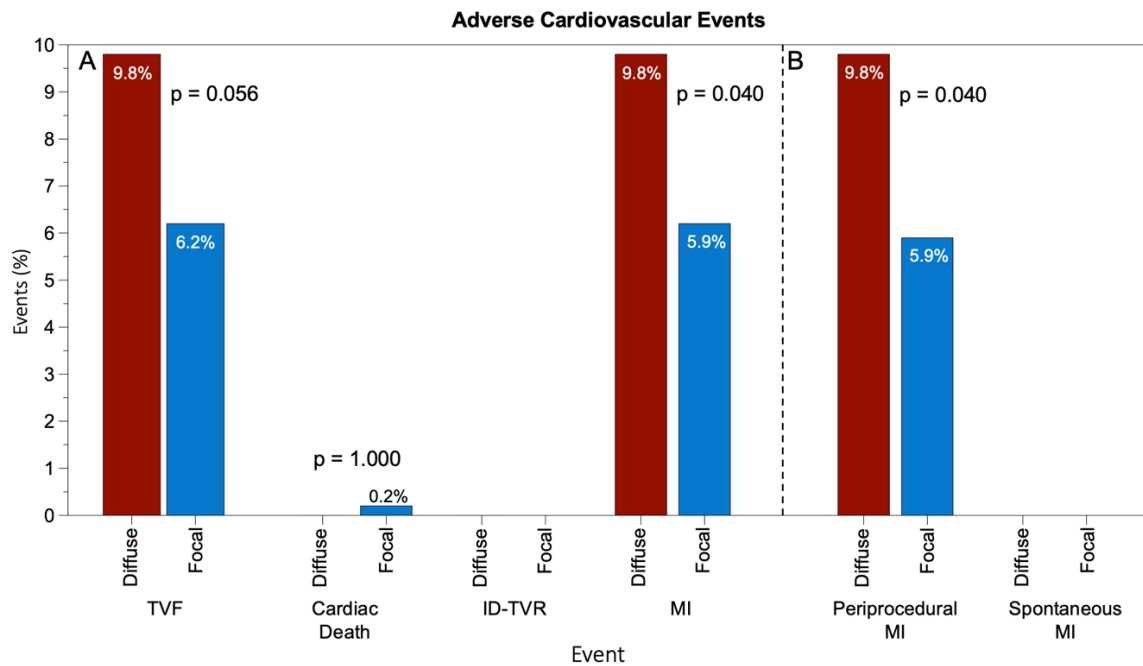
References

1. Hwang D, Koo BK, Zhang J, Park J, Yang S, Kim M, Yun JP, Lee JM, Nam CW, Shin ES, et al. Prognostic Implications of Fractional Flow Reserve After Coronary Stenting: A Systematic Review and Meta-analysis. *JAMA Netw Open*. 2022;5:e2232842. doi: 10.1001/jamanetworkopen.2022.32842

2. Collison D, Copt S, Mizukami T, Collet C, McLaren R, Didagelos M, Aetesam-Ur-Rahman M, McCartney P, Ford TJ, Lindsay M, et al. Angina After Percutaneous Coronary Intervention: Patient and Procedural Predictors. *Circ Cardiovasc Interv*. 2023;16:e012511. doi: 10.1161/circinterventions.122.012511

3. Collet C, Sonck J, Vandeloo B, Mizukami T, Roosens B, Lochy S, Argacha J-F, Schoors D, Colaiori I, Di Gioia G, et al. Measurement of Hyperemic Pullback Pressure Gradients to Characterize Patterns of Coronary Atherosclerosis. *Journal of the American College of Cardiology*. 2019;74:1772-1784. doi: 10.1016/j.jacc.2019.07.072

4. Mizukami T, Sonck J, Sakai K, Ko B, Maeng M, Otake H, Koo BK, Nagumo S, Nørgaard BL, Leipsic J, et al. Procedural Outcomes After Percutaneous Coronary Interventions in Focal and Diffuse Coronary Artery Disease. *J Am Heart Assoc*. 2022;11:e026960. doi: 10.1161/jaha.122.026960

5. Collet C, Collison D, Mizukami T, McCartney P, Sonck J, Ford T, Munhoz D, Berry C, De Bruyne B, Oldroyd K. Differential Improvement in Angina and Health-Related Quality of Life After PCI in Focal and Diffuse Coronary Artery Disease. *JACC Cardiovasc Interv*. 2022;15:2506-2518. doi: 10.1016/j.jcin.2022.09.048

6. Munhoz D, Collet C, Mizukami T, Yong A, Leone AM, Eftekhari A, Ko B, da Costa BR, Berry C, Collison D, et al. Rationale and Design of the Pullback Pressure Gradient (PPG) Global Registry. *Am Heart J*. 2023. doi: 10.1016/j.ahj.2023.07.016

7. Ohashi H, Mizukami T, Sonck J, Boussiet F, Ko B, Nørgaard BL, Mæng M, Jensen JM, Sakai K, Ando H, et al. Intravascular Imaging Findings After PCI in Patients With Focal and Diffuse Coronary Artery Disease. *J Am Heart Assoc*. 2024;13:e032605. doi: 10.1161/jaha.123.032605

8. Spertus JA, Winder JA, Dewhurst TA, Deyo RA, Prodzinski J, McDonell M, Fihn SD. Development and evaluation of the Seattle Angina Questionnaire: a new functional status measure for coronary artery disease. *J Am Coll Cardiol*. 1995;25:333-341. doi: 10.1016/0735-1097(94)00397-9

9. Thygesen K, Alpert JS, Jaffe AS, Chaitman BR, Bax JJ, Morrow DA, White HD. Fourth Universal Definition of Myocardial Infarction (2018). *J Am Coll Cardiol*. 2018;72:2231-2264. doi: 10.1016/j.jacc.2018.08.1038

10. Piroth Z, Otsuki H, Zimmermann FM, Ferenci T, Keulards DCJ, Yeung AC, Pijls NHJ, De Bruyne B, Fearon WF. Prognostic Value of Measuring Fractional Flow Reserve After Percutaneous Coronary Intervention in Patients With Complex Coronary Artery Disease: Insights From the FAME 3 Trial. *Circ Cardiovasc Interv*. 2022;15:884-891. doi: 10.1161/circinterventions.122.012542

11. Dujardin B, Van den Ende J, Van Gompel A, Unger JP, Van der Stuyft P. Likelihood ratios: a real improvement for clinical decision making? *Eur J Epidemiol*. 1994;10:29-36. doi: 10.1007/bf01717448

12. Sonck J, Mizukami T, Johnson NP, Nagumo S, Gallinoro E, Candreva A, Mileva N, Munhoz D, Shinke T, Svanerud J, et al. Development, validation, and reproducibility of the pullback pressure gradient (PPG) derived from manual fractional flow reserve pullbacks. *Catheter Cardiovasc Interv*. 2022;99:1518-1525. doi: 10.1002/ccd.30064

13. Piroth Z, Toth GG, Tonino PAL, Barbato E, Aghlmandi S, Curzen N, Rioufol G, Pijls NHJ, Fearon WF, Juni P, et al. Prognostic Value of Fractional Flow Reserve Measured Immediately After Drug-Eluting Stent Implantation. *Circ Cardiovasc Interv*. 2017;10. doi: 10.1161/circinterventions.116.005233

14. Rajkumar CA, Shun-Shin M, Seligman H, Ahmad Y, Warisawa T, Cook CM, Howard JP, Ganesananthan S, Amarin L, Khan C, et al. Placebo-Controlled Efficacy of Percutaneous Coronary Intervention for Focal and Diffuse Patterns of Stable Coronary Artery Disease. *Circ Cardiovasc Interv*. 2021;14:e009891. doi: 10.1161/circinterventions.120.009891

15. Shin D, Dai N, Lee SH, Choi KH, Lefieux A, Molony D, Hwang D, Kim HK, Jeon KH, Lee HJ, et al. Physiological Distribution and Local Severity of Coronary Artery Disease and Outcomes After Percutaneous Coronary Intervention. *JACC Cardiovasc Interv*. 2021;14:1771-1785. doi: 10.1016/j.jcin.2021.06.013

16. Collison D, Didagelos M, Aetesam-Ur-Rahman M, Copt S, McDade R, McCartney P, Ford TJ, McClure J, Lindsay M, Shaukat A, et al. Post-stenting fractional flow reserve vs coronary angiography for optimisation of percutaneous coronary intervention: TARGET-FFR trial. *Eur Heart J*. 2021. doi: 10.1093/eurheartj/ehab449

17. Sonck J, Nagumo S, Norgaard BL, Otake H, Ko B, Zhang J, Mizukami T, Maeng M, Andreini D, Takahashi Y, et al. Clinical Validation of a Virtual Planner for Coronary Interventions Based on Coronary CT Angiography. *JACC Cardiovasc Imaging*. 2022;15:1242-1255. doi: 10.1016/j.jcmg.2022.02.003

18. Nijjer SS, Sen S, Petraco R, Escaned J, Echavarria-Pinto M, Broyd C, Al-Lamee R, Foin N, Foale RA, Malik IS, et al. Pre-angioplasty instantaneous wave-free ratio pullback provides virtual intervention and predicts hemodynamic outcome for serial lesions and diffuse coronary artery disease. *JACC Cardiovasc Interv*. 2014;7:1386-1396. doi: 10.1016/j.jcin.2014.06.015

19. van Diemen PA, de Winter RW, Schumacher SP, Bom MJ, Driessen RS, Everaars H, Jukema RA, Somsen YB, Popelkova L, van de Ven PM, et al. Residual Quantitative Flow Ratio to Estimate Post-Percutaneous Coronary Intervention Fractional Flow Reserve. *J Interv Cardiol*. 2021;2021:4339451. doi: 10.1155/2021/4339451

20. Escaned J, Berry C, De Bruyne B, Shabbir A, Collet C, Lee JM, Appelman Y, Barbato E, Biscaglia S, Buszman PP, et al. Applied coronary physiology for planning and guidance of percutaneous coronary interventions. A clinical consensus statement from the European Association of Percutaneous Cardiovascular Interventions (EAPCI) of the European Society of Cardiology. *EuroIntervention*. 2023;19:464-481. doi: 10.4244/eij-d-23-00194

21. van Beek KAJ, van Steenbergen GJ, Vervaat FE, Mulders B, van Straten BH, van Nunen LX, Wijnbergen IF. Single center experience in the treatment of hemodynamically significant diffuse coronary artery disease of the left anterior descending. *Int J Cardiol*. 2022;352:40-44. doi: 10.1016/j.ijcard.2022.01.048

22. Shiono Y, Kubo T, Honda K, Katayama Y, Aoki H, Satogami K, Kashiyama K, Taruya A, Nishiguchi T, Kuroi A, et al. Impact of functional focal versus diffuse coronary artery disease on bypass graft patency. *Int J Cardiol*. 2016;222:16-21. doi: 10.1016/j.ijcard.2016.07.052

23. Sakai K, Mizukami T, Leipsic J, Belmonte M, Sonck J, Nørgaard BL, Otake H, Ko B, Koo BK, Maeng M, et al. Coronary Atherosclerosis Phenotypes in Focal and Diffuse Disease. *JACC Cardiovasc Imaging*. 2023. doi: 10.1016/j.jcmg.2023.05.018

24. Soeda T, Uemura S, Park SJ, Jang Y, Lee S, Cho JM, Kim SJ, Vergallo R, Minami Y, Ong DS, et al. Incidence and Clinical Significance of Poststent Optical Coherence

Tomography Findings: One-Year Follow-Up Study From a Multicenter Registry. *Circulation*. 2015;132:1020-1029. doi: 10.1161/circulationaha.114.014704

0.95

FFR

Length

312
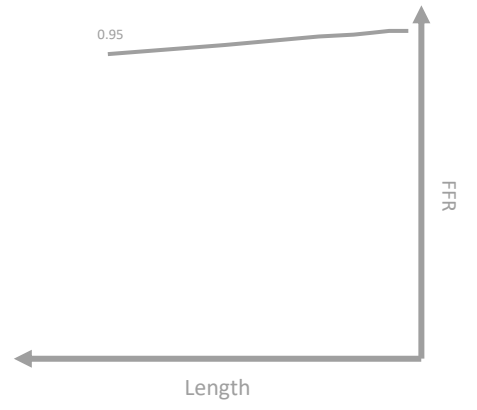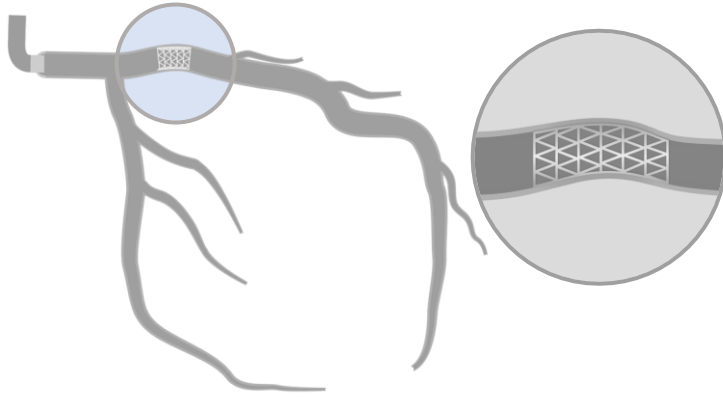
Part F. Discussion and conclusion

The present thesis supports the characterisation of atherosclerosis phenotypes in a spectrum of focal to diffuse CAD based on intracoronary pressure pullbacks. FFR pullbacks, performed manually or motorised, were accurate and reproducible in their ability to quantify the CAD using the PPG. Moreover, this provided valuable information in different clinical scenarios, such as serial lesions, to provide information for PCI guidance. Evaluation of serial lesions by pressure measurements is complex, as the functional contribution of each lesion is affected by the presence of the other lesions.[1] In vessels with serial lesions, three patterns of FFR pullback were described, each adequately identified by a spectrum of PPG values.

PCI success can be defined based on the improvement of coronary flow, improvement of angina, and, ultimately, reduction of cardiovascular events at follow-up. In Chapter 9, we demonstrated that improved blood flow with PCI is strongly linked to the pathophysiological patterns quantified by the PPG. In addition, we demonstrated that post-PCI FFR is affected by vessel size and subtended myocardial mass. We also showed how the distribution of pressure losses is associated with wall shear stress patterns in patients with flow-limiting stenosis. Finally, we validated these concepts clinically by demonstrating the association between post-PCI FFR and TVF. Furthermore, we described a distinct predictive ability of post-PCI FFR when stratified by the vessel type. The predictive capacity of FFR after PCI in the LAD is poor (AUC: 0.52; 95% CI: 0.47-0.58), while in non-LAD vessels, post-PCI FFR had a moderate predictive capacity (AUC: 0.66; 95% CI: 0.59-0.73; p = 0.005) for TVF. Consequently, we proposed that post-PCI be interpreted according to the vessel type.

The randomised clinical trial, TARGET-FFR, failed to show a benefit of physiologically guided PCI optimisation regarding the proportion of vessels achieving FFR after PCI ≥ 0.90.[2] In this thesis, we expanded the understanding of these results by demonstrating that the functional pattern of CAD affected TARGET-FFR's final result. Specifically, PIOS was applied more frequently to vessels with diffuse CAD. In patients

randomised to PIOS, those with focal disease achieved higher post-PCI FFR than patients with diffuse CAD. These findings suggest an interaction between the baseline pattern of CAD and the benefit of PCI optimisation based on coronary physiology.

One of the potential benefits of revascularisation is the reduction of spontaneous MI.[3,4] In untreated vessels, plaque morphology (i.e., high-risk plaques) is associated with MI.[5] We expanded this knowledge by showing an association between the functional pattern of CAD, quantified by the PPG, and plaque morphology, which could help refine patients' selection for PCI. Focal CAD had a higher plaque burden ($87 \pm 8\%$ vs $82 \pm 1\%$; p = 0.003), higher prevalence of circumferential lipid-rich plaque (37% vs 4%; p= 0.001) and TCFA (47% vs 10%; p= 0.002). Diffuse CAD had a higher prevalence of calcifications (Agatston score per vessel: 51 [IQR: 11-204] focal vs 158 [IQR: 52-341] diffuse; P= 0.024). Additionally, focal CAD by PPG predicted the presence of TCFA with an area under the curve of 0.73 (95% CI: 0.58-0.87). Wall shear stress descriptors, TSVI and time-average wall shear stress (TAWSS) predict MI.[6] We showed that TSVI was positively correlated with PPG. Vessels with focal CAD had significantly higher TAWSS and TSVI. PPG is associated with high-risk morphology and haemodynamics.

PPG standardises the assessment of the CAD pattern, allowing a reproducible definition of diffuse CAD. The PPG concept was validated clinically regarding the patient's response to PCI stratified by the pathophysiological CAD pattern. PCI in vessels with high PPG (focal CAD) resulted in higher post-PCI FFR (0.91 ± 0.07 vs 0.86 ± 0.05, P<0.001) and larger minimal stent area (6.3 ± 2.3 mm2 in focal versus 5.3 ± 1.8 mm2 in diffuse CAD, p=0.015) compared to vessels with low PPG (diffuse CAD). Furthermore, PPG improved the capacity to predict optimal PCI results compared to the angiographic assessment alone (AUC_{PPG} 0.81 [95% CI, 0.73– 0.88] vs AUC_{angio} 0.51 [95% CI, 0.42– 0.60]; P<0.001). Nevertheless, despite the leap in understanding CAD, the treatment of diffuse CAD remains an unmet clinical need.[7]

PCI in stable coronary artery disease improves angina in a placebo-controlled trial.[8] This thesis showed that this effect is heightened in patients with focal CAD who underwent PCI, as these patients had significantly higher SAQ-7 scores at follow-up than those with diffuse CAD. Residual angina after PCI was significantly less prevalent in those treated for focal CAD (27.5% vs 51.9%; p= 0.020). In summary, focal disease defined by high PPG correlates with the morphological features of plaques. It is associated with higher post-PCI FFR, larger minimal stent area, improvement in angina and quality of life.

To validate PPG as a predictor of PCI outcomes, we designed a prospective, investigator-initiated, multicentre, international, large-scale study. The study had prespecified adequately powered hypotheses. Patients with functionally significant coronary lesions (FFR≤0.80) intended to undergo PCI were included. The primary endpoint was the predictive capacity of PPG for post-PCI FFR. PPG was significantly correlated with the change in FFR after PCI (r=0.65, 95% CI 0.61-0.69, p<0.001) and demonstrated excellent predictive capacity for optimal revascularisation (AUC 0.82, 95% CI 0.79-0.84, p<0.001). PPG influenced treatment decisions in 14% of patients, deferring them from PCI. Periprocedural myocardial infarction occurred more frequently in patients with low PPG (<0.62) compared to those with focal disease (OR 1.83, 95% CI: 1.02-3.34). These findings establish PPG as a pre-procedural tool that predicts the safety and effectiveness of PCI. Future investigations will help better understand the benefit of a PPG-guided PCI strategy.

Conclusion

PPG, derived from FFR pullbacks, characterises the pathophysiological CAD patterns. High PPG was associated with high-risk plaque morphology. It also correlated with greater FFR improvement after PCI with higher rates of angina relief and a lower incidence of periprocedural MI compared to diffuse disease. Therefore, PPG adds clinical value to FFR in decision-making about revascularisation in patients with obstructive coronary artery disease.

The one-year follow-up of PPG Global is awaited and will confirm the differential outcomes of PCI in focal versus diffuse CAD.

References

1.   De Bruyne B, Pijls NH, Heyndrickx GR, Hodeige D, Kirkeeide R, Gould KL. Pressure-derived fractional flow reserve to assess serial epicardial stenoses: theoretical basis and animal validation. *Circulation*. Apr 18 2000;101(15):1840-7. doi:10.1161/01.cir.101.15.1840

2.   Collison D, McClure JD, Berry C, Oldroyd KG. A randomized controlled trial of a physiology-guided percutaneous coronary intervention optimization strategy: Rationale and design of the TARGET FFR study. *Clin Cardiol*. May 2020;43(5):414-422. doi:10.1002/clc.23342

3.   Chaitman BR, Alexander KP, Cyr DD, et al. Myocardial Infarction in the ISCHEMIA Trial: Impact of Different Definitions on Incidence, Prognosis, and Treatment Comparisons. *Circulation*. Feb 2021;143(8):790-804. doi:10.1161/CIRCULATIONAHA.120.047987

4.   Ferraro R, Latina JM, Alfaddagh A, et al. Evaluation and Management of Patients With Stable Angina: Beyond the Ischemia Paradigm: JACC State-of-the-Art Review. *J Am Coll Cardiol*. Nov 10 2020;76(19):2252-2266. doi:10.1016/j.jacc.2020.08.078

5.   Prati F, Romagnoli E, Gatto L, et al. Relationship between coronary plaque morphology of the left anterior descending artery and 12 months clinical outcome: the CLIMA study. *Eur Heart J*. Jan 14 2020;41(3):383-391. doi:10.1093/eurheartj/ehz520

6.   Candreva A, Pagnoni M, Rizzini ML, et al. Risk of myocardial infarction based on endothelial shear stress analysis using coronary angiography. *Atherosclerosis*. 02 2022;342:28-35. doi:10.1016/j.atherosclerosis.2021.11.010

7.   Baranauskas A, Peace A, Kibarskis A, et al. FFR result post PCI is suboptimal in long diffuse coronary artery disease. *EuroIntervention*. Dec 2016;12(12):1473-1480. doi:10.4244/EIJ-D-15-00514

8.   Rajkumar CA, Foley MJ, Ahmed-Jushuf F, et al. A Placebo-Controlled Trial of Percutaneous Coronary Intervention for Stable Angina. *N Engl J Med*. Dec 21 2023;389(25):2319-2330. doi:10.1056/NEJMoa2310610

Appendices

CURRICULUM VITAE

Name: Daniel Batista Munhoz

Date of birth: 06 June 1985

Nationality: Brazilian

Address: Albrechtlaan 19B, bus 15 Aalst, 9300 Belgium

E-mail: dbmunhoz@gmail.com

Phone: 0032 496 72 9319

Education

Research Fellowship in Interventional Cardiology, *Cardiovascular Center Aalst (2020-2023)*

Ph.D. in Cardiology*, University of Campinas, UNICAMP (2015-2020)*

Coronary Care Unit, *University Hospital of Campinas, University of Campinas, UNICAMP (2014-2015)*

Cardiology, *University Hospital of Campinas, Campinas University, UNICAMP (2012-2014)*

Internal Medicine, *Base Hospital of the Federal District, (2010-2012)*

Master's degree, *University of Brasília, UnB (2009-2011)*

Medicine (MD), *University of Brasília, UnB (2003-2009)*

Professional experience

Research Fellowship, *CoreAalst BV, Aalst, Belgium (2022-present)*

Staff Cardiology, *University Hospital of Campinas, Campinas University, UNICAMP (2015-2022)*

Staff Coronary Care Unit, *Galileo Hospital, Campinas (2015-2020)*

Staff Coronary Care Unit, *Medical Center of Campinas, Campinas (2016-2020)*

Staff Thrombolysis Care Unit, *Ouro Verde Hospital, Campinas (2013-2016)*

LIST OF PUBLICATIONS

Included in the thesis

1. Sonck J, Mizukami T, Johnson NP, **Munhoz D**, et al. Development, validation, and reproducibility of the pullback pressure gradient (PPG) derived from manual fractional flow reserve pullbacks. *Catheter Cardiovasc Interv*. Mar 02 2022;doi:10.1002/ccd.30064

2. Candreva A, Mizukami T, Sonck J, **Munhoz D**, et al. Hyperemic hemodynamic characteristics of serial coronary lesions assessed by pullback pressure gradients. *Catheter Cardiovasc Interv*. 11 01 2021;98(5):E647-E654. doi:10.1002/ccd.29868

3. Mileva N, Ohashi H, Paolisso P, **Munhoz D**, et al. Relationship between coronary volume, myocardial mass, and post-PCI fractional flow reserve. *Catheter Cardiovasc Interv*. Jun 2023;101(7):1182-1192. doi:10.1002/ccd.30664

4. **Munhoz D**, Sakai K, Collet C, Mizukami T. Triggering Stent Optimization by Coronary Physiology. *JACC Cardiovasc Interv*. Nov 14 2022;15(21):2228. doi:10.1016/j.jcin.2022.09.010

5. Collet C, Johnson NP, Mizukami T, **Munhoz D**, et al. Impact of Post-PCI FFR Stratified by Coronary Artery. *JACC Cardiovasc Interv*. Oct 09 2023;16(19):2396-2408. doi:10.1016/j.jcin.2023.08.018

6. Ohashi H, Collison D, Mizukami T, **Munhoz D**, et al. Fractional Flow Reserve-Guided Stent Optimisation in Focal and Diffuse Coronary Artery Disease. *Diagnostics (Basel)*. Aug 07 2023;13(15)doi:10.3390/diagnostics13152612

7. Candreva A, Gallo D, **Munhoz D**, et al. Influence of intracoronary hemodynamic forces on atherosclerotic plaque phenotypes. *Int J Cardiol*. Mar 15 2024;399:131668. doi:10.1016/j.ijcard.2023.131668

8. Sakai K, Mizukami T, Leipsic J, **Munhoz D**, et al. Coronary Atherosclerosis Phenotypes in Focal and Diffuse Disease. *JACC Cardiovasc Imaging*. Jul 06 2023;doi:10.1016/j.jcmg.2023.05.018

9. Mizukami T, Sonck J, Sakai K, **Munhoz D**, et al. Procedural Outcomes After Percutaneous Coronary Interventions in Focal and Diffuse Coronary Artery Disease. *J Am Heart Assoc*. Dec 06 2022;11(23):e026960. doi:10.1161/JAHA.122.026960

10. Collet C, Collison D, Mizukami T, **Munhoz D**, et al. Differential Improvement in Angina and Health-Related Quality of Life After PCI in Focal and Diffuse Coronary Artery Disease. *JACC Cardiovasc Interv*. Dec 26 2022;15(24):2506-2518. doi:10.1016/j.jcin.2022.09.048

11. **Munhoz D,** Collet C, Mizukami T, et al. Rationale and Design of the Pullback Pressure Gradient (PPG) Global Registry. *Am Heart J*. Aug 21 2023;doi:10.1016/j.ahj.2023.07.016

12. Nakayama M, Sakai K, **Munhoz D**, et al. Discordance in the Pattern of Coronary Artery Disease Between Resting and Hyperemic Conditions. *JACC Cardiovasc Interv*. 05 23 2022;15(10):*e113-e116. doi:10.1016/j.jcin.2022.01.303*

13. Collet C, **Munhoz D**, Mizukami T, et al. Influence of Pathophysiological Patterns of Coronary Artery Disease on Percutaneous Coronary Intervention Outcomes Originally published 14 May 2024; *Circulation. 2024;0* https://doi.org/10.1161/CIRCULATIONAHA.124.069450

Published articles, not included in thesis

14.   **Munhoz D,** Kodeboina M, Nagumo S, et al. Simplified Assessment of the Index of Microvascular Resistance. *J Interv Cardiol*. 2021;2021:9971874. doi:10.1155/2021/9971874

15.   Gallinoro E, Paolisso P, Candreva A, **Munhoz D,** et al. Microvascular Dysfunction in Patients With Type II Diabetes Mellitus: Invasive Assessment of Absolute Coronary Blood Flow and Microvascular Resistance Reserve. *Front Cardiovasc Med*. 2021;8:765071. doi:10.3389/fcvm.2021.765071

16.   Candreva A, Pagnoni M, Rizzini ML, **Munhoz D,** et al. Risk of myocardial infarction based on endothelial shear stress analysis using coronary angiography. *Atherosclerosis*. 02 2022;342:28-35. doi:10.1016/j.atherosclerosis.2021.11.010

17.   Bertolone DT, Gallinoro E, Esposito G, **Munhoz D,** et al. Contemporary Management of Stable Coronary Artery Disease. *High Blood Press Cardiovasc Prev*. May 2022;29(3):207-219. doi:10.1007/s40292-021-00497-z

18.   Mileva N, Nagumo S, Mizukami T, **Munhoz D,** et al. Prevalence of Coronary Microvascular Disease and Coronary Vasospasm in Patients With Nonobstructive Coronary Artery Disease: Systematic Review and Meta-Analysis. *J Am Heart Assoc*. 04 05 2022;11(7):e023207. doi:10.1161/JAHA.121.023207

19.   Sonck J, Nagumo S, Norgaard BL, **Munhoz D,** et al. Clinical Validation of a Virtual Planner for Coronary Interventions Based on Coronary CT Angiography. *JACC Cardiovasc Imaging*. Jul 2022;15(7):1242-1255. doi:10.1016/j.jcmg.2022.02.003

20.   Paolisso P, Gallinoro E, Andreini D, **Munhoz D,** et al. Prospective evaluation of the learning curve and diagnostic accuracy for Pre-TAVI cardiac computed tomography analysis by cardiologists in training: The LEARN-CT study. *J Cardiovasc Comput Tomogr*. Mar 12 2022;doi:10.1016/j.jcct.2022.03.002

21.   Paolisso P, Gallinoro E, Vanderheyden M, **Munhoz D,** et al. Absolute coronary flow and microvascular resistance reserve in patients with severe aortic stenosis. *Heart*. Dec 13 2022;109(1):47-54. doi:10.1136/heartjnl-2022-321348

22.   Bermpeis K, Esposito G, Gallinoro E, **Munhoz D,** et al. Safety of Right and Left Ventricular Endomyocardial Biopsy in Heart Transplantation and Cardiomyopathy Patients. *JACC Heart Fail*. Dec 2022;10(12):963-973. doi:10.1016/j.jchf.2022.08.005

23.   Vandeloo B, Andreini D, Brouwers S, **Munhoz D,** et al. Diagnostic performance of exercise stress tests for detection of epicardial and microvascular coronary artery disease: the UZ Clear study. *EuroIntervention*. Sep 23 2022;doi:10.4244/EIJ-D-22-00270

24.   Mileva N, Paolisso P, Gallinoro E, **Munhoz D,** et al. Diagnostic and Prognostic Role of Cardiac Magnetic Resonance in MINOCA: Systematic Review and Meta-Analysis. *JACC Cardiovasc Imaging*. Mar 2023;16(3):376-389. doi:10.1016/j.jcmg.2022.12.029

25.   Fabbricatore D, Buytaert D, Valeriano C, **Munhoz D,** et al. Ambulatory pulmonary vein isolation workflow using the Perclose ProglideTM suture-mediated vascular closure device: the PRO-PVI study. *Europace*. Apr 15 2023;25(4):1361-1368. doi:10.1093/europace/euad022

26.   Gallinoro E, Bertolone DT, Mizukami T, **Munhoz D,** et al. Continuous vs Bolus Thermodilution to Assess Microvascular Resistance Reserve. *JACC Cardiovasc Interv*. Nov 27 2023;16(22):2767-2777. doi:10.1016/j.jcin.2023.09.027

27.   Andreini D, Belmonte M, Penicka M, **Munhoz D,** et al. Impact of coronary CT image quality on the accuracy of the FFR. *Eur Radiol*. Apr 2024;34(4):2677-2688. doi:10.1007/s00330-023-10228-8

28.   Fawaz S, **Munhoz D,** Mahendiran T, et al. Assessing the Impact of Prolonged Averaging of Coronary Continuous Thermodilution Traces. *Diagnostics (Basel).* Jan 28 2024;14(3)doi:10.3390/diagnostics14030285

29.   Candreva A, Lodi Rizzini M, **Munhoz D,** Calò K, et al. Association Between Automated 3D Measurement of Coronary Luminal Narrowing and Risk of Future Myocardial Infarction. *J Cardiovasc Transl Res.* Mar 01 2024;doi:10.1007/s12265-024-10500-2

30.   Gallinoro E, Monizzi G, Sonck J, **Munhoz D,** et al. Physiological and angiographic outcomes of PCI in calcified lesions after rotational atherectomy or intravascular lithotripsy. *Int J Cardiol.* Apr 01 2022;352:27-32. doi:10.1016/j.ijcard.2022.01.066

ACKNOWLEDGMENTS

First and foremost, I thank my wife. You are a stronghold, my biggest supporter in science, my fiercest critic, and the bravest woman I know. I appreciate you coming along my adventure abroad and expanding our worlds. It seems now you are ready to start a new adventure of your own! Eu te amo, Linda.

My parents who have supported me in my first steps and since then. You are the shoulders in which I stand. Thank you so much for your wholehearted support and for always understanding me. Mama, eu te amo imensamente. Obrigado por me compreender de uma forma que eu sequer consigo entender. Dad, thanks for being a computer nerd. It helped a lot in this thesis!

My sisters and brother, you have built your lives but always kept in touch. I'm eager to keep learning from you. Lulu, eu sinto muito a sua falta aqui desse lado do oceano.

Some friends seem far away now, but Gustavo and Alex are always somewhere in my heart. Thank you for believing in me so thoroughly. I hope to live up to it!

I want to thank the fellows I met in Europe, many of them leading authors and co-authors in this thesis. Even in the grey and cold Aalst, each of you could find something good to add. I appreciate getting a better understanding of such diverse cultures while discussing the heart. A special thanks to Marta who has always been kind and helpful, even from Italy!

I also thank the many co-authors I've met and those who I didn't had the chance yet. I'm looking forward to new collaborations. The team of CoreAalst should also not be overlooked. I really appreciate your support in making research possible. Particularly, I thank Ms. Pardaens for being a great counselor during this period and Dimi who is always ready to help.

The staff members of the Cardiovascular Center Aalst for their support in developing research and their patience in the many times I would be there asking to enroll a PPG Global patient. The team of nurses and research nurses for their support and effort to communicate, even if sometimes I was not de allerbeste luisteraar.

Finally, I would like to acknowledge the cardiology team of UNICAMP for making me a Cardiologist. Thank you for all the support and all the knowledge. Prof. Andrei, thank you for being more than a promoter, being the master!

Of course, I appreciate Popper's support. The only one by my side until the thesis is finished (and it is indeed, his second Thesis).

0.95

FFR

Length